PHARMACOKINETIC AND PHARMACODYNAMIC MECHANISMS FOR REDUCED TOXICITY OF CPT-11 BY THALIDOMIDE AND ST. JOHN'S WORT

XIAOXIA YANG

(MSc, National Institute for the Control of

Pharmaceutical & Biological Products, P.R. China)

A THESIS SUBMITTED

FOR THE DEGREE OF DOCTOR OF PHILOSOPHY

DEPARTMENT OF PHARMACY

NATIONAL UNIVERSITY OF SINGAPORE

2006

Acknowledgements

First and foremost, I would like to express my deepest gratitude to Associate Professor Chan Sui Yung. Her help started from the first day when I came to the University and never stopped. I would like to take this opportunity to extend my sincere appreciation to Prof. Chan for her great support.

Special appreciation should also be given to the graduate committee members of our department who gave me continuous support and instruction for my Ph.D. study. I would also like to acknowledge the technical assistance given by all the laboratory officers and students in our department.

I am very grateful for the scholarship from National University of Singapore and the generous support of the National University of Singapore Academic Research Funds.

Finally, I want to make a special acknowledgement to my family for their great moral support.

Table of Contents

Summary

Gastrointestinal toxicity and myelosuppression hinder the clinical use of CPT-11-based dose-intensified regimens. Clinical studies indicated that combination with thalidomide or St. John's wort (SJW) alleviated CPT-11 induced toxicity. However, the underlying mechanisms involved are not fully understood. In this thesis, a rat model with dose-limiting toxicity profiles that are similar to those observed in patients was developed and used to study the modulations of thalidomide and SJW on CPT-11 induced toxicities. Furthermore, the underlying pharmacodynamic and pharmacokinetic components involved were explored. The study demonstrated that coadministered thalidomide or SJW significantly ameliorated the gastrointestinal and hematological toxicities of CPT-11 in rats, as indicated by alleviation of late-onset diarrhea and up-regulation of decreased leukocyte counts as well as alleviated macroscopic and microscopic intestinal damages. Combination of thalidomide or SJW brought down increased interleukins (IL-1β and IL-6), interferon-γ (IFN-γ), and tumor necrosis factor-α (TNF-α) protein levels as well as *TNF-α* mRNA levels in the intestines. In addition, both thalidomide and SJW reduced intestinal epithelial apoptosis compared to rats treated with CPT-11 alone. Furthermore, coadministered thalidomide increased the area under plasma concentration-time curve (AUC) of CPT-11 but decreased that of SN-38, while combination of SJW decreased maximum plasma concentration (C_{max}) of SN-38. The hydrolytic products of thalidomide significantly reduced the formation of SN-38 from CPT-11 in rat liver microsomes and H4-II-E cells (a rat hepatoma cell line). The ethanolic extracts of SJW significantly reduced SN-38 glucuronidation in rat liver microsomes but the ethanolic and aqueous extracts of SJW, hyperforin, and quercetin increased SN-38

glucuronidation in H4-II-E cells. Additionally, hydrolytic products of thalidomide increased the cellular accumulation of SN-38 and CPT-11 in H4-II-E cells, whereas hypericin and hyperforin inhibited the intracelluar accumulation of CPT-11 and the extracts of SJW and its major components increased the intracellular accumulation of SN-38. These results indicated that both pharmacodynamic and pharmacokinetic components play important roles in the protective effects of thalidomide and SJW against the gastrointestinal and hematological toxicities of CPT-11. Combination of CPT-11 with thalidomide will be a promising strategy to alleviate CPT-11 induced toxicities and possibly enhance its anti-tumor activity in view of the anti-neoplastic and anti-angiogenic activities of thalidomide. However, combination of SJW may compromise overall anti-tumor activity of CPT-11 by reducing the SN-38 plasma levels. Therefore, patients receiving CPT-11 treatment should refrain from SJW coadministration and specific dosing guidelines should be taken when patients have to receive such a combination. The increased understanding for CPT-11 induced toxicity and the protective effects of thalidomide and SJW may provide effective strategies to circumvent CPT-11 induced toxicities using anti-TNF-α agents through the inhibition of pro-inflammatory cytokine expression and intestinal epithelial cellular apoptosis. In addition, pharmacokinetic studies on the combination of SJW with CPT-11 indicated that caution is needed when combining chemotherapeutic agents which are substrates of cytochrome P450 and MDR1 P-glycoprotein with herbal medicines that are modulators of such enzymes and transporters, considering the pharmacokinetic profiles of the anti-cancer agents might be changed, leading to a deleterious treatment outcome.

List of Tables

List of Figures

List of Abbreviations

AE	Aqueous extracts
ANOVA	One-way analysis of variance
APC	7-ethyl-10-[4-N-(5-aminopentanoic acid)-1-piperidino] carbonyloxycamptothecin
AUC	Area under the plasma concentration-time curve
$AUC_{0-\infty}$	Areas under plasma concentration-time curve from time zero to infinity
AUC_{0-t}	Areas under plasma concentration-time curve from time zero to the last quantifiable time point
Bcl-2	B-cell leukemia/lymphoma 2
BNPP	bis (p-nitrophenyl) phosphate sodium salt
BW	Body weight
C_0	Initial drug concentration
CE	Carboxylesterase
CL	Total body clearance
C_{max}	Maximum plasma concentration
cMOAT	Canalicular multispecific organic anion transporter
COX-2	Cyclooxygenase-2
CPT	Camptothecin
CPT-11	7-ethyl-10-[4-(1-piperidino)-1-piperidino] carbonyloxycamptothecin
CYP	Cytochrome P-450
DEPC	Diethyl pyrocarbonate
DMEM	Dulbecco's modified Eagle's medium
DMSO	Dimethyl sulfoxide
DMXAA	5,6-dimethylxanthenone-4-acetic acid
EDTA	Ethylenediaminetetraacetic acid
EE	Ethanolic extracts
ELISA	Enzyme-linked immunosorbent assay
f_u	Fraction of unbound
HBSS	Hank's balanced salt solution
hCE	Human carboxylesterase
HE	Hematoxylin-eosin
HEPES	N-[2-hydroxyethyl]piperazine-N'-4-butanesulfonic acid
HPLC	High performance liquid chromatography
i.p.	Intraperitoneal
I.S.	Internal standard
i.v.	Intravenous
IFN-γ	Interferon-γ
IL	Interleukin
LC-MS	Liquid chromatography mass spectrometry
MRP	Multidrug resistance associated protein
MTT	3-(4, 5-dimethylthiazol-2-yl)-2, 5-diphenyltetrazonium bromide
NF-κB	Nuclear factor-κB
NPC	7-ethyl-10-[4-amino-1-piperidino]carbonyloxycamptothecin
PBS	Phosphate buffered saline
PGA	Phthaloyl glutamic acid
PGE_2	Prostaglandin E_2
Pgp	P-glycoprotein

rTdT	Recombinant terminal deoxynucleotidyl transferase
RT-PCR	Reverse transcription and polymerase chain reaction
SD	Standard deviation
SJW	St. John's wort (*Hypericum perforatum)*
SN-38	7-ethyl-10-hydroxycamptothecin
SN-38G	SN-38 glucuronide
$t_{1/2\alpha}$	half-life at α phase
$t_{1/2\beta}$	Terminal half-life
TH	Thalidomide
TNF	Tumor necrosis factor
Topo I	Topoisomerase I
TRAIL	TNF-related-apoptosis-inducing-ligand
TUNEL	Terminal deoxynucleotidyl transferase-mediated dUTP nick-end labeling
UDPGA	Uridine diphosphate glucuronic acid
UGT	Uridine diphosphate glucuronosyltransferase
V_d	Volume of distribution
V_{dss}	Volume of distribution at steady-state
VEGF	Vascular endothelial growth factor
β-glu	β-glucuronidase

CHAPTER 1 GENERAL INTRODUCTION

1.1   CANCER CHEMOTHERAPY

In this section, basic concepts, mechanisms of action, drug resistance, and toxicity associated with chemotherapeutic agents as well as approaches to improve anti-tumor activity for cancer chemotherapy will be discussed.

Cancer is a disease that occurs when cells in the body develop abnormally and grow in an uncontrolled way. It is now a leading killer worldwide [1]. Cumulative evidence has shown that cancer is a disease with accumulation of genetic alterations in cells [2]. To date, the major modalities for treating cancer include surgery, radiation, chemotherapy, and immunotherapy [3]. However, these therapies are only successful for certain types of cancer (e.g. leukemia) or when the cancer is detected at an early stage. Conventional chemotherapy aims to kill or disable tumor cells by inhibiting DNA synthesis in one way or another through direct or indirect mechanisms, while preserving the normal cells in the body by the use of natural or synthetic compounds [4]. Chemotherapeutic agents generally have narrow margins of safety, and are usually given at maximum tolerated doses to achieve maximal cancer cell killing effects [5]. They kill tumor cells by direct cytotoxicity, or activating host immune response, inhibiting the proliferative processes of tumor cells and/or inducing the apoptosis of tumor cells [3].

Apoptosis, also called programmed cell death, is an active energy-dependent mode of cell death, which is regulated by tightly controlled intracellular signalling events [6]. The term apoptosis was originally defined to describe certain morphological characteristics, including nuclear and cytoplasmic shrinkage and

chromatin condensation. Apoptosis was observed in many different tissues, both healthy and neoplastic, adult and embryonic [7]. Recently, it has been clearly proven that there are two apoptotic signalling pathways: intrinsic and extrinsic [8, 9]. Following severe cellular stress such as DNA damage and cell cycle defects, the intrinsic pathway is activated, which involves activation of the pro-apoptotic members of the B-cell leukemia/lymphoma 2 (Bcl-2) family and subsequent release of apoptosis-inducing factors such as cytochrome C from the mitochondria. The extrinsic pathway involves members of the tumor necrosis factor (TNF)-superfamily, such as Fas and TNF-related-apoptosis-inducing-ligand (TRAIL), and plays a role in apoptosis induced by chemotherapy and cellular immunity. Apoptosis plays important roles in the development and maintenance of homeostasis and in the maturation of nervous and immune systems. It is also a major defence mechanism of the body, removing unwanted and potentially dangerous cells such as self-reactive lymphocytes, virus-infected cells and tumor cells. In contrast to its beneficial effects, the inappropriate activation of apoptosis may contribute to a variety of pathogenic processes such as the extensive T cell death in AIDS as well as the loss of neuronal cells in Alzheimer's disease [10-12].

Although chemotherapy plays an important role in cancer treatment, it may fail due to drug resistance and dose-limiting toxicities. Tumor cells can develop acquired drug resistance due to a number of tumor-, host- and drug-associated factors. Tumor cells may have intrinsic resistance to current chemotherapeutic agents or develop resistance after exposure to the drugs. Tumor-related cellular factors include defective drug transport (e.g. reduced drug influx or increased drug efflux), altered drug activation or inactivation, enhanced repair after DNA damage, and/or deficient apoptotic response to DNA damage [13-16]. Host factors

2

include sanctuary sites for tumors, lack of bioactivation, increased inactivation, and/or dose-limiting normal organ/tissue toxicity, leading to inadequate tumor cell exposure [17-20]. Most anti-cancer drugs exhibit a greater toxicity in tissues with high growth fractions such as the bone marrow, gastrointestinal epithelium, hair follicles, and gonadal tissue. Most cytotoxic drugs [e.g. alkylating agents, topoisomerase I (Topo I) inhibitors] produce substantial hematological and gastrointestinal toxicities in many cancer patients. Such dose-limiting toxicities hinder the effective use of dose-intensified regimens in chemotherapy. Although supportive (e.g. growth factors and stem cells) and protective approaches have been widely used in combination with chemotherapeutic agents, toxicity is still a major hindrance for the success of chemotherapy. Therefore, there is a need for new approaches that decrease the toxicities of cytotoxic agents without compromising the anti-tumor activity. In addition, pharmacokinetic parameters of many anti-cancer drugs are associated with clinical treatment outcomes (e.g. response and/or toxicity). Most anti-cancer agents have wide interindividual pharmacokinetic variabilities, which affect the absorption, distribution, metabolism and excretion of anti-cancer drugs, thus resulting in unpredictable toxicity, drug resistance and various clinical responses in cancer patients.

In order to obtain better therapeutic efficacy for cancer chemotherapy, many approaches have been developed. Among which, co-administration of multiple anti-cancer agents has become a standard regimen for the treatment of nearly all carcinomas. Combination chemotherapy has several important advantages. Firstly, combination therapy usually results in a decreased incidence of resistance. Secondly, there is often a greater than additive or synergistic effect of the drugs due to complementary mechanisms of action. Finally, by using drugs with

different types of toxic effects, the overall toxicity or at least the toxicity to any one-organ system could be reduced. There are three generally accepted guidelines to choose drugs for combination chemotherapy: a) drugs that are active against the tumor when used alone should be selected for combination use; b) drugs with different mechanisms of action should be combined to obtain maximal tumor killing effect and to avoid combined resistance; and c) drugs with minimally overlapping toxicities are preferentially combined.

Aside from drug combination strategy, the development of new anti-cancer agents with improved anti-cancer activity and/or reduced toxicity represents another effective way to kill cancer cells more effectively and/or selectively. Newer and more recent chemotherapeutic agents as well as novel drug delivery systems, drug transporter inhibitors and signal transduction inhibitors have been developed based on the knowledge of cancer biology involving signal transduction, cell-cycle regulation, apoptosis, and angiogenesis [21-24]. In addition, biological response modifiers have also become an important complementary approach to cancer treatment. These are agents or approaches that modify the relationship between the host and tumor by modifying the host's biological response to tumor cells with resultant therapeutic effects. Most biological response modifiers appear to act by inhibiting angiogenesis, activating the reactivity of immunological effectors, or modulating cellular growth and/or apoptotic process [25-28]. Moreover, to decrease inter-individual pharmacokinetic differences, doses should ideally be tailored to the individual patient, which has been done by normalizing dose to body surface area, which is calculated from patient's height and weight. In addition, genotype-directed dosing and phenotype-based dosing have been applied to identify suitable doses to patients and to reduce inter-patient pharmacokinetic

variability [29-31]. In addition, population pharmacokinetic modelling has been developed to study the variability in plasma drug concentration between individuals who receive standard dosage regimens and those who represent the target patient population [32-34].

1.2 IRINOTECAN (CPT-11)

Following the general introduction of cancer chemotherapy, an introduction for CPT-11 including its anti-tumor activity, pharmacokinetic profiles, and related toxicities that limit its clinical application will be discussed.

1.2.1 Anti-tumor activity and mechanism of action of CPT-11

The camptothecins (CPTs), a relatively new group of anti-cancer compounds, are potent DNA topoisomerase I (Topo I) inhibitors [35-38]. DNA topoisomerases are a group of enzymes that alter the topology of DNA and are present in all organisms including bacteria, viruses, yeast, and mammalian including humans [39, 40]. There are two general types of topoisomerases, Type I and Type II. Type I cleaves and separates a single strand of DNA and alters the linkage quantity of DNA, whereas Type II cleaves both strands of DNA and changes the linking number of DNA by two [36, 37]. Mammalian Topo I is particularly important in supporting replication fork movement during DNA replication and relaxing supercoils formed during transcription [41], which were found to be targets for many anti-cancer drugs [42-44].

The camptothecins can induce tumor cell death due to the stabilization of Topo I-DNA complex and the generation of permanent DNA strand breaks [45]. The parental compound, CPT, is an anti-cancer alkaloid isolated from the Chinese tree,

5

Camptotheca acuminata, during a screen of plant extracts for finding anti-cancer agents [46]. The poor aqueous solubility (approximately 3.85µM in pure water [47, 48]) and unacceptable toxicity are major obstacles for the clinical use of CPT. In the past twenty years, more effort has been made to synthesize new derivatives of CPT with improved water solubility and potent anti-tumor activity. This has led to the discovery of a series of CPT analogs including CPT-11 (irinotecan, 7-ethyl-10-[4-(1-piperidino)-1-piperidino] carbonyloxycamptothecin), topotecan, lurtotecan, 9-amino-CPT, rubitecan (9-nitro-CPT, RFS2000), 10-hydroxy-CPT, silatecan (DB-67,7-tert-butyldimethylsilyl-10-hydroxy-CPT), and exatecan (DX-8951f, a hexacyclic analog of CPT) [35].

CPT-11, a water-soluble semi-synthetic derivative of CPT inhibiting DNA Topo I [49], has exhibited significant clinical anti-tumor activity with 9-43% response rate in non-small cell lung cancer, small cell lung caner, gastric cancer, malignant lymphoma, acute leukemia, cervical cancer, and pancreatic cancer [50-60]. The major indication for CPT-11 is advanced colorectal cancer when used as a first-line treatment in combination with 5-fluorouracil. CPT-11 has been approved by Food and Drug Administration of the USA for clinical use based on its 15-30% response rates in advanced colorectal cancer [61].

The cytotoxic mechanism of CPT-11 is multifaceted but is most commonly explained by the replication collision model [62]. In this model, CPT-11 interacts with cellular Topo I-DNA complexes and has an *S*-phase-specific cytotoxicity [63]. The collisions of the reversible Topo I-CPT-11-DNA cleavable complex with the advancing replication forks result in the formation of a double-strand DNA breaks, thus leading to irreversible arrest of the replication fork [64]. One or

more of these events eventually trigger other cellular responses, leading to the cell cycle arrest in the G_2 phase and to cell death.

1.2.2 Pharmacokinetics of CPT-11

In this section, the pharmacokinetics of CPT-11 were described starting with its plasma pharmacokinetic profiles followed by its metabolism, distribution, and excretion properties.

Plasma pharmacokinetics of CPT-11

The plasma pharmacokinetics of CPT-11 in humans have been addressed in many studies [65-68]. After intravenous (i.v.) infusion at 100-350 mg/m^2, maximum plasma concentrations (C_{max}) of CPT-11 are within the 1-10 mg/L range [66]. The area under the plasma concentration-time curve (AUC) of both CPT-11 and SN-38 increased proportionally to the administered dose, although marked inter-patient variability has been observed. Enterohepatic recirculation may be related to the rebound peak in the plasma concentration-time curve. Plasma concentration profiles of CPT-11 can be described using a two- or three-compartment model with a mean terminal half-life ($t_{1/2\beta}$) of 5-27 hr. Its volume of distribution at steady-state (V_{dss}) ranges from 136 to 255 L/m^2, and the total body clearance (CL) is 8-21 L/hr/m^2. Maximum concentrations of SN-38 are reached about 1 hr after the beginning of a short intravenous infusion. SN-38 plasma decay follows closely that of the parental compound with an apparent $t_{1/2\beta}$ ranging from 6 to 30 hr [32, 66, 69, 70].

Though i.v. infusion is the major way for CPT-11 treatment in clinical use, oral administration is a likely route for CPT-11 dosing to achieve a better therapeutic

outcome. Two clinical studies using oral delivery of CPT-11 have shown encouraging efficacy and toxicity profiles [71, 72]. A linear relationship was found between dose, C_{max}, and AUC for both CPT-11 and SN-38 lactone, implying no saturation in the conversion of CPT-11 to SN-38. The mean metabolic ratio ($[AUC_{SN-38} + AUC_{SN-38G}]/AUC_{CPT-11}$) was 0.7-0.8, which suggests that oral dosing results in presystemic conversion of CPT-11 to SN-38. An average of 72% of SN-38 was maintained in the lactone form during the first 24 hr after administration. The maximum-tolerated dose and recommended phase II dosage for oral CPT-11 is 66 mg/m^2/day in patients younger than 65 years of age and 50 mg/m^2/day in patients 65 or older, administered daily for 5 days every 3 weeks. The dose-limiting diarrhea was similar to that observed with i.v. administration of CPT-11. The biologic activity and favorable pharmacokinetic characteristics make oral administration of CPT-11 an attractive option for further clinical development. However, a low bioavailability (< 20%) and high variability (50%) in AUC were encountered, which may limit the oral use of CPT-11 [72].

Metabolism

The metabolism of CPT-11 is complicated and involves several drug metabolizing enzymes (Figure 1-1). CPT-11 is hydrolyzed by human carboxylesterases 1 and 2 (hCE1 and 2) [73-77] to the active metabolite SN-38 (7-ethyl-10-hydroxycamptothecin), which is 100 to 1000-fold more cytotoxic than the parental molecule [78, 79]. SN-38 is subsequently conjugated to SN-38 glucuronide (SN-38G) by uridine diphosphate glucuronosyltransferase (UGT1A1/1A9) enzymes [80].
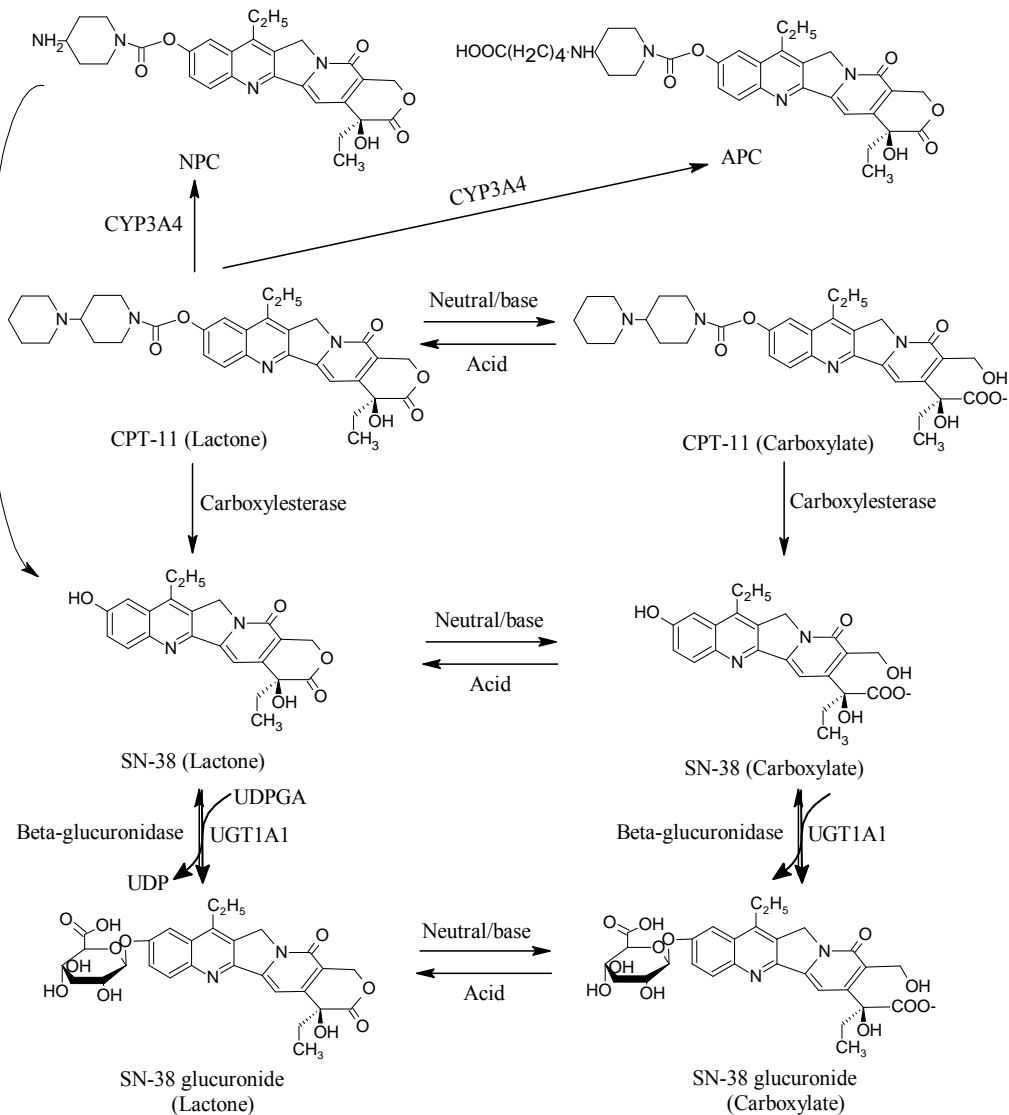
Figure 1-1. Metabolism of CPT-11 in humans. APC, 7-ethyl-10-[4-N-(5-aminopentanoic acid)-1-piperidino]-carbonyloxycamptothecin; NPC, 7-ethyl-10-[4-amino-1-piperidino]-carbonyloxycamptothecin; CYP3A4, cytochrome P450 3A4; UGT1A1, UDP-glucuronosyltransferase 1A1.

SN-38G has only weak anti-tumor activity, which can be converted to SN-38 by intestinal β-glucuronidase (β-glu) and reabsorbed into the plasma. Such enterohepatic recirculation of SN-38 may contribute to the increased exposure of the intestinal epithelium to SN-38 and the late SN-38 double peaks in the plasma [20, 81]. SN-38G and CPT-11 can also be reabsorbed into the enterohepatic circulation to a certain extent by intestinal cells [82, 83].

A second major metabolism pathway of CPT-11 is cytochrome P-450 (CYP3A4 and CYP3A5)-mediated bipiperidine side chain oxidation to form 7-ethyl-10-[4-N-(5-aminopentanoic acid)-1-piperidino)]carbonyloxycamptothecin (APC) and 7-ethyl-10-[4-amino-1-piperidino]carbonyloxycamptothecin (NPC) [84-86]. NPC, but not APC, can undergo hydrolysis to form SN-38 by human hepatic and plasma carboxylesterases *in vitro* [87, 88]. Both APC and NPC lack cytotoxicity [89]. The peak plasma concentrations and AUC values of NPC are very low after CPT-11 administration [90], suggesting that there is a rapid and virtually complete conversion of this compound to SN-38 in the systemic circulation. In addition, SN-38 is possibly oxidized by CYP3A4 [91].

Conversion of CPT-11 lactone and carboxylate forms

CPT-11, SN-38 and SN-38G are in equilibrium with their active lactone and inactive carboxylate forms. The lactone form has a closed α-hydroxy-δ-lactone ring, which can be reversibly hydrolyzed to form the open-ring hydroxyl acid (carboxylate form). The rate of hydrolysis is dependent on pH [92-94], ionic strength [93], and protein concentration [94, 95]. The lactone form has been found to be essential for the stabilization of the DNA-Topo I complex and the tumor inhibitory activity of the lactone form is significantly greater than the carboxylate form [96]. Recent studies showed that in isolated intestinal cells, CPT-11 and SN-38 lactones were both passively transported, whereas their respective carboxylate forms were actively transported [97]. There is no significant difference between the intestinal uptake rate of CPT-11 and SN-38 lactone and carboxylate. However, the respective intestinal uptake of CPT-11 and SN-38 lactone is about 10 times greater than those of the carboxylate form [98].

Plasma protein binding

CPT-11 over 0.1-4.0 mg/ml is 60-66% bound to human plasma and SN-38 is 94-96% bound over 0.05-0.2 mg/ml [99]. Albumin is the major binding protein of CPT-11 and SN-38 in human plasma. In human blood, CPT-11 is mainly bound to plasma proteins (47%) and localized in erythrocytes (33%). The binding of SN-38 to blood is high (99%) and most of SN-38 in blood is located in blood cells (approximately 66%) [99]. The lactone forms of CPT-11 and SN-38 are more stable in the presence of albumin, while the lifetimes of their carboxylate forms are insensitive to the addition of albumin [100, 101]. Binding isotherms constructed by the method of fluorescence lifetime titration showed that human albumin bound preferentially the carboxylate forms of CPT-11 and SN-38 over their lactone forms with a 150-fold higher affinity, providing an explanation for the shift to the carboxylate forms upon addition of human albumin [100].

Transport of CPT-11 across cellular membrane

Several drug transporters have been implicated in the active efflux of CPT-11 when multidrug resistance was studied. P-glycoprotein (Pgp) and the canalicular multispecific organic anion transporter [cMOAT, namely, multidrug resistance protein 2 (MRP2)] conferred resistance to CPT-11 by effluxing the drug out of the tumor cells [17] (Figure 1-2). In drug-resistant tumor cells overexpressing Pgp, the cellular accumulation of CPT-11 and SN-38 are decreased [102].

CPT-11 and SN-38 in unconjugated and conjugated forms are also actively effluxed out of cells by MRP1 [103]. Moreover, the breast cancer resistance protein can transport CPT-11 and SN-38, conferring resistance to the two

compounds [104, 105]. The high-level expression of these transporters in tumor cells has been implicated in tumor resistance to CPT-11.
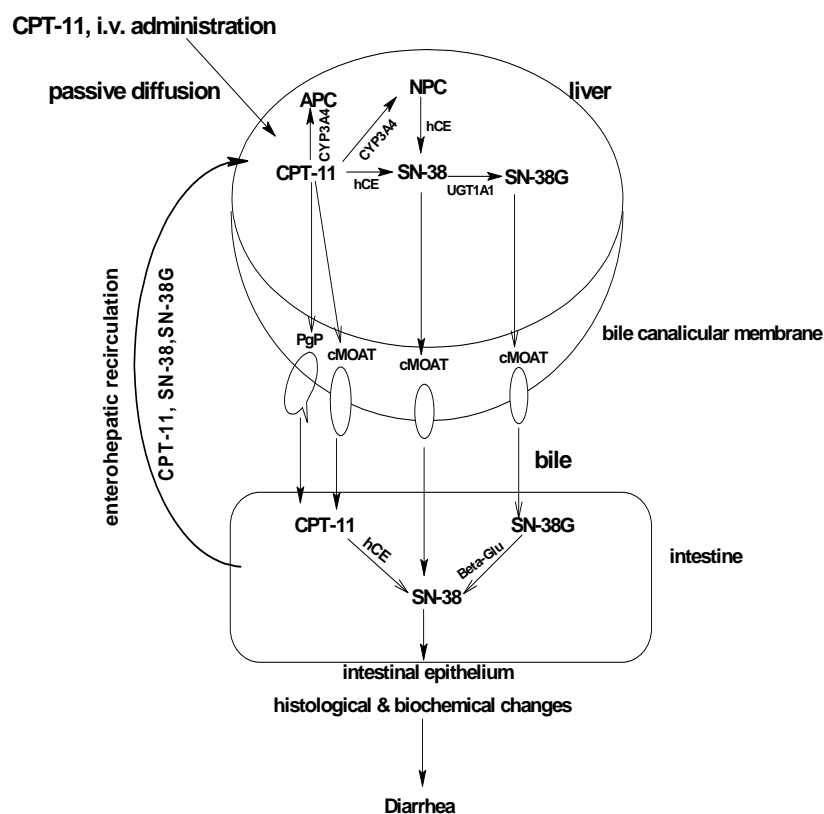
Figure 1-2. Primary active transport systems for CPT-11 and its metabolites in the bile canalicular membrane of humans. APC, 7-ethyl-10-[4-N-(5-aminopentanoic acid)-1-piperidino]-carbonyloxycamptothecin; NPC, 7-ethyl-10-[4-amino-1-piperidino]-carbonyloxycamptothecin; SN-38G, SN-38 glucuronide; CYP3A4, cytochrome P450 3A4; UGT1A1, UDP glucuronosyltransferase 1A1; β-glu, β-glucuronidase; hCE, human carboxylesterase; Pgp, P-glycoprotein; cMOAT, canalicular multispecific organic anion transporter.

The mechanisms for the intestinal and biliary transport of CPT-11 and its metabolites have not been fully defined, although Pgp and cMOAT have been suggested to play an important role [106, 107]. In rat and human bile canalicular membrane vesicles, Pgp and cMOAT have been demonstrated to mediate the efflux of CPT-11 and SN-38 [108]. The involvement of Pgp and cMOAT in the efflux of CPT-11 and SN-38 has been further demonstrated in wild-type rats and

rats defective in cMOAT *in vivo* [109, 110]. Intestinal efflux of CPT-11 by Pgp and/or cMOAT may be responsible for the low oral absorption of CPT-11.

Excretion

CPT-11 is predominantly eliminated in faeces with unchanged parental drug as the major excretion product (about 64% of the total dose) followed by smaller amounts of SN-38 and APC [111, 112] (Figure 1-3). On the average, 0.25 and 3% of the dose is excreted in the urine as SN-38 and SN-38G, respectively [20]. Similar results have been observed in rats where 34-55%, 7-9%, and 2-22% of CPT-11, SN-38 and SN-38G, respectively, were excreted into the bile over 24 hr and about 18% of the biliary radioactivity was reabsorbed from the intestine [113-115].
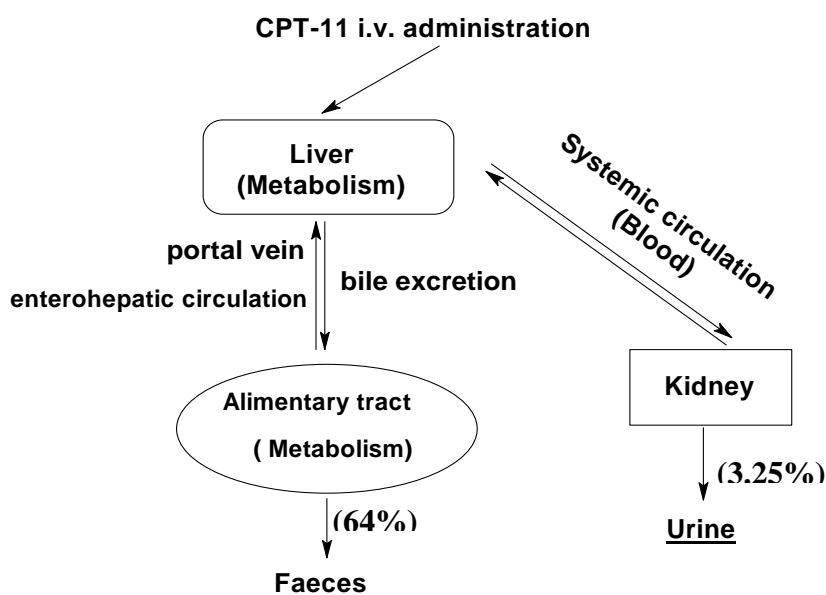
Figure 1-3. Clearance profile of CPT-11 after i.v. administration.

Both CPT-11 and SN-38 can be reabsorbed into the enterohepatic circulation from the intestine following biliary excretion. Plasma concentrations of SN-38

gradually increased to reach peak levels within 1.5-3 hr after start of the i.v. administration and slowly began to decline thereafter, and a secondary peak appeared at 7-9 hr in some patients which contributed to 10-20% increase of the AUC of SN-38 [20, 111]. SN-38 is released from SN-38G due to intestinal β-glu mediated hydrolysis and followed by intestinal uptake [111]. This deconjugation and reabsorption may contribute to the observed considerable variabilities of pharmacokinetic parameters of CPT-11 and SN-38, as well as severe late-onset diarrhea caused by the increased exposure of the intestinal epithelium to SN-38, and the late SN-38 double peaks in the plasma caused by enterohepatic recirculation [20, 81, 116]. High faecal SN-38 concentrations and its enterohepatic circulation can be of clinical significance, as a potential recycling of SN-38 reduces the effective clearance and may add a distributional compartment by way of the enteric circuit.

1.2.3 Toxicities of CPT-11

Following the introduction of anti-tumor activity and pharmacokinetic profiles of CPT-11, the toxicities caused by CPT-11 will be discussed here.

Although CPT-11 has been widely used for cancer treatment, its clinical application was circumvented by its dose-limiting toxicities, which are myelosuppression and gastrointestinal toxicity, in particular unpredictable severe diarrhea [17, 20], including early- or late-onset (< 24 hr or ≥ 24 hr after administration respectively). Early-onset diarrhea is observed immediately after CPT-11 infusion and probably due to the inhibition of acetylcholinesterase activity as it can be eliminated by atropine [117]. However, severe late-onset diarrhea of 3 (severe) or 4 (life threatening) grade, based on National Cancer

Institute Common Toxicity Criteria, occurring in up to 40% patients treated with CPT-11 after an average period of 6 days [118], complicates the clinical use of CPT-11 [119, 120].

Pharmacokinetic-toxicity relationship

The relationship between pharmacokinetic parameters and pharmacodynamic effects of CPT-11 may help to elucidate the cause of inter-patient variation in side effects and can be used to predict the incidence of late-onset diarrhea to some extent [77, 78]. Most investigations found that the AUC values for both CPT-11 and SN-38 significantly correlated with the severity of diarrhea, which were also related to the anti-cancer activity [121-123]. However, some studies showed that the correlation existed only for AUC and C_{max} of CPT-11 [124-126] or only for those of SN-38 in mice and human [121, 127]. In addition, some researchers reported a positive correlation between the AUC of SN-38G and diarrhea [29, 68]. β-glu activity, but not intestinal tissue carboxylesterase activity, had been directly correlated with the severity of CPT-11-induced diarrhea [20, 83]. This gave a mechanistic support for treatment of diarrhea by limiting intestinal glucuronidase activity. At the same time, some studies suggested that there is a correlation between diarrhea and the biliary index of SN-38, a surrogate measure of biliary excretion, which is the product of the relative area ratio of SN-38 to SN-38G and the total CPT-11 AUC, calculated as $AUC_{CPT-11} \times (AUC_{SN-38}/AUC_{SN-38G})$ [20, 68, 128], suggesting that diarrhea is a function of the intraluminal exposure to SN-38 [68, 129]. On the other hand, some trials found that this relationship only exists for AUC of CPT-11 and SN-38G, but not for SN-38 or biliary excretion [65] and some studies failed to find any relationship between diarrhea and any

15

pharmacokinetic parameters [130-132]. All these findings reflect the complexity of pharmacokinetic-pharmacodynamic relationship for anti-cancer agents such as CPT-11.

Biochemical mechanisms for CPT-11 induced diarrhea

Many studies have been carried out to explore the underlying biochemical mechanisms for CPT-11 induced toxicities. It is found that the early-onset toxicity is related to the adverse cholinergic effects of CPT-11, which acts as a specific acetylcholinesterase blocker or an acetylcholine receptor (including muscarinic and nicotinic receptors) agonist [133]. The piperidino side chain of CPT-11 is similar to dimethylphenylpiperazinium [134], which is a highly selective and potent stimulator of nicotinic receptors in the autonomic ganglion. Such cholinergic activity of CPT-11 intensifies intestinal contractility and leads to the disturbance in internal mucosal absorptive and secretory functions [133, 135].

However, the biochemical mechanism for CPT-11-induced late-onset diarrhea is not fully identified, but several potential mechanisms have been suggested. One potential mechanism of late-onset diarrhea caused by CPT-11 is direct histological damage of SN-38 on the intestinal mucosa [136]. Intestinal bacterial microflora and human intestinal CE in the small intestine are involved in the etiopathogenesis of this effect [137-139]. Accumulation of SN-38 can cause direct damage to the intestinal mucosa by interfering with DNA Topo I. CPT-11 also increased cyclooxygenase-2 (COX-2) expression associated with an increase in prostaglandin E_2 (PGE_2) [140], which is secreted by the mucosa and smooth muscle of the small intestine. PGE_2 is able to stimulate colonic secretion and hyperperistalsis of the gut, inhibit Na^+,K^+-ATPase which affects the absorption of

electrolytes [141], trigger Cl^- secretion and water loss [142]. Additionally, administration of CPT-11 stimulated the production of thromboxane A_2, which has been shown to be a potent physiological stimulant of water and Cl^- secretion in the colon [143, 144]. Thus, it appears that the late-onset diarrhea is in part a consequence of thromboxane A_2 and PGE_2 induction secondary to colonic mucosal damage after CPT-11 treatment [145]. In addition, CPT-11 may induce secretion of cytokines such as tumor necrosis factor-α (TNF-α) in mouse and human mononuclear cells. TNF-α exerts cytotoxic effects on a wide range of tumor cells and is also a key pro-inflammatory cytokine and a primary mediator of immune regulation [146]. Induction of TNF-α has been associated with diarrhea induced by chemotherapy [147, 148].

Agents capable of inhibiting CPT-11 induced diarrhea

Based on the knowledge of pharmacokinetic-toxicity relationship for CPT-11 and the possible underlying biochemical mechanisms related to CPT-11 induced toxicity, many approaches have been explored to overcome the CPT-11 induced diarrhea. Early treatment of severe late-onset diarrhea with high-dose loperamide has decreased patient morbidity [136]. Extensive studies have been conducted to identify other possible preventive approaches to ameliorate diarrhea. These included intestinal alkalization [149], oral antibiotics (e.g. neomycin) [150], enzyme inducers (e.g. phenobarbital), Pgp inhibitors (e.g. cyclosporine) [109], COX-2 inhibitors (e.g. celecoxib) [145], and blockade of biliary SN-38 secretion (e.g. probenecid and valproic acid) [151] (Table 1-1).

Table 1-1. Experimental therapies and possible modes of action for CPT-11 induced diarrhea.

Diarrhea Type	Experimental Therapy	Possible Modes of Action	References
Early-onset	• Atropine • Scopolamine • Aminoglycoside antibiotics (e.g. streptomycin)	• Anti-cholinergic and anti-muscarinic effects	[152-154]
Late-onset	• Morphine analogue (loperamide) • Loperamide + acetorphan	• Opiate agonism • Block of calcium channels • Block of the calmodulin system in the colonic epithelium • Acetorphan is a potent enkephalinase inhibitor and antisecretory agent without significant effect on intestinal transit time • Inhibition of biliary excretion of CPT-11	[155, 156]
	• CYPs inducers: Phenytoin, carbamazepine, & phenobarbital • UGT1A1 inducers: Phenobarbital & dexamethasone • β-Glucuronidase inhibitors: D-saccharic acid 1.4-lactone, Kampo medication Hange-shashin-to (TJ-14) & baicalin • Inhibitors of the human intestinal CE: Sulfonamide derivatives • Inhibitors of β-glucuronidase production: Penicillin, streptomycin, neomycin & bacitracin	• All agents of this type are capable of interfering with the metabolism of CPT-11 and SN-38, to reduce the intestinal level of toxic SN-38 and increased formation of APC and inactive SN-38G	[151, 157-162]
	• Transport inhibitors: Cyclosporine A & probenecid • Agents that reduce intestinal drug uptake: Sodium bicarbonate, magnesium oxide, base water & ursodeoxycolic acid	• Inhibition of biliary excretion of CPT-11 and SN-38 • Inhibition of intestinal uptake of CPT-11 and SN-38	
	• Anti-inflammatory cytokines: IL-2 & IL-15 • Cytokine inducers: JBT-3002 • TNF-α inhibitor: Thalidomide • Corticosteroid: Budesonide • COX2 inhibitor: Celecoxib	• Reduction of inflammatory cytokines • Increase of anti-inflammatory cytokines • Inhibition of COX2 activity • Inhibition of PGs	[118, 163-170]
	• Cytoprotectant: Amifostine • Proliferative agents: Glutamine • Octreotide	• Protection of intestinal epithelium • Restoring intestinal epithelium • A long-acting somatostatin analogue • Reduces the secretion of some pancreatic and intestinal hormones • Prolongs intestinal transit time • Increases intestinal absorption of fluids and electrolytes	[171, 172]
	• Adsorbents: activated charcoal & oral carbonaceous adsorbent (Kremezin)	• Adsorbtion of SN-38 & CPT-11 in intestine	[173, 174]
	• Miscellaneous agents - Intestinal growth factors: transforming growth factor-β and keratinocyte growth factor, stem-cell factor & glucagons-like peptide 2 - Fish oil supplements - Valproic acid & ceftriaxone - Sucralfate & nifuroxazide - Activated charcoal	• Promoting epithelial growth • Protection of intestinal epithelium • Anti-diarrhea effect	[175, 176]

Interestingly, a pilot clinical study in colorectal cancer patients indicated that co-administered thalidomide almost eliminated CPT-11 induced gastrointestinal toxicities including nausea and diarrhea. In addition, a pilot study in 5 cancer patients found that oral treatment of St. John's wort (SJW) at 900 mg/day for 18 days alleviated irinotecan-induced toxicity [177]. However, the mechanisms for these protective effects are not very clear yet. In the present study, the protective effects of its combination with thalidomide or SJW on CPT-11 induced toxicities using a rat model would be investigated and the underlying pharmacodynamic and pharmacokinetic components involved using this rat model and *in vitro* models would be explored, which may provide a new treatment approach for chemotherapy-associated histological damages based on these mechanistic findings.

1.3 THALIDOMIDE

A brief introduction on the clinical activity, pharmacokinetic profile, and toxicity of thalidomide will be given in this section.

Thalidomide (α-phthalimidoglutarimide) was first developed and introduced as a sedative to relieve nausea during pregnancy in the 1950s, but withdrawn from the market in 1961 due to its infamous teratogenicity [178]. It is a derivative of glutamic acid, containing two amide rings and a single chiral center. The interconversion between the enantiomers of thalidomide is very rapid at physiological pH in aqueous medium and biological matrices such as plasma, undergoing rapid spontaneous hydrolysis [179].

1.3.1 Clinical activity and mechanism of action of thalidomide

19

Clinical activity of thalidomide

Potential activity has been observed in clinical trials for various hematological and solid tumor cancers including relapsed and/or refractory multiple myeloma [180], myelodysplastic syndrome [181], mantle cell lymphoma [182], glioma [183], renal cell carcinoma [184, 185], metastatic melanoma [185], pancreatic cancer and androgen-independent prostate cancer [186, 187]. Thalidomide was administered to patients with myeloma based upon the observations that bone marrow angiogenesis was prominent in active myeloma [187, 188]. More than 50,000 patients with multiple myeloma have been treated with thalidomide to date [188-190]. Research with thalidomide provides clear and convincing evidence that thalidomide monotherapy is efficacious in relapsed and refractory multiple myeloma. Results typically show a consistent ~30% response rate [191]. Thalidomide has an apparent synergistic activity when used in combination with dexamethasone in newly diagnosed and relapsed and/or refractory multiple myeloma, and could even reduce the median response time when compared with thalidomide alone [191]. In addition, thalidomide has been used to treat complex regional pain syndrome related to multiple myeloma [192].

In recent years, there is an increased use of oral thalidomide for the management of a variety of autoimmune diseases including erythema nodusum leprosum, graft-versus-host disease [193, 194], microsporidiosis [195], and Crohn's disease [196]. Thalidomide has also shown activity in various dermatological conditions such as erythema nodosum leprosum, prurigo nodularis, aphthous ulcers, and actinic prurigo [197]. In addition, as an anti-angiogenic agent, thalidomide has been

clinically used for combination therapy with cancer chemotherapeutical agents to obtain additive or synergistic anti-tumor effects [198-201].

Mechanisms of actions

The mechanisms of the actions of thalidomide have been studied. It is possible that angiogenesis inhibition, direct cytotoxic effects on tumor cells, increasing tumor cell susceptibility to apoptotic triggers, immunomodulation, cytokine modulation and attenuation of metastatic potential of tumor cells by reducing TNF-α-induced upregulation of adhesion molecules on endothelial cells individually or in combination, are all implicated [202]. Its very wide range of activities may be explained to a great extent by its effects on nuclear factor-κB (NF-κB) activity through suppression of IkappaB kinase activity. NF-κB is involved in the transcriptional regulation of many genes including cytokines [e.g. TNF-α, interleukins (IL-6 and IL-12)], proteins involved in apoptosis [e.g. cellular inhibitor of apoptosis protein 2, Fas-associated death domain protein, Bcl-2 family members], and angiogenic factors [e.g. vascular endothelial growth factor (VEGF), TNF-α, and IL-8]. Therefore, NF-κB plays a central role in the regulation of pivotal processes including proliferation, tumor growth, apoptosis, and immune responses. Since thalidomide is able to suppress NF-κB activity [203], this drug has an impact on all of these processes.

In preclinical models, growth inhibition of tumor cells by thalidomide has been reported against several tumor types. These effects of thalidomide are probably mainly due to an enhanced susceptibility to apoptosis. Thalidomide affects both pathways of apoptosis: the intrinsic pathway by reducing levels of the anti-apoptotic members of the Bcl-2 family [204] and the extrinsic pathway by down-

regulating proteins conferring resistance against Fas- or TRAIL-mediated apoptosis [200]. Another mechanism leading to growth inhibition is reduction of growth stimulating factors.

Thalidomide also inhibits the production of TNF-α by monocytes, as well as T cells [205]. In addition, thalidomide enhances the production of IL-2, which itself may possess anti-tumor activities or may modulate the immune system [206]. Its effects on interferon-γ (IFN-γ) production are stimulatory or inhibitory but more reports have shown it to increase IFN-γ production than to inhibit it [207]. Thalidomide also inhibits IL-6, IL-10 and IL-12 production [208], and enhances IL-4 and IL-5 production [200]. IL-6 is a potent growth factor for malignant plasma cells, and its inhibition may be partly responsible for the action of thalidomide in myeloma [209]. In addition to increasing total lymphocyte counts as well as CD4$^+$ and CD8$^+$ T cells, thalidomide is a potent co-stimulator of T lymphocytes. Thalidomide also augments natural killer cell cytotoxicity in myeloma.

Additionally, thalidomide has been shown to inhibit angiogenesis [210] by which thalidomide exerts its anti-tumor activity. Thalidomide inhibits the angiogenesis-stimulating property of angiogenic factors [211, 212]. In addition, it reduces the levels of angiogenesis promoting factors, such as TNF-α, VEGF, and IL-6 [212]. Furthermore, thalidomide inhibits lipopolysaccharide-mediated induction of COX-2 biosynthesis in murine macrophages [213], providing insights into the anti-neoplastic properties of thalidomide. Angiogenesis, the formation of new blood vessels, is fundamental to wound repair, reproduction, and development. It is also a critical process for the growth, development, and metastasis of solid tumors

[214]. The growth of tumor beyond a size of 1 to 2 mm^3 requires the assembly of a vascular network, so that tumor that is unable to elicit angiogenesis will exist in a dormant state. The pioneering work by Folkman et al. [215] has defined angiogenesis as an appealing target for the development of anti-neoplastic drugs. Anti-angiogenic therapy is recently becoming a research focus of cancer pharmacology and dozens of angiogenic inhibitors including antibody against VEGF (Avastin), small molecule VEGF receptor, and tyrosine kinase inhibitor are undergoing clinical evaluations [216-219]. Therefore, anti-angiogenic therapy is becoming the fifth therapeutic modality in addition to surgery, chemotherapy, radiotherapy, and immunotherapy. A strategy combining continuous low-dose chemotherapy with anti-angiogenic inhibitors has been developed recently [220]. These studies have pointed out that this combination suppressed the growth of experimental tumors more effectively than conventional therapy alone and also circumvent drug resistance to a certain extent. The attractiveness of anti-angiogenic therapy in cancer treatment is its generally low toxicity, broad efficacy, and that the target, the neovasculature endothelial cell, is genetically stable and unlikely to develop acquired resistance.

1.3.2 Pharmacokinetics of thalidomide

Following the introduction for thalidomide clinical activity and mechanisms, pharmacokinetic profiles and toxicities for thalidomide will be described here.

Oral absorption of thalidomide (typically 200 mg, as the US FDA-approved capsule formulation) is slow and extensive, with time to C_{max} of 4-10 μM at 2-4 hr, apparent $t_{1/2\beta}$ of 6 hr, apparent CL of 10 L/hr and an estimated bioavailability of 80-100% [221-225]. With larger doses ($\geq$ 200 mg), its absorption rate decreases

23

considerably, and thus a variable and lower bioavailability is expected. This has been partly ascribed to the poor solubility of thalidomide in intestinal fluids that resulted in thalidomide's rate-limited pharmacokinetics (the 'flip-flop' phenomenon), with its elimination rate being faster than its absorption rate. Thalidomide is spontaneously hydrolysed into numerous products, whereas CYP2C-catalyzed metabolism plays a minor role in its elimination *in vivo* [226]. Protein bindings for the *(R)*- and *(S)*-enantiomers in plasma are 55% and 65%, respectively. More than 90% of the absorbed drug is excreted in urine and faeces within 48 hr. Pharmacokinetic parameters for oral dose of racemic thalidomide and its separate enantiomers have been determined in healthy volunteers and patients [227].

A one-compartment model with first-order absorption and elimination best describes thalidomide pharmacokinetics. Multiple doses of thalidomide at 200 mg/day over 21 days caused no change in the pharmacokinetics, with a steady-state C_{max} of 1.2 mg/L. Multiple-dose thalidomide treatment studies in cancer patients show pharmacokinetics comparable with those in healthy populations at similar dosages. Thalidomide exhibits a dose-proportional increase in AUC at doses from 50 to 400 mg [228]. Furthermore, some stereo-selective pharmacokinetic and pharmacodynamic profiles exist for thalidomide. The (*S*)-isomer has been associated with the teratogenicity of thalidomide [224]. Due to the variable absorption caused by oral dose or disease states where patients experience nausea, oral pain or other swallowing problems, an i.v. formulation of thalidomide would be of clinical interest, but this is hindered by its poor solubility and rapid degradation in aqueous media [224].

1.3.3 Toxicities of thalidomide

The most common adverse events were somnolence, asthenia, rash, peripheral oedema, paresthesia, dizziness, constipation, dyspnoea, and leucopenia [229]. The most frequently observed adverse effects are related to the sedative action which appear to be dose-related [230]. Drowsiness, dizziness, and mood changes were observed in 33-100% patients. Loss of libido, nausea, pruritus, hypothyroidism, serious dermatological reactions including Steven-Johnson syndrome and menstruation abnormalities have been occasionally observed [231]. In addition, thalidomide can cause toxic peripheral neuropathy, which can sometimes be irreversible [231]. Changes in nerve conductivity are frequent and unpredictable adverse effects of thalidomide. Known or possible teratogenicity is of course an absolute contraindication to the use of thalidomide. A single dose of thalidomide may be sufficient for inducing malformation [232].

1.4 ST. JOHN'S WORT

Following the general introduction on thalidomide, the pharmacodynamic, pharmacokinetic and toxicological properties of St. John's wort will be described. St. John's wort (*Hypericum perforatum*, SJW) is one of the most commonly used herbal medicines for the treatment of mild to moderate depression [233]. SJW contains over two dozen constituents, among which hyperforin and hypericin are the major active components (Figure 1-4).

1.4.1 Pharmacodynamics of SJW

Alcoholic extracts of SJW are mainly used for the treatment of mild to moderate depression as an alternative to classic anti-depressant, with a favorable side-effect

profile [233]. However, current evidence regarding the anti-depressive effects of hypericum extracts is inconsistent and confusing. In patients who met criteria for major depression, several recent placebo-controlled trials suggest that the tested hypericum extracts have minimal beneficial effects while other trials suggest that hypericum and standard anti-depressants have similar beneficial effects [234]. The anti-depressant effect of SJW extract is unlikely due to an interaction of hypericin with central neurotransmitter receptors. The main *in vitro* effects of hyperforin (at concentrations of 0.1-1 μM) are non-specific presynaptic effects, resulting in the nonselective inhibition of the uptake of many neurotransmitters, and the interaction with dopamine D1 and opioid receptors.

However, it is still unclear whether these mechanisms can be applied *in vivo*, since after administration of SJW extract, brain concentrations of hyperforin are well below those active *in vitro*. In the rat, SJW extract might indirectly activate sigma receptors *in vivo* (through the formation of an unknown metabolite or production of an endogenous ligand), suggesting a new target for its anti-depressant effects [235, 236]. In addition, SJW has been reported to have anti-inflammatory effects. There are some reports attributing the anti-inflammatory effects of SJW or its ingredients to the inhibition of nuclear factor-κB (NF-κB) activation [237, 238], inhibition of protein kinase C [239], and reduction of the lipopolysaccharide-, cytokine- or substance P-induced expression of COX-2, inducible nitric-oxide synthase or IL-6 [240, 241].

SJW and its components (in particular hyperforin and hypericin) have demonstrated *in vitro* cytotoxicity and apoptosis-inducing effect by triggering activation of caspases in several tumor cell lines (e.g. HT-1080, C-26, K562, and

SK-N-BE) [242]. Hyperforin is also shown to inhibit matrix metalloproteinases, extracellular signal-regulated kinase 1/2, and leukocyte elastase [242]. The cytotoxicity of SJW has been shown to be partially related to the inhibition of protein kinase C [243] and formation of oxygen radicals [244]. SJW inhibited the growth and metastasis of human prostatic carcinoma orthotopically implanted in nude mice [245]. In a metastatic mouse model using C-26 or B16-LU8 tumor cells, daily intraperitoneal (i.p.) administration of hyperforin remarkably decreased the size of metastases with C-26 (38%) and the number of lung metastases with B16-LU8 (22%), with preservation of apparently healthy and active behaviour. Moreover, several studies showed that hypericin is a potent photosensitizer with powerful *in vivo* and *in vitro* anti-neoplastic and apoptosis-inducing activity upon photoactivation with either visible or UV light [246]. These findings indicate that both hyperforin and hypericin are potent inducers of tumor cell apoptosis by targeting multiple signalling molecules. This may provide a rationale for the combined use of SJW or its components with other chemotherapeutic agents for increasing efficacy.

1.4.2 Pharmacokinetic interactions of drugs with SJW

However, possible pharmacokinetic interactions should be taken into account when SJW was combined with other chemotherapeutic agents. Extensive preclinical and clinical studies have been reported on the inducing effects of SJW (mainly via hyperforin) on CYP2B6/CYP3A4 and Pgp [247]. Hyperforin, but not hypericum extracts, resulted in a significant induction of CYP3A4 expression after treatment of primary human hepatocytes. SJW extracts and its major components have been reported to inhibit the activities of recombinant CYP1A2,

2C9, 2C19, 2D6, and 3A4 [248]. Direct evidence for induction of Pgp by SJW *in vivo* is provided by the finding that long-term pretreatment increased Pgp expression in the rat intestine [249, 250] and also human peripheral blood lymphocytes [251].

I3,II8-biapigenin

Chlorogenic acid

Hyperforin

Hypericin

Quercetin
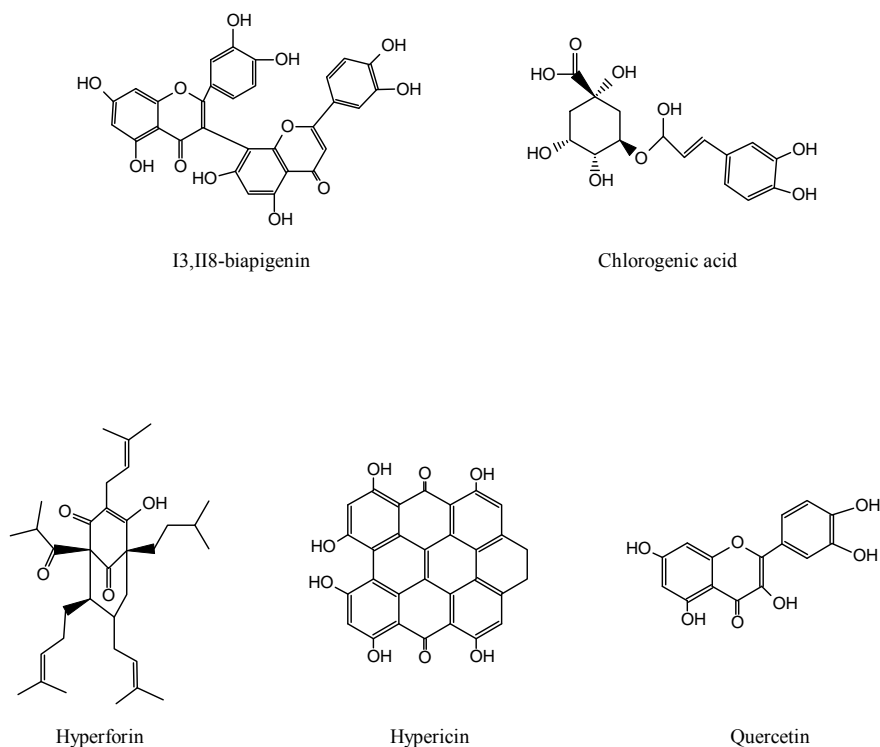
Figure 1-4. Chemical structures of the major constituents of St. John's wort.

More importantly, a number of pharmacokinetic and/or pharmacodynamic interactions of SJW with other clinically important drugs (e.g. cyclosporine, amitriptyline, digoxin, and methadone) have been reported [251]. The induction of hepatic and intestinal CYP3A4 and/or Pgp may partly explain most of these interactions, because CYP3A4 is involved in the metabolism of more than 50% of current therapeutic drugs and Pgp mediates the intestinal and hepatic transport of many drugs. However, the clinical importance of drug interaction with SJW

depends on a number of factors that are associated with coadministered drugs, herbs and patients. In most cases, the extent of drug interactions with SJW varies markedly among individuals, depending on inter-individual differences in drug metabolizing enzymes and transporters, existing medical conditions, age and other factors.

1.4.3 Side effects of SJW

In addition, observational studies with preparations of SJW have recorded adverse events among those treated of between 1 and 3% [252]. The most common adverse events are reactions of the skin exposed to light. Investigations in volunteers have shown that the threshold dose for an increased risk of photosensitization is about 2-4 g/day of a usual commercial extract (equivalent to approximately 5-10 mg of the hypericin). Recently, it has been reported that hypericum preparations must not be taken at the same time as other anti-depressants. If co-medication with coumarin-type anti-coagulants is unavoidable, it must only be undertaken provided the physician closely monitors clotting parameters. Concomitant administrations with cyclosporine and indinavir, and for the time being, other protease inhibitors used in anti-HIV treatment, are absolutely contraindicated [251].

1.5 OBJECTIVES OF THE THESIS

As mentioned above, histological damage is a common dose-limiting toxicity associated with cancer chemotherapy, especially in the treatment of colorectal cancer by use of irinotecan (CPT-11), 5-fluouracil and oxaliplatin [253, 254]. The occurrence of severe, uncontrollable diarrhea has limited the further evaluation of

more aggressive anti-tumor regimens using CPT-11. Despite great interest in diarrhea induced by CPT-11 and a large amount of effort put into its investigation, effective strategies are still needed to circumvent such toxicity, thus allowing safer delivery of this potential agent in the clinical setting.

A good response rate and acceptable tolerability regarding gastrointestinal effects were demonstrated in a pilot study of the irinotecan/thalidomide combination in patients with metastatic colorectal cancer [165, 255, 256]. Although the modulation of CPT-11 plasma pharmacokinetic profiles and the beneficial biological response modifying effects of thalidomide have been implicated, the underlying mechanisms involved are not fully understood. In addition, a clinical pilot study in 5 patients indicated that combination of SJW with CPT-11 significantly alleviated CPT-11 induced neutropenia, accompanied with decreased plasma levels of SN-38, which might be attributed to the induction effect of SJW on CYP3A4 expression [177]. Based on this finding, the authors advised that patients administered with CPT-11 should refrain from taking SJW as the combination may have a deleterious impact on treatment outcome. However, the underlying mechanisms for the modifying effects of SJW on both pharmacokinetics and toxicity of CPT-11 have not been fully examined.

In the present study, a rat model with dose-limiting toxicity profiles that are similar to those observed in patients treated with CPT-11 was developed and used to study the modulations of CPT-11 induced gastrointestinal and hematological toxicities by the combinations of thalidomide and SJW. The rat was chosen to be used in this study as: a) the metabolic pathways of CPT-11 in rats and humans are qualitatively similar, despite the presence of species differences in the

contribution of enzymes for individual pathways including variation in the kinetics of hydrolysis of CPT-11 between humans and rats; b) the transport and elimination routes of CPT-11 in rats and humans are also similar; c) the rat is sensitive to CPT-11 and it has been previously used in CPT-11 toxicity studies; and d) rats facilitate pharmacokinetic studies by allowing repeated blood sampling and have been widely used for CPT-11 pharmacokinetic studies [257]. Therefore, the underlying pharmacodynamic and pharmacokinetic components involved in the protective actions of thalidomide and SJW were explored using this rat model and various *in vitro* models. Furthermore, the similarities and differences in terms of the protective abilities against CPT-11 induced toxicity by thalidomide and SJW as well as the underlying mechanisms involved were evaluated.

Based on these findings, these two combination therapies can be further evaluated. Moreover, these mechanistic examinations for CPT-11 induced histological damages and the protective effects of thalidomide and SJW may provide some insights for identifying new effective strategies to circumvent CPT-11 induced toxicities. The achievements in abolition of CPT-11-induced complication may reduce mortality caused by severe diarrhea and inflammation, as well as avoid overall reduction in effectiveness of therapy caused by interruptions or dose reductions during treatment [224, 258-262]. In addition, the kinetic study of the combination of SJW with CPT-11 using *in vitro* models may provide some insights into the pharmacokinetic interactions of chemotherapeutic agents with herbal medicines that have modulation effects on cytochrome P450 and/or drug transporting proteins.

CHAPTER 2 THALIDOMIDE REDUCED THE DOSE-LIMITING TOXICITIES OF CPT-11 IN THE RAT

2.1 INTRODUCTION

Irinotecan (CPT-11), a potent DNA topoisomerase I inhibitor, has been widely used for the treatment of advanced colorectal cancer as a first-line therapy in combination with 5-fluororacil [263]. However, its gastrointestinal and hematological toxicities have become unpredictably severe in certain patients, thus compromising the success of CPT-11-based chemotherapy.

Thalidomide has been used alone and more often in combination with other anti-cancer agents for treatment of a variety of tumors and substantial responses have been observed in patients with multiple myeloma [258]. Murine studies have demonstrated that thalidomide is able to potentiate the activity of a number of anti-cancer agents including melphalan, celecoxib, angiostatin, fludarabine, dacarbazine, paclitaxel, sulindac, cyclophosphamide [264-267]. More importantly, a variety of clinical studies found that combined use of thalidomide with carboplatin [218], cyclophosphamide [268], paclitaxel [185, 269], epirubicin [270], temozolomide [271], carmustine [183], dexamethasone [272], IL-2 [273], or IFN-α2b [274] resulted in improved clinical response and reduced resistance coupled with reduced or unchanged toxicity in cancer patients.

A good response rate and acceptable tolerability regarding gastrointestinal effects were demonstrated in a pilot study of the irinotecan/thalidomide combination in patients with metastatic colorectal cancer [146, 165, 255, 256, 275]. However, the mechanisms underlying this striking protective effect are not very clearly elucidated

yet, although the beneficial biological response modifying effects of thalidomide have been implicated.

In addition, studies have shown that CPT-11 induced secretion of TNF-α in murine and human mononuclear cells [276]. TNF-α is a key pro-inflammatory cytokine and a primary mediator of immune regulation [277]. There exists a close interaction between epithelial cellular apoptosis and pro-inflammatory cytokines expression in intestines. TNF-α has been shown to play an essential role in regulating intestinal epithelial cell apoptosis and/or survival during chronic inflammation [278]. TNF-α also plays a critical role in initiation of chemotherapy-induced primary mucosal damage responses including early damage to connective tissue and endothelium, reduction of epithelial oxygenation, and ultimately, epithelial basal-cell death and injury. Therefore, TNF-α may also play an important role in the intestinal inflammation and damage induced by CPT-11. Thus, down-regulatory effect on TNF-α expression by thalidomide may provide another rationale for the combination with thalidomide to reduce toxicity of CPT-11 in our study. Furthermore, as a potential anti-angiogenic agent, thalidomide may exert its anti-tumor activity when combined with CPT-11.

In the present study, based on the pilot clinical report and the hypothesis that using anti-TNF-α agents may alleviate CPT-11-induced complication, a rat model was developed to investigate whether combination of thalidomide could attenuate gastrointestinal and hematological toxicities caused by CPT-11. In addition, the potential pharmacodynamic mechanisms involved for this interaction were explored by examining the cytokine expressions and epithelial cellular apoptosis using this model. The increasing understanding of the molecular events that lead to

33

chemotherapy-induced intestinal mucosal injury and the protective effect of thalidomide may allow us to identify new approaches to arrest chemotherapy-induced intestinal damages, which may then reduce mortality caused by severe diarrhea and inflammation and avoid overall reduction in effectiveness of therapy caused by interruptions or dose reductions during treatment.

2.2   MATERIALS AND METHODS

2.2.1   Chemicals

CPT-11 lactone form (diethyl-4,11 hydroxy-4 (piperidino-4 piperidino-carbonyloxy)-9 1H-pyrano (3', 4', 6, 7) indolizino (1, 2-b) quinolein-(4H, 12H) dione-3, 14 hydrochloride trihydrate, Irinotecan, > 99% purity as determined by high performance liquid chromatography (HPLC), molecular weight = 677.20) was purchased from SinoChem Ningbo Import and Export Co. (Ningbo, China). CPT-11 was protected from light exposure to avoid degradation. An injectable formulation of CPT-11 was prepared by dissolving CPT-11 (20 mg/ml), D-sorbitol (45 mg/ml) and D-lactic acid (0.9 mg/ml) in Milli-Q water heated to 70-90ºC for 5-10 min. The pH of this clear solution was adjusted to 3.5 by 1 M NaOH. The resulting solution was sterile-filtered (0.22 μm, Millipore, MA, USA) and stored at 4ºC under dark condition until use [135]. Thalidomide was provided by Celgene Co. (MA, USA). D-sorbitol, D-lactic acid, protease inhibitor cocktail, diethyl pyrocarbonate (DEPC), formaldehyde and Bradford reagent were all purchased from Sigma Chemical Co. (St. Louis, Mo, USA). Trizol and RNase away reagent were purchased from Invitrogen (Carlsbad, CA, USA). The water used was of Milli-Q grade purified by a Milli-Q UV Purification System

(Millipore, Bedford, MA, USA). All other chemicals were of analytical grade or HPLC grade obtained from commercial sources.

2.2.2 Animals

Healthy male Sprague Dawley rats (200-220 g, purchased from the Laboratory Animals Centre, National University of Singapore, Singapore) were used in the study after 2-4 days' acclimatization with free access to water and regular diet. All animal procedures were approved by the Institutional Animal Care and Use Committee (IACUC) of the National University of Singapore. Rats were kept in a room under controlled temperature (23-24ºC) with a 12-hr light-dark cycle and housed in wire-bottom cages with paper lining beneath.

2.2.3 Drug administration schedules

To set up a CPT-11 induced toxicity model (including myelosuppression and gastrointestinal damages) in male Sprague Dawley rats, we adopted the dosing schedule [60 mg/kg i.v. once daily for four consecutive days (days 1-4)] reported previously by the Kurita and the Takasuna groups [125] . Using this CPT-11's regimen, the diarrhea throughout days 5-8 was similar to human diarrhea in terms of being resistant to conventional anti-diarrhea agent, which was considered to be late-onset diarrhea, which prevented the adoption of CPT-11 in aggressive chemotherapy [125, 145]. Rats were randomly divided into three groups. One group was treated with CPT-11 at a dose of 60 mg/kg/day by i.v. injection (3 ml/kg/day) for four consecutive days (days 1-4). DMSO (1%, v/v) without thalidomide was also given at 1 ml/kg/day by i.p. injection to this group of rats for eight consecutive days (starting one day before the first CPT-11 injection) as control vehicle. Treatment group of rats was administered with CPT-11 at 60

mg/kg/day by i.v. for four consecutive days in combination with thalidomide in 1% DMSO (v/v) (100 mg/kg/day by i.p. for eight consecutive days, starting one day before the first CPT-11 injection). A dose of 100 mg/kg for thalidomide was used as this level of dose is reported to elicit significant biological response in extensive previous studies [267, 279-281]. In addition, another group of rats without any drug treatment was also included as blank. Each group consisted of 4 -7 rats.

2.2.4 Monitoring of CPT-11 induced diarrhea

The severity of diarrhea and changes in body weight were monitored twice a day throughout the study (for a total of 12 days from the first administration of thalidomide). In Sprague Dawley male rats, diarrhea observed after the final administration (beginning from day 5) was considered to be late-onset diarrhea. The severity of diarrhea was scored according to the following standard as described previously [282, 283]:

- 0: normal, normal stool or absent;

- 1: slight, slightly wet and soft stool;

- 2: moderate, wet and unformed stool with moderate perianal staining of the coat;

- 3: severe, watery stool with severe perianal staining of the coat.

2.2.5 Counting of blood cells

Rat blood (about 300 μl) was collected using a K_2-ethylenediaminetetraacetic acid (EDTA) treated tube (Microtainer®, Becton Dickison and Company, Franklin Lakes, NJ, USA) before drug administration (day 0) and on days 5, 7, 9, and 11.

Leucocytes including lymphocyte and neutrophil were counted with a XE-2100 Hematology Analyzer (Sysmex, Illinois, USA).

2.2.6　Evaluation of intestinal damages

Total 12 groups of rats (n = 4-6 per group) were included to examine intestinal damages on days 5, 7, 9, 11 after treatment of CPT-11 alone or combination with thalidomide.

Among which, four groups of rats were treated with i.v. CPT-11 injection at 60 mg/kg/day for four consecutive days and 1% DMSO (v/v) (control vehicle) by i.p. injection at 1 ml/kg/day for eight consecutive days starting one day before the first CPT-11 injection. The rats in the four groups were sacrificed on days 5, 7, 9, and 11, respectively, and the macroscopic and microscopic gastrointestinal toxicities were monitored.

For microscopic evaluation, intestinal tissues (ileum, caecum, and colon) were extirpated after exsanguination and fixed in 10% neutral buffered formaldehyde. After routine processing (Leica TP 1050 automated vacuum tissue processor, Leica Microsystems AG, Wetzlar, Germany), segments were embedded in paraffin wax (Leica EG1160 paraffin embedding station, Leica Microsystems AG, Wetzlar, Germany). Slices of 4-5 μm were taken by a Leica RM 2135-Rotary Microtome (Leica Microsystems AG, Wetzlar, Germany), stained with hematoxylin-eosin (H&E) and subjected to light microscopic examination (Leica DMRXA Microscope, Leica Microsystems AG, Wetzlar, Germany) in a blinded manner by covering the ID of each sample. Semi-quantitative scoring systems for macroscopic and microscopic evaluations of intestinal damages were used based

on the methods previously described [284]. Briefly, the macroscopic evaluation of intestinal tissues was based on the severity of gut wall thickening, hyperemia, hemorrhage, formation of pseudomembrane-like substance, ulceration, adhesion, diarrhea and stomach swelling. The microscopic evaluation was based on the severity of ulceration, destruction of normal mucosal architecture, crypt abscesses, degeneration of crypts, globlet cell mucus depletion, infiltration of leucocytes, muscle thickening, and edema (i.e. swelling) (Table 2-1 and Table 2-2).

Table 2-1. The scoring criteria for the macroscopic evaluation of intestinal damages in rats.

S/N	Observation	Score	Details of damage
1	Wall thickening	0 1 2 3	Absence Slight Mild Severe
2	Hyperemia	0 1 2 3	Absence Slight Mild Severe
3	Hemorrhage	0 1 2 3	Absence Slight Mild Severe
4	Formation of pseudo membrane-like substance	0 2	Absence Presence
5	Ulceration (ulcerative damages)	0 2 4 6	Absence Ulceration with inflammation at 1 site More sites of ulceration and inflammation Ulceration extending > 1 cm along the intestine
6	Adhesions	0 1 2 3	Absence Slight: can be easily separated from other tissue Mild: difficult to be separated from other tissue Severe: can not be separated from other tissue
7	Diarrhea	0 1 2 3	Normal: normal stools or absent Slight: wet and soft stools Moderate: wet and unformed stools with moderate perianal staining of the coat Severe: watery stools with severe perianal staining of the coat
8	Stomach swell	0 1 2 3	Absence Slight Mild Severe

Four groups of rats received i.v. CPT-11 injections at 60 mg/kg/day with thalidomide at 100 mg/kg/day by i.p. injections and the rats were sacrificed on days 5, 7, 9, and 11, respectively, with close monitoring of their toxicity. Four

additional groups of rats used as blank controls without any drug treatment were also included and sacrificed on days 5, 7, 9, and 11, respectively.

Table 2-2. The scoring criteria for the microscopic evaluation of intestinal damages in rats.

S/N	Observation	Score	Details of damage
1	Ulceration	0	Absence (normal appearance)
		1	Damage of surface epithelium
		2	Focal mucosal or transmucosal damage
		3	Extensive mucosal or transmucosal damage
2	Extent of destruction of normal mucosal architecture	0	Normal
		1	Slight
		2	Mild
		3	Severe
3	Crypt abscesses	0	Absence
		1	Slight
		2	Mild
		3	Severe
4	Degeneration of crypts	0	Absence
		1	Slight
		2	Mild
		3	Extensive
5	Goblet cell mucus depletion	0	Absence
		1	Slight
		2	Mild
		3	Severe
6	Degree of infiltration	0	Absence
		1	Slight
		2	Mild
		3	Severe (maximal infiltration)
7	Muscle thickening	0	Absence
		1	Slight
		2	Mild
		3	Severe (maximal thickness)
8	Edema (swelling)	0	Absence
		1	Slight
		2	Mild
		3	Severe

2.2.7 Terminal deoxynucleotidyl transferase-mediated dUTP nick-end labeling (TUNEL) assay

The assay of nuclear DNA fragmentation for apoptotic cell death in paraffin-embedded tissue sections was performed by TUNEL staining assay. TUNEL staining was done with standard methods according to the manufacturer's recommendations (DeadEnd™ Fluorometric TUNEL System, Promega, Madison, WI, USA). This system measures the fragmented DNA of apoptotic cells by

catalytically incorporating fluorescein-12-dUTP at 3'-OH DNA ends using the recombinant terminal deoxynucleotidyl transferase (rTdT). rTdT forms a polymeric tail using the principle of the TUNEL assay. The fluorescein-12-dUTP-labeled DNA can be visualized directly using fluorescence microscopy.

Tissue sections embedded in paraffin as described before were first prepared by deparaffinization using xylene. After being rehydrated in graded ethanol and fixed by immersing the slides in 4% methanol-free formaldehyde solution, the tissues were exposed to proteinase K solution to help permeabilize tissues to the staining reagents. To label double-stranded DNA breaks, 50 μl of rTdT incubation buffer was added and incubated at 37°C for 60 min in a humidified chamber. The reaction was terminated by immersing the slides in 2 × standard saline citrate. After removing unincorporated fluorescein-12-dUTP, the samples were stained by immersing in propidium iodide solution which was freshly diluted to 1 μg/ml in phosphate buffered saline (PBS) for 15 min at room temperature in the dark. Then, samples were immediately analyzed under a fluorescence microscope (Olympus micro image analysis system with retiga exi mono 12 bit cooled camera) using a standard fluorescence filter set to view the green fluorescence at 520 ± 20 nm; red fluorescence of propidium iodide at > 620 nm. In the meantime, negative control (using incubation buffer without rTdT) and positive control (using DNase I treatment to result in fragmentation of the chromosomal DNA and exposure of multiple 3'-OH DNA ends for labelling) were also included.

2.2.8 Quantitation of cytokines by enzyme-linked immunosorbent assay (ELISA)

Blood samples were also collected and allowed to clot at room temperature before centrifuging at 2,000 × g and 4ºC for 15 min. The serum was then immediately collected and aliquoted, and stored at -80ºC until analysis. Tissues (including liver, spleen, ileum, caecum, and colon) were harvested from rats killed on days 0, 5, 7, 9, and 11 after the first CPT-11 injection and snap-frozen in liquid nitrogen and then stored at -80ºC. Prior to assay, specimens were thawed and homogenized in a 50 mM Tris-HCl buffer containing 100 mM NaCl (pH 7.4) and 1% (v/v) protease inhibitor cocktail (Sigma, St. Louis, Mo. USA) on ice using a Heidolph homogenizer (Heidolph Instruments GmbH & Co. KG, Germany). The resultant homogenates were then centrifuged at 4,000 × g for 5 min at 4°C. The supernatant was then aliquoted and stored at -80°C for further analysis.

Cytokine levels of IL-1β, IL-2, IL-6, IFN-γ, and TNF-α in rat sera and various tissues were measured using a sandwich ELISA method. The Quantikine® immunoassay kits for IL-1β and IL-2 determination were purchased from R&D Systems (Minneapolis, MN, USA); while the analyses of IL-6, IFN-γ and TNF-α determination were processed using BD OptEIA™ ELISA Sets (BD Biosciences, San Jose, CA, USA). The sensitivities for the assays of IL-1β, IL-2, IL-6, IFN-γ and TNF-α were 5, 15, 4, 15, and 15 pg/ml, respectively. Standards and samples to be assayed were added to pre-coated 96-well plates. In some cases, the liver samples were diluted 10 times to bring the concentrations of IL-1β and IL-6 to the assay linear range. Samples and standards were incubated with biotinylated detection antibody for 2 hr. After the addition of avidin-horseradish peroxidase conjugate, the colour product was developed using tetramethylbenzidine substrate solution. The reaction was terminated by the addition of the stop solution (1M phosphoric solution) and the resultant optical density determined at a wavelength

of 450 nm within 30 min using a microplate reader (TECAN Group Ltd, Switzerland).

Cytokine levels in each sample were calculated by reference to a standard curve constructed for each assay by plotting the net absorbance versus the concentration of standards on a logarithmic scale. Protein content of the samples was determined by the Bradford assay [35] according to the manufacturer's recommendations (Sigma Chemical Co. St. Louis, Mo, USA). The cytokine levels in each tissue sample (in pg/ml) were then normalized by the protein content of each tissue sample, to give a final cytokine result expressed as pg/mg protein. The cytokine levels in sera were expressed as pg/ml.

2.2.9 Determination of protein concentration

The total protein concentration in tissue homogenates was determined by the Bradford method [17, 20] (Sigma, St. Louis, MO. USA) with bovine serum albumin as the standard. Protein samples were thawed, and then diluted appropriately with fresh NaOH (1 M) to make all protein soluble and to ensure that the concentrations are within measurable ranges of the calibration curve (100-fold dilution for liver and 50-fold dilution for other tissues). Bovine serum albumin was dissolved in Milli-Q water and further diluted with 1 M NaOH to prepare the standards with the concentration of 0.1-1.4 mg/ml. The standards and digested protein samples as well as 5 µl 1 M NaOH (used as blank control) were added in duplicate to a 96-well ELISA plate (NUNC, Rochester, NY). The Bradford reagent (250 µl) was then added to each well and mixed on a shaker for 30 sec. The absorbance was read at 595 nm using a microplate reader (TECAN, Switzerland). Standard curves were obtained by plotting the net absorbance versus

the protein concentration of standards. The protein concentration of the unknown samples was calculated using the standard curves.

2.2.10 Reverse transcription and polymerase chain reaction (RT-PCR) assay

mRNA Extraction

RNA was extracted from intestinal samples by using Trizol reagent (Invitrogen, Carlsbad, CA, USA) according to the manufacturer's protocol. Briefly, tissues of ileum, caecum, and colon were collected from rats killed on days 0, 5, 7, 9, and 11 and mixed with Trizol, then immediately transferred into liquid nitrogen and stored at -80°C prior to use.

Before extraction, the tissues were thawed on ice and homogenized in Trizol. Chloroform was then added to precipitate DNA and protein. After incubating for 2-3 min at room temperature and centrifuging at $12,000 \times g$ for 15 min at 4°C, the aqueous phase of RNA was collected carefully and 0.5 ml of isopropanol was added to the aqueous phase to precipitate RNA. The mixture was vortexed, incubated for 10 min at room temperature and centrifuged at $12,000 \times g$ for 10 min at 4°C. The RNA precipitate formed a gel-like pellet on the side and the bottom of the tube. After discarding the supernatant (isopropanol), 1 ml of 75% ethanol (made up with 0.1% DEPC-treated water) was added to wash the RNA. After centrifugation at $7,500 \times g$ for 5 min at 4°C, the ethanol was removed and the RNA was dried under vacuum. Finally, the RNA pellet was mixed with 100 µl 0.1% DEPC-treated water by pipetting up and down and then the solution was stored at -80°C until analysis. The purity of RNA was determined using a UV spectrophotometer (Shimadzu, Japan) by comparing its absorbance at 260 nm

(peak for RNA) and 280 nm (peak for proteins). The concentration of total RNA in µg/ml was calculated by the following formula:

$$RNA\ concentration = Absorbance \times 40$$

RT-PCR procedure

RT-PCR amplification of *TNF-α* mRNA was processed using the Access RT-PCR System (Promega, Madison, WI, USA). The RT-PCR reaction was performed in a 200 µl thin-wall test tube containing 10 µl AMV/Tfl 5 × reaction buffer, 1 µl dNTP Mix (0.2 mM each), 0.5 µM downstream primer and 0.5 µM upstream primer, 1.5 mM MgSO$_4$, 1 µl AMV reverse transcriptase (5 u/µl) and 1 µl Tfl DNA polymerase (5 u/µl), and 1 µg *TNF-α* mRNA sample. In addition to the *TNF-α* primer, the housekeeping gene *β-actin* was also used in the same reaction as a reference for standardization of the PCR procedure used. The specific oligonucleotide primers of *TNF-α* (Rattus) and *β-actin* (Rattus) were designed according to sequences published earlier. The specificity of these primers was confirmed using standard nucleotide-nucleotide BLAST. The sequences were as follows: *TNF-α* primer sense, 5'-TAC TGA ACT TCG GGG TGA TCG GTC G-3'; TNF-α primer antisense, 3'-CAG CCT TGT CCC TTG AAG AGA ACC-5', Genebank accession No. NM_012675 (about 300bp); *β-actin* sense, 5'-GCC ACT GCC GCA TCC TCT T-3'; *β-actin* antisense, 3'-ATC GTA CTC CTG CTT GCT GA-5', Genebank accession No. NM_031144 (about 408bp). RT-PCR was carried out using Flexigene Thermal Cycler (Techne, Burlington, NJ, USA) at 45ºC for 45 min and 94ºC for 2 min. Amplifications were then carried out using 25 cycles of 94ºC for 30 sec, 60ºC for 1 min, and 68ºC for 2 min, followed by 68ºC for 7 min and soaked at 4ºC. Initial experiments were carried out to optimize the RT-PCR conditions using a variety of annealing temperatures, primer and magnesium

concentrations. For both of the oligonucleotide pairs, preliminary analyses applying various PCR cycles were conducted to define the appropriate range of cycles consistent with an exponential increase of the amount of the DNA product. In addition, the absence of contaminants was routinely checked by RT-PCR of negative control samples, in which RNA samples were replaced with sterile water.

PCR products and molecular weight markers were subjected to 1% agarose gel (Seakem LE Agarose, Cambres Bio Science Rockland Inc., Rockland, ME, USA) electrophoresis (Bio-Rad Mini-Sub Cell GT system, Hercules, CA, USA) and visualized by means of ethidium bromide (Promega, Madison, WI, USA) staining. The gel images were digitally captured using Gel-Doc (Bio-Rad, Hercules, CA, USA) and densitometric analysis was performed with Quantity One 1-D Analysis software (Bio-Rad, Hercules, CA, USA). The levels of *TNF-α* mRNA were normalized to that of *β-actin* present in the same sample, expressed as *TNF-α*-to-*β-actin* ratio (band intensity). Final results were expressed as fold increase in band intensity compared to that at day 0 (i.e. rats killed on day 0 that received no drug treatment).

2.2.11 Statistical analysis

Data were expressed as mean ± SD (standard deviation), except otherwise indicated. Diarrhea scores were analyzed using Wilcoxon rank sum test. Statistical comparisons for multiple groups were performed using a one-way analysis of variance (ANOVA) followed by Student's Newman-Keuls test. Differences between two groups were analysed using unpaired Student's *t*-test. Statistical significance was set as $P < 0.05$.

2.3 RESULTS

2.3.1 Effects of thalidomide on CPT-11 induced toxicities
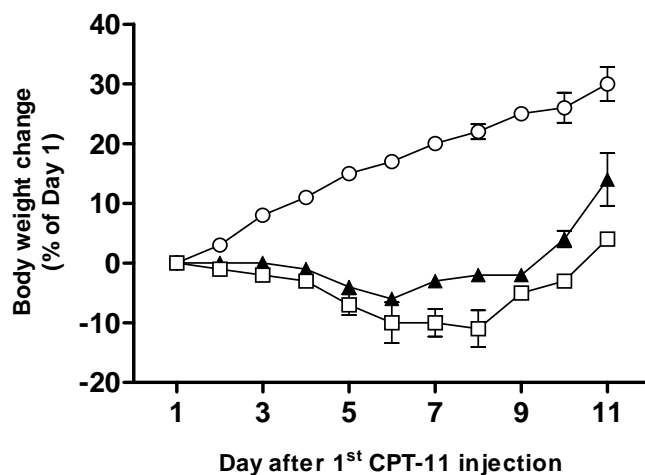
Figure 2-1. Body weight changes (% compared to that on day 1) in two groups of rats treated with CPT-11 and the control vehicle (1% DMSO, v/v) or CPT-11 in combination with thalidomide. Symbols: ○, Blank (without drug treatment); ▲, CPT-11+ Thalidomide; □, CPT-11+ Control vehicle (1% DMSO, v/v) (N = 4-6).

The present study investigated body weight changes, leukocyte counts, and histological damages, cytokine expressions as well as apoptosis throughout the gastrointestinal tract including ileum, caecum, and colon tissues for the combination of thalidomide with CPT-11 throughout the whole study. Rats treated with CPT-11 and control vehicle (1% DMSO, v/v) experienced rapid decrease in body weight, reached a nadir by day 8 with a decrease of 11% compared to the baseline (day 1), and recovered to 104% of the baseline by day 11 (Figure 2-1). Co-administration of thalidomide with CPT-11 resulted in lesser body weight loss compared to rats receiving CPT-11 and control vehicle (1% DMSO, v/v), with a decrease of 2% by day 8 and recovery to 114% of the baseline by day 11 ($P <$ 0.05). Rats without any drug treatment increased body weight over 11 days continously.

Table 2-3. Incidence of early- and late-onset diarrhea in rats treated with CPT-11 and control vehicle (1% DMSO, v/v) or CPT-11 in combination with thalidomide. The values are the number of animals (n) with scores of severity of diarrhea.

Treatment Group	n	Early-onset diarrhea score [a]																				
		Day 1					Day 2					Day 3					Day 4					
		0	1	2	3	Mean	0	1	2	3	Mean	0	1	2	3	Mean	0	1	2	3	Mean	
Blank	5	10				0	10				0	10				0	10				0	
CPT-11+ Thalidomide	6	12				0	10	2			0.17	10		1	1	0.42	5		3	4	1.5	
CPT-11+ 1% DMSO (v/v)	6	8	2	2		0.50	8	3	1		0.42	5	2	4	1	1.08	3	2	1	6	1.83	

Treatment Group	n	Late-onset diarrhea score [a]																				
		Day 5					Day 6					Day 7					Day 8					
		0	1	2	3	Mean	0	1	2	3	Mean	0	1	2	3	Mean	0	1	2	3	Mean	
Blank	5	10				0	10				0	10				0	10				0	
CPT-11+ Thalidomide	6	7			5	1.25	6	1	2	3	1.17*	5	4	3	0	0.83*	10	2			0.17	
CPT-11+ 1% DMSO (v/v)	6	4			8	2.00	2	1		9	2.33	1	3	3	5	2.00	7	3	2		0.58	

$*P < 0.05$ *vs.* CPT-11+ control vehicle (1% DMSO, v/v) group. Mean = Sum of scores (1-3)/rat number;
[a] Two observations each animal/day.

Treatment of rats with CPT-11 at 60 mg/kg/day by i.v. for four consecutive days and control vehicle (1% DMSO, v/v) by i.p. for eight consecutive days induced severe early- (days 1-4) and late-onset (days 5-8) diarrhea, with mean severity scores of 0.5, 0.42, 1.08, 1.83, 2.0, 2.33, 2.0, and 0.58 by days 1-8, respectively (Table 2-3). The severity scores for late-onset diarrhea were significantly ($P < 0.05$, by Wilcoxon rank sum test) brought down in rats treated with CPT-11 in combination of thalidomide (100 mg/kg/day, i.p.) on days 6 and 7. Rats without any drug treatment did not experience any diarrhea.

The counts of leucocytes were also monitored in the toxicity study on days 0, 5, 7, 9, and 11, respectively. The numbers of neutrophils and lymphocytes were decreased and reached a minimum by day 7 in rats treated with CPT-11 and control vehicle (1% DMSO, v/v) (Figure 2-2). However, combination of CPT-11 with thalidomide increased the numbers of lymphocyte ($P < 0.05$) and neutrophil on day 7 ($P < 0.01$). Rats receiving either CPT-11 with control vehicle or CPT-11 plus thalidomide had increased neutrophil numbers after day 7. This may be due to systemic response to severe inflammation of intestines. Rats without any drug treatment did not induce any detectable blood toxicities.

Marked macroscopic and microscopic gastrointestinal damages were induced in rats treated with CPT-11 and control vehicle (1% DMSO, v/v). Typical macroscopic intestinal damages included wide wall thickening and swelling, hyperemia, haemorrhage, ulceration, as well as adhesion. Combination of thalidomide significantly reduced these damages on day 5 (10.5 *vs.*17.5, $P < 0.01$), on day 7 (6.8 *vs.* 12.0, $P < 0.05$), on day 9 (4.6 *vs.* 9.2, $P < 0.001$), and on day 11 (3.2 *vs.* 6.7, $P < 0.05$), respectively (Figure 2-3).

A Lymphocyte
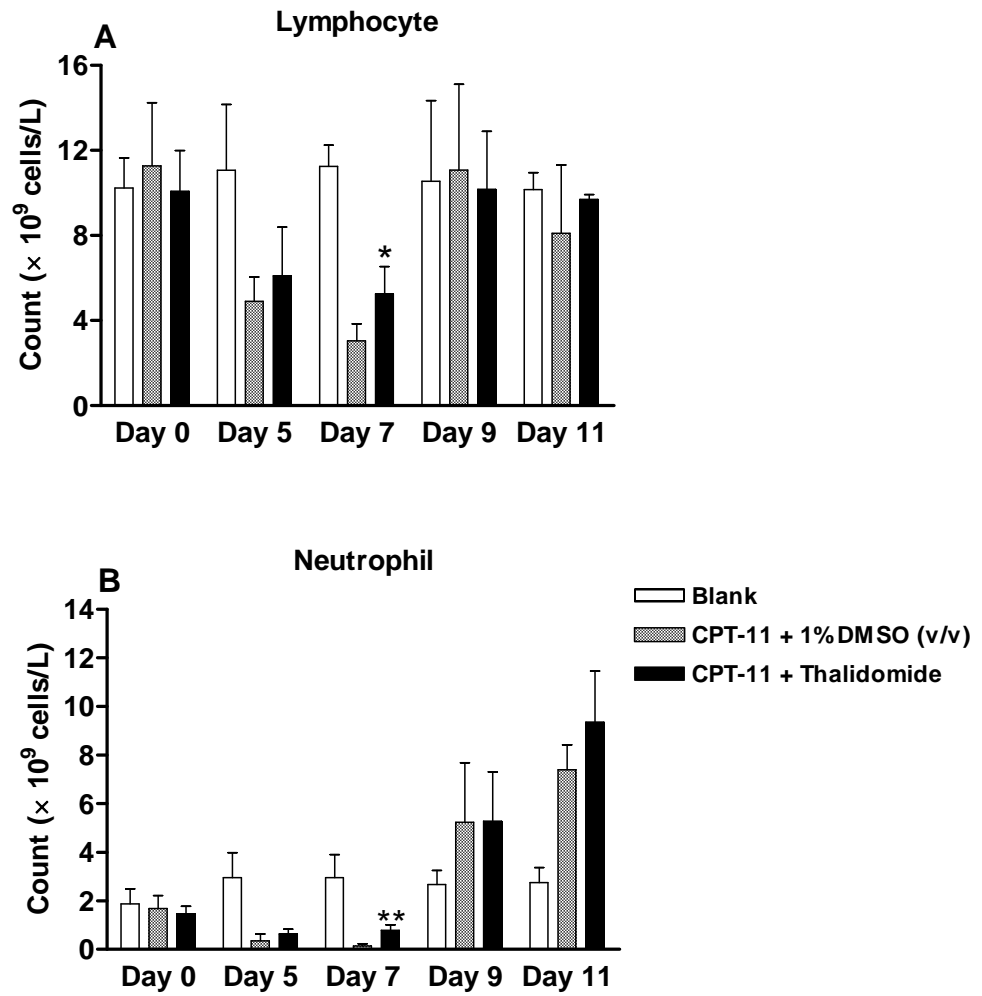
B Neutrophil

Figure 2-2. Comparison of lymphocyte and neutrophil counts on days 0, 5, 7, 9, and 11 in rats treated with CPT-11 and control vehicle (1% DMSO, v/v) or in combination with thalidomide. *P < 0.05; **P < 0.01 (N = 4-6).
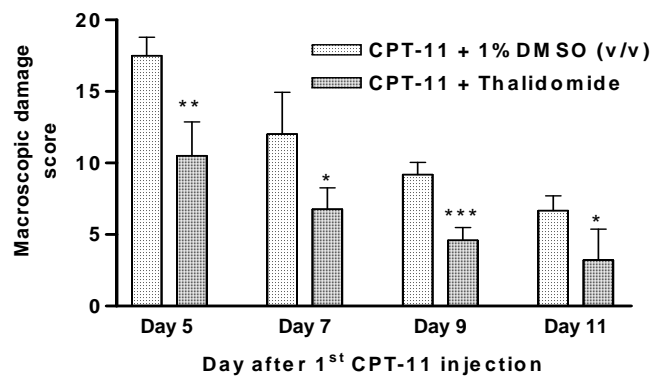
Figure 2-3. Scores of macroscopic intestinal (including ileum, caecum, and colon) damages by days 5, 7, 9, and 11 induced by CPT-11 in rats pretreated with thalidomide or the control vehicle (1% DMSO, v/v). *P < 0.05; **P < 0.01; ***P < 0.001 (N = 4-6).

49

	CPT-11 + 1% DMSO (v/v)	CPT-11+ Thalidomide
Day 0		
Day 5		
Day 7		
Day 9		
Day 11		
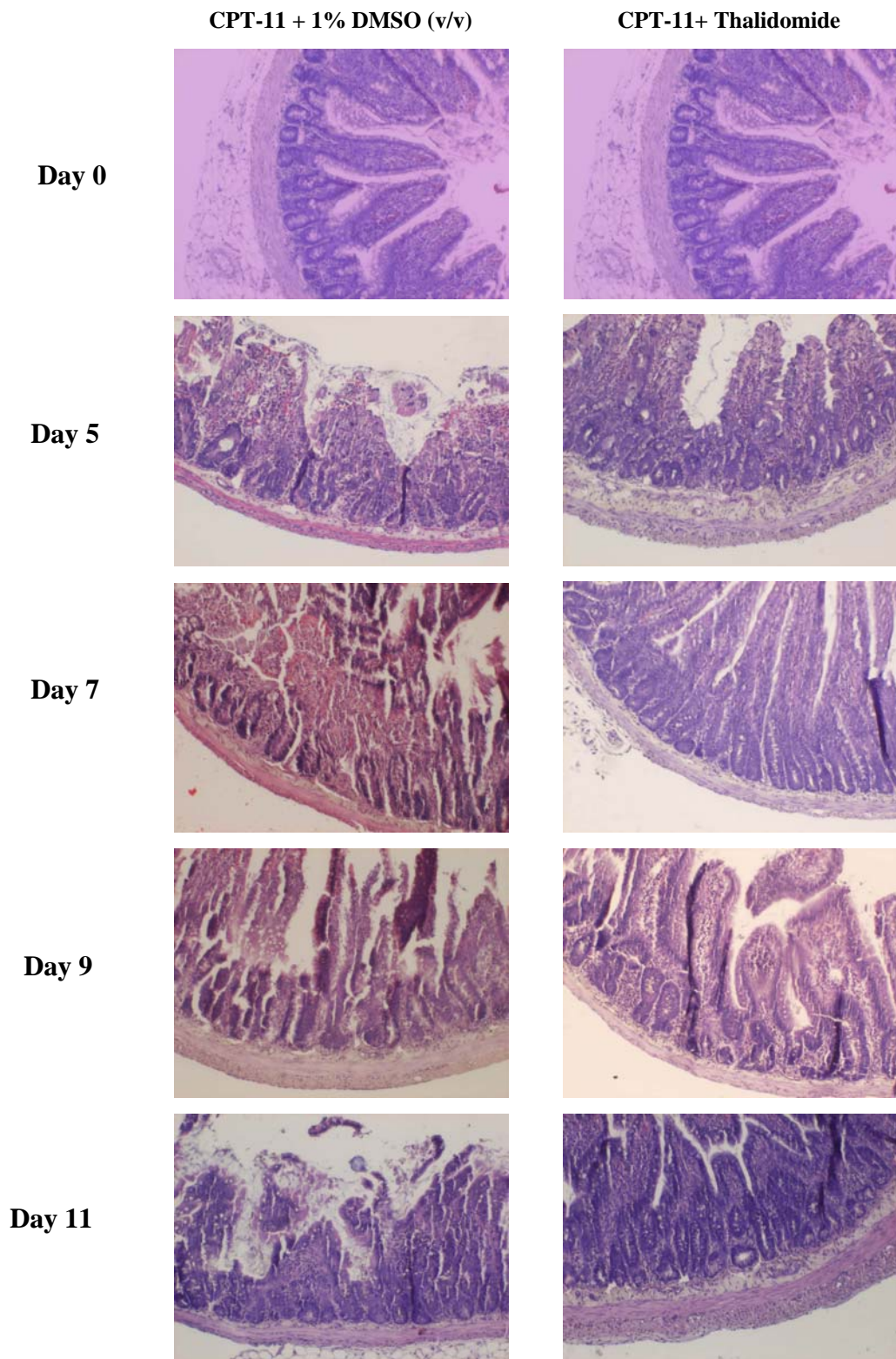
Figure 2-4. Micrographs (magnification × 100) of ileum showing histological damages on days 0, 5, 7, 9, and 11 in rats. The rats were treated with CPT-11 and the control vehicle (1% DMSO, v/v), or CPT-11 in combination with thalidomide.

CPT-11 + 1% DMSO (v/v)   **CPT-11+ Thalidomide**

Day 0

Day 5

Day 7

Day 9

Day 11
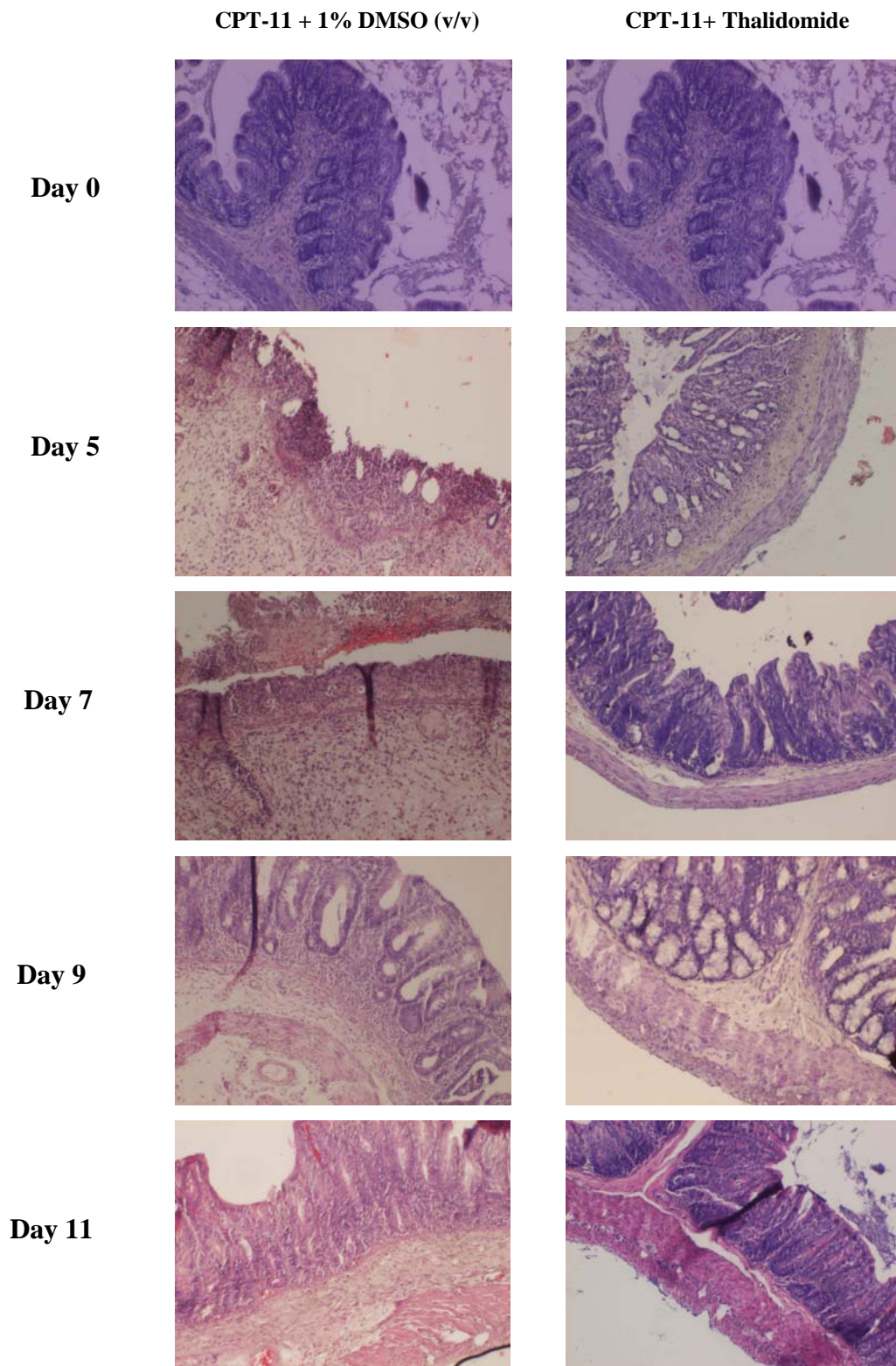
Figure 2-5. Micrographs (magnification × 100) of caecum showing histological damages on days 0, 5, 7, 9, and 11 in rats. The rats were treated with CPT-11 and the control vehicle (1% DMSO, v/v), or CPT-11 in combination with thalidomide.

	CPT-11 + 1% DMSO (v/v)	**CPT-11 + Thalidomide**
Day 0		
Day 5		
Day 7		
Day 9		
Day 11		
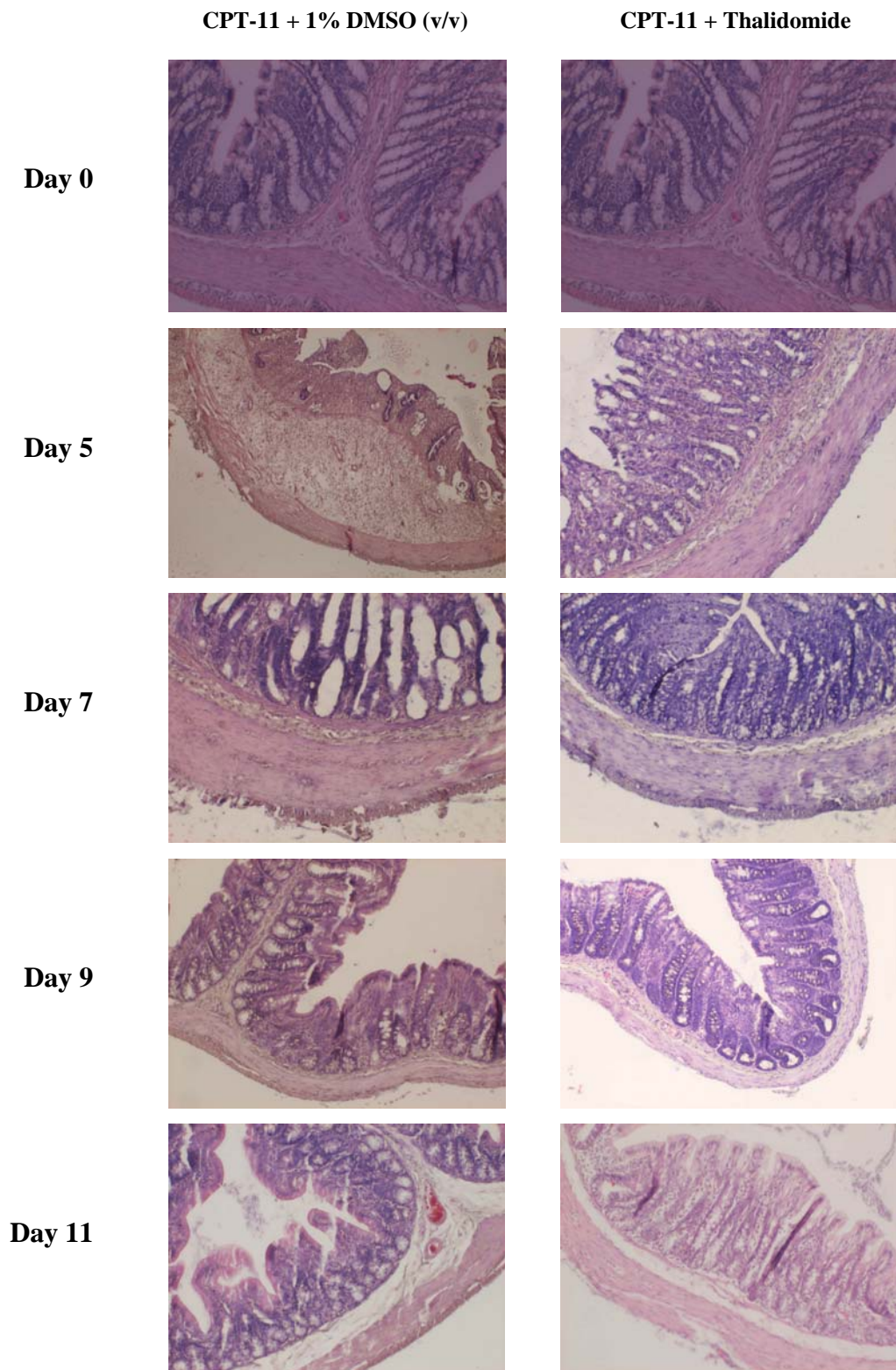
Figure 2-6. Micrographs (magnification × 100) of colon showing histological damages on days 0, 5, 7, 9, and 11 in rats. The rats were treated with CPT-11 and the control vehicle (1% DMSO, v/v), or CPT-11 in combination with thalidomide.
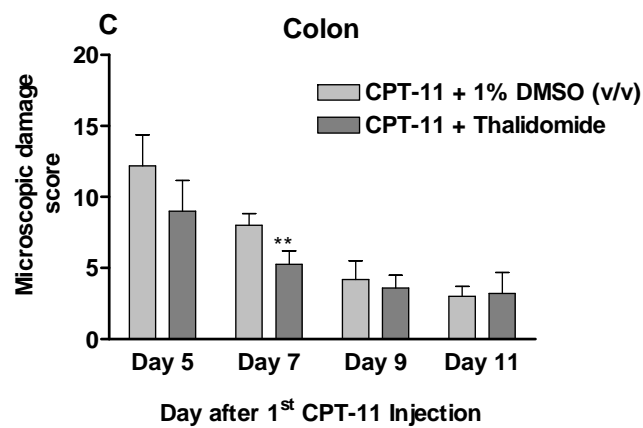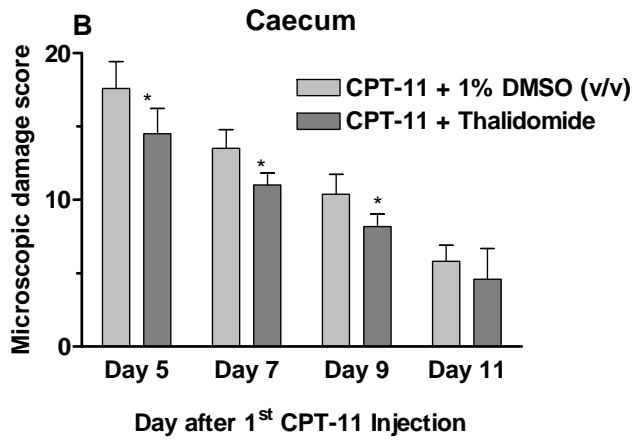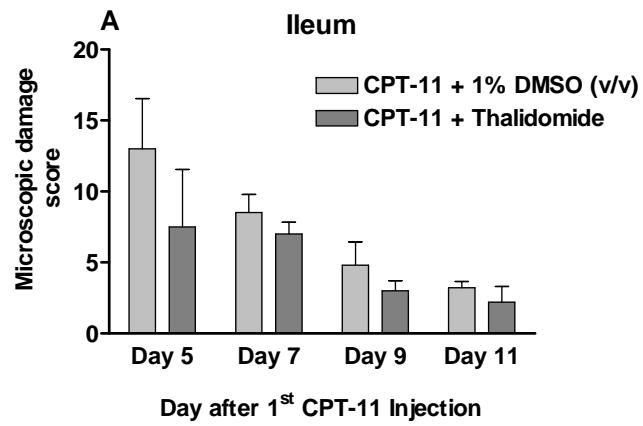
Figure 2-7. Scores of microscopic intestinal (including ileum, caecum, and colon) damages on days 5, 7, 9, and 11 induced by CPT-11 in rats pretreated with thalidomide or the control vehicle (1% DMSO, v/v). *$P < 0.05$; **$P < 0.01$ (N = 4-6).

Typical microscopic injuries included severe damages of the mucosal surface of the intestines characterized by stubby villi, goblet cell mucus depletion, epithelial vacuolation, crypt abscesses and inflammatory cellular infiltration noted by HE staining (Figure 2-4, Figure 2-5, and Figure 2-6). In particular, these histological damages were extremely severe in the caecum on day 5 and day 7 compared to the small intestine and colon. These impairments, however, were significantly decreased in rats treated with CPT-11 in combination with thalidomide in the caecum and colon (Figure 2-7).

2.3.2 TUNEL assay

In normal rats without any drug treatment, the number of epithelial apoptotic cells per crypt in ileum, caecum, and colon were 2.0 ± 0.7, 5.0 ± 1.6 and 3.2 ± 1.3, respectively. CPT-11 caused a maximal epithelial apoptosis (62.6 ± 11.5 per crypt) on day 5 in the ileum, and then decreased thereafter (12.2-40.2 per crypt over 7-11 days). Combination of thalidomide significantly reduced ileal epithelial apoptosis on day 5 by 47.9% ($P < 0.01$), on day 7 by 39.3% ($P < 0.01$), and on day 11 by 52.5 % ($P < 0.05$) compared to rats received CPT-11 and the control vehicle [1% DMSO (v/v)] (Figure 2-8 and Figure 2-11).

Similarly, maximal epithelial apoptosis was detected in the caecum and colon on day 5. Thalidomide pretreatment caused less epithelial apoptosis by 52.4% on day 5 ($P < 0.01$), by 45.7% on day 7 ($P < 0.001$), and by 35.8% on day 11 ($P < 0.01$) in the caecum (Figure 2-9 and Figure 2-11). In addition, coadministered thalidomide reduced the apoptosis by 47.0% on day 5 ($P < 0.01$), by 34.1% on day 7 ($P < 0.05$), and by 28.4% on day 9 ($P < 0.05$) in the colon (Figure 2-10 and Figure 2-11).

CPT-11 + 1% DMSO (v/v)   **CPT-11 + Thalidomide**

Day 0

Day 5

Day 7

Day 9

Day 11
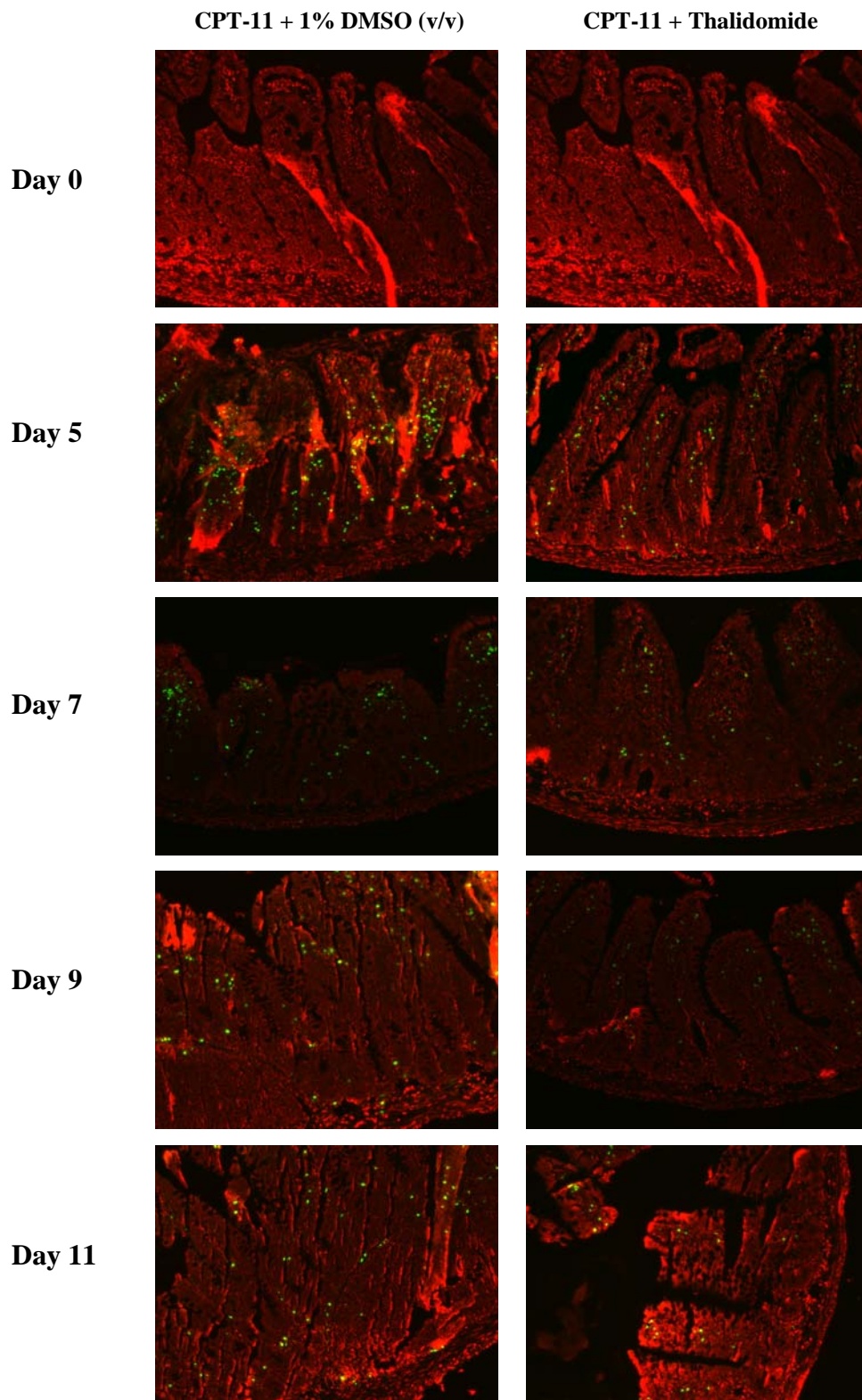
Figure 2-8. Detection of apoptotic cells in ileum (4-μm slices) using TUNEL assay. The fragmented DNA of TUNEL-positive apoptotic cells (green spots) were incorporated with fluorescein-dUTP at free 3'-hydroxyl ends and visualized by fluorescence microscopy (magnification × 100).

CPT-11 + 1% DMSO (v/v)   **CPT-11 + Thalidomide**

Day 0

Day 5

Day 7

Day 9

Day 11
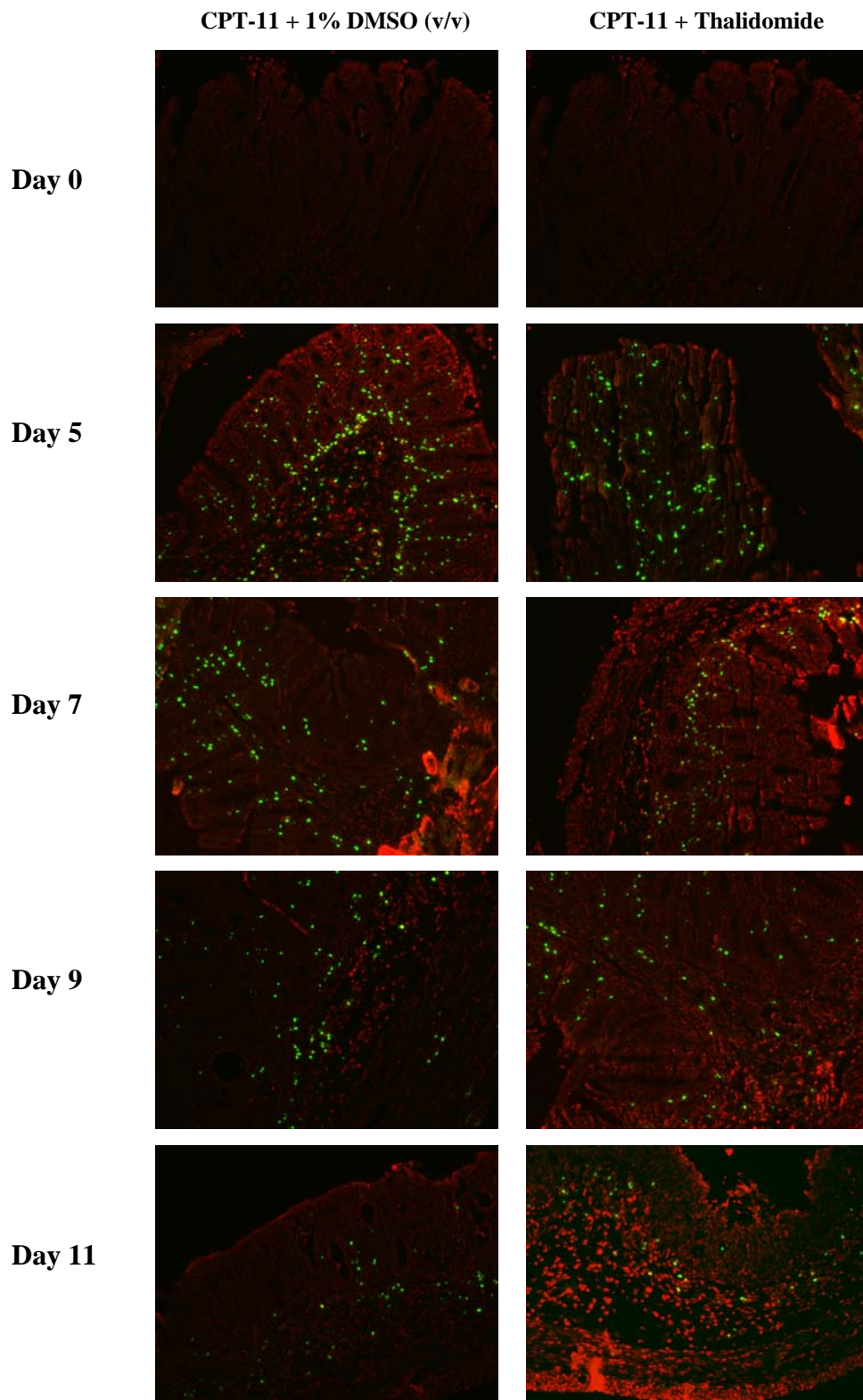
Figure 2-9. Detection of apoptotic cells in caecum (4-μm slices) using TUNEL assay. The fragmented DNA of TUNEL-positive apoptotic cells (green spots) were incorporated with fluorescein-dUTP at free 3'-hydroxyl ends and visualized by fluorescence microscopy (magnification × 100).

CPT-11 + 1% DMSO (v/v) **CPT-11 + Thalidomide**

Day 0

Day 5

Day 7

Day 9

Day 11
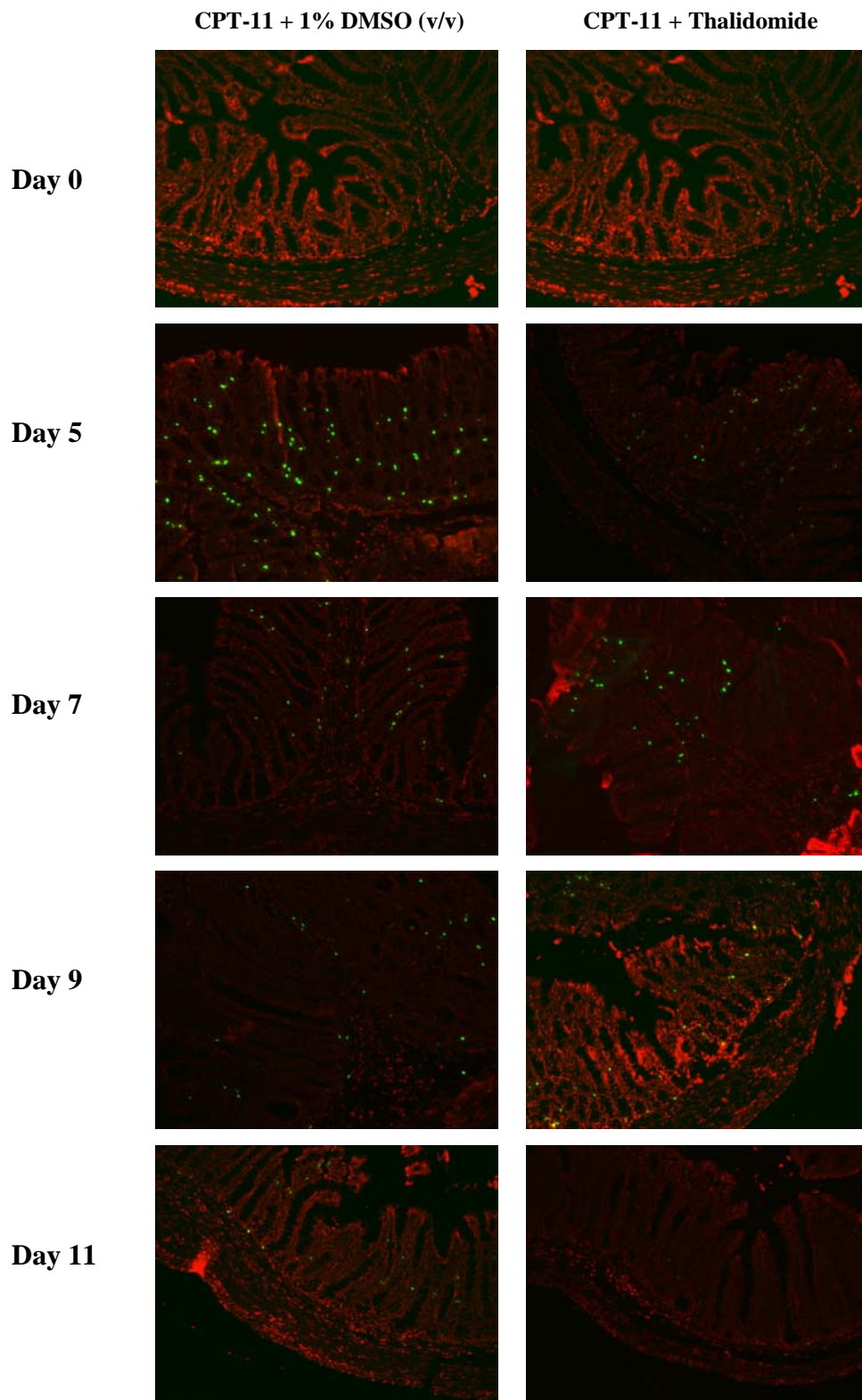
Figure 2-10. Detection of apoptotic cells in colon (4-µm slices) using TUNEL assay. The fragmented DNA of TUNEL-positive apoptotic cells (green spots) were incorporated with fluorescein-dUTP at free 3'-hydroxyl ends and visualized by fluorescence microscopy (magnification × 100).
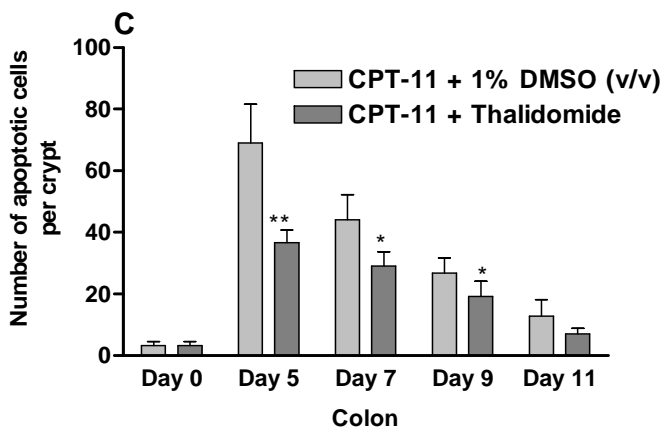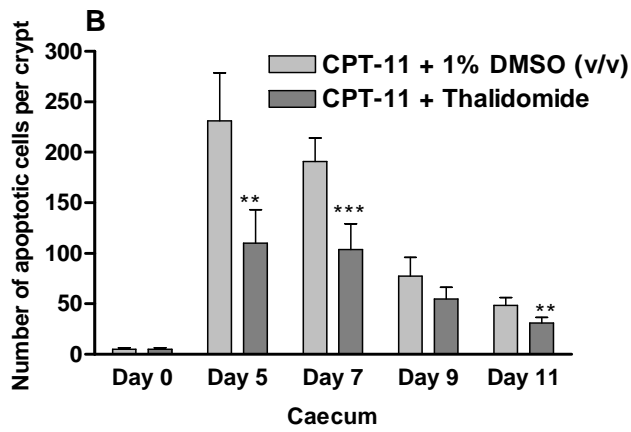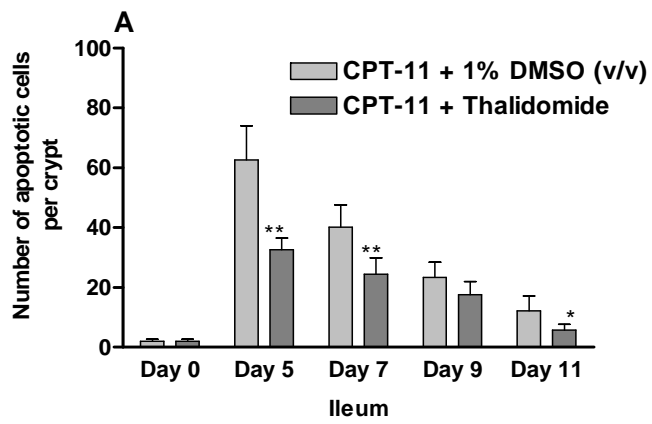
Figure 2-11. Number of intestinal epithelial apoptotic cells per crypt in rats treated with CPT-11 and 1% DMSO (v/v) or in combination with thalidomide. $*P < 0.05$; $**P < 0.01$; $***P < 0.001$ (N = 4-6).

2.3.3 Quantitation of cytokines by ELISA

The levels of TNF-α, IFN-γ, IL-1β, IL-2, and IL-6 in intestinal tissues and liver, spleen as well as serum are shown in Figures 2-12, 2-13, 2-14, 2-15, and 2-16, respectively. Treatment of CPT-11 generally increased the levels of TNF-α, IFN-γ, IL-1β, and IL-6 compared to day 0, which achieved peak levels by day 5 or day 9 and declined thereafter, while the level of IL-2 generally decreased compared to day 0, reaching minimum level by day 5 or day 7 in the above tissues.

Significant inhibition of TNF-α was seen in ileum from rats treated with combination therapy on day 5 by 64.9% ($P < 0.05$) and on day 7 by 59.0% ($P < 0.01$); and in caecum on day 5 by 44.9% and on day 7 by 46.6% ($P < 0.05$), respectively, compared to the control group. Coadministered thalidomide caused no significant effects on IFN-γ expression in all tissues examined except that the splenic IFN-γ level in the combination group was increased more that 3-fold compared to that in the control group that received CPT-11 and 1% DMSO (v/v) on day 5 ($P < 0.05$). Combination of thalidomide caused significant inhibitory effects on IL-1β expression in spleen by 39.7% on day 9 and by 38.0% on day 11 ($P < 0.05$). Similar inhibitory effect was observed in the combination group for IL-2 level in serum by 60.5% ($P < 0.001$) on day 11. In addition, IL-6 levels were significantly brought down by the combination with thalidomide in ileum on day 5 by 67.3% ($P < 0.05$); in colon on day 5 by 41.3% ($P < 0.05$); in spleen on days 5 and 7 by 62.1% and 48.5% ($P < 0.05$), respectively.
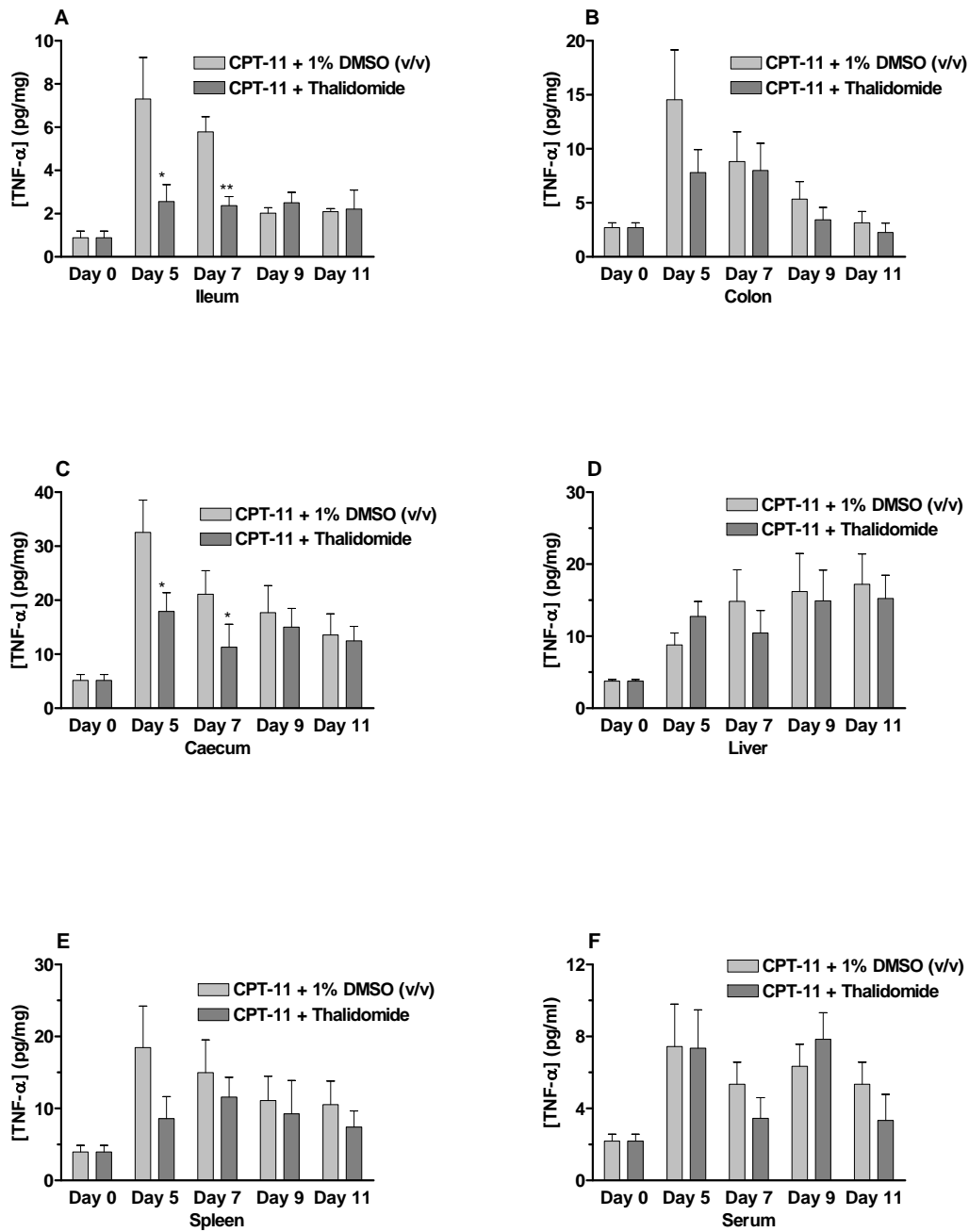
Figure 2-12. Protein levels of TNF-α in ileum (A), colon (B), caecum (C), liver (D), spleen (E), and serum (F) on days 0, 5, 7, 9, and 11 after CPT-11 administration in the control group treated with CPT-11 and 1% DMSO (v/v) and the combination group treated with CPT-11 and thalidomide. *$P < 0.05$; **$P < 0.01$ (N = 4-6).
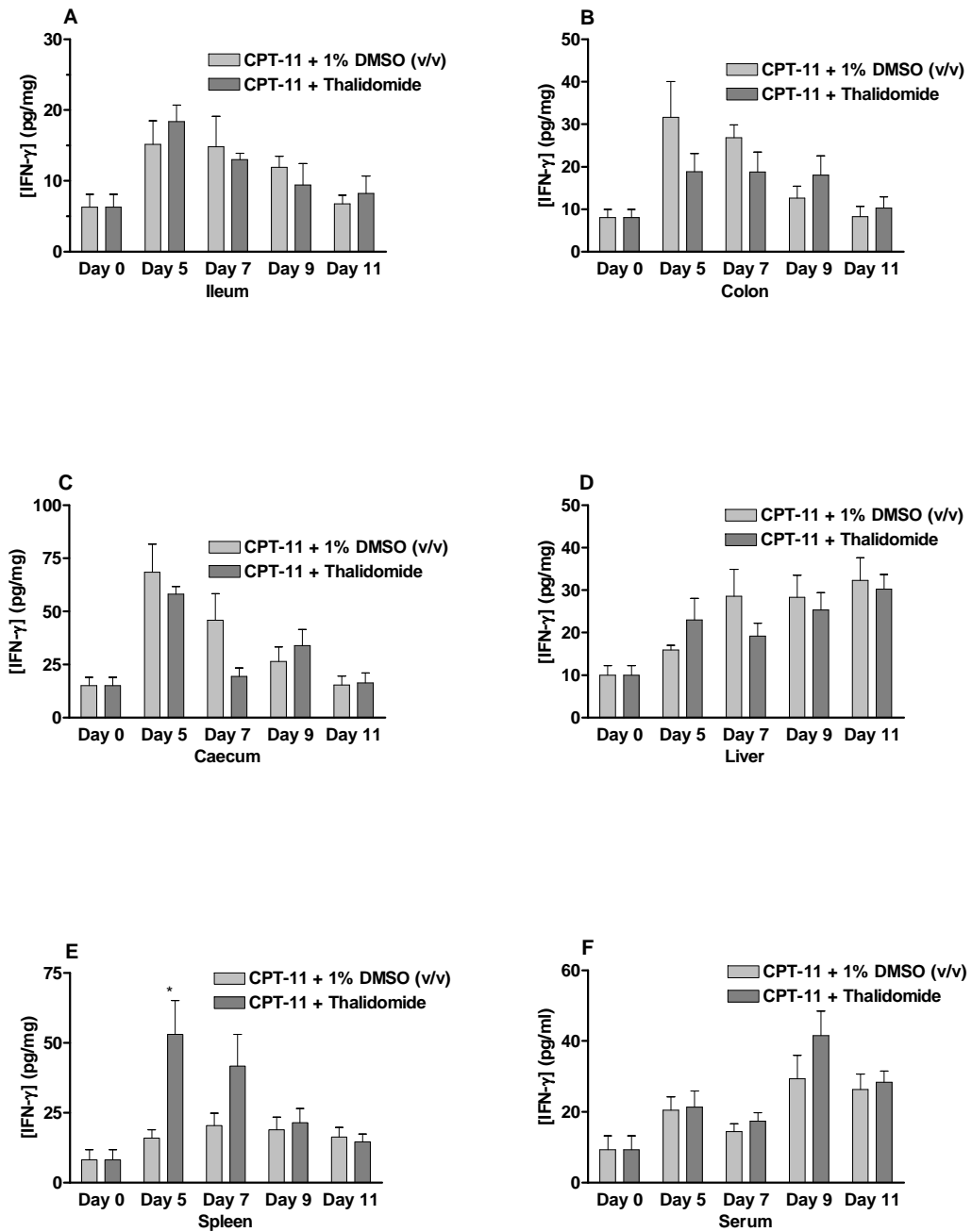
Figure 2-13. Protein levels of IFN-γ in ileum (A), colon (B), caecum (C), liver (D), spleen (E), and serum (F) on days 0, 5, 7, 9, and 11 after CPT-11 administration in the control group treated with CPT-11 and 1% DMSO (v/v) and the combination group treated with CPT-11 and thalidomide. *$P < 0.05$ (N = 4-6).
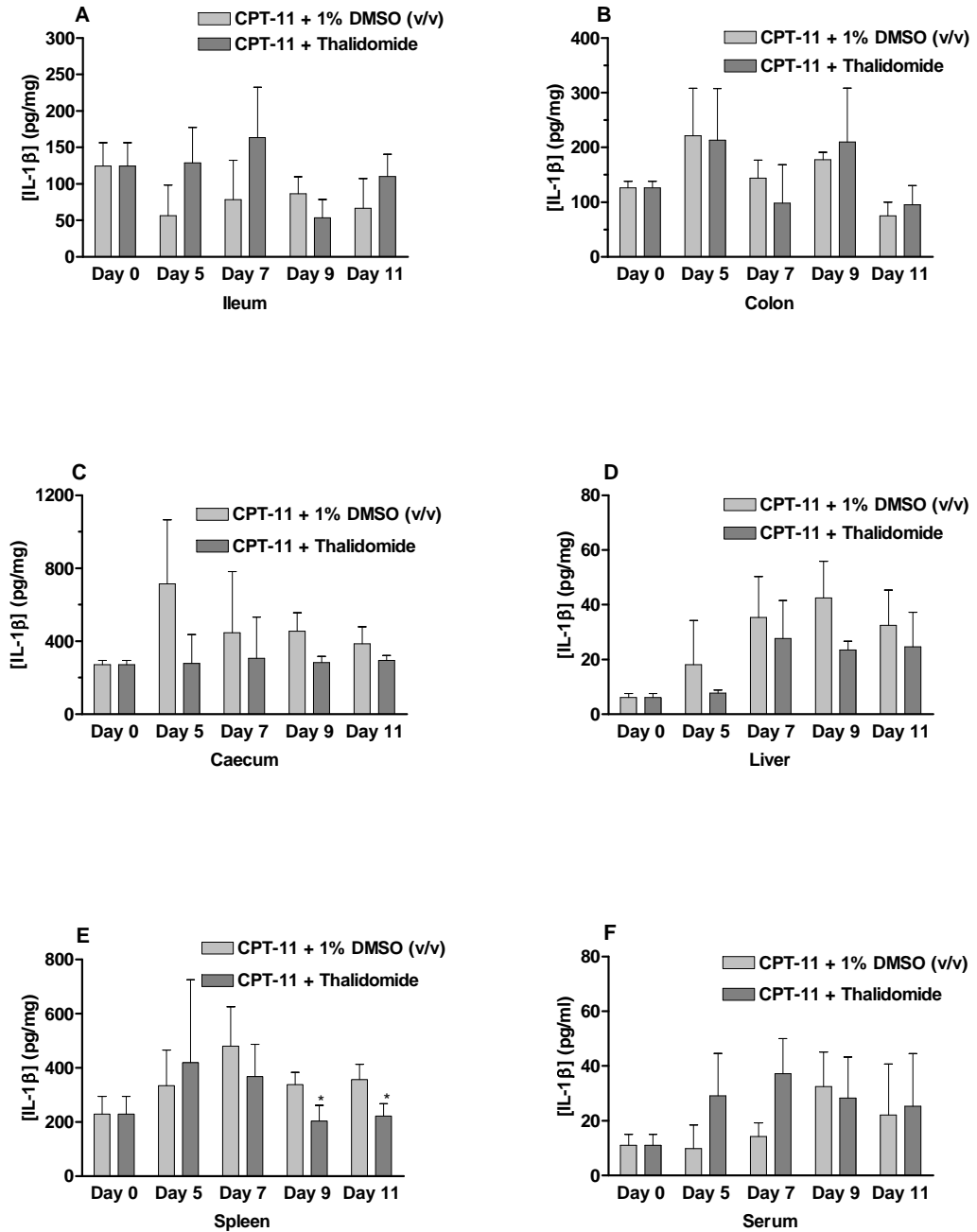
Figure 2-14. Protein levels of IL-1β in ileum (A), colon (B), caecum (C), liver (D), spleen (E), and serum (F) on days 0, 5, 7, 9, and 11 after CPT-11 administration in the control group treated with CPT-11 and 1% DMSO (v/v) and the combination group treated with CPT-11 and thalidomide. *P < 0.05 (N = 4-6).
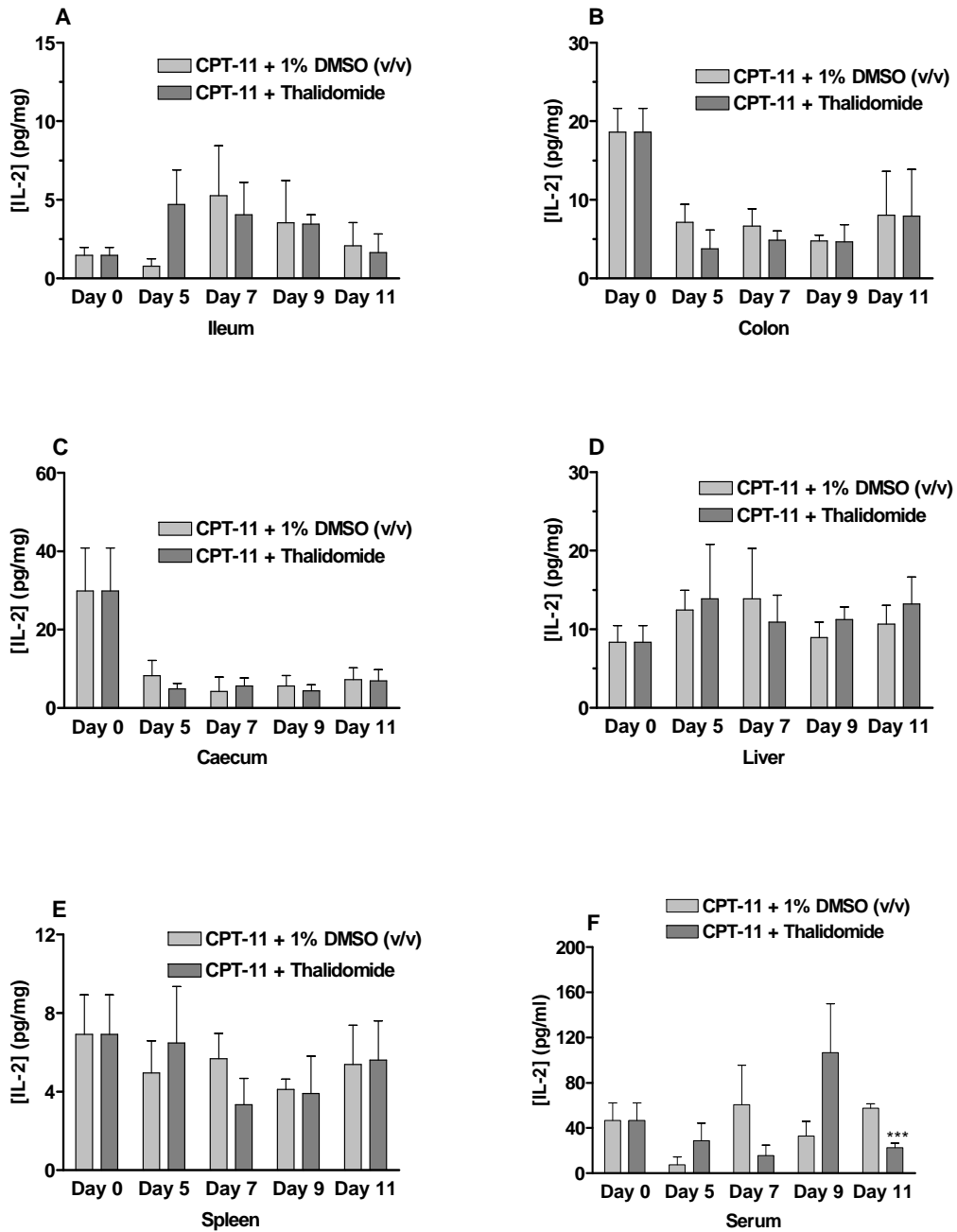
Figure 2-15. Protein levels of IL-2 in ileum (A), colon (B), caecum (C), liver (D), spleen (E), and serum (F) on days 0, 5, 7, 9, and 11 after CPT-11 administration in the control group treated with CPT-11 and 1% DMSO (v/v) and the combination group treated with CPT-11 and thalidomide. ***P < 0.001 (N = 4-6).
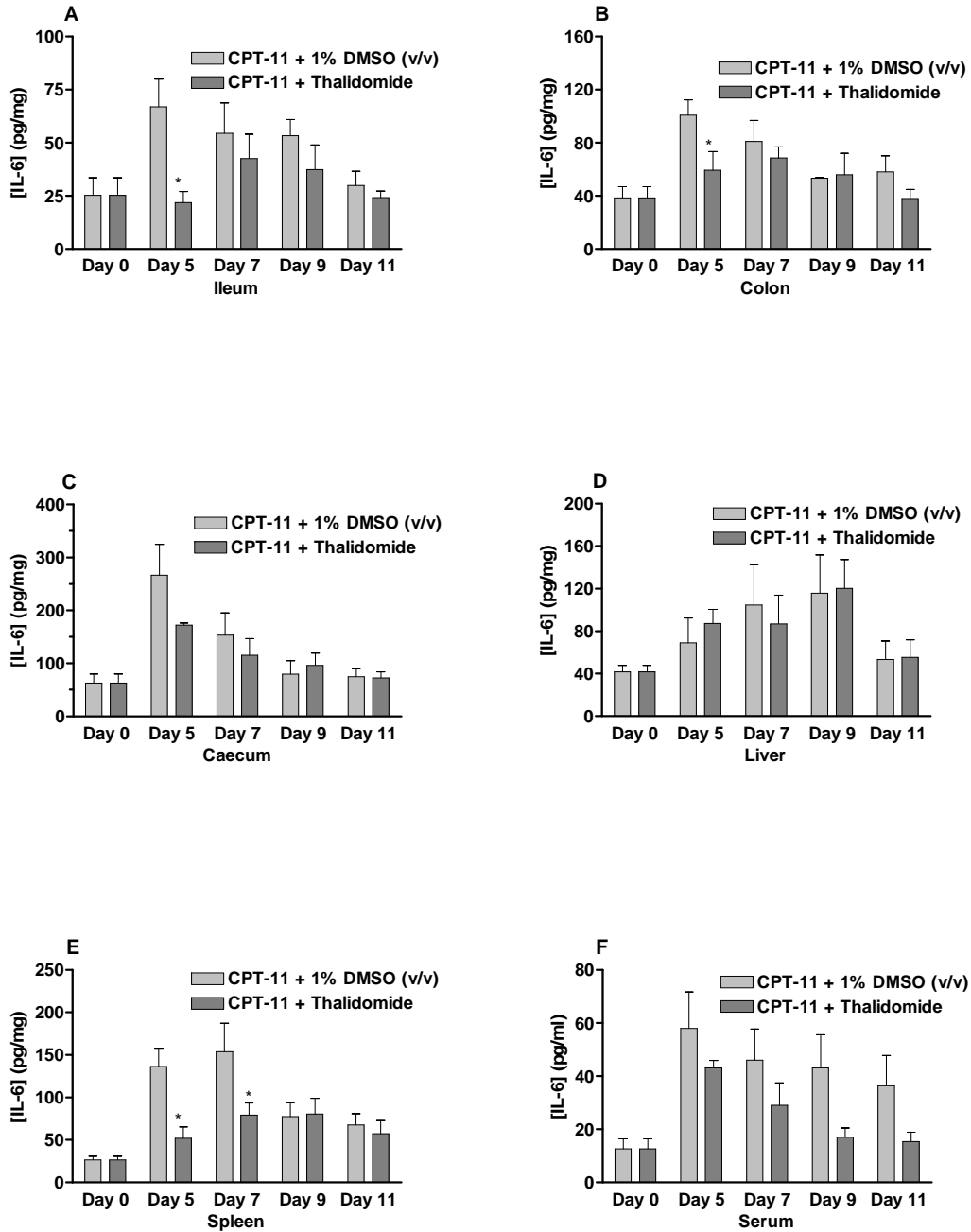
Figure 2-16. Protein levels of IL-6 in ileum (A), colon (B), caecum (C), liver (D), spleen (E), and serum (F) on days 0, 5, 7, 9, and 11 after CPT-11 administration in the control group treated with CPT-11 and 1% DMSO (v/v) and the combination group treated with CPT-11 and thalidomide. *P < 0.05 (N = 4-6).

2.3.4 *TNF-α* mRNA expression

We examined the expression pattern and kinetics of the transcripts for *TNF-α* genes over 11 days after administration of CPT-11 in intestinal tissues including ileum, caecum, and colon (Figure 2-17). The transcripts for *TNF-α* in ileum were detectable in healthy rats without any drug therapy. The band intensity increased after CPT-11 injection and reached a peak level on day 9 (2.8-fold increase compared to that of day 0) and then started to drop on day 11. However, combination with thalidomide brought down the increased expression levels of *TNF-α* mRNA, as indicated by decreasing fold-increase in band intensity compared to that of day 0 on days 7 and 9 by 29.2% and 29.1%, respectively ($P <$ 0.05).

Although the transcripts for *TNF-α* in caecum were almost undetectable from healthy rats, they were readily detectable on days 5 to 11, with gradual decrease in the expression level after CPT-11 administration. Decreased *TNF-α* transcript was observed in the group treated with combined thalidomide over 11 days. The fold-increase of band intensity was brought down by 61.4% on day 7 ($P <$ 0.05), 95.7% on day 9 ($P <$ 0.01), and 95.6% on day 11 ($P <$ 0.01). The transcripts for *TNF-α* were almost undetectable on days 9 and 11 in the rats receiving combination therapy.

The transcripts for *TNF-α* were detectable from healthy colon. They were increased after CPT-11 injection and achieved the maximum level on day 7 in the control group treated with CPT-11 and 1% DMSO (v/v) and then decreased. Similar trends could be seen in the combination group with decreased expression levels of *TNF-α* over 11 days. However no significant influence was observed.
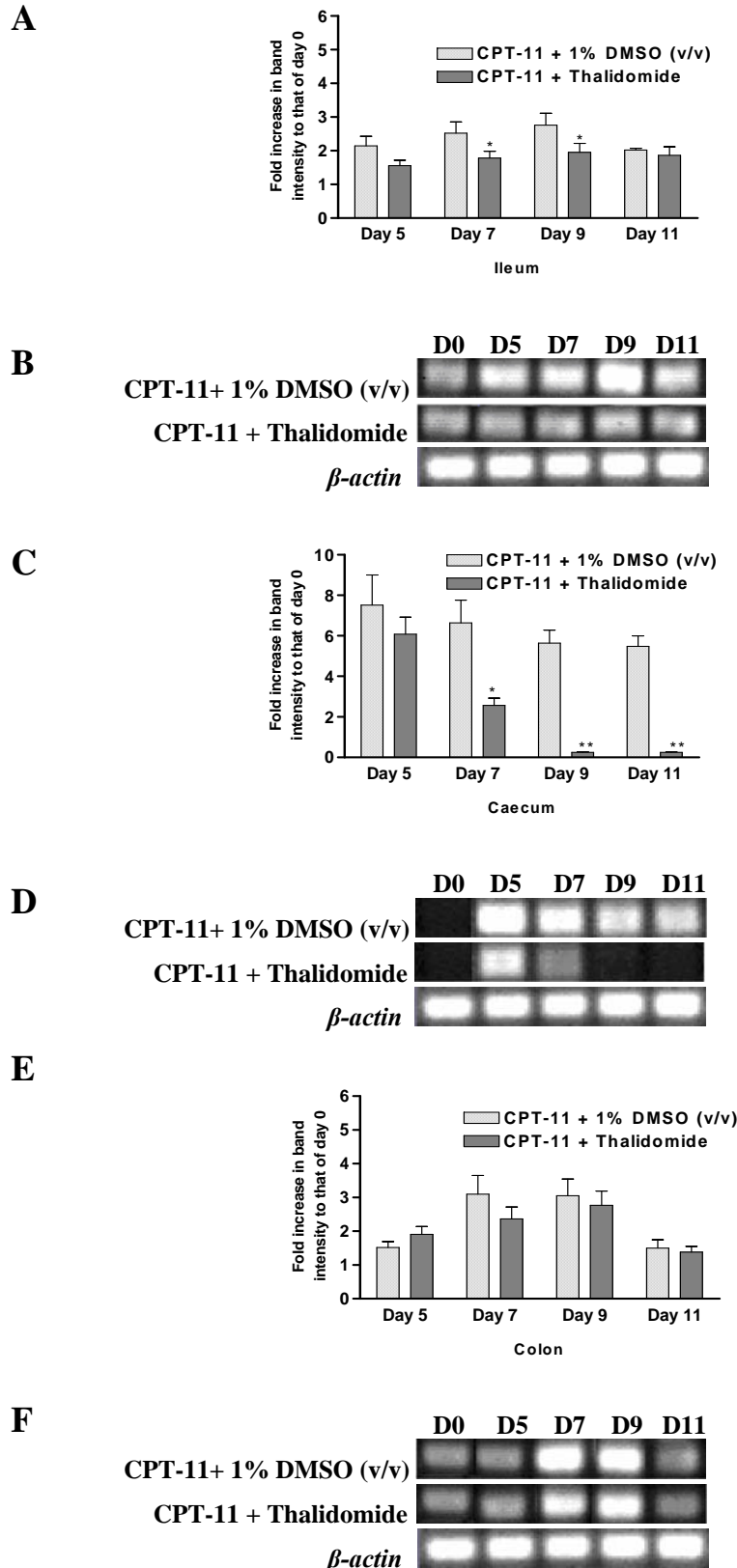
Figure 2-17. Representative illustrations of the development pattern of *TNF-α* expression in ileum (A & B), caecum (C & D), and colon (E & F) after CPT-11 injection on days 0, 5, 7, 9, and 11 from rats treated with CPT-11 with 1% DMSO (v/v) or CPT-11 with thalidomide. B, D, and F, RT-PCR analysis of *TNF-α*; A, C, and E, fold-increase in band intensity compared to that at day 0, obtained from three independent experiments. Significant differences compared with values obtained in rats treated with CPT-11 and 1% DMSO (v/v): *$P < 0.05$; **$P < 0.01$ (N = 4-6).

2.4 CONCLUSION & DISCUSSION

CPT-11 has been widely used for the treatment of a variety of cancers due to its substantial antitumor activity when dose-intensified regimens are applied. However, diarrhea, especially late-onset diarrhea has been observed at higher incidence than with other chemotherapies, which limited the further evaluation of more aggressive regimens using CPT-11 [285, 286]. Although loperamide is used as a standard therapy for management of CPT-11-induced diarrhea, some patients do not respond to it. Therefore, alternative approaches are needed to alleviate the dose-limiting toxicities of CPT-11.

The present study investigated histological changes, cytokine expressions and apoptosis throughout the gastrointestinal tract including ileum, caecum, and colon tissues for the combination of thalidomide with CPT-11. The results demonstrated that coadministered thalidomide ameliorated the gastrointestinal and hematological toxicities of CPT-11 in the rat, as indicated by alleviation of late-onset diarrhea and body weight loss, up-regulation of decreased leukocyte counts, and alleviation of macroscopic and microscopic intestinal damages. These results are consistent with those reported in cancer patients when thalidomide was combined with CPT-11 [277]. In addition, the data showed that combination of thalidomide suppressed the increased intestinal TNF-α and IL-6 as well as splenic IL-6 and IL-1β levels. Furthermore, thalidomide exhibited marked *in vivo* anti-apoptotic effects in intestinal epithelial cells in our study.

Increasing evidence show that chemotherapy-induced intestinal mucositis appears to be associated with intestinal exposure to these drugs which induce epithelial

apoptosis characterized by the generation of DNA fragments through the action of endogenous endonucleases, decreased crypt cell renewal, and destruction of the mucosal architecture, thus leading to the increased Cl^- and Na^+ secretion and severe diarrhea [277]. The findings in our study further support the apoptosis-associated mechanism for CPT-11 induced toxicity. In addition, over-expressions of TNF-α and other pro-inflammatory cytokines such as IL-1 and IL-6 in intestinal mucosa have been reported to be associated with intestinal toxicities induced by cancer chemotherapy agents [287-289]. TNF-α plays a critical role in initiation of chemotherapy-induced primary mucosal damage responses including early damage to connective tissue and endothelium, reduction of epithelial oxygenation, and ultimately, epithelial basal-cell death and injury [278]. In our study, administration of CPT-11 for four consecutive days in rats showed significant increase in TNF-α production in rat intestinal tissues both at protein and mRNA levels, associated with severe diarrhea and histological damages. These findings may support the hypothesis that the intestinal damage induced by CPT-11 results from increased production of pro-inflammatory cytokines like TNF-α.

The combination of thalidomide resulted in decreases in TNF-α production at both protein and mRNA levels compared to the control group treated with CPT-11 alone, accompanied with decreased intestinal IL-6 expression. Studies have shown that blockade of TNF-α also abrogated the production of IL-6 [289]. In addition, co-administered thalidomide showed a marked inhibitory effect on intestinal epithelial cellular apoptosis. A close interaction between intestinal epithelial cellular apoptosis and intestinal pro-inflammatory cytokines expression has been observed. TNF-α has been proven to play an essential role in regulating

intestinal epithelial cellular apoptosis and/or survival during chronic inflammation. The inhibition of intestinal apoptosis by thalidomide might be partially ascribed to the inhibition of TNF-α expression. Thus, the protective effect of thalidomide on CPT-11 induced toxicity might be ascribed to its down-regulatory effect on TNF-α expression. Furthermore, the effects of thalidomide on the inhibition of TNF-α protein expression might be due to its effect on mRNA level of *TNF-α*. As shown in our data, the combination of thalidomide reduced the transcription product levels of *TNF-α* mRNA compared to the group treated with CPT-11 alone, which might be attributed to the increased degradation of *TNF-α* mRNA by thalidomide.

In summary, the increasing understanding for the involvement of TNF-α in CPT-11 induced toxicity and the modulation effects of thalidomide against CPT-11 associated histological damages via regulation of TNF-α expression may provide a new treatment for chemotherapy-associated histological damages by anti-TNF-α agent through the inhibition of inflammatory cytokines expression and intestinal epithelial cellular apoptosis.

CHAPTER 3 EFFECTS OF THALIDOMIDE ON THE PHARMACOKINETICS OF CPT-11 AND THE UNDERLYING MECHANISMS

3.1 INTRODUCTION

Pharmacokinetic study is important for combination cancer therapy given that cytotoxic agents have narrow therapeutic indices. Such information of pharmacokinetic profiles is useful for developing a combination therapy strategy, since the chance for treatment success can be compromised by the failure to anticipate the likely changes in plasma concentration over time when the pharmacokinetics of a drug is significantly altered by concurrent drug administration, or the toxicity of either agent is significantly enhanced.

Clinical study and our study in rats have shown that the combination of thalidomide ameliorated the toxicity induced by CPT-11 [255]. The modulation of cytokine levels (in particular TNF-α inhibition) and intestinal epithelial cellular apoptosis might partially explain this effect; however, pharmacokinetic mechanisms could also be involved. Though spontaneous hydrolysis is the major elimination pathway of thalidomide and CYP2C-mediated metabolism plays only a minor role in its elimination [290], thalidomide can be hydrolyzed to more than a dozen of metabolites *in vivo* [291], which may have modulating effects on the metabolism and transport of other drugs. Preclinical studies have found that co-administration of thalidomide increased the $t_{1/2\beta}$ of the investigational anti-cancer agent DMXAA [292] and decreased the CL of cyclophosphamide and its metabolites from plasma and tissue, with corresponding increases in the AUC. A

recent clinical study in 14 cancer patients revealed that oral administration of thalidomide at 400 mg/day increased the plasma level of CPT-11 by 33.4% ($P <$ 0.05), which may suggest a possible reduced metabolism of CPT-11 to SN-38 and a modest increase in SN-38 glucuronidation by thalidomide [164, 255]. In addition, another study also found a decreased metabolism of irinotecan into SN-38 and SN-38G when it was administered with thalidomide. However, the *in vitro* pharmacokinetic interactions have yet to be investigated to explain the in vivo kinetic changes.

In the present study, we sought to explore the potential kinetic interactions between the two compounds using *in vivo* and *in vitro* models. The rats were chosen in this study as: a) the metabolic pathways of CPT-11 in rats and humans are similar, despite the presence of species differences in the contribution of enzymes for individual pathways; b) the transport and elimination routes of CPT-11 in rats and humans are also similar; and c) rats facilitate pharmacokinetic studies by allowing repeated blood sampling. Thus, the data on CPT-11 arising from rats might be readily extrapolated to humans. Furthermore, the effect of thalidomide and its hydrolytic products on the rat plasma protein binding of CPT-11 and SN-38 was examined. Moreover, rat liver microsomes and a rat hepatoma cell line, H4-II-E cells, were used to study the possible metabolic interactions between these two drugs. In addition, H4-II-E cells were also used to investigate the effect of thalidomide and its hydrolytic products on the transport of CPT-11 and SN-38. This cell line has been widely used to investigate drug metabolism and transport *in vitro* since it expresses substantial Phase I and Phase II drug metabolizing enzymes and drug transporters such as Pgp [293].

3.2   MATERIALS AND METHODS

3.2.1   Chemicals

CPT analogues including irinotecan (CPT-11), CPT and SN-38, verapamil hydrochloride (all compounds with a purity > 99.0%) were purchased from SinoChem Ningbo Import and Export Co. (Ningbo, China). The ion-pairing reagent sodium 1-heptane-sulfonate, lyophilized type IX-A β-glucuronidase (from Escherichia coli, with activity of 1,724,400 units per gram solid form), probenecid, nifedipine, bilirubin, bis (p-nitrophenyl) phosphate sodium salt (BNPP), uridine diphosphate glucuronic acid (UDPGA), D-saccharic acid 1,4-lactone, N-[2-hydroxyethyl]piperazine-N'-4-butanesulfonic acid (HEPES), Hank's balanced salt solution (HBSS), Dulbecco's modified Eagle's medium (DMEM), trypan blue were all purchased from Sigma Chemical Co. (St. Louis, Mo. USA). The leukotriene antagonist MK-571 was a gift from Dr. Ford Hutchinson (Merck Frosst Canada, Inc.) [294]. Fetal bovine serum was obtained from Hyclone Lab Inc. (Logan, UT, USA). Phthaloyl glutamic acid (PGA, a hydrolytic product of thalidomide, with a purity > 99.0% as determined by HPLC) was a gift provided by Dr. Tom Pui-Kai Li, School of Pharmacy, Ohio State University, Cincinnati, USA. All other reagents were of analytical or HPLC grade as appropriate. The hydrolytic products of thalidomide were prepared by incubation of thalidomide with 0.1 M phosphate buffer at pH 7.4 overnight at room temperature (22°C).

3.2.2   Animals

Refer to Section 2.2.2.

3.2.3   Drug administration and sampling

Single-dose thalidomide treatment and multiple-dose thalidomide treatment pharmacokinetic studies for the combination of CPT-11 and thalidomide were carried out. For the single-dose thalidomide treatment study, rats were randomized to two groups with one group receiving CPT-11 at 60 mg/kg by i.v. and control vehicle (1% DMSO, v/v) by i.p. at 1 ml/kg given 30 min before CPT-11 injection, and another group of rats treated with CPT-11 at 60 mg/kg by i.v. in combination with thalidomide (100 mg/kg by i.p. given 30 min prior to CPT-11 injection). Blood samples (200 μl) were collected in heparinised tubes at 0.25, 0.5, 1, 2, 4, 6, 8, and 10 hr following CPT-11 administration. Plasma was obtained by immediate centrifugation at $1,500 \times g$ for 10 min at 4ºC. After protein precipitation and simple liquid extraction procedure, plasma concentrations of CPT-11 and its major metabolites were determined by a validated HPLC method. Similar blood sampling procedure was used for the 5-day multiple-dose thalidomide treatment study, whereas thalidomide or the control vehicle (1% DMSO, v/v) at 1 ml/kg/day by i.p. was given for five consecutive days before CPT-11 injection. CPT-11 was administered by i.v. injection 30 min after thalidomide injection on the 5th day.

Similar schedule was also adopted for the study of the effect of CPT-11 on the plasma pharmacokinetics of thalidomide except that CPT-11 was given 30 min before thalidomide injection. To account for the effect of the delivery vehicle (i.e. vehicle used for dissolving CPT-11), another group of rats treated with thalidomide (100 mg/kg, i.p.) was also pre-treated with the delivery vehicle [sterile-filtered D-sorbitol (45 mg/ml) and D-lactic acid (0.9 mg/ml) in Milli-Q water, pH 3.5] by i.v. injection.

73

3.2.4 Rat plasma and liver microsome preparation

Livers and blood were collected from healthy male Sprague Dawley rats and livers were stored at -80°C until used. Plasma was freshly separated by centrifugation at 1000 × g for 15 min. Hepatic microsomes were prepared by differential centrifugation as described. Briefly, liver samples were thawed and weighed, and then 3 volumes of ice-cold homogenisation medium (0.1 M sodium phosphate buffer with 1.5% KCl at pH 7.4) were added. This and all the subsequent operations were carried out on ice. The tissue samples were chopped using scissors, and homogenised with a Heidolph homogenizer (Heidolph Instruments GmbH & Co. KG, Germany) at 500 rpm for 2 min on ice. The resultant homogenates were transferred to centrifuge tubes, and centrifuged at 9,000 × g for 20 min at 4°C. The supernatant (S9) was collected and centrifuged at 105,000 × g for 1 hr at 4°C using an ultracentrifuge (Type 70 Ti Rotor, Beckman Coulter, Inc. Fullerton, CA, USA). The supernatant fraction served as a cytosol source. The microsome pellet was resuspended with homogenization medium. Hepatic microsomal suspensions were aliquoted (0.5 ml) into a 1.5-ml test tube and stored at -80°C until used. Microsomal protein concentration was determined by the Bradford method (Sigma, St. Louis, MO. USA) with bovine serum albumin as the standard.

3.2.5 *In vitro* plasma protein binding assay

The effects of thalidomide (25 and 250 μM) and its hydrolytic products (total concentration of 10 μM) on the protein binding of CPT-11 and SN-38 were investigated in drug-free fresh plasma from healthy male Sprague Dawley rats using an ultrafiltration method followed by drug determination using HPLC. CPT-

11 or SN-38 was added to rat plasma, followed by addition of thalidomide or its hydrolytic products. The samples (500 µl) were incubated at 37°C for 30 min in a water bath with gentle shaking. Control incubations with 1% DMSO (v/v) were also undertaken, which showed no significant effects on CPT-11 or SN-38 plasma protein binding. After incubation, an aliquot (400 µl) of the plasma sample was transferred to the Centrisart ultrafiltration device (20,000 molecular weight cut-off, Sartorius Corporation, Germany), and centrifuged at 2,000 $\times$ g for 30 min at 37°C. Samples were capped to minimize changes in pH during filtration. After centrifugation, an aliquot (100 µl) was taken from the ultrafiltrate to determine the CPT-11 or SN-38 concentration using a validated HPLC method. Before ultrafiltration, an aliquot of plasma sample (50 µl) was taken to measure the total concentration of CPT-11 or SN-38. The fraction of unbound (f_u) CPT-11 or SN-38 was calculated by the ratio of the drug concentration in the ultrafiltrate to that in the rat plasma before ultrafiltration.

3.2.6 Hepatic microsomal incubation and metabolic inhibition study

In vitro rat hepatic microsomal incubation conditions for CPT-11 and SN-38 metabolism were optimized with regard to microsomes concentration, incubation time, and substrate concentration. In particular, incubation time (5-90 min) and microsomal protein concentration (0.125-10 mg protein/ml) were tested to identify optimal conditions that resulted in quantifiable and linear formation of SN-38 and SN-38G. The formation of SN-38 from CPT-11 and formation of SN-38G from SN-38 were determined using a validated HPLC method. For SN-38G, it was converted to SN-38 by incubation with β-glu.

To investigate the effect of thalidomide (25 and 250 µM) and its hydrolytic products (total concentration of 10 µM) on CPT-11 hydrolysis and SN-38 glucuronidation in rat hepatic microsomes, CPT-11 or SN-38 was incubated with hepatic microsomes (2.0 mg protein/ml for CPT-11 and 1.0 mg protein/ml for SN-38) in 200 µl incubation buffers containing either thalidomide or its hydrolytic products for 30 min. The incubation buffer was 0.1 M sodium phosphate buffer (pH 7.4) for CPT-11 and 0.1 M sodium phosphate buffer (pH 6.8) containing 4 mM UDPGA, 10 mM $MgCl_2$, 1 mM D-saccharic acid 1,4-lactone for SN-38. Both low and high concentrations of CPT-11 (0.5 or 78 µM, that corresponded to the high-affinity K_{m1} and low-affinity K_{m2} obtained from the best fit two-binding site model) or SN-38 (5.0 µM or 18.2 µM, which is the K_m obtained from one-enzyme equation) were used. Control incubations with 1% DMSO (v/v) were also undertaken, which showed no significant effect on the liver microsomal metabolism of CPT-11 and SN-38. SN-38 and SN-38G formation was measured as pmol/min/mg protein. In addition, the known CE inhibitor nifedipine (100 µM) and BNPP (100 µM) were used as positive control for CPT-11 hydrolysis; while nifedipine (100 µM) and bilirubin (100 µM) were used as positive control for SN-38 glucuronidation. Inhibition was expressed as percentage of the control.

3.2.7 Cell culture

H4-II-E cells were obtained from the American Type Culture Collection (Rockville, MD) and cultured in complete DMEM supplemented with 10% fetal bovine serum, 100 U/ml penicillin G and 100 µg/ml streptomycin. The cells were grown in an atmosphere of 5% CO_2 /95% air at $37^{o}C$ and given fresh medium

every 3 or 4 days. Experiments were performed on cells within 10 passages. Viable cells were counted using the trypan blue exclusion method.

3.2.8 Cytotoxicity assay in rat hepatoma H4-II-E cells

The cytotoxic effects of CPT-11, SN-38, thalidomide, and its hydrolytic products on H4-II-E cells were determined using the 3-(4,5-dimethylthiazol-2-yl)-2,5-diphenyltetrazonium bromide (MTT) assay. Drugs were diluted in culture medium and added to the cultures 24 hr after cell seeding. Cells were exposed to drugs at different concentrations in culture medium for 4 or 48 hr, after which 0.05 mg MTT was added to each well, and the plates were further incubated for 4 hr. Thereafter, supernatants were removed and the purple precipitates were dissolved in 100 µl DMSO each. The absorbance of formazan, a metabolite of MTT, was measured at a wavelength of 595 nm using a microplate reader (Tecan Instrument Inc., Research Triangle Park, NC, USA). The cytotoxicity was reported as IC_{50} value that is the drug concentration causing 50% of growth inhibition compared with the control (1% DMSO, v/v). The IC_{50} values were the means of at least three independent experiments, each performed in replicate of eight for each drug concentration.

3.2.9 Metabolic inhibition assay for CPT-11 and SN-38 in rat hepatoma H4-II-E cells

For the metabolism study, H4-II-E cells were grown in BD Falcon^{TM} cell culture dishes (BD Biosciences, San Jose, CA, USA). Different concentrations of CPT-11 (0.5-50 µM) and SN-38 (0.1-5.0 µM) in DMEM medium were added to confluent cell cultures. An aliquot of the culture medium (0.1 ml) was collected from each

dish over 120 min, mixed with 300 μl extraction solution (0.01 M HCl : methanol, 1:1, v/v) containing the internal standard (I.S.), CPT. After vortex-mixing and centrifugation at $3,000 \times g$ for 10 min, the concentration of the supernatant was analyzed by HPLC. The production of SN-38G was determined by the conversion of SN-38G to SN-38 by incubating it with β-glu. Viable cells were monitored using the trypan blue exclusion method and the productions of SN-38 and SN-38G were expressed as pmol/min/10^6 cells.

The effects of thalidomide (25 and 250 μM) and its hydrolytic products (total concentration of 10 μM) on CPT-11 hydrolysis and SN-38 glucuronidation in rat hepatoma H4-II-E cells were investigated in triplicate using optimized incubation conditions. Briefly, cells were preincubated with thalidomide or its hydrolytic products for 2 hr. After removal of the tested drugs, the cells were washed twice with PBS and then exposed to CPT-11 (10 μM) or SN-38 (1 μM) for 5 min. Thalidomide or its hydrolytic products were also added to the culture together with CPT-11 or SN-38 to test their co-incubation effects on CPT-11 or SN-38 metabolism. Control incubations containing an equal amount of 1% DMSO (v/v) were also conducted. DMSO was also used to dissolve inhibitors. In addition, the positive controls for the microsomal metabolic inhibition studies as described above were also conducted here.

Because fetal bovine serum in the culture medium might interfere with the metabolism of CPT-11 and SN-38, incubations were also done in HBSS containing 10 mM HEPES to rule out the serum effect on the metabolism of these drugs by thalidomide and its hydrolytic products.

3.2.10 Inhibition assay for intracellular accumulation of CPT-11 and SN-38 in rat hepatoma H4-II-E cells

The intracellular accumulation of CPT-11 and SN-38 in H4-II-E cells was examined in confluent cell cultures grown in BD Falcon^{TM} cell culture dishes (BD Biosciences, San Jose, CA, USA) as described [138]. CPT-11 (0.5-50 µM) or SN-38 (0.1-5.0 µM) in DMEM medium was added to exponentially growing cell cultures. The medium was aspirated off at the indicated times over 120 min, and the dishes were rapidly washed five times with ice-cold PBS. HPLC analysis of final washes ensured that they contained no residual CPT-11 or SN-38. The cells were then scraped off and each cell pellet was suspended in 200 µl extraction solution (0.01M HCl: methanol, 1:1, v/v) containing CPT (used as the I.S.). After vortex-mixing, the cellular homogenates were sonicated and centrifuged at 15,000 × g for 15 min, and the supernatants were analyzed by HPLC. The intracellular accumulation of CPT-11 and SN-38 was expressed as pmol/min/10^6 cells.

The effects of thalidomide (25 and 250 µM) and its hydrolytic products (total concentration of 10 µM) on CPT-11 and SN-38 intracellular accumulation in rat hepatoma H4-II-E cells were investigated in triplicate using optimized incubation conditions. Briefly, cells were preincubated with thalidomide or its hydrolytic products for 2 hr. After removal of these tested drugs, the cells were washed twice with PBS and exposed to CPT-11 (10 µM) for 30 min or SN-38 (1 µM) for 5 min. Thalidomide or its hydrolytic products were also added to the cell culture together with CPT-11 or SN-38 to test their co-incubation effects on CPT-11 or SN-38 accumulation. In addition, the effects of the Pgp or MRP inhibitors including MK-571 (100 µM), verapamil (200 µM), probenecid (200 µM), and nifedipine (100

μM) on the intracellular accumulation of CPT-11 or SN-38 were also examined. Similar incubations of CPT-11 or SN-38 were also performed in HBSS containing HEPES to avoid the interference of fetal bovine serum in the cell culture studies.

3.2.11 Determination of CPT-11, SN-38, and SN-38 glucuronide and thalidomide by HPLC methods

A Shimadzu HPLC system (Shimadzu Corporation, Japan) was used to quantify the CPT-11, SN-38, SN-38G, and thalidomide concentrations in different biological matrices. The chromatographic system consisted of a Shimadzu SCL-10A$_{VP}$ system controller, a LC-10AT$_{VP}$ pump, a DGU-14A degasser, a RF-10A XL fluorescence detector (for CPT-11 and SN-38) or a SPD-M10A$_{VP}$ diode array detector (for thalidomide), and a SIL-10AD$_{VP}$ autoinjector. Data were monitored and analysed using the CLASS VP software. A stainless steel (200 mm × 4.6 mm i.d.) analytical column packed with 5 μm Hyperclon ODS (C18) material (Phenomenex, Torrance, CA, USA) preceded by a Phenomenex C18 guard cartridge was used for separation of test compounds.

The mobile phase for the determination of CPT-11 and its metabolites was composed of acetonitrile-50 mM disodium hydrogen phosphate buffer containing 10 mM sodium 1-heptane-sulfonate, with the pH adjusted to 3.0 with 85% (w/v) orthophosphoric acid (27/73, v/v). The mobile phase was delivered at a flow-rate of 1.0 ml/min, and the column effluent was monitored at 540 nm with an excitation wavelength of 380 nm.

Plasma concentrations of CPT-11, SN-38, and SN-38G in rats were determined. Briefly, the rat plasma was divided into 2 aliquots (50 μl each): one for CPT-11

and SN-38 analysis and the other for SN-38G determination using β-glu. For CPT-11 or SN-38 concentration determination, each sample was allowed to thaw at room temperature, and 50 µl of a solution of CPT (I.S.) (4 µg/ml) and 100 µl of a mixture of acetonitrile-1mM orthophosphoric acid (90:10, v/v) were added to 50 µl plasma. The tube was vortex-mixed for 10 sec, and centrifuged at 6,000 × g for 10 min. An aliquot of 150 µl of the resultant supernatant was added to 175 µl 50 mM disodium hydrogen phosphate (pH 3.0) buffer. After vortex-mixing, 100 µl of this mixture was injected into the HPLC system. For SN-38G analysis, the β-glu was dissolved in the 0.1 M sodium phosphate buffer (pH 6.4) to obtain a concentration of 20,000 units/ml. An aliquot of rat plasma sample (50 µl) was incubated in water bath with 50 µl of the solution of β-glu (1,000 units) for 2 hr at 37ºC. Then the samples were processed by the same procedures as for CPT-11 and SN-38, except that the volumes of all the added solutions were doubled.

The CPT-11 and SN-38 concentrations in the ultrafiltrate were determined by mixing an aliquot of ultrafiltrate (100 µl) with 200 µl H_3PO_4-acetonitrile (10:90, v/v) and 100 µl CPT (I.S.). After vortex-mixing, an aliquot (100 µl) of the mixture was injected into the HPLC system. The CPT-11 and SN-38 concentrations in the cell homogenate, culture medium or microsome were determined after simple liquid extraction by the addition of 0.01M HCl: methanol mixture (1:1, v/v) or H_3PO_4: acetonitrile (10:90, v/v), both containing CPT as I.S.

The plasma concentrations of thalidomide in rats were determined. Briefly, the plasma protein was precipitated by the addition of 200 µl of ice-cold acetonitrile: methanol (1:1, v/v) containing 2% (v/v) acetic acid and 10 µl of 2.79 mM phenacetin solution (used as I.S.) to 100 µl of plasma samples, then centrifuged at

3,000 × *g* for 10 min. An aliquot (20 μl) of the supernatant was injected into the HPLC system with the eluted peaks monitored using a UV detector at 220 nm. The mobile phase consisting of acetonitrile-10 mM ammonium acetate buffer (pH 5.5) (28/72, v/v) was delivered at a flow rate of 0.8 ml/min. Acidifying and quick chilling of the plasma samples by ice-cold organic solvents with 2% acetic acid (to pH 4.0) were used to prevent the spontaneous degradation of thalidomide.

All HPLC methods used in this study were well validated. Calibration curves were linear over the concentration ranges (CPT-11 and SN-38: 0.01-10 μM; thalidomide: 0.02-50 μM) with mean correlation coefficients being greater than 0.995 (n ≥ 3). All methods had acceptable accuracy (85-115% of true values) and precision (intra- and inter-assay coefficient variations < 15%) over the concentration ranges (CPT-11 and SN-38: 0.01-10 μM; thalidomide: 0.02-50 μM). For higher concentrations exceeding the linear concentration range, validation for the dilution was also conducted and resulted in acceptable accuracy and precision. The limits of quantitation for CPT-11, SN-38, and SN-38G in rat plasma or in rat plasma ultrafiltrate were 0.005 μM, and 0.003 μM for CPT-11 and 0.002 μM for SN-38 in cellular homogenate and culture medium. This value was 0.02 μM for thalidomide in rat plasma. Assay specificities for CPT-11, SN-38, and SN-38G determination were indicated by the absence of interfering chromatographic peaks in rat plasma or plasma ultrafiltrate in the presence of potentially combined drugs such as thalidomide, or its hydrolytic products, nifedipine, probenecid, MK-571, or verapamil. Similarly, a lack of interfering peaks in rat plasma in the presence of drugs such as CPT-11, SN-38, and CPT indicated good assay specificity for thalidomide determination.

3.2.12 Liquid chromatography-mass spectrometry (LC-MS)

The liquid chromatography-mass spectrometry (LC-MS) analysis was conducted to confirm the structures of metabolites of CPT-11 formed in rat liver microsomes and rat hepatoma H4-II-E cells. A Finnigan MS system (Thermo Finnigan, Egelsbach, Germany) equipped with an electrospray ionization source was used for mass analysis. Mass spectrometric analysis was performed in the positive ion mode and set up in the selected ion monitoring mode. Nitrogen was used as the sheath gas and the auxiliary gas. The capillary temperature was at $350^{\circ}C$. The spray voltage was set at 3,500 V. The protonated molecule $[M+H]^{+}$ was identified as quantifying ion.

3.2.13 Pharmacokinetic calculation

The plasma concentration-time curves were obtained by plotting the mean plasma concentrations of each analyte versus time on a semi-logarithmic scale. Pharmacokinetic parameters were calculated by standard model-independent pharmacokinetic formulae using WinNonlin program (Scientific Consulting Inc., North Carolina, USA). The $t_{1/2\beta}$ value was calculated as $0.693/\beta$, where β is the elimination rate constant calculated from the terminal linear portion of the log plasma concentration-time curve. The total areas under plasma concentration-time curve from time zero to the last quantifiable time point (AUC_{0-t}) and from time zero to infinity ($AUC_{0-\infty}$) were calculated using the log trapezoidal rule. The CL was estimated by dividing the total administered dose by the $AUC_{0-\infty}$. The C_{max} for thalidomide and the metabolites of CPT-11 (SN-38 and SN-38G) was obtained by visual inspection of the plasma concentration-time curve, whereas the initial drug concentration (C_0, the extrapolated concentration at zero time) of CPT-11

83

was calculated by back extrapolation of the plasma concentration-time curve to Y-axis. Alternatively, C_0 can be calculated by Dose/V_d. The volume of distribution (V_d) was calculated by dividing CL by β. The apparent CL and V_d values of thalidomide (i.e. CL/F and V_d/F) were determined as for CPT-11 herein, assuming its bioavailability was complete after i.p. injection (100%).

3.2.14 Statistical analysis

Refer to 2.2.11.

3.3 RESULTS

3.3.1 Thalidomide altered the plasma pharmacokinetics of CPT-11

For the single-dose thalidomide treatment study, co-administered thalidomide significantly ($P < 0.05$) increased the AUC_{0-10hr} and $AUC_{0-\infty}$ of CPT-11 by 32.50% and 39.02%, respectively. By contrast, these values for SN-38 were significantly ($P < 0.01$) decreased by 24.58% and 42.62%, respectively (Figure 3-1 and Table 3-1). The value of $t_{1/2\beta}$ for SN-38 in rats treated with CPT-11 in combination with thalidomide was significantly lower compared to rats treated with CPT-11 and control vehicle (1% DMSO, v/v) (4.37 *vs.* 7.18 hr, $P < 0.01$). However, the combination of thalidomide did not significantly alter the pharmacokinetic parameters of SN-38G.
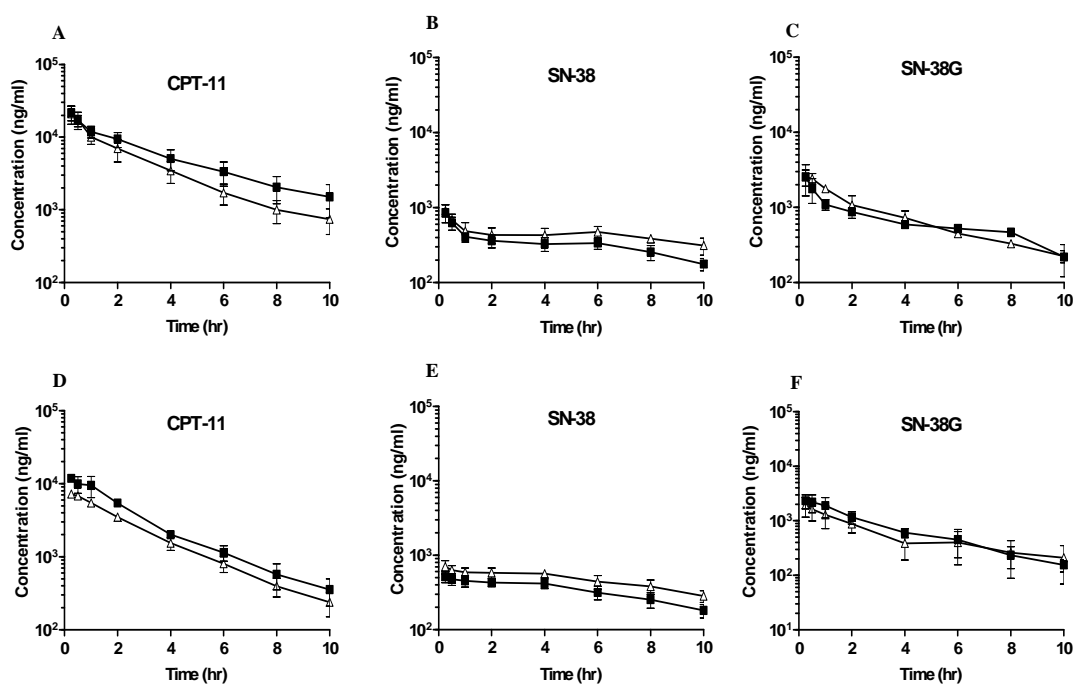
Figure 3-1. Plasma concentration-time profiles for CPT-11, SN-38, and SN-38 glucuronide (SN-38G) in rats treated with CPT-11 and 1% DMSO (v/v) (control vehicle) or CPT-11 in combination with thalidomide. A, B, & C, single-dose thalidomide treatment kinetic study; D, E, & F, 5-day multiple-dose thalidomide treatment kinetic study. ■, CPT-11 + Thalidomide; Δ, CPT-11 + 1% DMSO (v/v) (N = 5).

For the 5-day multiple-dose thalidomide treatment study, pretreatment of rats with thalidomide at 100 mg/kg by i.p. significantly increased the C_0, $AUC_{0-10hr,}$ and $AUC_{0-\infty}$ of CPT-11 by 85.56% ($P < 0.05$), 45.49% ($P < 0.01$), and 44.82% ($P < 0.01$), respectively, but decreased the V_d and CL of CPT-11 by 38.98% and 43.03%, respectively ($P < 0.01$) (Figure 3-1 and Table 3-2). The values of AUC_{0-10hr} and $AUC_{0-\infty}$ for SN-38 were significantly decreased in rats treated with CPT-11 in combination with thalidomide by 28.12% ($P < 0.05$) and 37.53% ($P < 0.01$), respectively, compared with rats receiving CPT-11 and the control vehicle (1% DMSO, v/v). However, there was no significant change in the pharmacokinetic parameters of SN-38G.

Table 3-1. Comparison of pharmacokinetic parameters between two groups of rats treated with a single dose of CPT-11 and control vehicle (1% DMSO, v/v) or a single dose of CPT-11 with thalidomide (N = 5). ns, not significant.

Parameters	Treatment Groups		Change (%)	P value*
	CPT-11 + Thalidomide	CPT-11 + 1% DMSO (v/v)		
CPT-11				
C_0 (µg/ml)	30.11 ± 19.19	25.23 ± 7.59	19.36	ns
$t_{1/2\beta}$ (hr)	2.93 ± 0.64	2.59 ± 0.51	13.16	ns
AUC_{0-10hr} (µg·hr/ml)	60.91 ± 11.57	45.97 ± 10.96	32.50	<0.05
$AUC_{0-\infty}$ (µg·hr/ml)	67.29 ± 14.96	48.40 ± 11.79	39.02	<0.05
V_d (L/kg)	3.77 ± 0.27	4.87 ± 1.39	-22.51	ns
CL (L/hr/kg)	0.94 ± 0.26	1.34 ± 0.49	-29.68	ns
SN-38				
C_{max} (µg/ml)	0.86 ± 0.23	0.92 ± 0.17	-5.91	ns
$t_{1/2\beta}$ (hr)	4.37 ± 0.64	7.18 ± 1.48	-39.05	<0.01
AUC_{0-10hr} (µg·hr/ml)	3.31 ± 0.42	4.39 ± 0.70	-24.58	<0.01
$AUC_{0-\infty}$ (µg·hr/ml)	4.45 ± 0.66	7.75 ± 1.85	-42.62	<0.01
SN-38G				
C_{max} (µg/ml)	2.57 ± 1.15	2.57 ± 0.58	0.04	ns
$t_{1/2\beta}$ (hr)	4.38 ± 1.72	3.74 ± 1.32	17.02	ns
AUC_{0-10hr} (µg·hr/ml)	6.86 ± 0.95	7.74 ± 0.39	-11.39	ns
$AUC_{0-\infty}$ (µg·hr/ml)	8.54 ± 0.14	8.97 ± 0.27	-4.81	ns

*Comparison of the two groups using Student's unpaired *t*-test.

Table 3-2. Comparison of pharmacokinetic parameters between two groups of rats treated with CPT-11 and control vehicle (1% DMSO, v/v) or CPT-11 in combination with thalidomide for 5 consecutive days (N = 5). ns, not significant.

Parameters	Treatment Groups		Change (%)	P value*
	CPT-11 + Thalidomide	CPT-11 + 1% DMSO (v/v)		
CPT-11				
C_0 (µg/ml)	14.28 ± 1.25	7.70 ± 0.27	85.56	<0.05
$t_{1/2\beta}$ (hr)	2.13 ± 0.58	1.91 ± 0.13	11.33	ns
AUC_{0-10hr} (µg·hr/ml)	29.60 ± 1.32	20.35 ± 2.23	45.49	<0.01
$AUC_{0-\infty}$ (µg·hr/ml)	30.28 ± 0.93	20.91 ± 2.35	44.82	<0.01
V_d (L/kg)	4.85 ± 1.10	7.95 ± 0.71	-38.98	<0.01
CL (L/hr/kg)	1.65 ± 0.45	2.90 ± 0.36	-43.03	<0.01
SN-38				
C_{max} (µg/ml)	0.52 ± 0.08	0.70 ± 0.14	-26.36	ns
$t_{1/2\beta}$ (hr)	5.06 ± 1.50	6.86 ± 1.82	-26.31	ns
AUC_{0-10hr} (µg·hr/ml)	3.43 ± 0.53	4.78 ± 0.66	-28.12	<0.05
$AUC_{0-\infty}$ (µg·hr/ml)	4.80 ± 0.93	7.68 ± 0.84	-37.53	<0.01
SN-38G				
C_{max} (µg/ml)	2.40 ± 0.75	1.93 ± 0.75	24.56	ns
$t_{1/2\beta}$ (hr)	2.50 ± 0.18	3.92 ± 2.21	-36.12	ns
AUC_{0-10hr} (µg·hr/ml)	7.38 ± 1.67	5.68 ± 2.43	29.92	ns
$AUC_{0-\infty}$ (µg·hr/ml)	7.90 ± 1.74	6.99 ± 4.04	13.01	ns

*Comparison of the two groups using Student's unpaired *t*-test.

3.3.2 CPT-11 did not alter the plasma pharmacokinetics of thalidomide
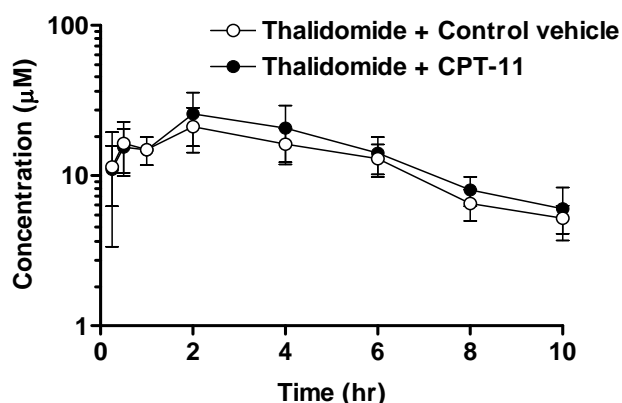
Figure 3-2. Plasma concentration-time profiles for thalidomide in rats treated with thalidomide and control vehicle or thalidomide in combination with CPT-11 (N = 5).

Figure 3-2 shows the representative plasma concentration-time profiles of thalidomide in animals treated with thalidomide and the control vehicle, or thalidomide in combination with CPT-11. Co-administration of CPT-11 (i.v., 60 mg/kg) insignificantly ($P > 0.05$) increased the C_{max} and plasma AUC_{0-10hr} of thalidomide by 32.29% and 11.66%, respectively, as compared to the control rats (Table 3-3). These results indicated that coadministered CPT-11 did not significantly alter the plasma pharmacokinetic of thalidomide in rats.

Table 3-3. Pharmacokinetic parameters of thalidomide in rats treated with thalidomide and control vehicle or thalidomide in combination with CPT-11 (N = 5). ns, not significant.

| Parameter | Treatment | | Change % | P value* |
	Thalidomide + CPT-11	Thalidomide + Control vehicle		
Dose/kg (mg)	100 (258 μmol)	100 (258 μmol)	-	-
C_{max} (μM)	25.72 ± 10.00	19.44 ± 7.00	32.29	ns
T_{max} (hr)	2.00 ± 0.00	2.00 ± 0.00	0	ns
AUC_{0-10hr} (μM·hr)	149.02 ± 52.58	133.46 ± 39.17	11.66	ns
V_d/F (L/kg)	11.88 ± 3.44	13.89 ± 7.30	-14.51	ns
β (1/hr)	0.19 ± 0.03	0.20 ± 0.06	-3.43	ns
$t_{1/2\beta}$ (hr)	3.71 ± 0.69	3.75 ± 1.00	-0.89	ns
$AUC_{0-\infty}$ (μM·hr)	186.74 ± 56.56	165.10 ± 37.55	13.10	ns
CL/F (L/hr/kg)	2.24 ± 0.71	2.49 ± 0.79	-10.04	ns

*Comparison of the two groups using Student's unpaired *t*-test.

3.3.3 Effects of thalidomide and its hydrolytic products on the plasma protein binding of CPT-11 and SN-38

CPT-11 and SN-38 are 80% and 99% bound in blood, respectively [65]. Since pharmacokinetic parameters of highly plasma protein bound drugs can be significantly altered by plasma protein binding displacement by combined drugs, we examined whether thalidomide and its hydrolytic products altered the plasma protein binding of CPT-11 and SN-38.

As expected, our data showed that CPT-11 and SN-38 were bound extensively to the rat plasma proteins (Table 3-4). Thalidomide (25 and 250 μM) and its hydrolytic products (total concentration at 10 μM) did not significantly alter the plasma protein binding of CPT-11 and SN-38.

Table 3-4. Effects of thalidomide and its hydrolytic products on the plasma protein binding of CPT-11 and SN-38.

Substrate concentration (μM)	Inhibitor concentration (μM)	f_u (Mean ± SD)	N
CPT-11			
1	0 (Control)	0.047 ± 0.007	3
	25 (TH)	0.041 ± 0.002	3
	250 (TH)	0.044 ± 0.000	3
20	0 (control)	0.109 ± 0.004	6
	10 (TH hydrolytic products)	0.113 ± 0.003	6
50	0 (Control)	0.164 ± 0.003	3
	25 (TH)	0.163 ± 0.004	3
	250 (TH)	0.176 ± 0.007	3
SN-38			
0.5	0 (Control)	0.237 ± 0.007	3
	25 (TH)	0.232 ± 0.003	3
	250 (TH)	0.233 ± 0.006	3
1.0	0 (Control)	0.201 ± 0.003	6
	10 (TH hydrolytic products)	0.200 ± 0.000	6
2.5	0 (Control)	0.217 ± 0.006	3
	25 (TH)	0.220 ± 0.004	3
	250 (TH)	0.216 ± 0.015	3

TH = Thalidomide.

3.3.4 Effects of thalidomide and its hydrolytic products on the hepatic microsomal metabolism of CPT-11 and SN-38

For the hydrolysis of CPT-11, linear SN-38 formation was observed with incubation time from 5 to 90 min and with rat liver microsomes from 0.125 to 4.0 mg microsomal protein/ml. An optimal protein concentration of 2.0 mg/ml and incubation time of 30 min were chosen for further inhibition studies. For the glucuronidation of SN-38, linear SN-38 formation was observed with incubation times of 15 to 60 min and with rat liver microsomes of 0.25 to 2.0 mg microsomal protein/ml. Thus, a protein concentration of 1.0 mg microsomal protein/ml and an incubation time of 30 min were chosen for further inhibition studies. By comparing the models, hydrolysis of CPT-11 to form SN-38 in rat liver microsomes was best fitted by a two binding-site model with an estimated K_{m1} and K_{m2} of 0.5 and 78 μM, respectively, and V_{max1} and V_{max2} of 0.58 and 2.34 pmol/min/mg protein, respectively (Figure 3-3 and Table 3-5). In addition, glucuronidation of SN-38 in rat liver microsomes was best fitted by a one-enzyme equation with an estimated K_m of 18.2 μM and a V_{max} of 185.6 pmol/min/mg protein.

The effects of thalidomide and its hydrolytic products on CPT-11 hydrolysis and SN-38 glucuronidation are shown in Figure 3-5 and Figure 3-4, respectively. Thalidomide (25 μM or 250 μM) had no inhibitory effects on CPT-11 (0.5 and 78 μM) hydrolysis; while the hydrolytic products of thalidomide (10 μM) significantly ($P < 0.01$) decreased the CPT-11 (0.5 μM) hydrolysis by 15.6%. The hydrolytic products of thalidomide significantly inhibited CPT-11 (0.5 μM)

hydrolysis in a concentration-dependent manner. However, both thalidomide and

its hydrolytic products had no significant effects on SN-38 glucuronidation.
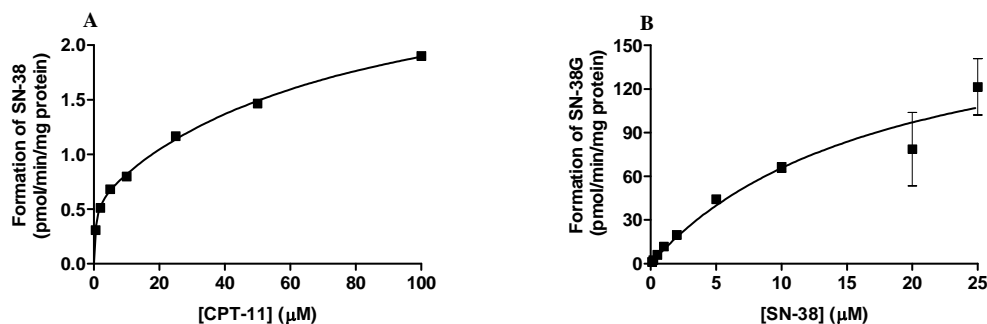
Figure 3-3. Effects of substrate concentration on the formation of SN-38 from CPT-11 (A) and SN-38 glucuronide from SN-38 (B) in rat liver microsomes. The curves represent the best fit of two- and one-binding site models, respectively.

Table 3-5. Estimated K_m and V_{max} values for the metabolism or intracellular accumulation of CPT-11 and SN-38 *in vitro* (N = 3).

Substrate/Reaction or transport	Best fit model	K_m (µM)		V_{max} [a]	
		K_{m1}	K_{m2}	V_{max1}	V_{max2}
Rat liver microsomes					
CPT-11/hydrolysis	Two binding-site	0.50	78	0.58	2.34
SN-38/glucuronidation	One binding-site		18.20		185.60
H4-II-E cells					
CPT-11/hydrolysis (DMEM)	One binding-site		43.80		9.68
CPT-11/SN-38G formation (DMEM)	One binding-site		21.22		1.59
CPT-11/hydrolysis (HBSS)	One binding-site		44.47		6.53
CPT-11/SN-38G formation (HBSS)	One binding-site		30.81		1.01
SN-38/glucuronidation (DMEM)	One binding-site		2.50		278.8
SN-38/glucuronidation (HBSS)	One binding-site		3.62		221.9
CPT-11/accumulation (DMEM)	One binding-site		32.71		24.53
CPT-11/accumulation (HBSS)	One binding-site		19.77		40.55
SN-38/accumulation (DMEM)	One binding-site		3.71		1.02
SN-38/accumulation (HBSS)	One binding-site		1.55		0.89

DMEM = Dulbecco's modified Eagle's medium; HBSS = Hank's balanced salt solution.
[a]The unit was pmol/min/mg protein for rat liver microsomes, and pmol/min/10^6 cells for metabolism and accumulation of CPT-11 and SN-38 in H4-II-E cells**.**

As expected, nifedipine (100 µM) significantly reduced CPT-11 hydrolysis (0.5

µM) by 23.4% ($P < 0.001$), while it had no significant effect for CPT-11

hydrolysis at a higher concentration (78 µM). By contrast, BNPP at 100 µM

showed significant ($P < 0.001$) inhibitory effect on CPT-11 hydrolysis at 0.5 µM

(53.7% decrease) or at 78 µM substrate concentration (41.1% decrease). In addition, nifedipine (100 µM) had significant ($P < 0.001$) inhibitory effect on the glucuronidation of SN-38 at 5.0 µM (60.0% decrease). However, bilirubin at 100 µM had no significant effect on SN-38 glucuronidation (5.0 µM and 18.2 µM). These results indicated the effectiveness of our microsomal system in the metabolic inhibition studies.
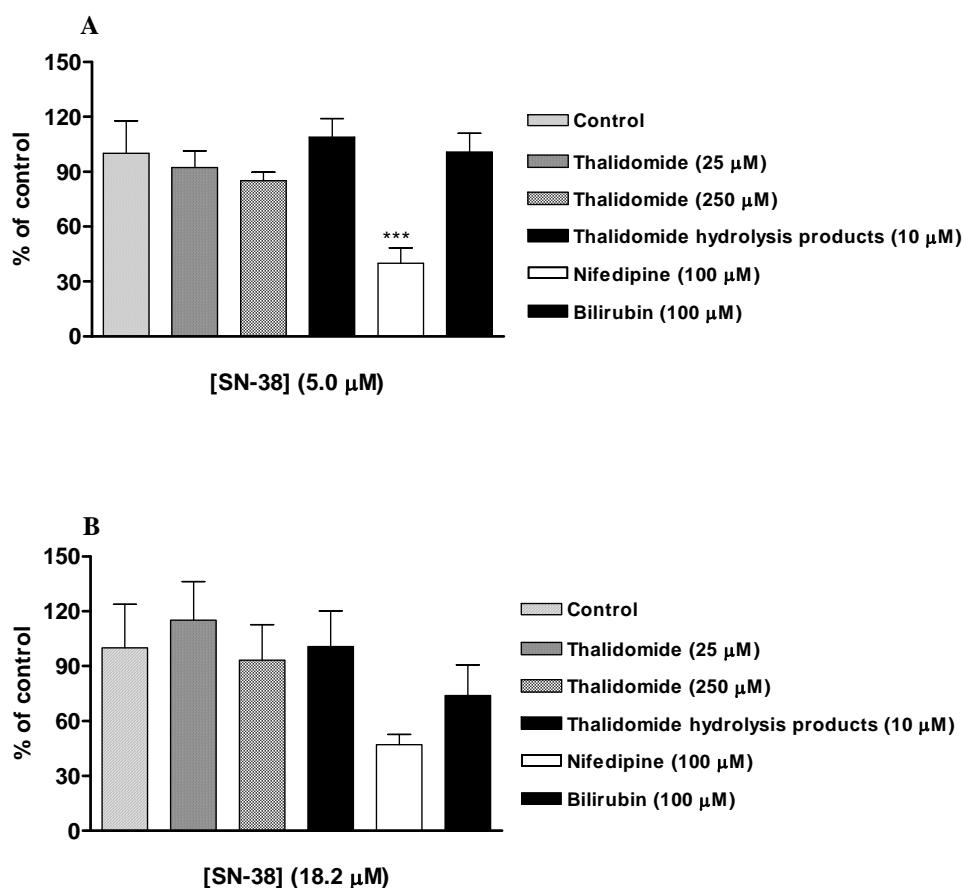
Figure 3-4. Effects of thalidomide, total thalidomide hydrolytic products, nifedipine, and bilirubin on SN-38 glucuronidation at 5.0 µM (A) and 18.2 µM (B) in rat liver microsomes. Data are expressed as percentage of the control. ***$P < 0.001$ compared to the control group (N = 3).
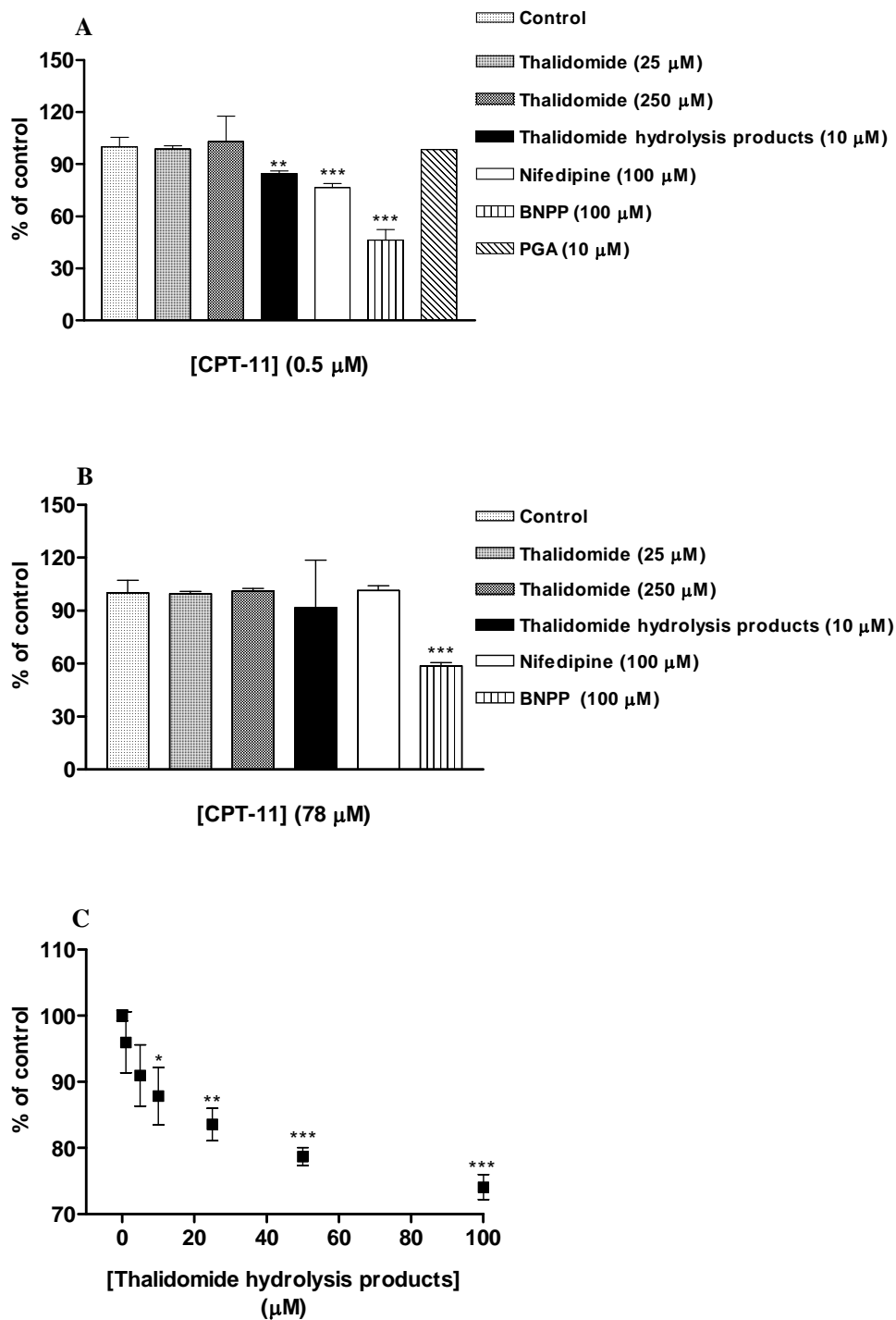
Figure 3-5. Effects of thalidomide, its total hydrolytic products, phthaloyl glutamic acid (PGA), nifedipine, and bis (p-nitrophenyl) phosphate sodium salt (BNPP) on the hydrolysis of CPT-11 at 0.5 (A & C) or 78.0 μM (B) in rat liver microsomes. (C) represents the concentration effects of thalidomide hydrolytic products on CPT-11 (0.5 μM) hydrolysis in rat liver microsomes. Data are expressed as the percentage of the control group. *$P < 0.05$; **$P < 0.01$; ***$P < 0.001$ compared to the control group (N = 3).

3.3.5 Cytotoxicity of CPT-11, its metabolites and thalidomide in rat hepatoma H4-II-E cells
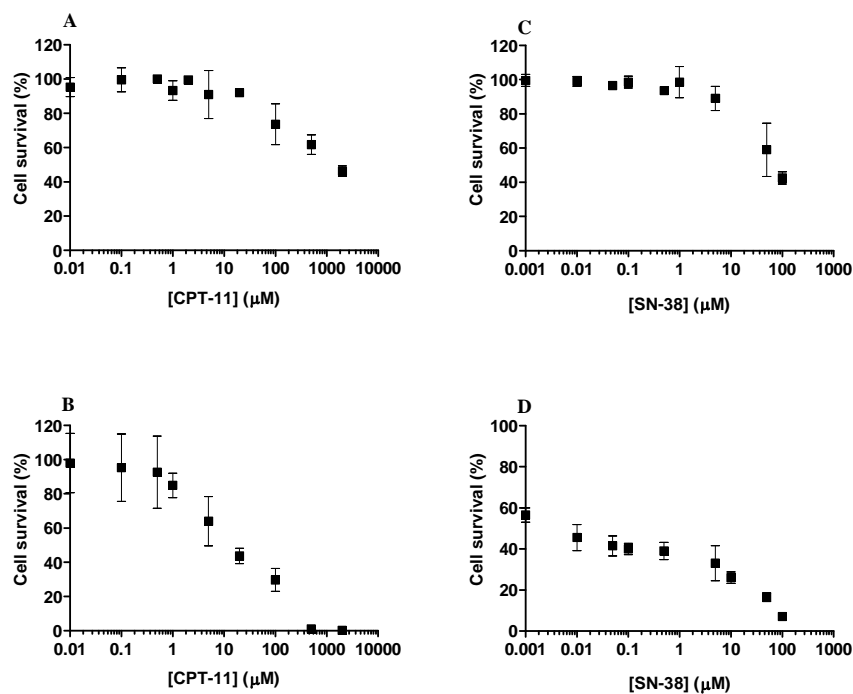
Figure 3-6. Cytotoxic effects of CPT-11 (A and B) and SN-38 (C and D) in rat hepatoma H4-II-E cells when incubated for 4- (A and C) or 48-hr (B and D) (N = 3).

When incubated for 48 hr, CPT-11 and SN-38 caused significant cell growth inhibition with estimated IC_{50} of 7.50 ± 1.36 μM and 13.37 ± 5.91 nM, respectively (Figure 3-6). SN-38 was 560-fold more cytotoxic to the cells than CPT-11. The IC_{50} for CPT-11 and SN-38 increased to 692.29 μM and 47.20 μM, respectively when the drug-exposure time was shortened to 4 hr. By contrast, incubation of thalidomide at concentrations up to 1,000 μM or its hydrolytic products at the total concentration of up to 100 μM for 48 hr exhibited little or no cytotoxic effects in H4-II-E cells.

3.3.6 Effects of thalidomide and its hydrolytic products on the metabolism of CPT-11 and SN-38 in rat hepatoma H4-II-E cells

The metabolism of CPT-11 and SN-38 in H4-II-E cells incubated with DMEM or HBSS with regard to incubation time and substrate concentration is shown in Figure 3-7.

Both SN-38 and SN-38G were detectable and achieved peak levels after incubating CPT-11 with H4-II-E cells for 5 min; thereafter, the formation of both metabolites rapidly declined over 180 min in both DMEM and HBSS. The formation of both SN-38 and SN-38G in H4-II-E cells increased with increasing CPT-11 concentration and followed Michaelis-Menten kinetics with the one-binding site model being the best fit. The estimated K_m and V_{max} for SN-38 formation in DMEM were 43.8 µM and 9.68 pmol/min/10^6 cells, respectively. For SN-38G formation, the K_m and V_{max} were 21.22 µM and 1.59 pmol/min/10^6 cells, respectively (Table 3-5). These constants were similar for the formation of SN-38 (K_m = 44.47 µM; V_{max} = 6.53 pmol/min/10^6 cells) and SN-38G (K_m = 30.81 µM; V_{max} = 1.01 pmol/min/10^6 cells) in HBSS.

In addition, when SN-38 was incubated with H4-II-E cells, SN-38G appeared rapidly in the medium or HBSS and then declined over 120 min. The formation of SN-38 increased in a substrate concentration-dependent manner and followed Michaelis-Menten kinetics. One-binding site model was the best fit for the formation of SN-38G in both DMEM and HBSS, with comparable K_m and V_{max} values (K_m, DMEM *vs*. HBSS: 2.50 *vs*. 3.62 µM; V_{max}, DMEM *vs*. HBSS: 278.8 *vs*. 221.9 pmol/min/10^6 cells).
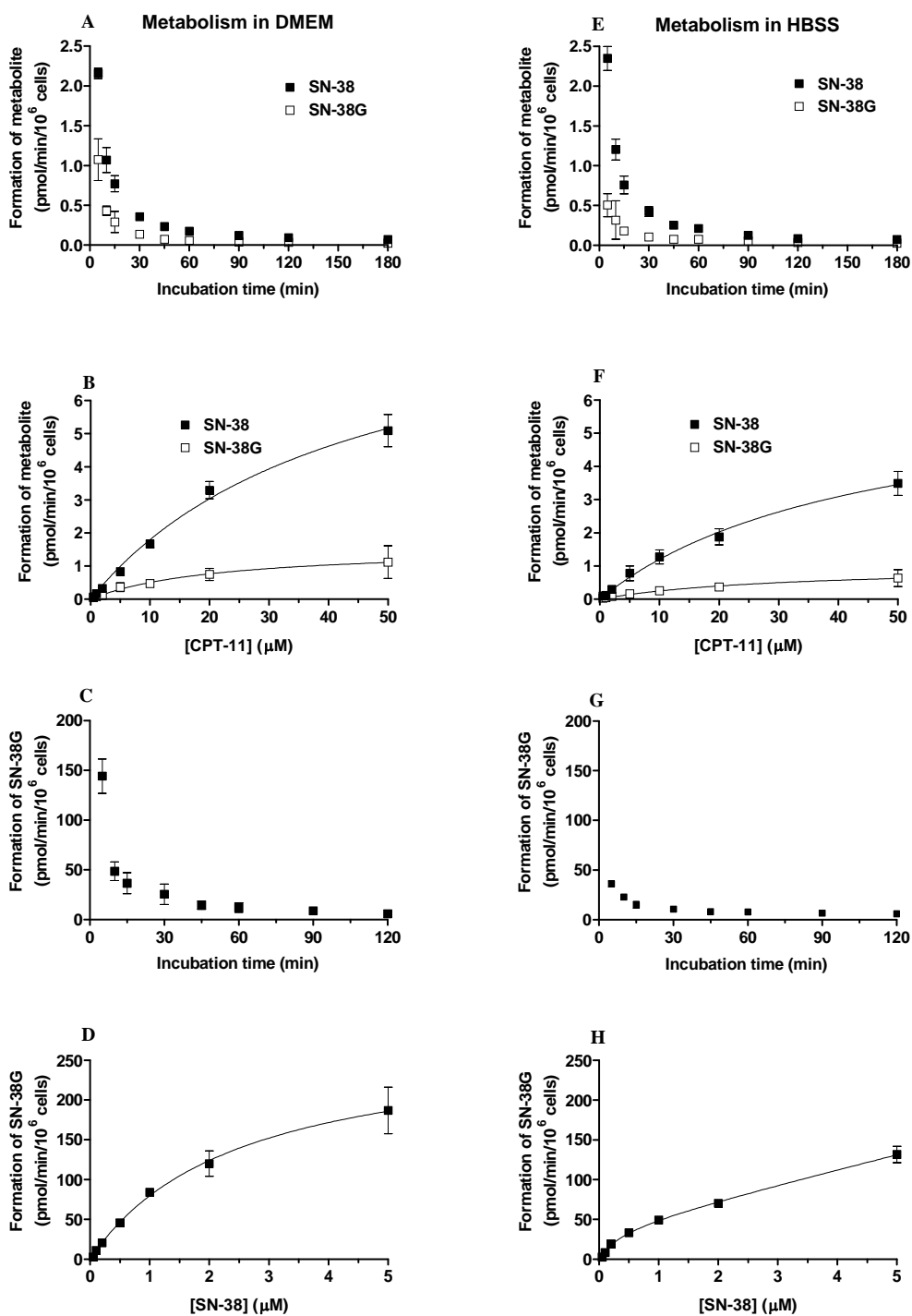
Figure 3-7. Effects of incubation time and substrate concentration on hydrolysis of CPT-11 (A, B, E, & F) and SN-38 glucuronidation (C, D, G, & H) in H4-II-E cells in DMEM (A, B, C, & D) or HBSS (E, F, G, & H). The curves in plots B, D, F, & H represent the best fit of one-binding site model (N = 3).

The effects of thalidomide and its hydrolytic products on CPT-11 and SN-38 metabolism in H4-II-E cells in DMEM are shown in Figure 3-8. Co-incubation of thalidomide at 25 μM, PGA at 10 μM or its total hydrolytic products at 10 μM significantly inhibit the hydrolysis of CPT-11 by 10.3% ($P < 0.01$), 20.3% ($P < 0.001$), and 9.6% ($P < 0.05$), respectively. However, co-incubation or 2-hr pre-incubation of thalidomide at 25 μM and 250 μM and its hydrolytic products at 10 μM did not show any significant effects on SN-38 glucuronidation.

Of the control inhibitors, BNPP and nifedipine at 100 μM significantly inhibited the hydrolysis of CPT-11 by 9.8% ($P < 0.01$) and 6.8 % ($P < 0.05$) and nifedipine at 100 μM significantly inhibited the glucuronidation of SN-38 by 14.3% ($P < 0.05$). By contrast, bilirubin had no inhibitory effect on SN-38 glucuronidation.

3.3.7 Effects of thalidomide and its hydrolytic products on the intracellular accumulation of CPT-11 and SN-38 in rat hepatoma H4-II-E cells

The intracellular accumulation of CPT-11 and SN-38 in H4-II-E cells in DMEM or HBSS was investigated. As shown in Figure 3-9, the accumulation of CPT-11 or SN-38 in DMEM or HBSS was not significantly dependent on the incubation time, but their accumulation increased depending on the substrate concentration and followed Michaelis-Menten kinetics with one-binding site model being the best fit. The K_m for CPT-11 was 32.71 and 19.77 μM in DMEM and HBSS, respectively; and the V_{max} for CPT-11 was 24.53 and 40.55 pmol/min/10^6 cells, respectively. For SN-38, the K_m was 3.71 and 1.55 μM in DMEM and HBSS, respectively; and the V_{max} was 1.02 and 0.89 pmol/min/10^6 cells, respectively (Table 3-5).
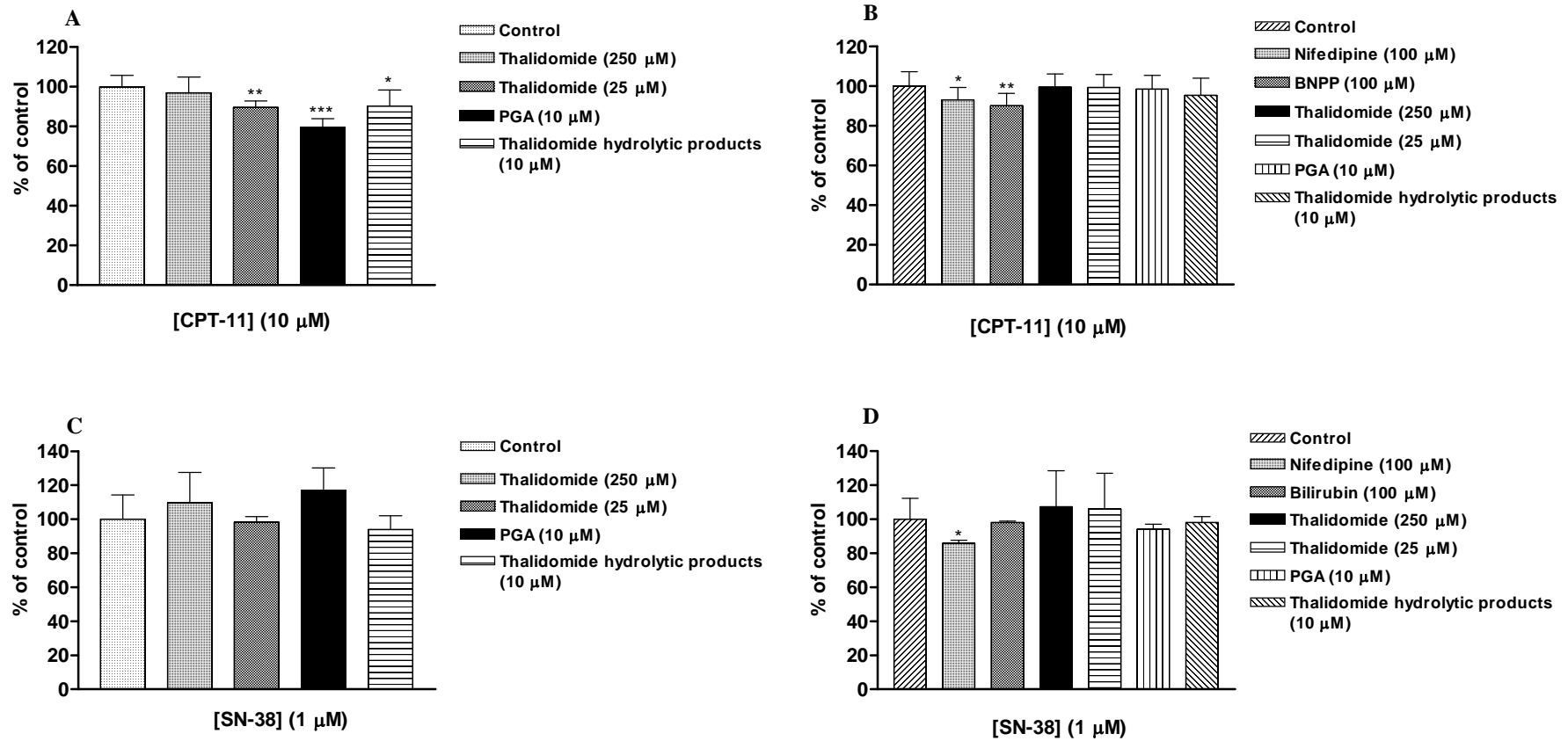
Figure 3-8. Effects of thalidomide, phthaloyl glutamic acid (PGA), total thalidomide hydrolytic products, nifedipine, bilirubin and and bis (p-nitrophenyl) phosphate sodium salt (BNPP) on CPT-11 hydrolysis (A & B) and SN-38 glucuronidation (C & D) in H4-II-E cells cultured in DMEM. A & C, co-incubation with the inhibitor; B & D, 2-hr pre-incubation with the inhibitor. *$P < 0.05$; **$P < 0.01$ compared to the control group (N = 3).

The effects of co-incubation and 2-hr pre-incubation of thalidomide and its hydrolytic products on the intracellular accumulation of CPT-11 and SN-38 are shown in Figure 3-10. Co-incubation or pre-incubation of PGA at 10 μM both increased CPT-11 uptake by 21.9% and 10.5% ($P < 0.05$). Pre-incubation of thalidomide at 25 μM decreased CPT-11 uptake by 11.3 % ($P < 0.05$). Pre-incubation of thalidomide at 250 μM, PGA at 10 μM, or total thalidomide hydrolytic products (10 μM) increased the intracellular accumulation of SN-38 by 174.0%, 113.3%, and 191.5%, respectively ($P < 0.001$). However, co-incubation of thalidomide and its hydrolytic products did not show any significant effects on the intracellular accumulation of SN-38. Not surprisingly, MK-571 at 100 μM increased the accumulation of CPT-11 by 35.6% ($P < 0.001$). Verapamil (200 μM), MK-571 (100 μM) and probenecid (200 μM) also increased the intracellular accumulation of SN-38 by 85.0% ($P < 0.05$), 670.5% ($P < 0.01$), and 36.3% ($P < 0.01$), respectively.

3.4   CONCLUSION & DISCUSSION

The pharmacokinetic study revealed that a single dose of co-administered thalidomide significantly increased the $AUC_{0-\infty}$ of CPT-11 but decreased the $AUC_{0-\infty}$ of SN-38. Similar results were found in the 5-day multiple-dose thalidomide treatment study. Furthermore, in the 5-day multiple-dose thalidomide treatment study, administration of thalidomide increased the C_0 but decreased V_d and CL of CPT-11. Prolonged administration of thalidomide caused greater modulating effect on the plasma pharmacokinetics of CPT-11 and SN-38 compared with short-term (one-day) treatment.
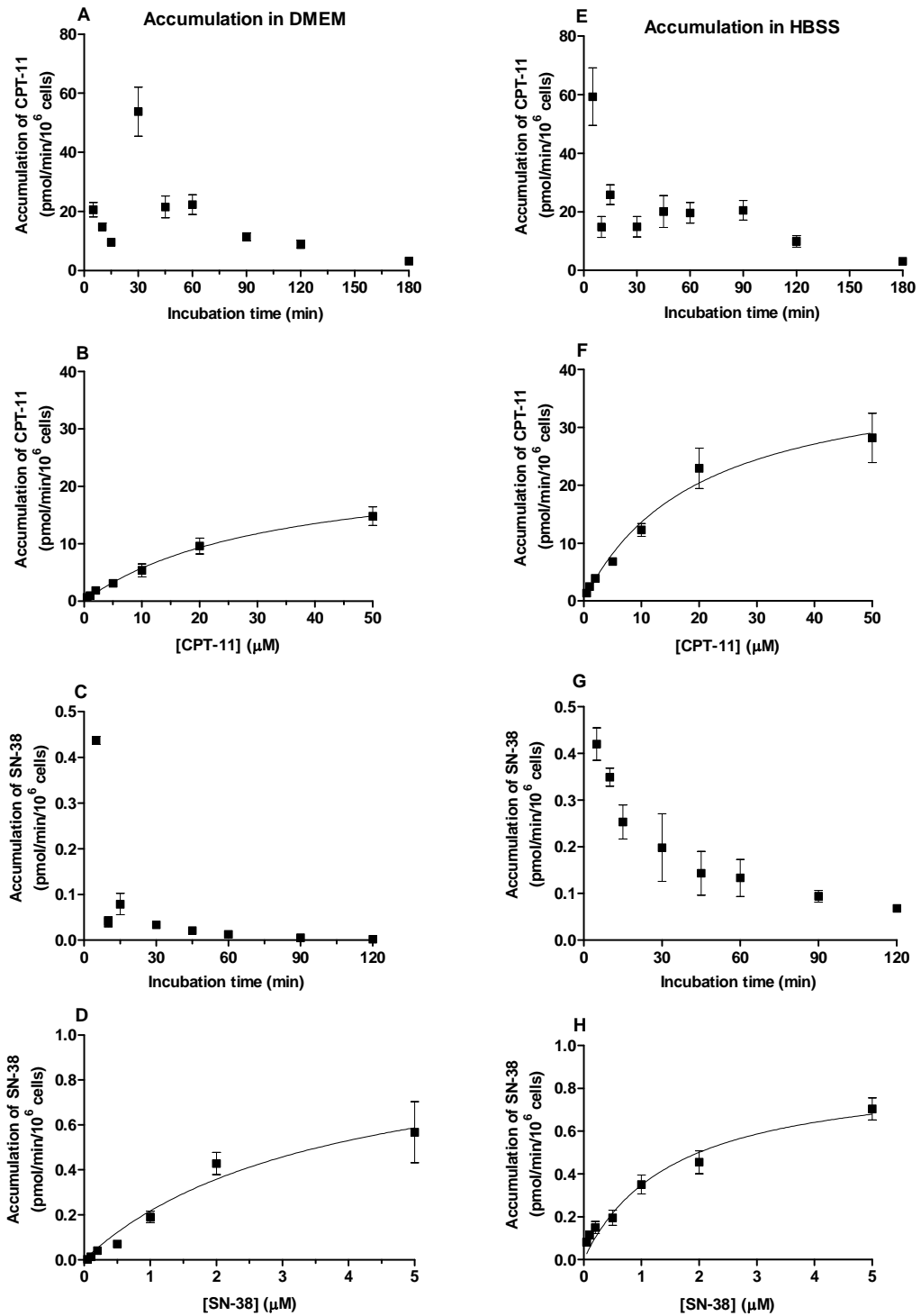
Figure 3-9. Effects of incubation time and substrate concentration on the intracellular accumulation of CPT-11 (A, B, E, & F) and SN-38 (C, D, G, & H) in H4-II-E cells cultured in DMEM (A, B, C, & D) or in HBSS (E, F, G, & H). The curves in plots B, D, F, & H represent the best fit of one-binding site model (N = 3).

99
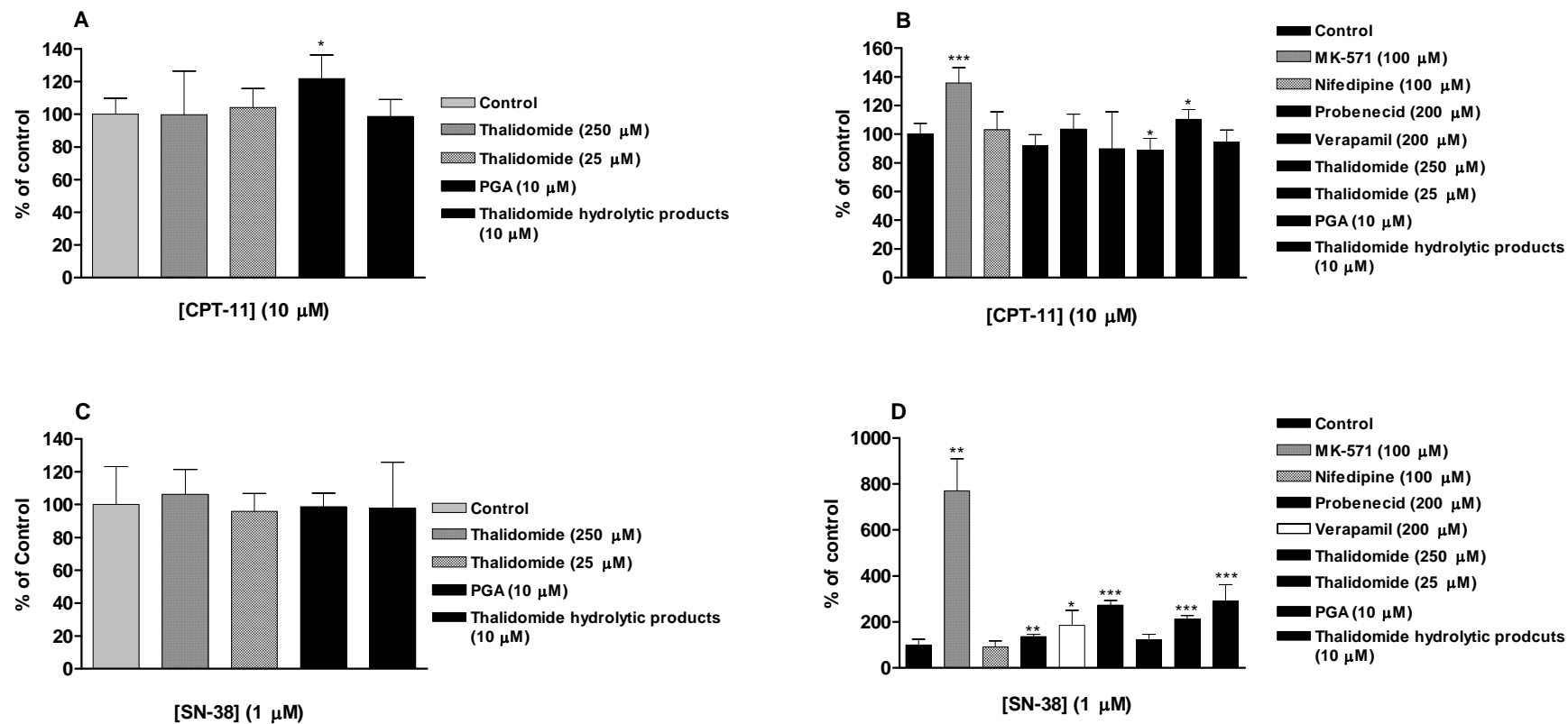
Figure 3-10. Effects of thalidomide, total thalidomide hydrolytic products, phthaloyl glutamic acid (PGA), nifedipine, probenecid, MK-571, and verapamil on the intracellular accumulation of CPT-11 (A & B) and SN-38 (C & D) in H4-II-E cells cultured in DMEM. A & C, co-incubation of the cells with the inhibitor; B & D, 2-hr pre-incubation of the cells with the inhibitor. $*P < 0.05$; $**P < 0.01$; $***P < 0.001$ compared to the control group (N = 3).

Exposure of intestines to SN-38 is believed to be the main reason for the occurrence of CPT-11 induced late-onset diarrhea. There is a clear correlation between the toxicity of CPT-11 and its pharmacokinetic parameters for AUC and C_{max} of SN-38 in cancer patients [295]. Thus, our pharmacokinetic findings may suggest that the protective effect of thalidomide against the gastrointestinal toxicity of CPT-11 might be partially attributed to the reduced plasma levels of SN-38.

In vitro models including rat liver microsomes and the rat hepatoma cell line, H4-II-E cells, were used to investigate the *in vitro* kinetic interactions. In rat liver microsomes, a 15.6% decrease ($P < 0.05$) in the hydrolysis of CPT-11 at 0.5 µM by the hydrolytic products of thalidomide (10 µM), instead of thalidomide, was observed. In addition, co-incubation of thalidomide at 25 µM, PGA at 10 µM or thalidomide hydrolytic products at total concentration of 10 µM caused a decrease in CPT-11 hydrolysis in H4-II-E cells. The inhibition of CPT-11 hydrolysis caused by the combination of thalidomide observed in the rat liver microsome and rat hepatoma cells may explain the increased plasma level of CPT-11 but decreased that of SN-38, as indicated in the plasma pharmacokinetic studies. It seemed that thalidomide could affect the main metabolic pathway of CPT-11 that yields SN-38 though, up to date, little is known concerning drugs that could interact with CE, except for ciprofloxacin and loperamide [296].

We further examined the effects of thalidomide and its hydrolytic products on CPT-11 and SN-38 cellular accumulation in H4-II-E cell line. Incubation of PGA at 10 µM increased CPT-11 accumulation, while thalidomide at 25 µM decreased CPT-11 accumulation in H4-II-E cells. In addition, thalidomide at 250 µM, PGA

at 10 µM, or total hydrolytic products of thalidomide at 10 µM all increased the cellular accumulation of SN-38 in H4-II-E cells. The increased accumulation of SN-38 in rat hepatoma cells might increase its metabolism via glucuronidation due to increased substrate availability for UGT1As, resulting in decreased SN-38 plasma levels. The mechanism for the increased accumulation of SN-38 by thalidomide and its hydrolytic metabolites is unknown, but their inhibitory effects on SN-38 transporters such as Pgp and MRP2 are implicated. Tumor cells generally exhibit high levels of expression of Pgp or MRPs, thus co-administration of thalidomide might enhance the anticancer effects of CPT-11 by inhibiting these transporters.

Since thalidomide is a poor substrate for CYPs and that it does not inhibit the metabolism of CYP-specific substrates, thalidomide is not involved in clinically important drug-drug interactions caused by an inhibition of CYP-mediated drug metabolism. However, given that thalidomide can be hydrolysed to more than a dozen metabolites *in vivo* [297], it can be expected that these hydrolytic metabolites may have a modulating effect on the metabolism and transport of CPT-11 and SN-38 and thus cause altered pharmacokinetics *in vivo*, as shown in our study. However, the specific thalidomide hydrolytic products responsible for these effects are not identified. Further studies are needed to identify these hydrolytic products and this may allow development of new CE and drug transporter modulators.

Taken together, the protective effects of thalidomide on CPT-11 induced gastrointestinal and blood toxicities might be attributed to the inhibition of pro-inflammatory cytokine expression and intestinal epithelial cellular apoptosis as

well as modulation of CPT-11 pharmacokinetic profiles. The abolition or alleviation of chemotherapy-induced complication may reduce mortality caused by severe diarrhea and inflammation and avoid overall reduction in effectiveness of therapy caused by interruptions or dose reductions during treatment. Therefore, administration of higher dose chemotherapy regimens with improved tumor regression might be achieved.

The major concern of this combination is that the plasma levels of SN-38 were reduced, accompanied with a decrease in TNF-α levels, which may compromise the anti-tumor activity of CPT-11. However, drug concentration and TNF-α level in tumor tissues play more important roles in the anti-tumor activity of cancer chemotherapeutic agent. In addition, combination of chemotherapeutic agent CPT-11 with thalidomide, an anti-angiogenic agent, may strengthen the anti-tumor activity of CPT-11 by targeting endothelial cells, which might be a new approach to resolve both toxicity and resistance phenomena for conventional cancer treatment. So further studies will be valuable to evaluate the anti-tumor activity for the combination of CPT-11 with thalidomide before this combination could be successfully used clinically. In addition, the protective effects of thalidomide on CPT-11 induced complications may provide a new treatment approach for chemotherapy-associated histological damages using anti-TNF-α agents through the inhibition of pro-inflammatory cytokine expression and intestinal epithelial cellular apoptosis.

CHAPTER 4 ST. JOHN'S WORT MODULATED DOSE-LIMITING TOXICITIES OF CPT-11 IN THE RAT

4.1 INTRODUCTION

A pilot clinical study in 5 cancer patients found that oral treatment of SJW at 900 mg/day for 18 days significantly alleviated irinotecan-induced neutropenia, accompanied with a decrease in SN-38 plasma level that may have a deleterious impact on treatment outcome of CPT-11 [177, 298]. However, the underlying pharmacodynamic mechanisms are not explored although this protective effect of SJW on CPT-11 induced toxicity may be partially attributed to the pharmacokinetic interactions as indicated by a decrease in the plasma level of SN-38. SJW has been reported to show anti-inflammatory effects which may help to reduce the toxicity of cytotoxic anti-cancer agents. In addition, SJW has shown anti-cancer effect and thus it may enhance the anti-tumor activity when combined with anti-cancer agents [299-301].

In the present study, we sought to use a rat model to demonstrate if combination of SJW would modulate the histological and hematological toxicities induced by CPT-11, and this model was further used to explore the potential pharmacodynamic mechanisms for this interaction by examining the intestinal epithelial apoptosis and cytokine expression. Although it was advised that patients receiving chemotherapeutic treatments such as CPT-11 should refrain from taking SJW, the mechanistic study for the protective effects of SJW on CPT-11 induced complications may provide some insights into the development of new treatment approaches for chemotherapy associated histological damages.

4.2   MATERIALS AND METHODS

4.2.1   Chemicals

CPT-11 was supplied by Sinochem Ningbo Import and Export Co. (Ningbo, China). An injectable formulation of CPT-11 was prepared as described in section 2.2.1. The SJW sugar-coated tablets [LI-160, 300 mg St. John's wort dry extract, DER 3-6:1, solvent methanol 80% (v/v)], purchased from local pharmacy of Singapore, were manufactured by Lichtwer Pharma GmbH (Berlin, Germany), and the SJW-free control vehicle (also formulated as sugar-coated tablet) was kindly supplied by Lichtwer Pharma GmbH (Berlin, Germany). The contents of hypericin and hyperforin in the SJW tablets have been standardized to 0.3% and 5%, respectively, by the manufacturer. Analysis using HPLC methods at our laboratory found similar contents of both compounds in the preparations. Prior to use, the sugar coat was peeled off before the tablets were ground to powder by mortar and pestle, then stored in the dryer protected from light. The administration form of SJW or vehicle was prepared by suspending SJW or vehicle powder in physiological saline for oral gavage administration. All other chemicals were of analytical grade or HPLC grade obtained from the same commercial sources as in section 2.2.1.

4.2.2   Animals

Refer to Section 2.2.2.

4.2.3   Drug administration schedules

The CPT-11 induced diarrhea model in male Sprague Dawley rats was developed as previously described. One group of rats (n = 4-7 per group) was treated with CPT-11 at a dose of 60 mg/kg/day by i.v. injection via tail vein for four consecutive days (days 1-4), and in combination with SJW (400 mg/kg/day by oral gavage for eight consecutive days, 6 ml/kg/day) starting one day before the first CPT-11 injection. The rats in control group received CPT-11 and SJW-free vehicle (400 mg/kg/day by oral gavage for 8 consecutive days, 6 ml/kg/day). These groups of rats were used to monitor diarrhea scores, body weight changes and counts of leucocytes. Doses used here for SJW in rats are higher than those used in humans (900 - 1,050 mg/day) [302, 303]. We adopted this dosage from other rat studies [247, 304, 305], where significant drug metabolizing enzyme and transporter inducing effects have been observed. This dose was reported to show no sign of toxicity in rats. Eight additional groups of rats (n = 4-6 per group) received CPT-11 for four consecutive days with or without SJW (400 mg/kg/day by p.o. for 5-8 consecutive days starting one day before CPT-11 injection, 6 ml/kg/day) combination and sacrificed on days 5, 7, 9, and 11 to monitor macroscopic and microscopic gastrointestinal damages. Physiological saline was given (3 ml/kg/day) by i.v. injection for four consecutive days for the blank groups. Tissues and serum samples were collected from these groups of rats for further cytokine quantification and examination of intestinal epithelial cellular apoptosis.

4.2.4 Toxicity evaluation and pharmacodynamic study

Refer to Section 2.2.4 for monitoring of CPT-11 induced diarrhea; Section 2.2.5 for counting of leucocytes; Section 2.2.6 for evaluation of intestinal damages;

Section 2.2.7 for TUNEL assay of intestinal epithelial cellular apoptosis; Section 2.2.8 for ELISA assay for cytokine protein levels; Section 2.2.9 for protein determination by Bradford method; Section 2.2.10 for RT-PCR assay for mRNA levels of *TNF-α*; and Section 2.2.11 for statistical analysis.

4.3   RESULTS

4.3.1   Effects of SJW on CPT-11 induced toxicities

Rats treated with CPT-11 alone experienced rapid decrease in body weight, reached a nadir by day 6 with a decrease of 10% compared to the baseline (day 1), and recovered to 108% of the baseline by day 11 (Figure 4-1). Co-administration of SJW with CPT-11 resulted in lower body weight loss compared to rats receiving CPT-11 alone, with a decrease of 3% by day 6 and recovery to 118% of the baseline by day 11. Rats that received physiological saline showed only a gradual increase of body weight over 11 days.
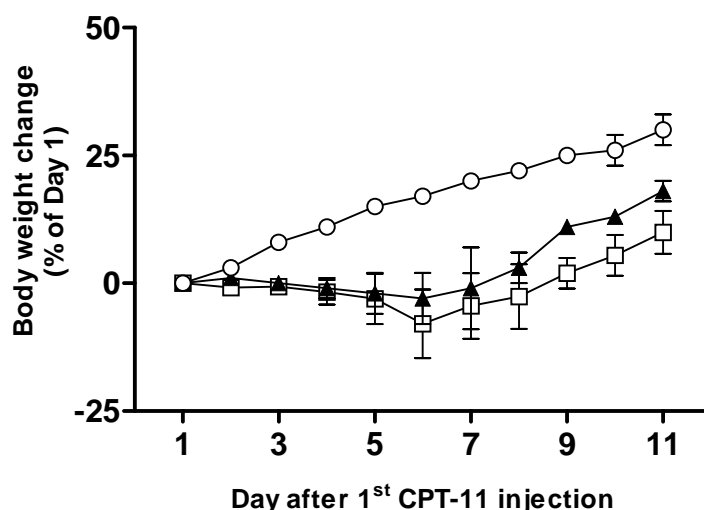
Figure 4-1. Body weight changes (% compared to day 1) in two groups receiving CPT-11 and control vehicle or CPT-11 in combination with St. John's wort. Data were expressed as mean ± SD. ○, Blank (without any drug treatment); ▲, CPT-11+ St. John's wort; □, CPT-11 + Control vehicle (N = 4-6).
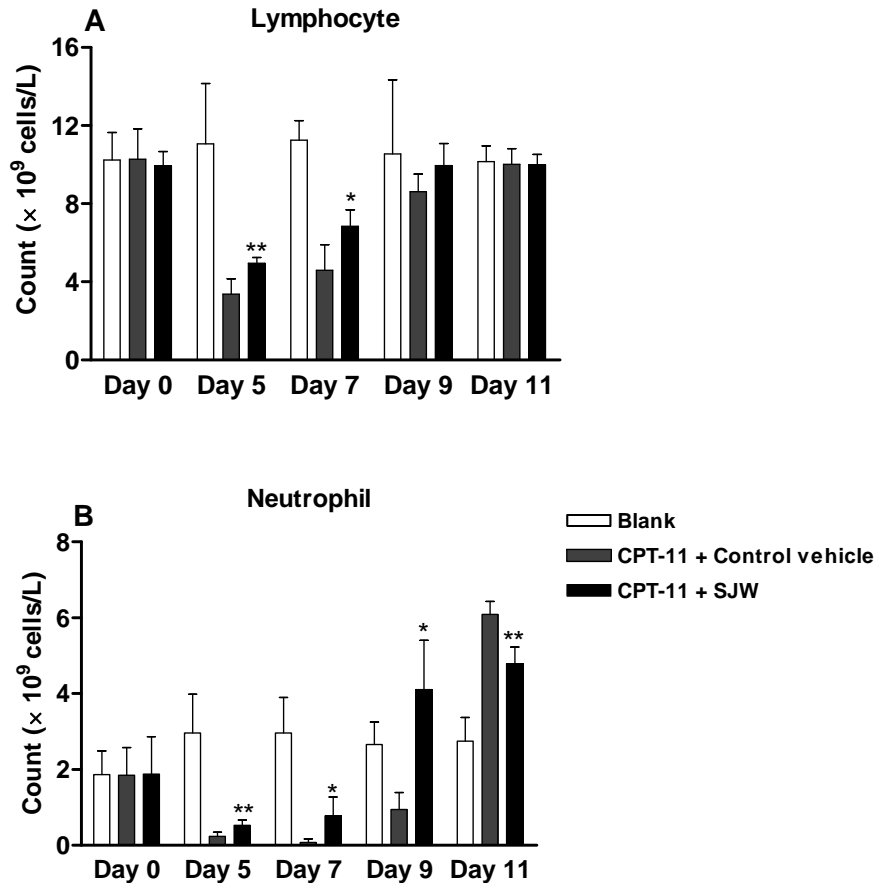
Figure 4-2. Changes of lymphocyte and neutrophil counts in rats treated with CPT-11 and control vehicle or in combination with St. John's wort. Asterisks (*P < 0.05; **P < 0.01) denote significant differences between rats pretreated with St. John's wort and control vehicle (N = 4-6).

Administration of CPT-11 alone at 60 mg/kg by i.v. for four consecutive days induced severe early- (days 1-4) and late-onset (days 5-8) diarrhea, with mean severity scores of 0.14, 0.14, 0.43, 1.43, 1.71, 2.07, 1.25, and 0.75 by days 1-8, respectively (Table 4-1). The severity scores for late-onset diarrhea were brought down in rats treated with CPT-11 and SJW (400 mg/kg, oral), with significant effect on day 5 (P < 0.05, Wilcoxon rank sum test).

The counts of neutrophils and lymphocytes were significantly decreased and reached a minimum by day 7 and day 5, respectively, in rats treated with CPT-11

alone. The combination of CPT-11 with SJW increased the numbers of lymphocytes on day 5 ($P < 0.01$) and day 7 ($P < 0.05$) compared to the control group receiving CPT-11 alone (Figure 4-2). The neutrophil numbers were also increased by the combination of SJW on days 5, 7, and 9 ($P < 0.05$).

Marked macroscopic pathological differences were observed in the gastrointestinal tissues between the rats receiving CPT-11 injection with or without SJW pretreatment. In the control rats receiving CPT-11 alone, wide macroscopic changes including wall thickening, hyperemia, hemorrhage, ulceration, and adhesion were observed in the intestinal tissues at days 5 and 7, although these symptoms were alleviated after day 9. Surprisingly, most of these rats experienced severe stomach swell at the same time. By contrast, gastrointestinal tissues from rats pretreated with SJW were significantly ($P <$ 0.05) less impaired (Figure 4-3). Marked microscopic pathological damages were also observed in the intestinal tissues treated with CPT-11 and control vehicle. However, these damages were significantly alleviated in the rats receiving CPT-11 with SJW pre-treatment (Figure 4-4, Figure 4-5, Figure 4-6, and Figure 4-7).
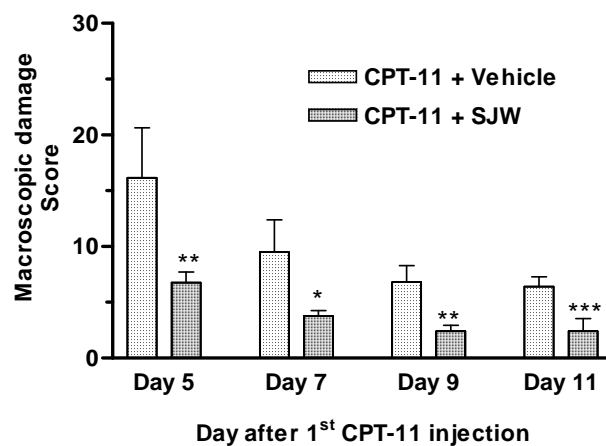
Figure 4-3. Scores of macroscopic intestinal (including ileum, caecum, and colon) damages by days 5, 7, 9, and 11 induced by CPT-11 in rats pretreated with St. John's wort (SJW) or control vehicle. Asterisks (*$P < 0.05$, **$P < 0.01$, ***$P < 0.001$) denote significant differences between rats pretreated with St. John's wort and control vehicle (N = 4-6).

Table 4-1. Incidence of early- and late-onset diarrhea in rats treated with CPT-11 and control vehicle or in combination with St. John's wort (SJW). The values are the number of animals with each score.

Early-onset diarrhea

Treatment Group	n	Diarrhea Score[a]																			
		Day 1					Day 2					Day 3					Day 4				
		0	1	2	3	Mean	0	1	2	3	Mean	0	1	2	3	Mean	0	1	2	3	Mean
Blank	5	10				0	10				0	10				0	10				0
CPT-11+ SJW	5	9	1			0.10	10				0	10				0	8	1	1		0.30
CPT-11+ vehicle	7	12	2			0.14	12	2			0.14	11	0	3	0	0.43	6	1	2	5	1.43

Late-onset diarrhea

Treatment Group	n	Diarrhea Score[a]																			
		Day 5					Day 6					Day 7					Day 8				
		0	1	2	3	Mean	0	1	2	3	Mean	0	1	2	3	Mean	0	1	2	3	Mean
Blank	5	10				0	10				0	10				0	10				0
CPT-11+ SJW	5	3	4	3	0	1.00*	3	1	3	3	1.60	5	2	3	0	0.80	9	1	0	0	0.10
CPT-11+ Vehicle	7[b]	2	3	6	3	1.71	2	3	1	8	2.07	1	4	3	0	1.25	2	6	0	0	0.75

*P < 0.05, CPT-11 + SJW *vs.* CPT-11 + Vehicle;
[a] Two readings at am and pm everyday;
[b] Three rats died of severe diarrhea on Day 7.
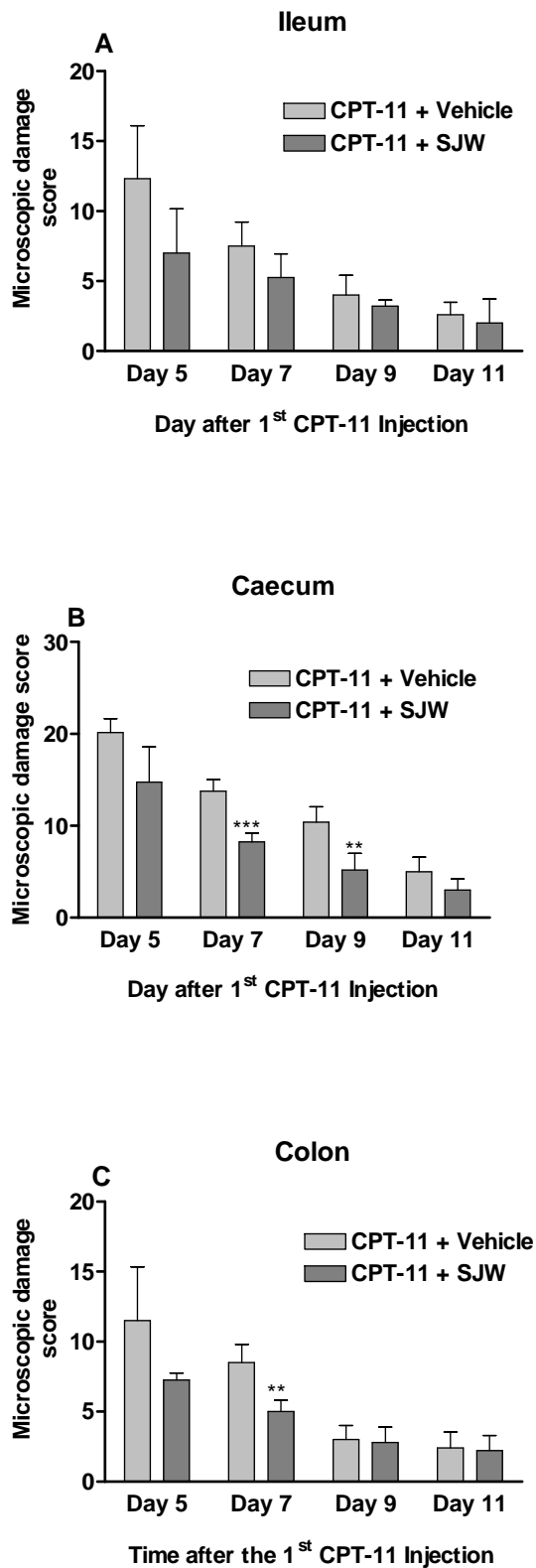
Figure 4-4. Scores of microscopic intestinal (including ileum, caecum, and colon) damages on days 5, 7, 9, and 11 induced by CPT-11 in rats pretreated with St. John's wort (SJW) or control vehicle. *$P < 0.05$; **$P < 0.01$; ***$P < 0.001$ (N = 4-6).

	CPT-11 + Vehicle	CPT-11+ SJW
Day 0		
Day 5		
Day 7		
Day 9		
Day 11		
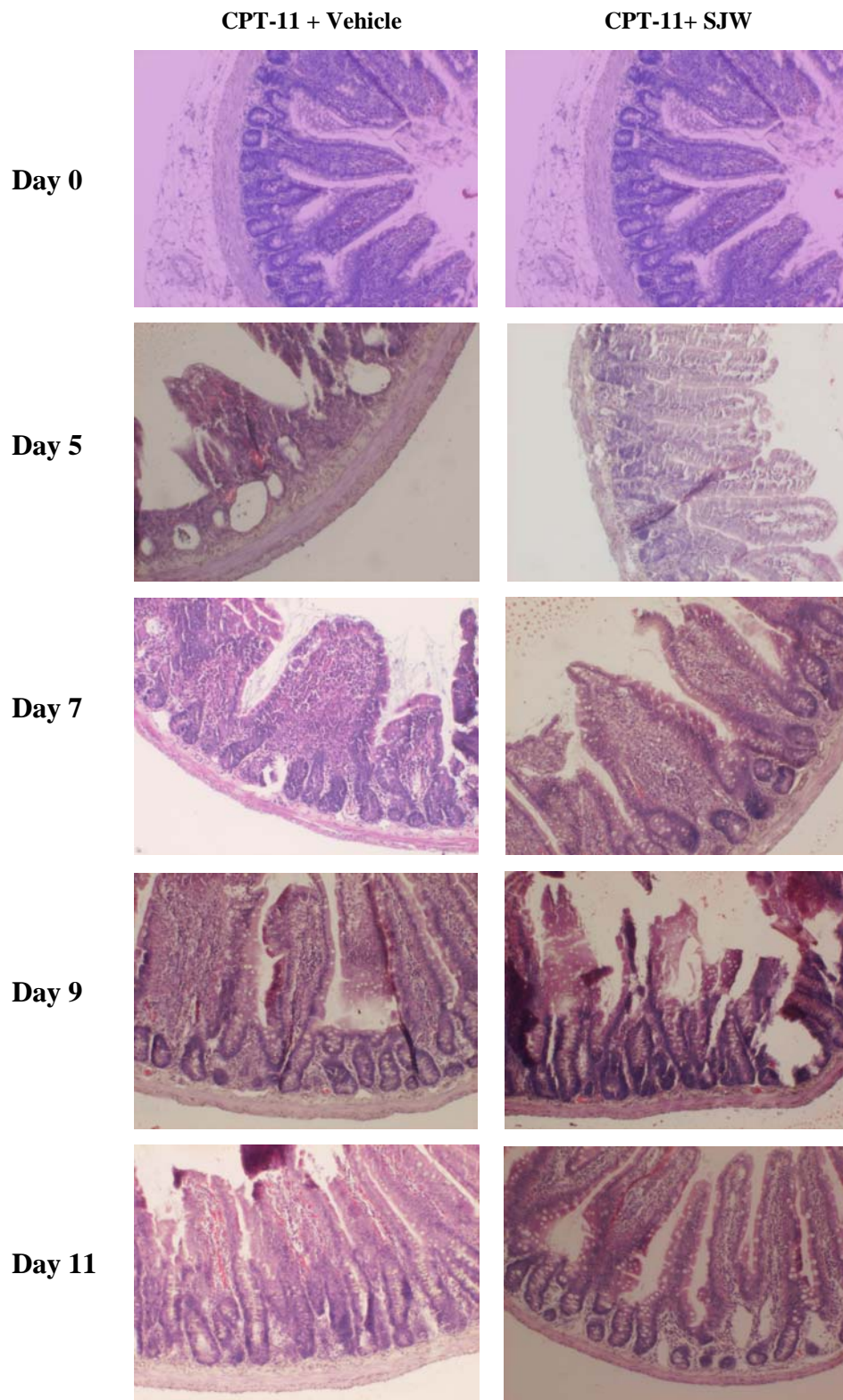
Figure 4-5. Micrographs (magnification $\times$ 100) of ileum showing histological damages on days 0, 5, 7, 9, and 11 in rats. The rats were treated with CPT-11 and control vehicle, or CPT-11 in combination with St. John's wort (SJW).

CPT-11 + Vehicle   **CPT-11 + SJW**

Day 0

Day 5

Day 7

Day 9

Day 11
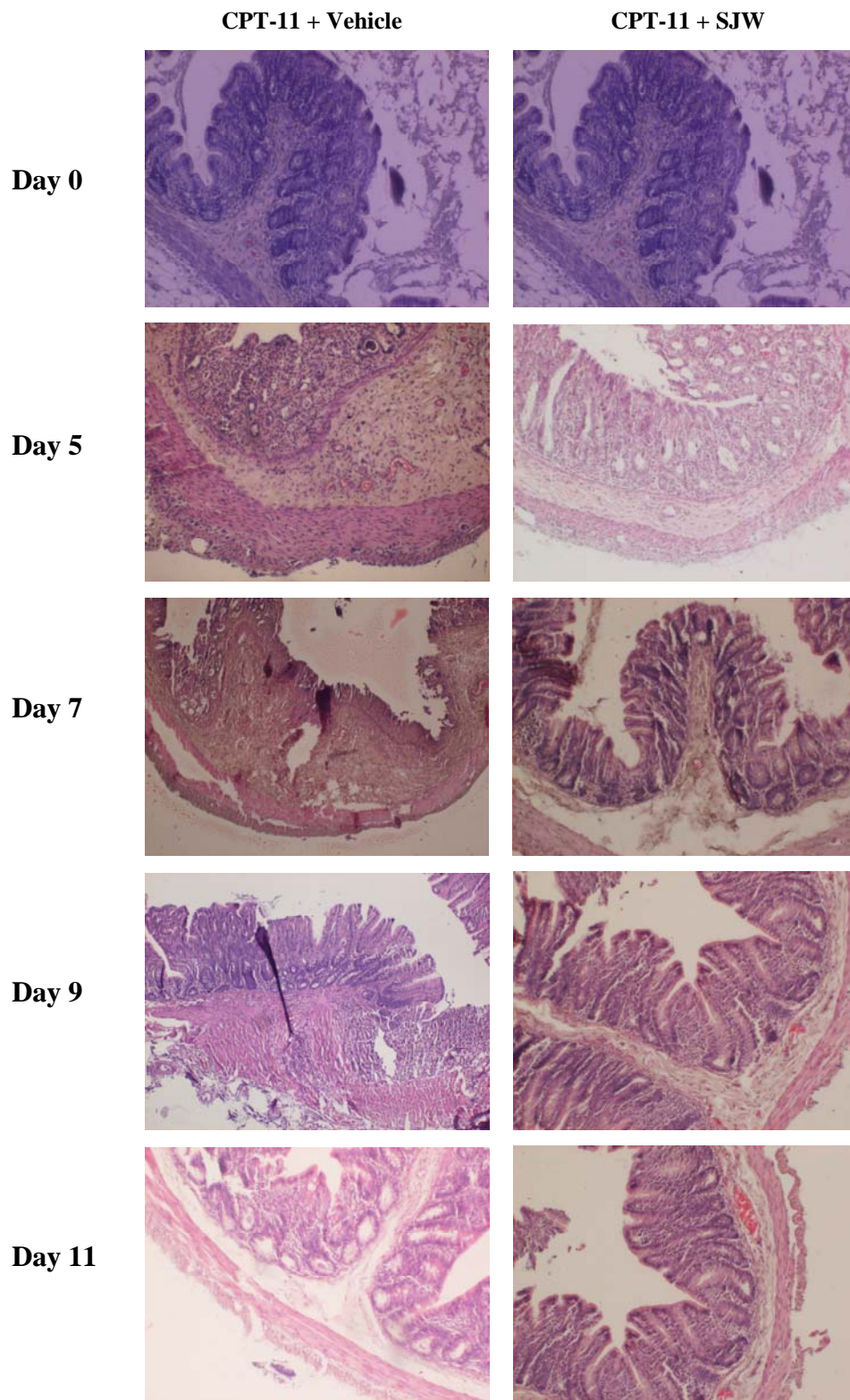
Figure 4-6. Micrographs (magnification × 100) of caecum showing histological damages on days 0, 5, 7, 9, and 11 in rats. The rats were treated with CPT-11 and control vehicle, or CPT-11 in combination with St. John's wort (SJW).

	CPT-11 + Vehicle	**CPT-11 + SJW**
Day 0		
Day 5		
Day 7		
Day 9		
Day 11		
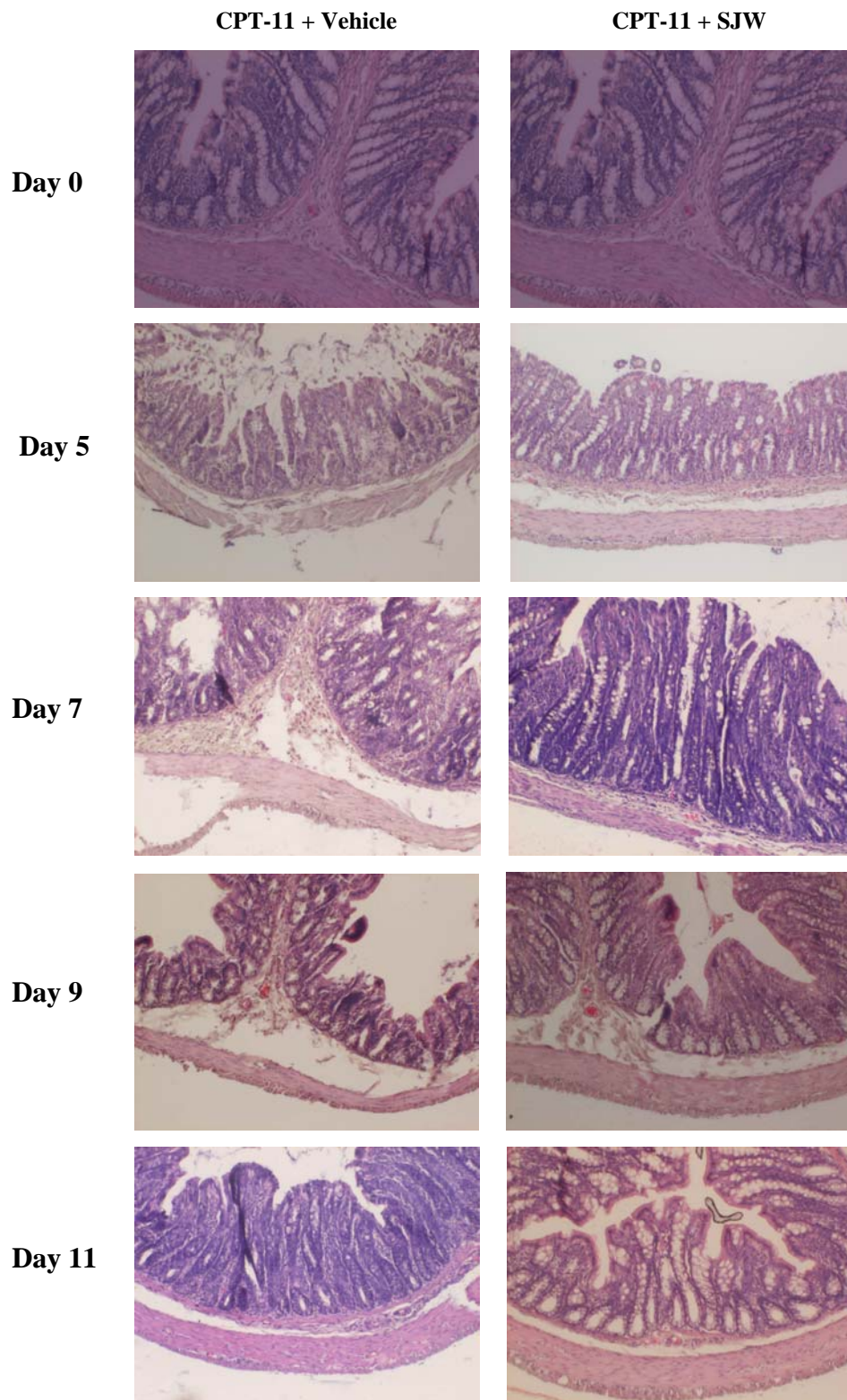
Figure 4-7. Micrographs (magnification $\times$ 100) of colon showing histological damages on days 0, 5, 7, 9, and 11 in rats. The rats were treated with CPT-11 and control vehicle, or CPT-11 in combination with St. John's wort (SJW).

4.3.2 TUNEL assay

CPT-11 + Vehicle **CPT-11 + SJW**

Day 0

Day 5

Day 7

Day 9

Day 11
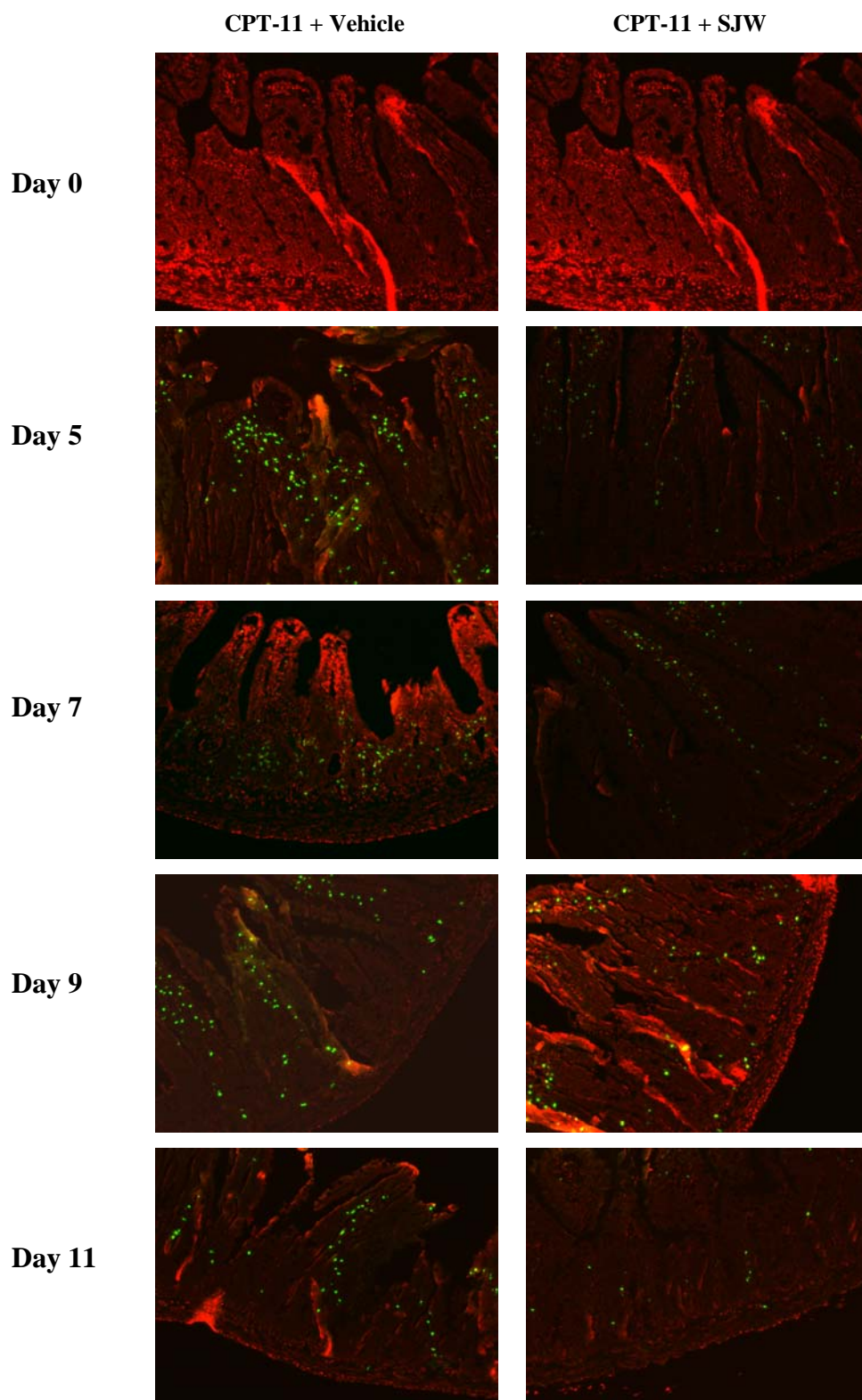
Figure 4-8. Detection of apoptotic cells in rat ileum (4-µm slices) using TUNEL assay. The fragmented DNA of TUNEL-positive apoptotic cells (green spots) were incorporated with fluorescein-dUTP at free 3'-hydroxyl ends and visualized by fluorescence microscopy (magnification × 100).
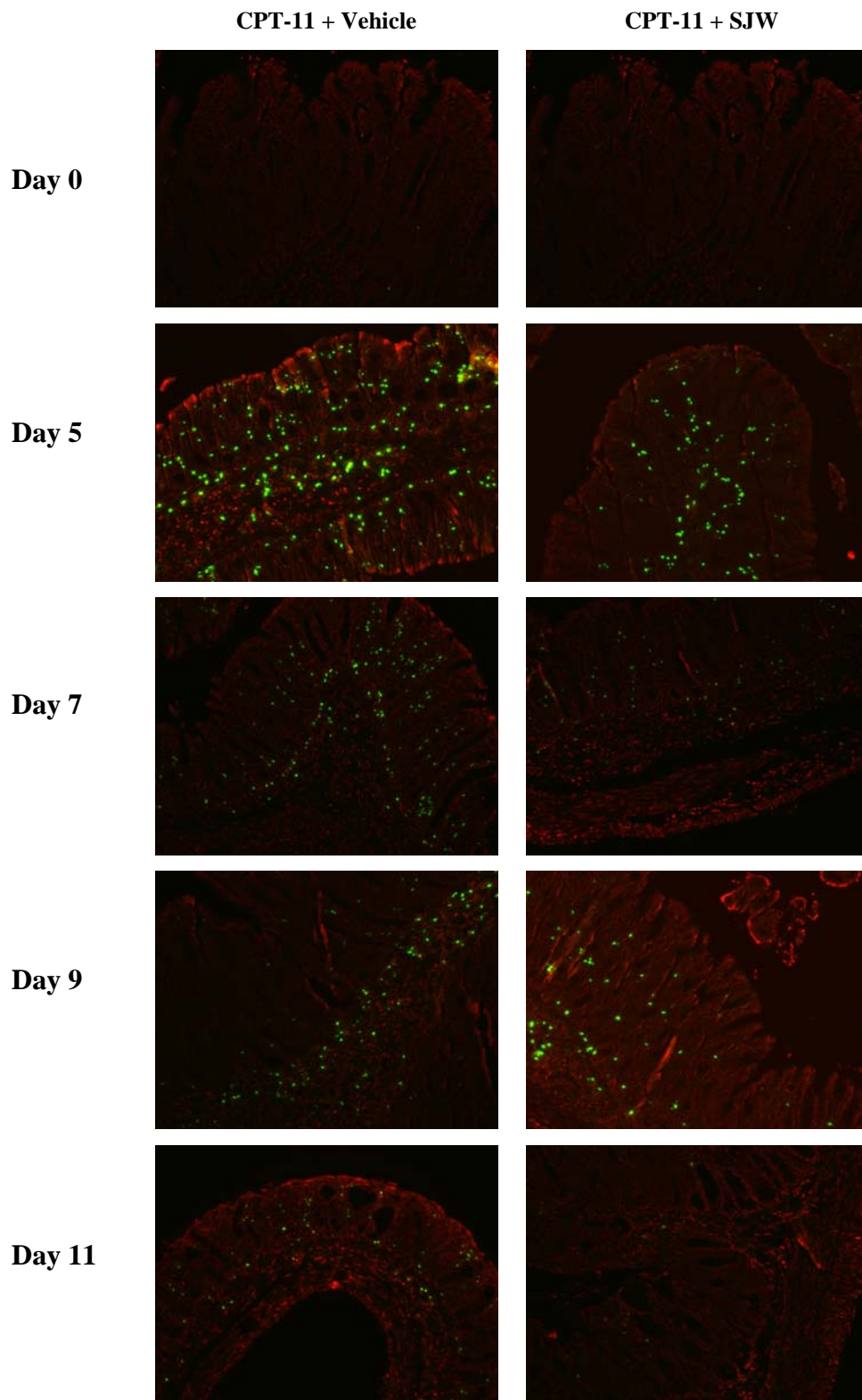
Figure 4-9. Detection of apoptotic cells in rat caecum (4-μm slices) using TUNEL assay. The fragmented DNA of TUNEL-positive apoptotic cells (green spots) were incorporated with fluorescein-dUTP at free 3'-hydroxyl ends and visualized by fluorescence microscopy (magnification × 100).

116

CPT-11 + Vehicle   **CPT-11 + SJW**

Day 0

Day 5

Day 7

Day 9

Day 11
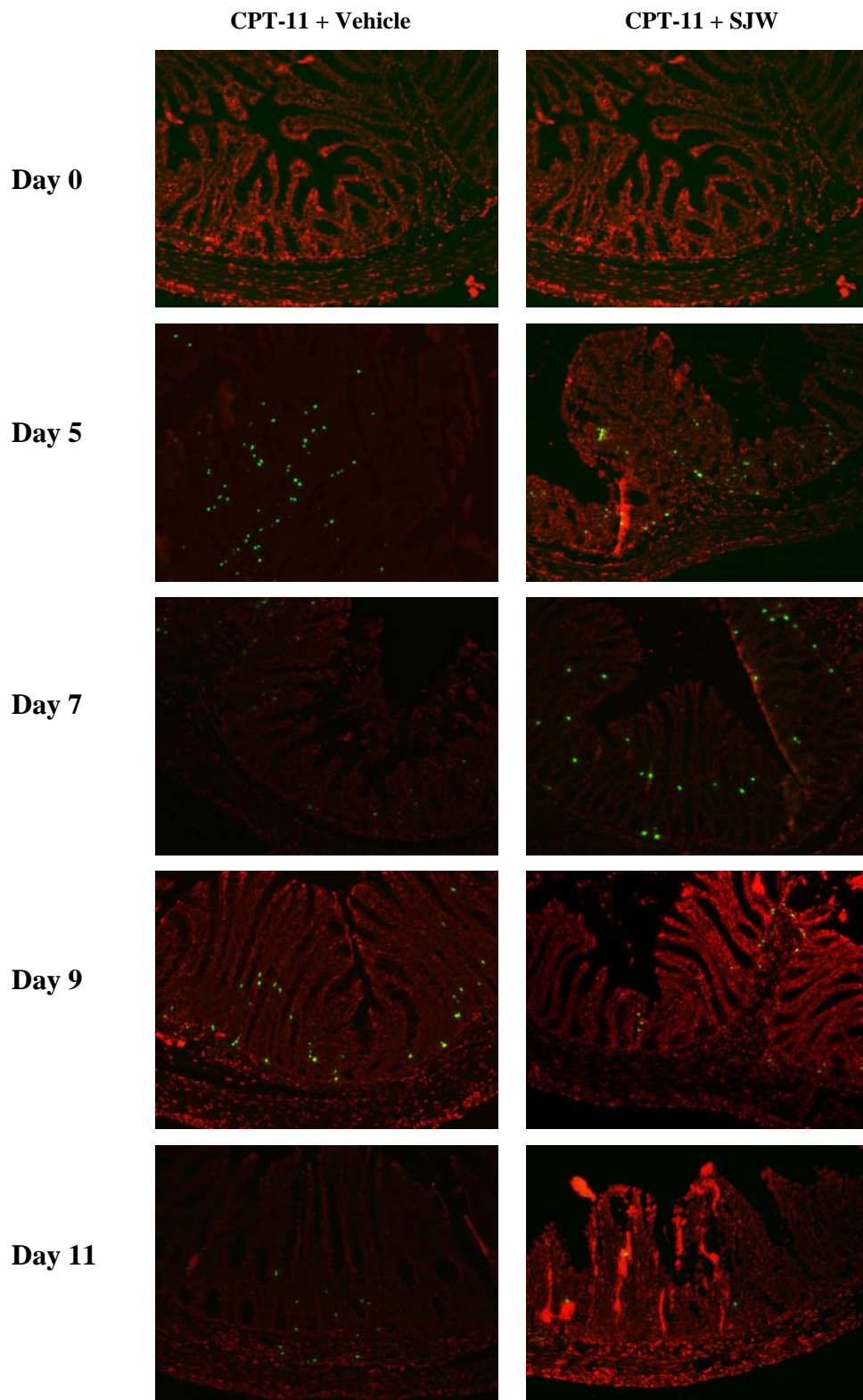
Figure 4-10. Detection of apoptotic cells in rat colon (4-µm slices) using TUNEL assay. The fragmented DNA of TUNEL-positive apoptotic cells (green spots) were incorporated with fluorescein-dUTP at free 3'-hydroxyl ends and visualized by fluorescence microscopy (magnification × 100).
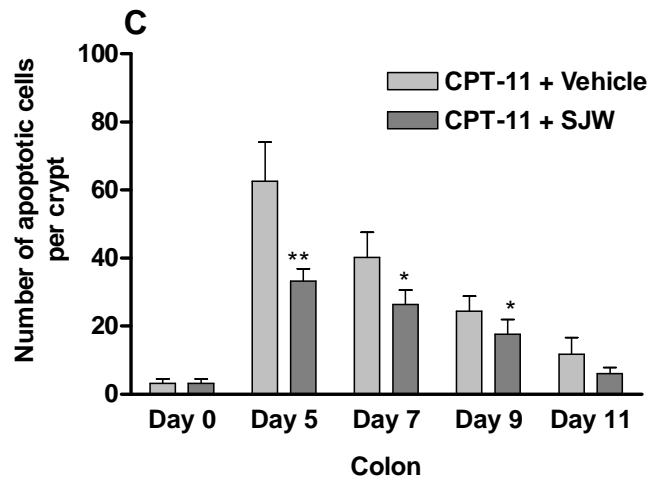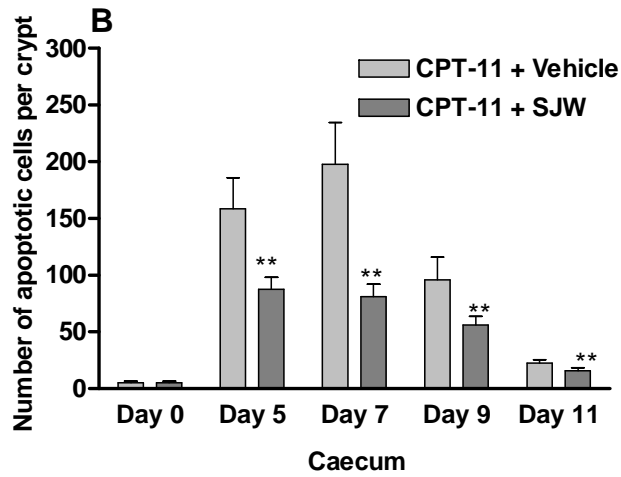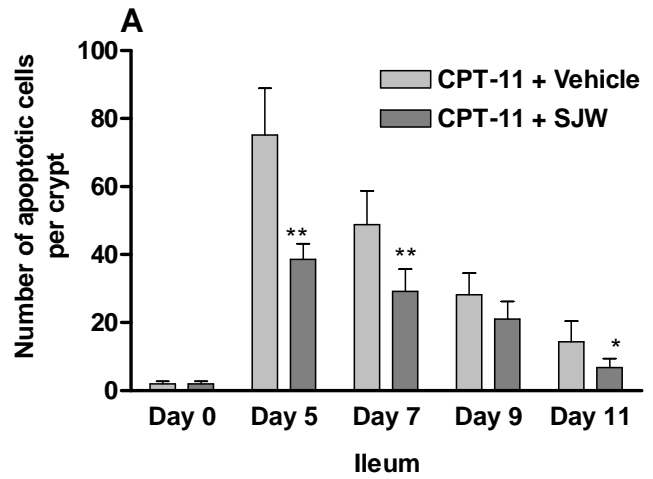
Figure 4-11. Counts of intestinal epithelial apoptotic cells per crypt in rats treated with CPT-11 and control vehicle or in combination with St. John's wort (SJW). $*P < 0.05$; $**P < 0.01$ (N = 4-6).

In normal rats without any drug treatment, the number of epithelial apoptotic cells per crypt in ileum, caecum, and colon were 2.0 ± 0.7, 5.0 ± 1.6, and 3.2 ± 1.3, respectively. Administration of CPT-11 with control vehicle caused a maximal epithelial apoptosis (75.2 ± 13.7 per crypt) on day 5 in the ileum, and then decreased thereafter. Combination of SJW significantly reduced ileal epithelial apoptosis on day 5 by 48.7% ($P < 0.01$), on day 7 by 40.2% ($P < 0.01$), and on day 11 by 52.8% ($P < 0.05$), respectively, compared to rats treated with CPT-11 alone (Figure 4-8 and Figure 4-11).

Similarly, maximal epithelial apoptosis was detected in the caecum and colon on day 7 and day 5, respectively. SJW pretreatment led to decreased CPT-11 induced epithelial apoptosis on day 5 by 44.8%, on day 7 by 59.0%, on day 9 by 41.3%, and on day 11 by 31.0% ($P < 0.01$) (Figure 4-9 and Figure 4-11) in the caecum, respectively. In addition, coadministered SJW reduced CPT-11 induced apoptosis on day 5 by 47.0% ($P < 0.01$), on day 7 by 34.3%, and on day 9 by 27.9% ($P < 0.05$) in the colon, respectively (Figure 4-10 and Figure 4-11).

4.3.3 Quantitation of cytokines by ELISA

The levels of TNF-α, IFN-γ, IL-1β, IL-2, and IL-6 in intestinal tissues and liver, spleen as well as serum were shown in Figure 4-12, Figure 4-13, Figure 4-14, Figure 4-15, and Figure 4-16, respectively. Treatment of CPT-11 generally increased the levels of TNF-α, IFN-γ, IL-1β, and IL-6 compared to day 0, which achieved peak levels by day 5 or day 9 and declined thereafter; while the level of IL-2 decreased compared to day 0, reaching minimum levels by day 5 or day 7 in above tissues.
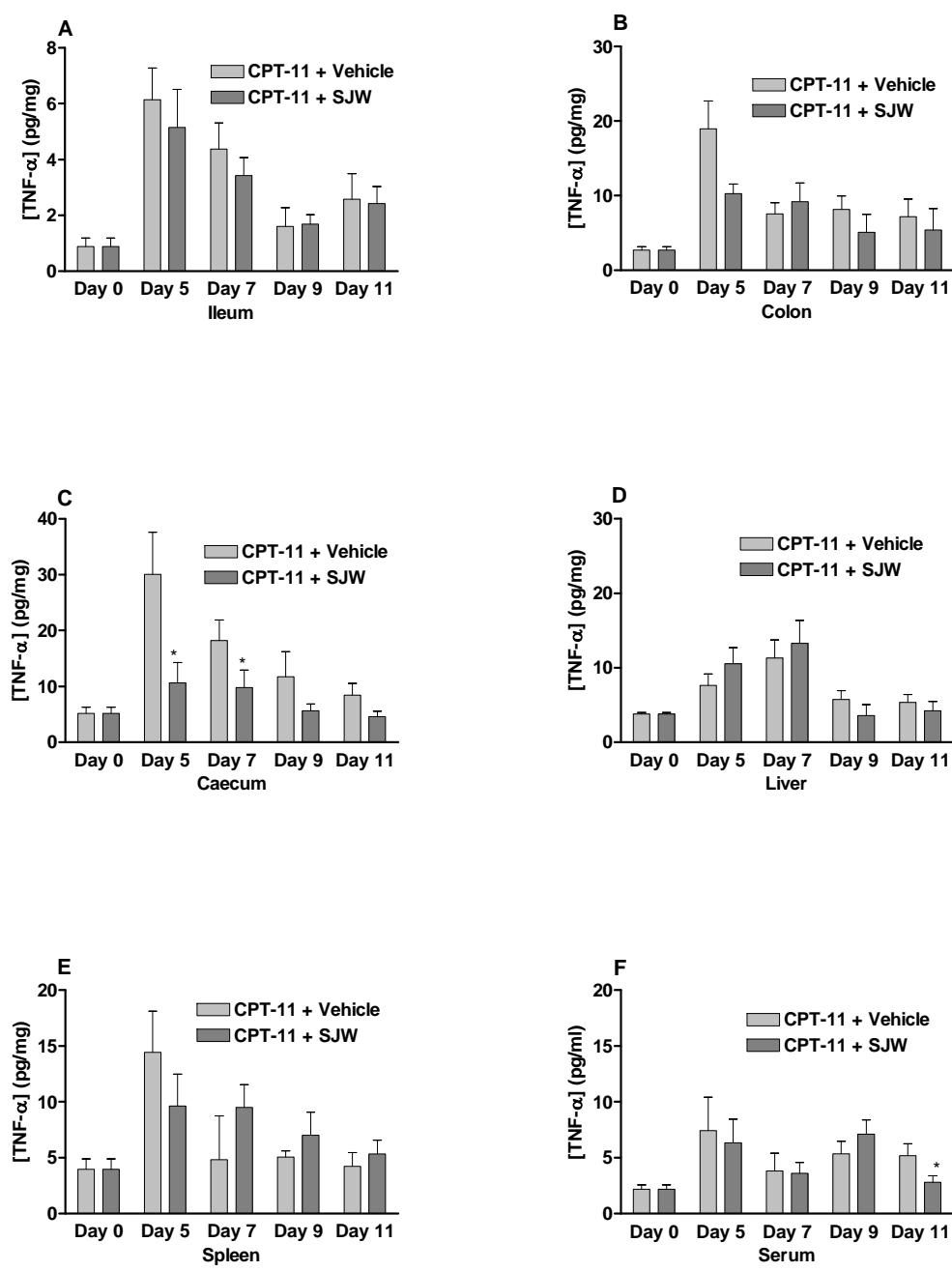
Figure 4-12. Protein levels of TNF-α in rat ileum (A), colon (B), caecum (C), liver (D), spleen (E), and serum (F) on days 0, 5, 7, 9, and 11 after CPT-11 administration in control group treated with CPT-11 and control vehicle and combination group treated with CPT-11 and St. John's wort (SJW). *$P < 0.05$ (N = 4-6).

.
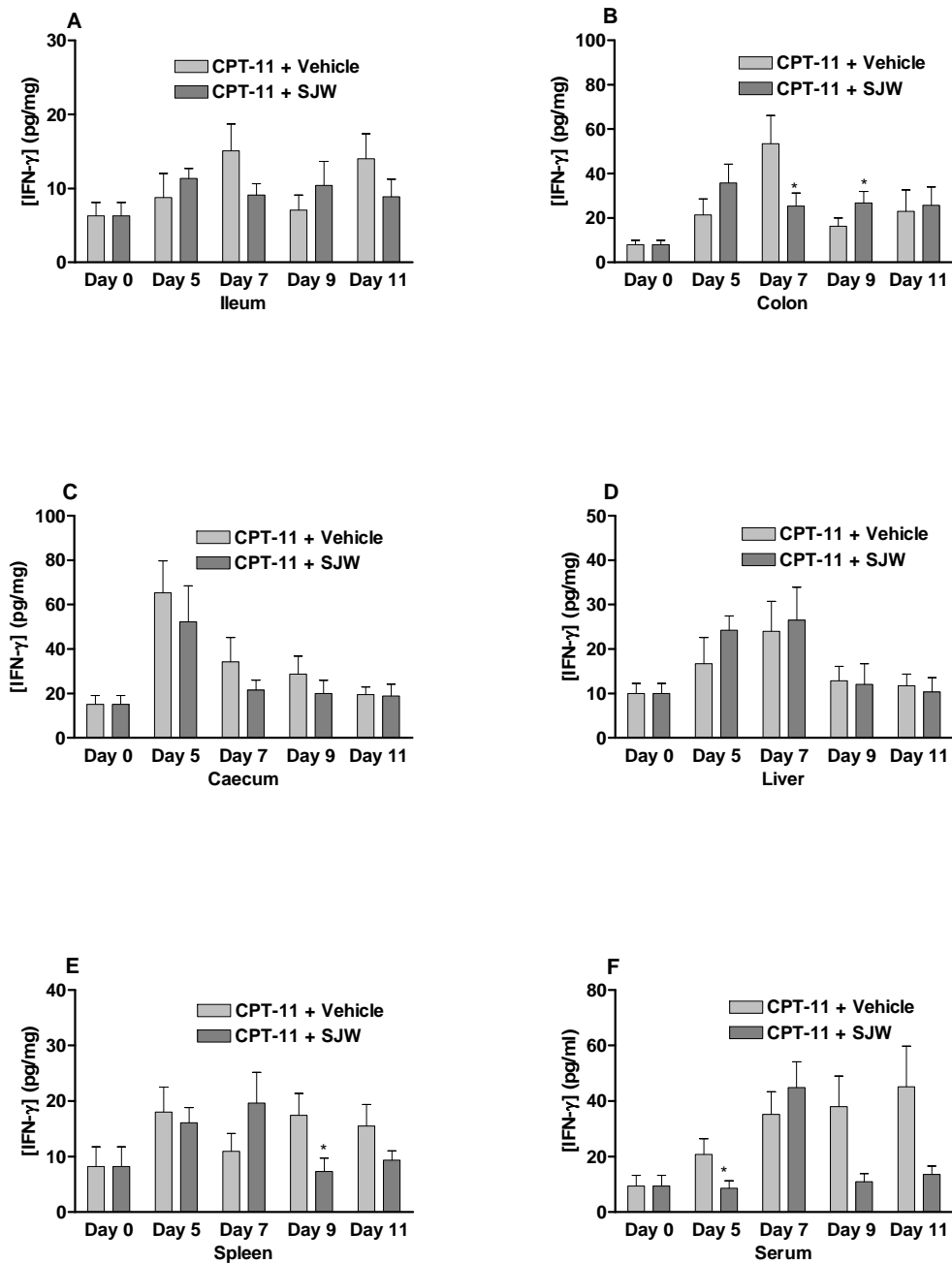
Figure 4-13. Protein levels of IFN-γ in rat ileum (A), colon (B), caecum (C), liver (D), spleen (E), and serum (F) on days 0, 5, 7, 9, and 11 after CPT-11 administration in control group treated with CPT-11 and control vehicle and combination group treated with CPT-11 and St. John's wort (SJW). *$P < 0.05$ (N = 4-6).
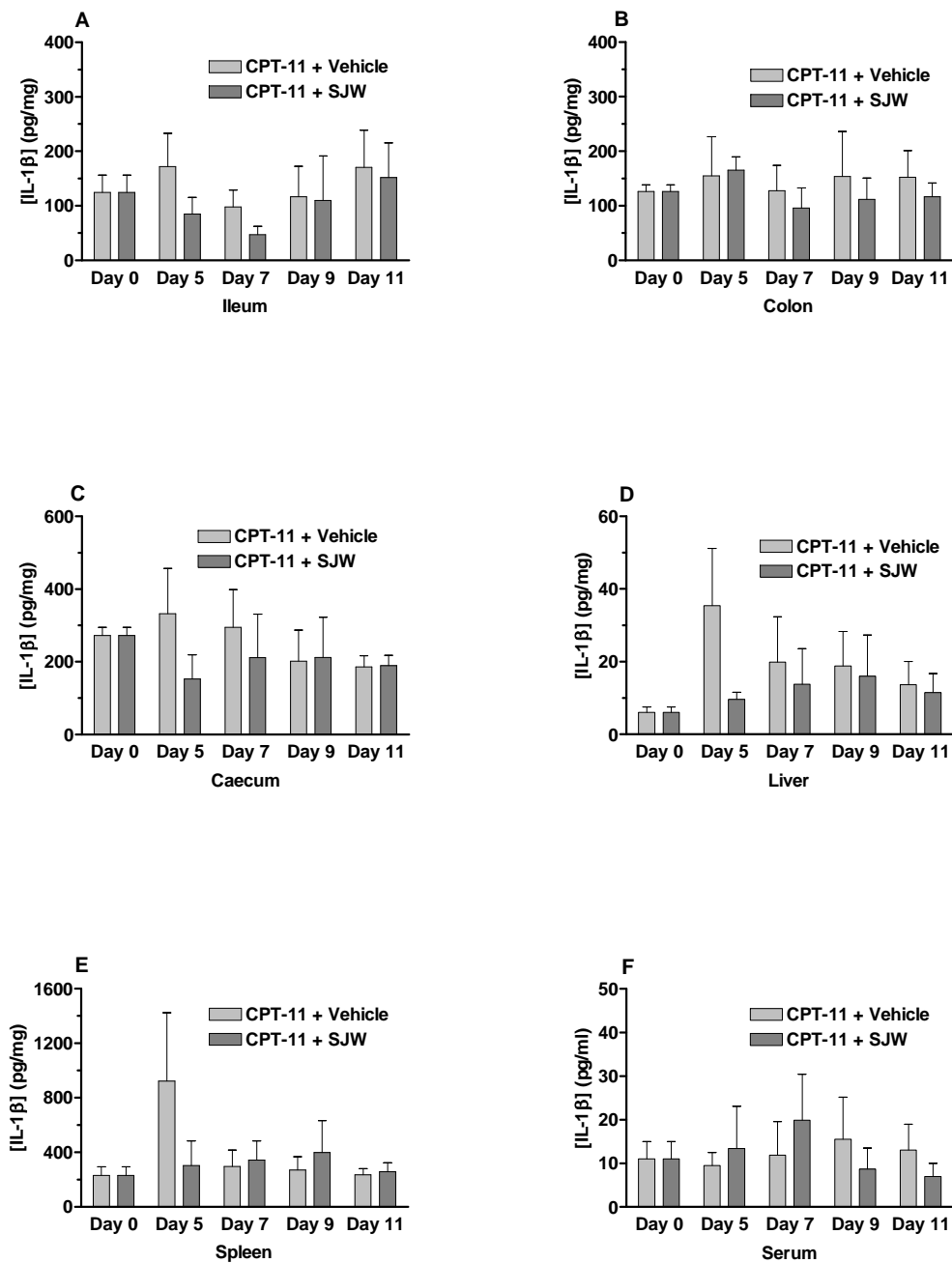
Figure 4-14. Protein levels of IL-1β in rat ileum (A), colon (B), caecum (C), liver (D), spleen (E), and serum (F) on days 0, 5, 7, 9, and 11 after CPT-11 administration in control group treated with CPT-11 and control vehicle and combination group treated with CPT-11 and St. John's wort (SJW) (N = 4-6).
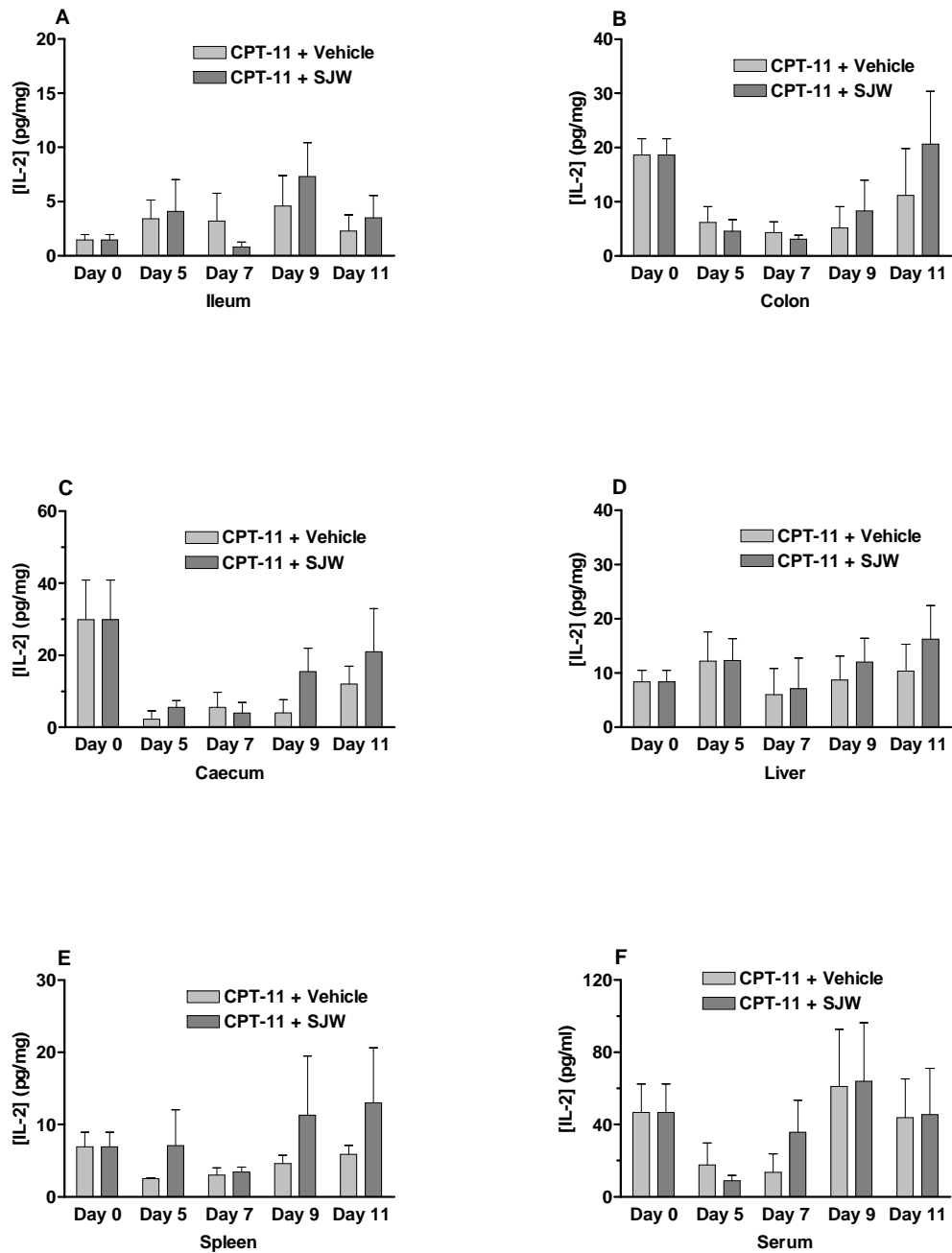
Figure 4-15. Protein levels of IL-2 in rat ileum (A), colon (B), caecum (C), liver (D), spleen (E), and serum (F) on days 0, 5, 7, 9, and 11 after CPT-11 administration in control group treated with CPT-11 and control vehicle and combination group treated with CPT-11 and St. John's wort (SJW) (N = 4-6).
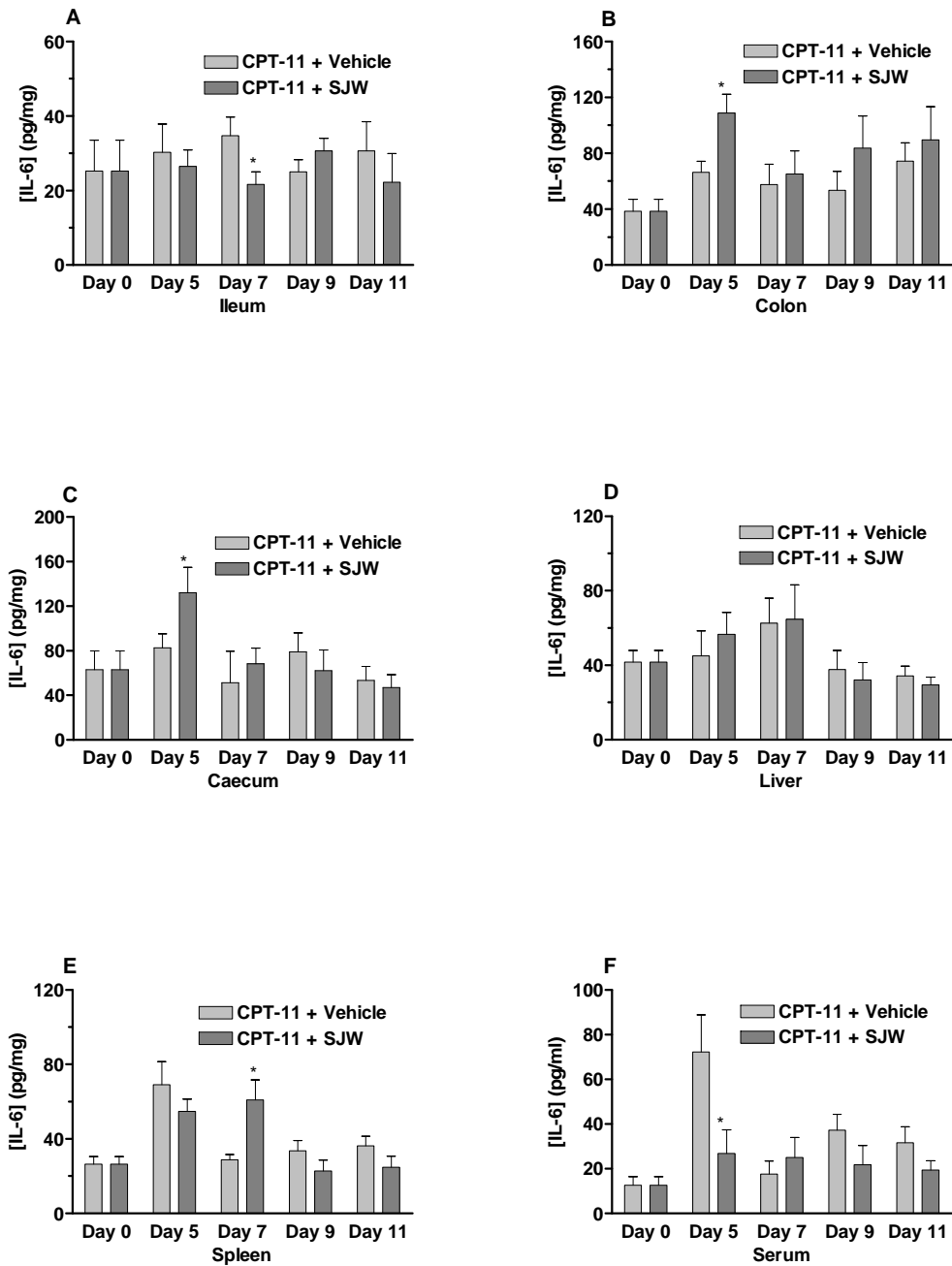
Figure 4-16. Protein levels of IL-6 in rat ileum (A), colon (B), caecum (C), liver (D), spleen (E), and serum (F) on days 0, 5, 7, 9, and 11 after CPT-11 administration in control group treated with CPT-11 and control vehicle and combination group treated with CPT-11 and St. John's wort (SJW). *$P < 0.05$ (N = 4-6).

Results showed that combination of SJW caused differential effects on protein levels of cytokine expressions in the tissues examined compared to the control group administered with CPT-11 alone.

Decreases in TNF-α expression were seen in the rats coadministered with SJW in caecum on day 5 by 64.5% and on day 7 by 46.3% ($P < 0.05$). Increased TNF-α was also suppressed in serum by coadministration of SJW on day 11 by 46.0% ($P < 0.05$).

Co-administered SJW caused differential effects on the levels of IFN-γ in different tissues. Co-administration of SJW significantly suppressed the increased protein level of IFN-γ in colon on day 7 by 52.6% ($P < 0.05$). Similar inhibitory effects on increased IFN-γ expression were observed in spleen on day 9 by 58.0% and serum on day 5 by 58.4% ($P < 0.05$). However, the combination of SJW resulted in an increase in protein levels of IFN-γ in colon on day 9 by 64.9% ($P < 0.05$) compared to rats treated with CPT-11 alone.

Combination of SJW reduced the expression of IL-6 in ileum on day 7 by 37.7% ($P < 0.05$) and in serum on day 5 by 62.7% ($P < 0.05$). However, protein levels of IL-6 were increased in the combination group compared to the control group in colon on day 5 by 63.6%, in caecum on day 5 by 60.1%, and in spleen on day 7 by 111.5% ($P < 0.05$), respectively.

Coadministered SJW had no significant effects on IL-1β and IL-2 expressions compared to the control group received CPT-11 alone.

4.3.4   *TNF-α* mRNA expression
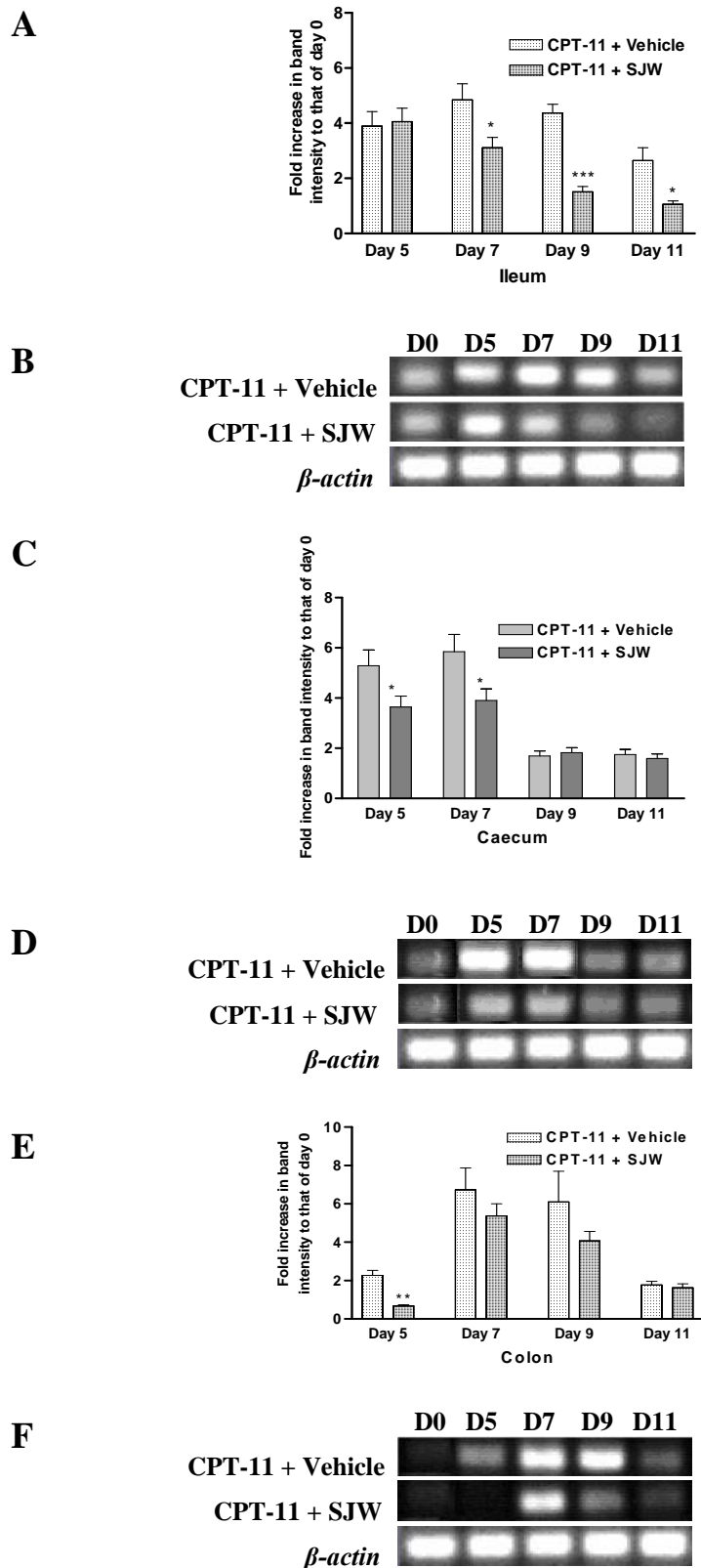
Figure 4-17. Representative illustrations of the expression pattern of *TNF-α* in ileum (A&B), caecum (C&D), and colon (E&F) after CPT-11 injection on days 0, 5, 7, 9, and 11 from rats in the absence or presence of SJW pretreatment. B, D, and F, RT-PCR analysis of *TNF-α*; A, C, and E, fold-increase in intensity of the bands compared to day 0 obtained from three independent experiments. Significant differences compared with values obtained in rats treated with CPT-11 alone: $*P < 0.05$; $**P < 0.01$; $***P < 0.001$ (N = 4-6).

126

The expression pattern and kinetics of the transcripts for *TNF-α* were examined over 11 days after administration of CPT-11 in intestinal tissues including ileum, caecum and colon (Figure 4-17). The transcripts for *TNF-α* were detectable in the ileum from healthy rats without any drug therapy. The intensity increased after CPT-11 injection and reached a peak level on day 7 (4.8-fold compared to that of day 0) in rats treated with CPT-11 alone and then dropped to day 11. However, combination of SJW brought down the expression levels of *TNF-α* mRNA, as indicated by reduced fold-increase of band intensity on days 7, 9 and 11 with a decrease of 35.8% ($P < 0.05$), 65.4% ($P < 0.001$) and 60.0% ($P < 0.05$), respectively.

Although the transcripts for *TNF-α* in the caecum were almost undetectable from healthy rats, they were readily detectable on days 5 to 11, with gradual decrease in the expression level after CPT-11 administration. Decreased *TNF-α* transcript was observed in the group treated with combined SJW over 11 days. The fold increase in band intensity was brought down by the combination of SJW on days 5 and 7 by 31.1% and 33.3% ($P < 0.05$), respectively.

The transcripts for *TNF-α* were detectable in the colon from healthy rats. They were increased after CPT-11 injection and achieved the maximum level on day 5 (6.7-fold compared to that of day 0) in the control group treated with CPT-11 and the control vehicle and then decreased. Similar expression pattern could be seen in the combination group but with dcreased levels of *TNF-α* over 11 days. Significant decrease in the fold increase in band intensity was observed on day 5 by 70.6% ($P < 0.01$).

4.4 CONCLUSION & DISCUSSION

The results showed that co-administered SJW ameliorated the dose-limiting toxicities of CPT-11 in rats by SJW attenuating the severity of late-onset diarrhea on day 5; increased the counts of neutrophil and lymphocyte on days 5, 7, and 9; alleviated the histological damages in intestinal tissues and subsequently reduced the stomach swell compared to the control rats without SJW pre-treatment. Serious leukopenia induced by CPT-11 administration would adversely allow the bacteria to infect the intestinal epithelium, thus exacerbating the intestinal toxicity. Therefore reduced hematological toxicity by the combination of SJW may help to alleviate CPT-11 induced histological damages by inhibiting opportunistic bacterial infections of the intestinal tissues.

These beneficial protective effects of SJW against CPT-11-induced toxicities are thought to be comparable to those caused by thalidomide. However, co-administration of thalidomide significantly alleviated body weight loss caused by CPT-11 and ameliorated late-onset diarrhea on both day 6 and day 7, while combination of SJW had no effect on body weight changes and only reduced late-onset diarrhea score on day 5 with significant effect. In the mean time, SJW increased leukocyte counts (including lymphocyte and neutrophil) with significant effects on days 5, 7, and 9 while thalidomide only increased leukocyte counts on day 7. Thus, by comparing, it seems that thalidomide might be more effective on CPT-11-induced gastrointestinal toxicity while SJW may be more efficient for CPT-11-induced hematological toxicity.

Our study showed that combination of SJW suppressed the protein expression of TNF-α and IFN-γ. Increased mRNA levels of *TNF-α* in intestinal tissues were

also brought down by the combination of SJW. The effects of SJW on the inhibition of TNF-α protein expression might be attributed to its effect on mRNA level of *TNF-α*. As shown in our data, the combination of SJW reduced the transcription product levels of *TNF-α* mRNA compared to the group treated with CPT-11 alone. However, inhibitory effects on the translation and post-translational modification of TNF-α by SJW can not be excluded.

Down-regulation of intestinal IFN-γ by SJW in the present study may be attributed to the inhibition of TNF-α production and/or direct inhibitory effects on the local immunocompetent cells. It has been advised that the immune responses of many other proinflammatory cytokines including IL-12 and IFN-γ could be potentiated by the increased TNF-α level. In addition, the inhibition of IFN-γ production by SJW was also indicated in human peripheral blood mononuclear cells [306].

Our study showed that coadministered SJW alleviated apoptosis in intestinal epithelial cells. SJW and quercetin have been reported to inhibit apoptosis induced by various mechanisms in several cell lines [307] and exerted a protective effect against H_2O_2-induced apoptosis in human neuroblastoma cells, cardiomyoblast cells and macrophages. Hypericin prevented the apoptosis induced in murine L-cells with recombinant TNF-α [308]. In addition, SJW extract modulated apoptosis in mice splenic lymphocytes *in vivo* [309]. This was consistent with our study that combination with SJW showed marked protective effect on CPT-11 induced leukocyte decrease, which might be ascribed to the modulation effect of SJW on apoptosis in leukocytes. Additionally, studies showed venous congestion induced mucosal apoptosis via TNF-α-mediated cell death in the rat small

intestine with a variety of intermediates and protein-protein interactions involved [310]. This finding is consistent with our result that congestion is observed in intestinal tissues accompanied with increased TNF-α level and apoptosis after CPT-11 treatment. The reduced TNF-α level after SJW combination also inhibited the intestinal damages caused by apoptosis, arising from venous congestion. In addition, as a pro-inflammatory cytokine, IFN-γ could sensitize intestinal epithelial cells to physiological and therapeutic inducers of apoptosis [311]. So the down-regulation of IFN-γ by SJW may also lead to the decreased apoptosis in intestinal epithelial cells.

In summary, these results provided additional support for the apoptosis- and TNF-α-associated mechanisms for CPT-11 induced toxicity and partially explained the protective effects of SJW on CPT-11 induced toxicity, which might be attributed to the modulation of relevant cytokines and intestinal epithelial cellular apoptosis.

CHAPTER 5 EFFECTS OF ST. JOHN'S WORT ON THE PHARMACOKINETICS OF CPT-11 AND THE UNDERLYING MECHANISMS

5.1 INTRODUCTION

Clinical study and our study in rats showed that the combination of SJW ameliorated the toxicities induced by CPT-11. The modulation of cytokine levels and intestinal epithelial apoptosis may partially explain this effect; however, pharmacokinetic interactions could also be involved. In an unblinded, randomized crossover study in 5 cancer patients, it was found that treatment of SJW (900 mg/day, oral) for 18 days decreased the plasma levels of the active metabolite SN-38 by 42%, which was accompanied by decreased myelosuppression [177]. The authors advised that patients on irinotecan treatment should refrain from taking SJW because of the dramatically reduced SN-38 plasma levels caused by combination with SJW which may have a deleterious impact on treatment outcome. However, the in vitro kinetic interactions for CPT-11 with SJW were not fully studied, although induction of CYP3A4 expression by SJW was indicated as a component for this interaction.

In the present study, we aimed to using the rat model and *in vitro* models to explore the potential kinetic interactions between CPT-11 with SJW. The effects of SJW extracts, hypericin, hyperforin, and quercetin on CPT-11 and SN-38 metabolism were conducted using rat liver microsomes and a rat hepatoma cell line, H4-II-E cells. H4-II-E cells were also used to investigate the effects of these compounds on the transport of CPT-11 and SN-38. The effect of the combination

of SJW with CPT-11 will be further evaluated. The greater understanding of the modulation effects of SJW on drug metabolizing enzymes and transporters for CPT-11 using *in vitro* models may also provide insights into the combination of chemotherapeutic agents with herbal medicines and their potential pharmacokinetic interactions.

5.2   MATERIALS AND METHODS

5.2.1   Chemicals

Refer to Sections 3.2.1 and 4.2.1. Hypericin, hyperforin, and quercetin were purchased from Sigma Chemical Co. (St. Louis, Mo, USA). The SJW aqueous extract (AE) were freshly prepared by suspending the SJW powder in 0.9% physiological saline at the concentration of 10 μg/ml, and ultrasonicating at room temperature for 10 min. After centrifugation at 6,000 × *g* for 15 min, the supernatant was collected for experimental use. For the preparation of ethanolic extract (EE) of SJW, the SJW powder was suspended in 80% ethanol (v/v) at a concentration of 1:9 (w/v). After vortex-mixing, the suspension was ultrasonicated at room temperature for 1 hr before evaporating the ethanol in a Heidolph LR4002 Control rotary evaporator (Heidolph Instruments GmbH & Co. KG, Germany). After that, the remaining was transferred into a tube and subjected to a freeze drier (FD3, Dynavac engineering, Sydney, Australia) until completely dry. So there will be more hydrophilic components in the aqueous extract and more lipophilic components in the ethanolic extract. However, the exact components for each extract would need to be identified. Hypericin and hyperforin were dissolved in DMSO and methanol, respectively, and stored in dark at -20°C.

5.2.2 Animals

Refer to Section 3.2.2.

5.2.3 Drug administration and sampling

The pharmacokinetic interaction studies included experiments with short-term (3 days) or long-term (14 days) administration of SJW to rats. Rats were randomized to four groups (at least 5 rats per group) receiving SJW at 400 mg/kg/day (6 ml/mg) or SJW-free control vehicle for 3 or 14 consecutive days by oral gavage before CPT-11 injection. On day 4 or 15, CPT-11 (60 mg/kg, i.v.) was administered via tail vein. Blood samples (~200 µl) were collected into heparinized tubes from tail vein 0.25, 0.5, 1, 2, 4, 6, 8, and 10 hr after CPT-11 injection. Plasma was obtained by immediate centrifugation at $1,500 \times g$ for 10 min at 4ºC, and stored at -80ºC until analysis. After deproteinization, plasma drug concentrations were analysed by HPLC.

5.2.4 Rat liver microsomal preparation

Refer to Section 3.2.4 for rat liver microsome preparation. In addition to normal rat liver microsomes, SJW-induced microsomes were also prepared using the same procedure in which rats were administered with SJW or SJW-free vehicle (as control group) by oral gavage (400 mg/kg/day) for 14 days continuously before the livers were collected.

5.2.5 Hepatic microsomal metabolic inhibition study

To investigate the effects of SJW AE (10 µg/ml), EE (5 µg/ml) and its major components including hypericin (20 nM and 200 nM), and hyperforin (1 µM) on

CPT-11 hydrolysis and SN-38 glucuronidation in rat hepatic microsomes, CPT-11 or SN-38 was incubated with hepatic microsomes (2.0 mg/ml for CPT-11 and 1.0 mg/ml for SN-38) in 200 µl incubation buffers containing either SJW extracts or its major components. For detailed incubation conditions refer to Section 3.2.6. Control incubations with 1% (v/v) DMSO were also undertaken, which showed no significant effect on the liver microsomal metabolism of CPT-11 and SN-38. SN-38 and SN-38G formation was measured as pmol/min/mg protein. Inhibition was expressed as percentage of the control. In addition, the known CE inhibitor nifedipine (100 µM) and BNPP (100 µM) [312, 313] were used as positive control for CPT-11 hydrolysis, while nifedipine (100 µM) and bilirubin (100 µM) were used as positive control for SN-38 glucuronidation [314-316]. The induction effects of SJW on rat hepatic microsomal enzyme activity were also evaluated by comparing the K_m and V_{max} values for CPT-11 hydrolysis and SN-38 glucuronidation in SJW-induced microsomes and SJW-free control vehicle pretreated microsomes.

5.2.6   Cell culture & cytotoxicity assay in rat hepatoma H4-II-E cells

The cytotoxic effects of SJW AE, SJW EE, hypericin, hyperforin, and quercetin on H4-II-E cells were determined using MTT assay. Refer to Section 3.2.7 for cell culture and 3.2.8 for cytotoxicity assay.

5.2.7   Metabolic and intracellular accumulation inhibition assay for CPT-11 and SN-38 in rat hepatoma H4-II-E cells

The effects of SJW AE, SJW EE, hypericin, hyperforin, and quercetin on CPT-11 hydrolysis and SN-38 glucuronidation as well as CPT-11 and SN-38 intracellular

accumulation in rat hepatoma H4-II-E cells were investigated in triplicate by pre-incubation of cell cultures with these compounds for 2 hr (short term) or 4 days (long-term, to observe whether there is induction effect).

5.2.8 Determination of CPT-11, SN-38, and SN-38 glucuronide by HPLC methods and LC-MS

Refer to Sections 3.2.11 and 3.2.12.

5.2.9 Pharmacokinetic calculation & statistical analysis

Refer to Sections 3.2.13 and 3.2.14.

5.3 RESULTS

5.3.1 SJW altered the plasma pharmacokinetics of CPT-11

Figure 5-1 shows the representative plasma concentration-time profiles for all analytes studied in rats receiving CPT-11 alone and in combination with SJW. For the short-term (3 days) study, pretreatment of rats with SJW (p.o. 400 mg/kg for consecutive 3 days) did not significantly alter the pharmacokinetic parameters for CPT-11 and its metabolites (Table 5-1) compared to rats receiving CPT-11 and control vehicle alone. For the long-term (14 days) study, pretreatment of rats with SJW (p.o. 400 mg/kg for consecutive 14 days) significantly decreased the C_{max} of SN-38 by 38.9 % ($P < 0.01$) (Table 5-2). However, the $AUC_{0-\infty}$ of SN-38 was not significantly altered. Pretreatment of rats with SJW for 14 days did not significantly alter the pharmacokinetic parameters of CPT-11 and SN-38G compared to the control group.

Table 5-1. Comparison of pharmacokinetic parameters between two groups of rats receiving CPT-11 and control vehicle or pretreated with St. John's wort (SJW) for 3 days (N = 5).

Parameters	Treatment Groups		Change (%)	*P* value*
	CPT-11 + SJW	CPT-11 + Vehicle		
CPT-11				
$C_0^{\#}$ (ng/ml)	8966.8 ± 1967.2	12140.0 ± 6695.3	-26.1	ns
$t_{1/2\beta}$ (hr)	1.68 ± 0.34	1.85 ± 0.32	-9.2	ns
$AUC_{0\text{-}10hr}$ (ng·hr/ml)	18523.3 ± 3265.2	20959.8 ± 3429.0	-11.6	ns
$AUC_{0\text{-}\infty}$ (ng·hr/ml)	18903.4 ± 3497.0	21472.7 ± 3532.1	-12.0	ns
V_d (ml/kg)	7799.7 ± 1382.0	7533.6 ± 1264.6	3.5	ns
CL (ml/hr/kg)	3263.0 ± 579.2	2856.8 ± 510.9	14.2	ns
SN-38				
C_{max} (ng/ml)	665.9 ± 277.3	846.9 ± 136.1	-21.4	ns
$AUC_{0\text{-}10hr}$ (ng·hr/ml)	4158.7 ± 1544.5	4824.6 ± 1079.6	-13.8	ns
$t_{1/2\beta}$ (hr)	3.70 ± 0.73	3.63 ± 0.72	1.9	ns
$AUC_{0\text{-}\infty}$ (ng·hr/ml)	5073.9 ± 1600.5	5759.6 ± 1360.9	-11.9	ns
SN-38G				
C_{max} (ng/ml)	2220.4 ± 463.3	3124.5 ± 1236.3	-28.9	ns
$AUC_{0\text{-}10hr}$ (ng·hr/ml)	7332.9 ± 1056.5	9943.7 ± 2936.8	-26.3	ns
$t_{1/2\beta}$ (hr)	2.88 ± 0.93	3.88 ± 0.71	-25.8	ns
$AUC_{0\text{-}\infty}$ (ng·hr/ml)	8074.6 ± 1063.7	11733.8 ± 3754.7	-31.2	ns

* Compared with the controls using Students' unpaired *t*-test. ns, not significant.
# Obtained by back-extrapolation to the zero time using WinNonlin program.

Table 5-2. Comparison of pharmacokinetic parameters between two groups of rats receiving CPT-11 and control vehicle or pretreated with St. John's wort (SJW) for 14 days (N = 5).

Parameters	Treatment Groups		Change (%)	*P* value*
	CPT-11 + SJW	CPT-11 + vehicle		
CPT-11				
$C_0^{\#}$ (ng/ml)	9358.4 ± 1971.4	15469.9 ± 6206.0	-39.5	ns
$t_{1/2\beta}$ (hr)	2.01 ± 0.31	1.73 ± 0.15	16.2	ns
$AUC_{0\text{-}10hr}$ (ng·hr/ml)	23227.6 ± 4847.1	28678.5 ± 9284.8	-19.0	ns
$AUC_{0\text{-}\infty}$ (ng·hr/ml)	23967.5 ± 5389.2	29104.7 ± 9368.2	-17.7	ns
V_d (ml/kg)	7393.9 ± 1077.5	5541.5 ± 1636.8	33.4	ns
CL (ml/hr/kg)	2597.1 ± 509.3	2242.4 ± 723.5	15.8	ns
SN-38				
C_{max} (ng/ml)	639.4 ± 200.3	1046.9 ± 232.2	-38.9	<0.01
$AUC_{0\text{-}10hr}$ (ng·hr/ml)	4342.7 ± 1250.0	5895.3 ± 1372.7	-26.3	ns
$t_{1/2\beta}$ (hr)	4.25 ± 1.63	4.82 ± 3.81	-11.8	ns
$AUC_{0\text{-}\infty}$ (ng·hr/ml)	5688.7 ± 1409.9	8644.4 ± 5543.2	-34.2	ns
SN-38G				
C_{max} (ng/ml)	2681.8 ± 963.1	2320.8 ± 544.8	15.6	ns
$AUC_{0\text{-}10hr}$ (ng·hr/ml)	7038.2 ± 1837.7	6523.4 ± 1577.1	7.9	ns
$t_{1/2\beta}$ (hr)	2.61 ± 0.50	2.79 ± 0.56	-6.5	ns
$AUC_{0\text{-}\infty}$ (ng·hr/ml)	7649.9 ± 2293.1	7073.1 ± 1688.3	8.2	ns

* Compared with the controls using Students' unpaired *t*-test. ns, not significant.
# Obtained by back-extrapolation to the zero time using WinNonlin program.
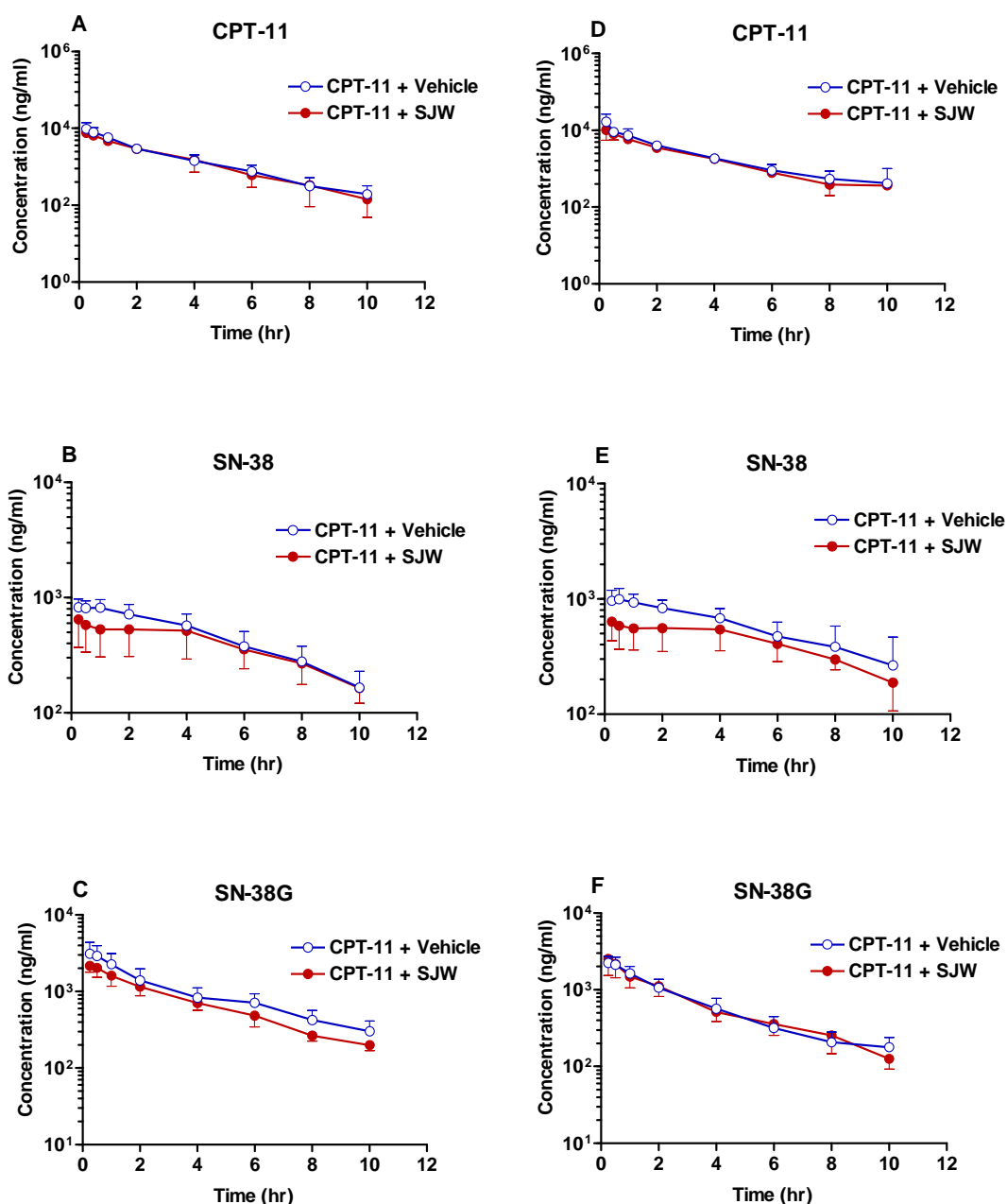
Figure 5-1. Plasma concentration-time profiles of CPT-11, SN-38, and SN-38G in rats receiving CPT-11 with control vehicle or in combination with St. John's wort (SJW). A, B, & C: Short-term (3 days) kinetic interaction study; D, E, & F: Long-term (14 days) kinetic interaction study (N = 5).

5.3.2 Effects of SJW extract and its major components on the hepatic microsomal metabolism of CPT-11 and SN-38

The effects of SJW AE, SJW EE, hyperforin, hypericin, nifedipine, BNPP and bilirubin on CPT-11 hydrolysis and SN-38 glucuronidation are shown in Figure 5-3. SJW extracts and its tested major compounds showed no inhibitory effects on

CPT-11 (0.5 and 78 µM) hydrolysis and SN-38 glucuronidation (5.0 µM and 18.2 µM) except that the ethanolic extract of SJW significantly decreased SN-38 (18.2 µM) glucuronidation by 45.1% ($P < 0.01$).

As expected, nifedipine (100 µM) significantly reduced CPT-11 hydrolysis (0.5 µM) by 23.4% ($P < 0.001$), while it had no significant effect on CPT-11 hydrolysis at a higher concentration (78 µM). By contrast, BNPP at 100 µM showed a significant ($P < 0.001$) inhibitory effect on CPT-11 hydrolysis at 0.5 µM (53.7% decrease) or at 78 µM substrate concentration (41.1% decrease). In addition, nifedipine (100 µM) also had significant inhibitory effect on the glucuronidation of SN-38 at 5.0 µM (60.0% decrease, $P < 0.001$) or at 18.2 µM (53.0% decrease, $P < 0.01$). However, bilirubin at 100 µM had no significant effect on SN-38 glucuronidation (5.0 µM) but inhibited SN-38 glucuronidation at 18.2 µM by 25.6% ($P < 0.05$). These results indicated the effectiveness of our microsomal system in the metabolic inhibition studies.

In our study, an optimal protein concentration of 2.0 mg/ml and incubation time of 30 min and a protein concentration of 1.0 mg microsomal protein/ml and an incubation time of 30 min were chosen for the CPT-11 hydrolysis and SN-38 glucuronidation study in control microsome and SJW-induced microsome (Figure 5-2). By comparing the fitted models, the hydrolysis of CPT-11 to form SN-38 in the control and SJW-induced rat liver microsomes is best represented by a one binding-site model with estimated K_m of 68.57 and 70.82 µM and V_{max} of 9.6 and 11.03 pmol/min/mg protein, respectively. In addition, the glucuronidation of SN-38 in rat liver microsomes is best represented by a one-enzyme equation in the control and SJW-induced rat liver microsomes with estimated K_m of 24.86 and

29.86 μM and V_{max} of 287.0 and 357.0 pmol/min/mg protein, respectively (Table 5-3).
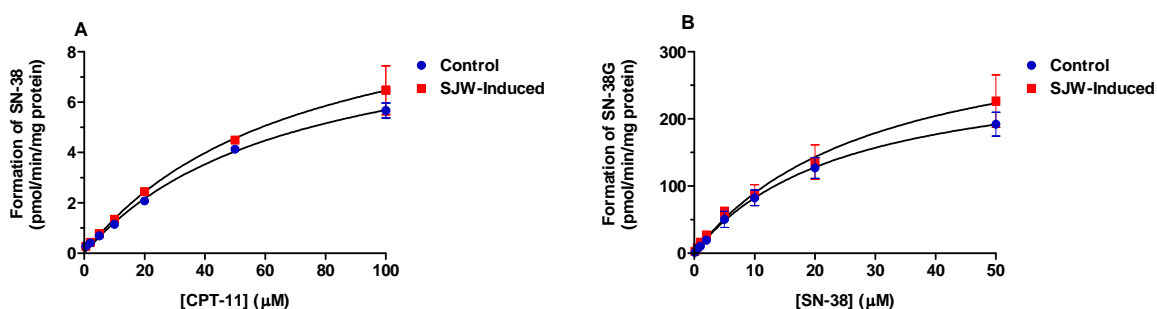
Figure 5-2. Effects of substrate concentration on the formation of SN-38 from CPT-11 (A) and SN-38 glucuronide from SN-38 (B) in control- and SJW-induced rat liver microsomes (N = 3).

Table 5-3. Estimated K_m and V_{max} values for the metabolism of CPT-11 and SN-38 in the control microsome and St. John's wort (SJW)-induced microsome (N = 3).

Substrate	Parameters	Control Microsome	SJW-induced Microsome
CPT-11	K_m (μM)	68.57	70.82
	V_{max} (pmol/min/mg protein)	9.60	11.03
SN-38	K_m (μM)	24.86	29.86
	V_{max} (pmol/min/mg protein)	287.00	357.00

5.3.3 Cytotoxicity of SJW extract and its major components in rat hepatoma H4-II-E cells

When incubated for 4 hr, hyperforin, hypericin, quercetin, and SJW EE caused significant cell growth inhibition with an estimated IC_{50} of 19.1, 44.1, 106.5μM, and 165.6 μg/ml, respectively (Figure 5-4). The IC_{50} for hyperforin, hypericin, quercetin, and SJW EE decreased to 9.1, 15.6, 19.0 μM, and 48.2 μg/ml, respectively when the drug-exposure time was increased to 48 hr (Figure 5-5). By contrast, incubation of SJW AE at concentrations up to 1,000 μg/ml for 48 hr exhibited little cytotoxic effects to H4-II-E cells.
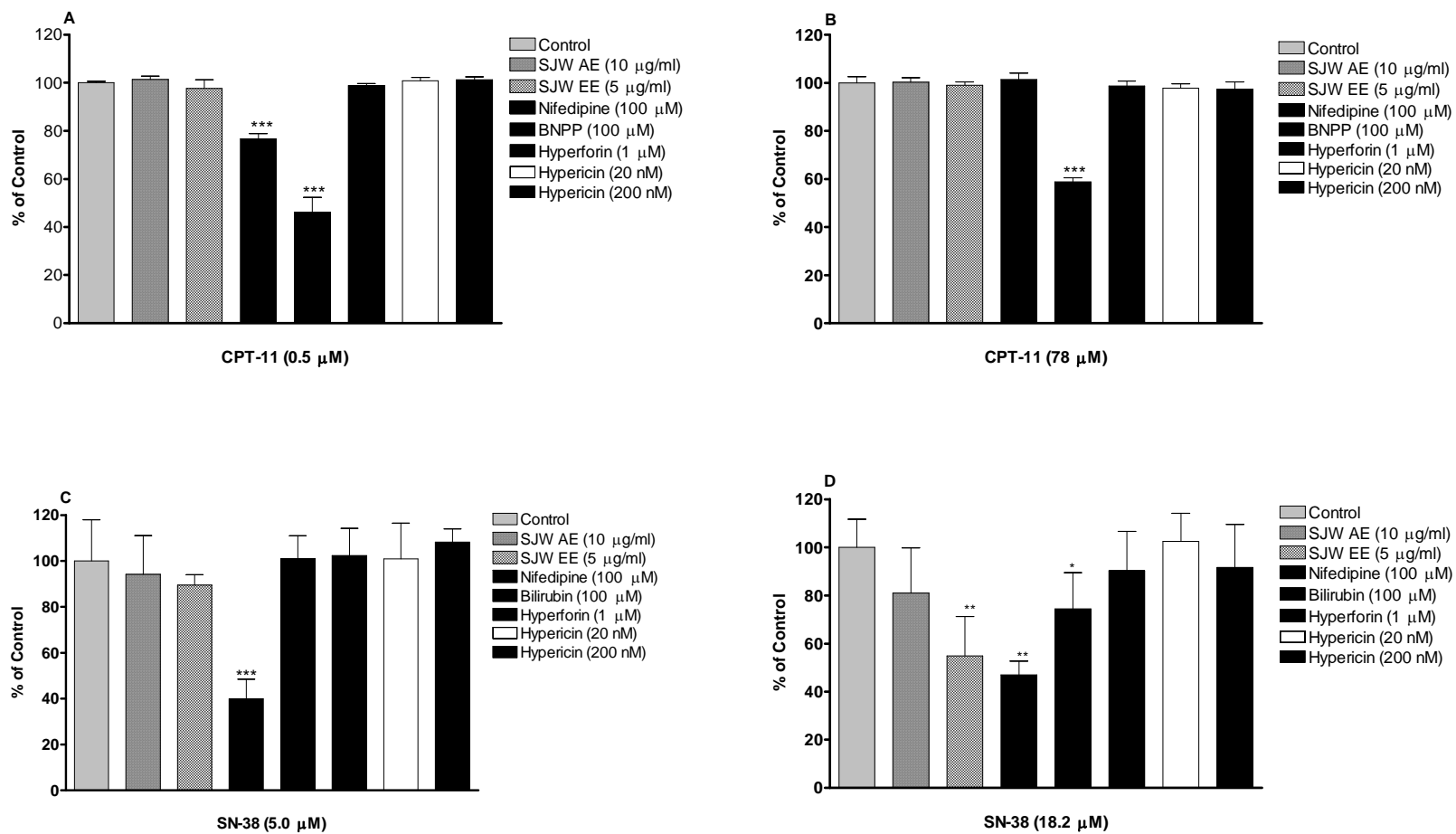
Figure 5-3. Effects of SJW aqueous extracts (AE), ethanolic extracts (EE), hyperforin, hypericin, nifedipine, bis (p-nitrophenyl) phosphate sodium salt (BNPP), and bilirubin on the hydrolysis of CPT-11 at 0.5 and 78 μM (A & B) or SN-38 at 5.0 and 18.2 μM (C & D) in rat liver microsomes. *$P < 0.05$; **$P < 0.01$; ***$P < 0.001$ (N = 3).
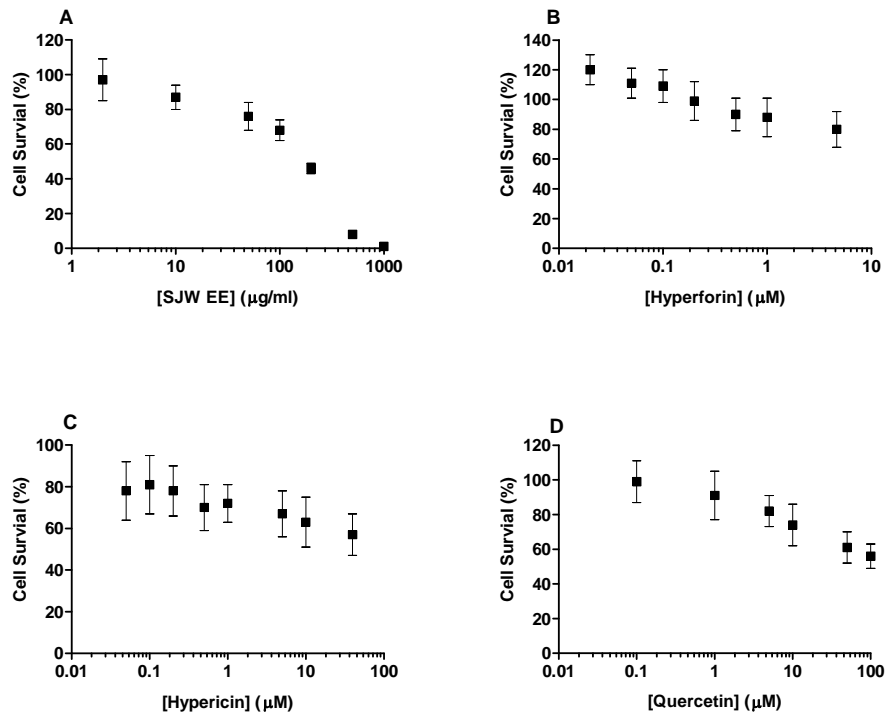
Figure 5-4. Cytotoxic effects of SJW ethanolic extracts (EE) (A), hyperforin (B), hypericin (C), and quercetin (D) in rat hepatoma H4-II-E cells when incubated for 4 hr (N = 3).
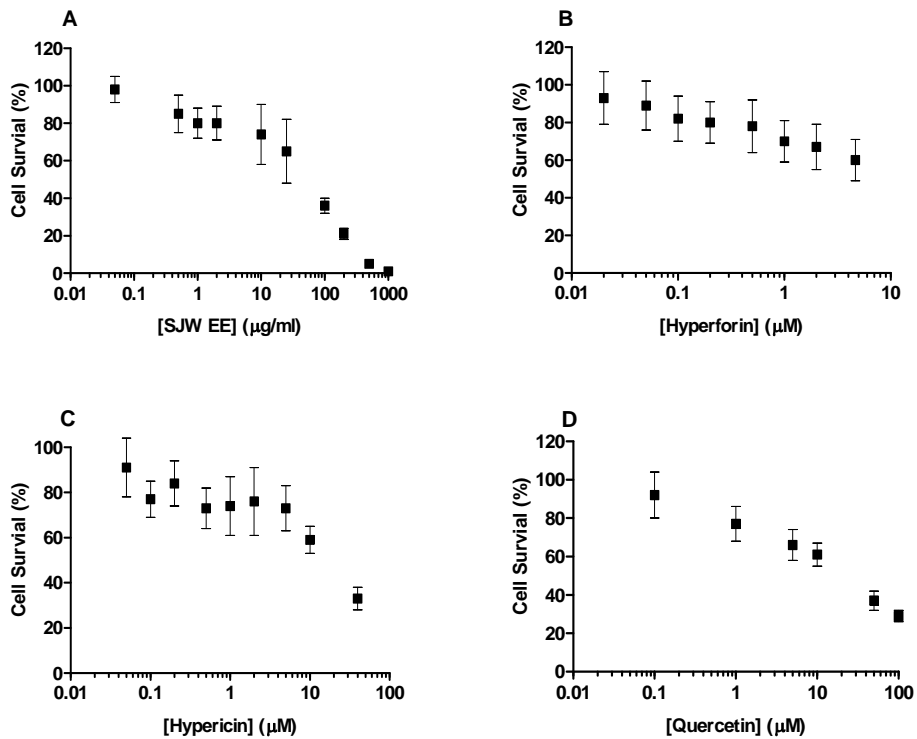
Figure 5-5. Cytotoxic effects of SJW ethanolic extracts (EE) (A), hyperforin (B), hypericin (C), and quercetin (D) in rat hepatoma H4-II-E cells when incubated for 48 hr (N = 3).

141

5.3.4 Effects of SJW extract and its major components on the metabolism of CPT-11 and SN-38 in rat hepatoma H4-II-E cells

The effects of SJW extract and its major components on CPT-11 and SN-38 metabolism in H4-II-E cells in DMEM are shown in Figure 5-6. Pre-incubation of SJW extract and its major components for 2 hr or 4 days had no inhibitory effects on CPT-11 hydrolysis. A 2-hr pre-incubation of SJW AE at 10 μg/ml and SJW EE at 5 μg/ml increased the glucuronidation of SN-38 by 15.1 and 13.9% ($P < 0.05$). A 4-day pre-incubation of SJW AE at 10 μg/ml, quercetin at 10 μM, and hyperforin at 1 μM all increased the conversion of SN-38 to SN-38G by 26.8% ($P < 0.01$), 35.2% ($P < 0.001$), and 57.7% ($P < 0.001$), respectively. In addition, BNPP and nifedipine at 100 μM significantly inhibited the hydrolysis of CPT-11 by 9.8% ($P < 0.01$) and 6.8% ($P < 0.05$) and nifedipine at 100 μM significantly inhibited the glucuronidation of SN-38 by 14.3% ($P < 0.05$). By contrast, bilirubin showed no inhibitory effect on SN-38 glucuronidation.

5.3.5 Effects of SJW extract and its major components on the intracellular accumulation of CPT-11 and SN-38 in rat hepatoma H4-II-E cells

The effects of SJW extract and its major components on CPT-11 and SN-38 cellular accumulation in H4-II-E cells in DMEM are shown in Figure 5-7. Pre-incubation of SJW EE and AE for 2 hr or 4 days had no inhibitory effects on CPT-11 cellular accumulation. A 2-hr pre-incubation of MK 571 at 100 μM increased the cellular accumulation of CPT-11 by 35.2% ($P < 0.001$).
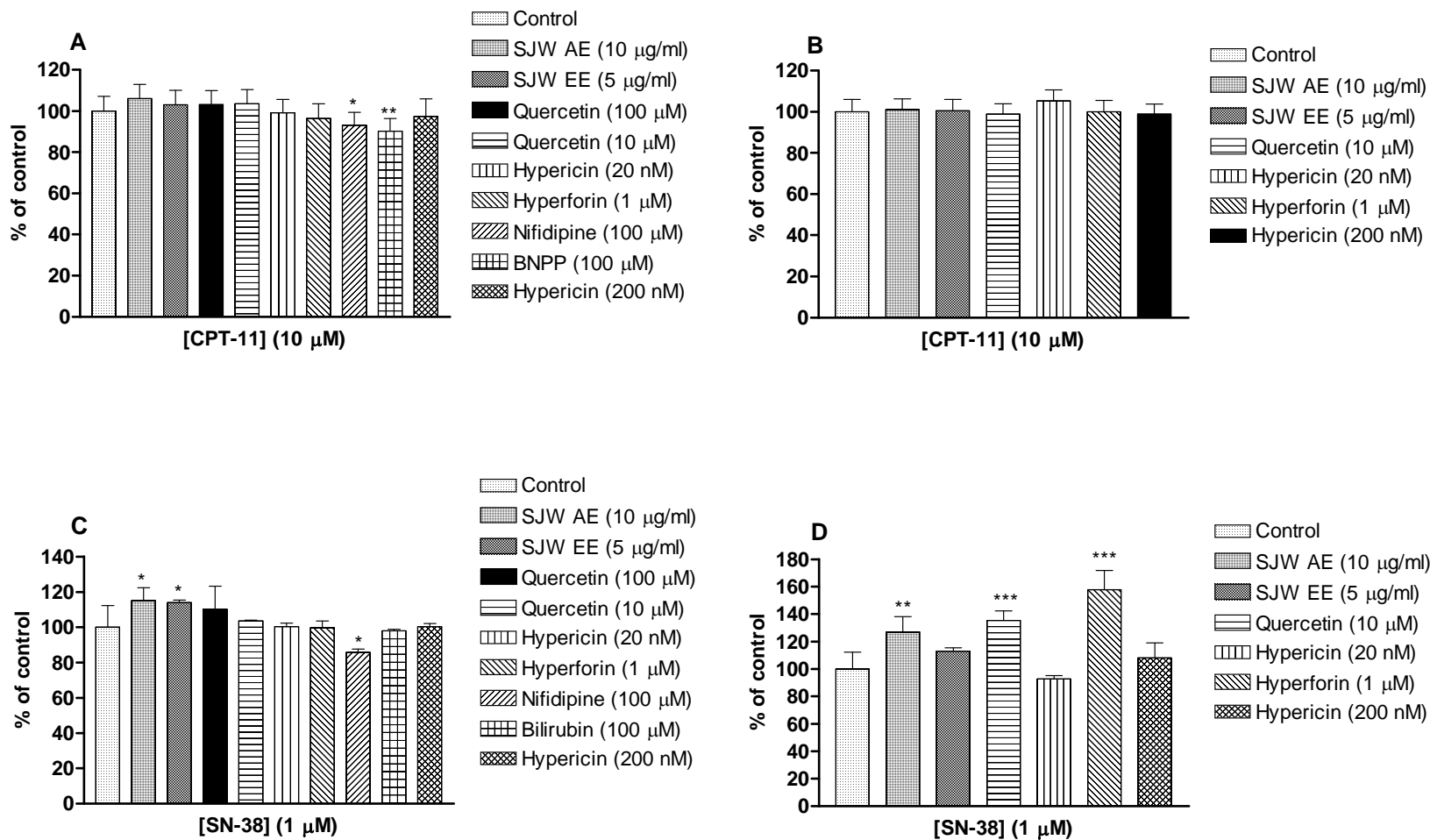
Figure 5-6. Effects of SJW ethanolic extracts (EE), SJW aqueous extracts (AE), hypericin, hyperforin, quercetin, nifedipine, BNPP, and bilirubin on CPT-11 hydrolysis (A & B) and SN-38 glucuronidation (C & D) in H4-II-E cells cultured in DMEM. A & C, 2-hr pre-incubation with the inhibitor; B & D, 4-day pre-incubation with the inhibitor. *P < 0.05; **P < 0.01; ***P < 0.001 (N = 3).
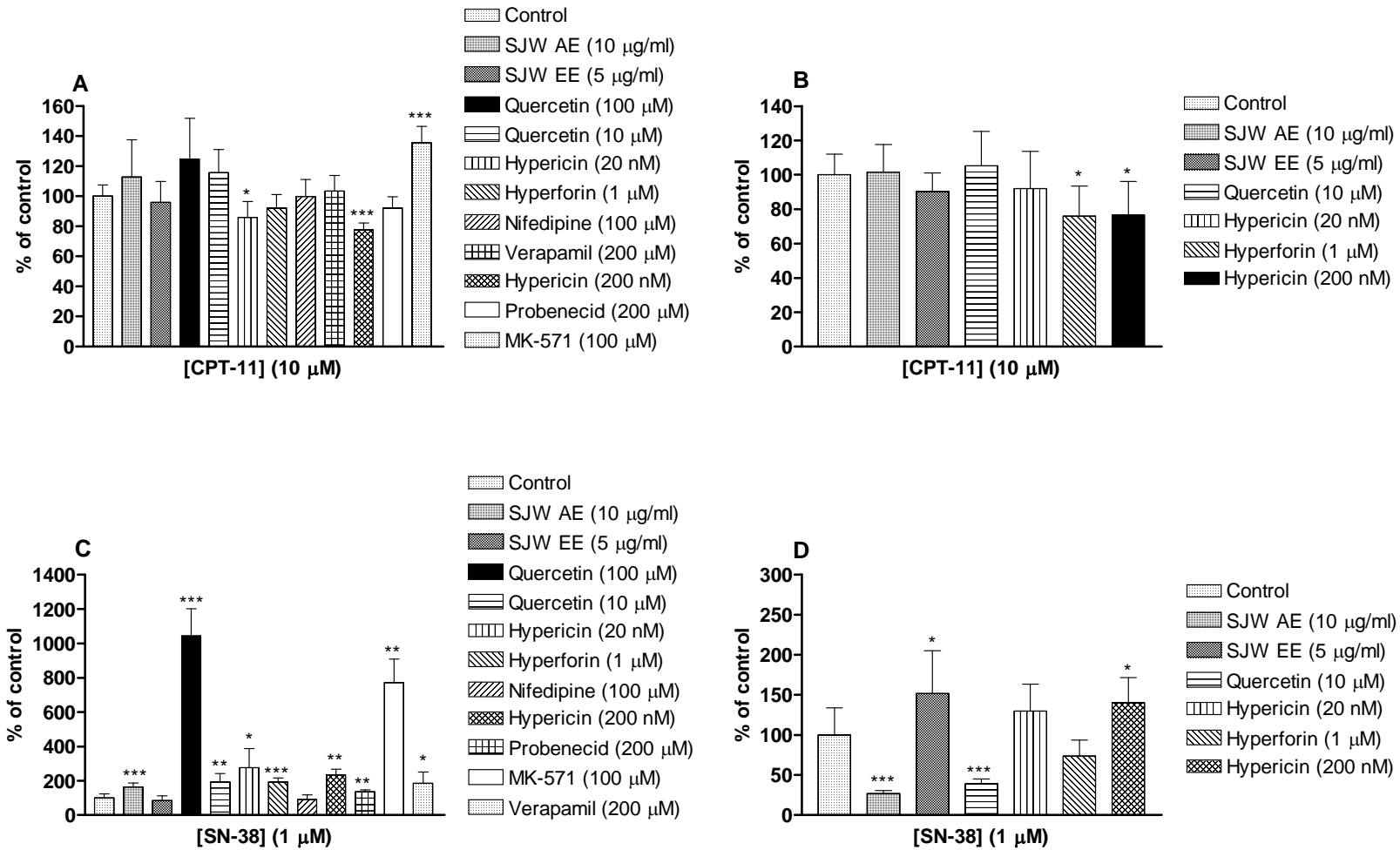
Figure 5-7. Effects of SJW ethanolic extracts (EE), SJW aqueous extracts (AE), hypericin, hyperforin, quercetin, nifedipine, verapamil, MK-571, and probenecid on cellular accumulation of CPT-11 (A & B) and SN-38 (C & D) in H4-II-E cells cultured in DMEM. A & C, 2-hr pre-incubation with the inhibitor; B & D, 4-day pre-incubation with the inhibitor. *$P < 0.05$; **$P < 0.01$; ***$P < 0.001$ (N = 3).

However, a 2-hr pre-incubation of hypericin at both 20 nM and 200 nM inhibited the cellular accumulation of CPT-11 by 14.0% ($P < 0.05$) and 22.3% ($P < 0.001$). Inhibitory effects could also be seen for a 4-day pre-incubation with hyperforin at 1 µM (by 24.0%, $P < 0.05$) and hypericin at 200 nM (by 23.6%, $P < 0.05$).

A 2-hr pre-incubation of hypericin at 20 nM, hypericin at 200 nM, hyperforin at 1 µM, quercetin at 10 µM and 100 µM, SJW AE (10 µg/ml), MK-571 at 100 µM, verapamil at 100 µM and probenecid at 200 µM all increased the cellular accumulation of SN-38 with significant effects by 176.2% ($P < 0.05$), 134.3% ($P < 0.01$), 91.9% ($P < 0.001$), 93.6% ($P < 0.01$), 944.1% ($P < 0.001$), 62.5% ($P < 0.001$), 670.5% ($P < 0.01$), 85.0% ($P < 0.05$), and 36.3% ($P < 0.01$), respectively. In addition, a 4-day pre-incubation with SJW EE at 5 µg/ml and hypericin at 200 nM increased the cellular accumulation of SN-38 by 51.6% ($P < 0.05$) and 40.1% ($P < 0.05$), respectively; while a 4-day pre-incubation with SJW AE at 10 µg/ml and quercetin at 10 µM inhibited the cellular accumulation of SN-38 by 73.2% ($P < 0.001$) and 61.0% ($P < 0.001$), respectively.

5.4   CONCLUSION & DISCUSSION

Results showed that co-administered SJW for 14 consecutive days significantly decreased the maximum plasma concentration (C_{max}) of SN-38. A clear correlation between the toxicity of CPT-11 and its pharmacokinetic parameters for C_{max} of SN-38 was observed in cancer patients [65]. Thus, the reduction in the C_{max} of SN-38 after SJW pre-treatment in our study may partially explain the finding that co-administered SJW reduced the gastrointestinal toxicity of CPT-11.

The reason for the reduced plasma SN-38 levels by SJW may be due to reduced formation of SN-38 and/or increased glucuronidation of SN-38. Reduced CE activity or induced CYP3A expression by SJW may result in reduced SN-38 formation. SJW is a potential inducer of CYP3A4 in human [315, 317]. In a rat study, the administration of SJW to rats for 14 days was reported to result in a 2.5-fold increase in hepatic CYP3A2 expression. This could subsequently lead to the increased metabolism from CPT-11 to APC and NPC, though the latter could be partially converted into SN-38 by carboxylesterases.

Hyperforin, hypericin and other flavonoids in SJW may be able to up-regulate UGT1A by stabilizing mRNA and increasing protein expression. Pre-incubation of SJW aqueous extract (AE) at 10 μg/ml, SJW EE, hyperforin at 1 μM, and quercetin at 10 μM, all significantly increased the glucuronidation of SN-38 in H4-II-E cells. However, surprisingly, in the rat hepatic microsomes, combination of SJW ethanolic extracts significantly reduced SN-38 glucuronidation by 45% ($P < 0.05$). In addition, the induction effects of SJW on CE and UGT1A activities were not clearly demonstrated in our study, as there was no significant difference between the K_m and V_{max} values for CPT-11 hydrolysis and SN-38 glucuronidation in SJW-induced microsomes and control microsomes. Additionally, in the long-term incubation study, the SN-38G levels were not significantly influenced by SJW, suggesting the lack of marked inducing effect of SJW on UGT1As or the induction of multiple drug metabolizing enzymes was masked by other effects.

In addition, the induction of Pgp (MDR1) and MRP1-2 by SJW may contribute to the altered pharmacokinetics of SN-38, given that CPT-11, SN-38 and SN-38G

are known substrates for Pgp, MRP1, and MRP2 [103, 318, 319]. Pre-incubation of hypericin (20 nM and 200 nM) and hyperforin (1 µM) inhibited the cellular accumulation of CPT-11 while pre-incubation of hypericin, hyperforin, SJW EE, and quercetin increased the cellular accumulation of SN-38. The increased accumulation of SN-38 into rat hepatoma cells might increase their metabolism via glucuronidation due to increased substrate availability for UGT1As. The increased accumulation cannot be attributable to damage of the cellular plasma membrane, which in turn could increase drug influx. The increased accumulation of the active metabolite of CPT-11, SN-38 by SJW and its major components has important clinical implication. Tumor cells generally exhibit high levels of expression of Pgp or MRPs, thus co-administration of SJW and its major components might enhance the anti-cancer effects of CPT-11 by inhibiting these transporters.

Taken together, the protective effects of SJW on CPT-11 induced gastrointestinal and blood toxicities could be attributed to the inhibition of pro-inflammatory cytokine expression and intestinal epithelial cellular apoptosis, as well as, modulation of CPT-11 pharmacokinetic profiles. The achievement in abolition or alleviation of chemotherapy-induced complication may reduce mortality caused by severe diarrhea and inflammation and avoid overall reduction in effectiveness of therapy caused by interruptions or dose reductions during treatment.

In addition, SJW and its major components have shown anti-cancer effects and thus may enhance the anti-tumor activity when combined with anti-cancer agents. Hypericin and hyperforin induced apoptosis in a variety of tumor cell lines and inhibited cancer invasion and metastasis. Some studies showed that quercetin

147

induced apoptosis and inhibited the growth of tumor cells *in vitro* and *in vivo*. More interestingly, studies indicated that the major component of SJW, hyperforin, phloroglucinol derivatives found in SJW related mainly to its anti-depressant effects, inhibits key steps of angiogenesis *in vitro* in bovine aortic endothelial cells, as well as *in vivo* in the chorioallantoic membrane assay, which may open the way for the possibility of a new pharmacological use of SJW for the treatment of angiogenesis-related malignancies [320]. The same was observed for hypericin [321], which may increase the anti-tumor activity when SJW was combined with other chemotherapeutic agents.

However, the co-administration of SJW leading to the decreased plasma level of SN-38, accompanied with decrease in TNF-α level, may compromise the anti-tumor activity of CPT-11. Although the major components of SJW, hypericin and hyperforin, have shown certain anti-tumor and anti-angiogenic properties, their contents in SJW, a complicated herbal medicine, are too low to exert their effects (0.3% and 5% for the contents of hypericin and hyperforin in the SJW tablets). Therefore it is strongly recommended that patients receiving chemotherapeutic treatments should refrain from taking SJW. Specific dosing guidelines should be followed for patients on such combinations. Further anti-tumor activity evaluation is necessary before the clinical application of the combination of SJW with CPT-11 although this combination could alleviate the toxicity induced by CPT-11. Therefore, based on the study of the interactions between CPT-11's pharmacokinetics and SJW, caution should be exercised with co-administration of chemotherapeutic agents and modulators of drug metabolizing enzymes and transporters such as CPT-11 with SJW, considering that the pharmacokinetic

profiles of the anti-cancer agents might be changed, and might lead to a deleterious impact on treatment outcome.

CHAPTER 6 GENERAL DISCUSSION & CONCLUSION

Chemotherapy is a major approach to treat cancer. However, intestinal mucositis accompanied with severe diarrhea is a common dose-limiting toxicity of many forms of cancer chemotherapy, especially in treatment of colorectal cancer by use of irinotecan (CPT-11), 5-fluorouracil, oxaliplatin, capecitabine, or raltitrexed [322, 323]. Mucositis has a significant impact on health, quality of life and economic outcomes that are associated with chemotherapy. It also indirectly affects the success of anti-neoplastic therapy by limiting the ability of patients to tolerate optimal dosing-intensified regimens. About 50-80% of patients administered with these chemotherapeutic agents alone or in combination in randomized phase III trials experienced severe diarrhea. For CPT-11, the incidence of grade 3 or 4 diarrhea increased to 40% [324]. Severe diarrhea causes dehydration, renal failure, and thromboembolic events, limiting the completion of optimal dosing regimens in many patients. Furthermore, diarrhea combined with severe neutropenia commonly leads to Gram-negative sepsis and such complications have contributed to the high incidence of mortality for patients who received CPT-11-based regimens. Invariably, high-dose loperamide is recommended to manage CPT-11-induced diarrhea, consisting of an initial dose of 4 mg followed by 2 mg every 2 hr until a 12-hr interval without loose motions [325]. However, a number of patients do not respond to this agent. Therefore efforts to reduce the incidence of severe diarrhea should be of considerable value.

This thesis has demonstrated that combination of thalidomide or SJW reduced the gastrointestinal and hematological toxicities induced by CPT-11 in the rat, as indicated by alleviation of late-onset diarrhea, body weight loss, macroscopic and

microscopic intestinal damages as well as hematological toxicity. The protective effects of thalidomide or SJW on CPT-11 induced toxicities might be partially explained by the pharmacokinetic interactions between CPT-11 and thalidomide or SJW. These interactions could be explained by the altered metabolism and transport of CPT-11 in rat liver microsomes and the rat hepatoma cell line, H4-II-E cells, by thalidomide, its hydrolytic products, SJW and its major components. The pharmacodynamic mechanisms, including the modulatory effects on cytokine expression and intestinal epithelial apoptosis by the co-administration of thalidomide or SJW, also played a role in the protective effects of these two drugs. These mechanistic findings for CPT-11 induced histological damages and the protective effects of thalidomide and SJW may provide some insights for new effective strategies to circumvent CPT-11 induced toxicities.

6.1 PROTECTION AGAINST CPT-11 INDUCED TOXICITY BY COMBINATION WITH THALIDOMIDE OR ST. JOHN'S WORT

The present study demonstrated that co-administered thalidomide or SJW both ameliorated the gastrointestinal and hematological toxicities of CPT-11, as indicated by alleviation of late-onset diarrhea, alleviation of macroscopic and microscopic intestinal damages as well as up-regulation of decreased leukocyte counts, in a rat model with dose-limiting toxicity profiles that are similar to those observed in patients treated with CPT-11. Our results also showed that both thalidomide and SJW had no protective effects on CPT-11 induced early-onset diarrhea, on day 1 to day 4 in our study. In addition, similar effects were observed for macroscopic and microscopic evaluations of histological damages for the combination with thalidomide and SJW.

151

However, coadministration of thalidomide significantly alleviated body weight loss caused by CPT-11 and ameliorated late-onset diarrhea on both day 6 and day 7, while the combination with SJW showed no body weight changes and only reduced late-onset diarrhea score on day 5 with significant effect. In the mean time, SJW up-regulated decreased leukocyte counts (including lymphocyte and neutrophil) with significant effects on days 5, 7, and 9 while thalidomide only increased leukocyte counts on day 7. Thus, our findings suggest that thalidomide might be more effective on CPT-11-induced gastrointestinal toxicity while SJW might be more efficient for CPT-11-induced haematological toxicity.

6.2 PHARMACODYNAMIC MECHANISMS OF THE PROTECTIVE EFFECTS OF THALIDOMIDE AND ST. JOHN'S WORT

There is increasing understanding of the molecular events that lead to chemotherapy-induced intestinal mucosal injury. The mucosal damages appear to be associated with intestinal exposure to these drugs which induce epithelial apoptosis, decreased crypt cell renewal, complicated inflammatory responses, and destruction of the mucosal architecture [326]. In addition, several possible mechanisms of CPT-11-induced diarrhea, especially late-onset diarrhea have been previously proposed, ranging from changes in architecture and large intestinal absorption rates to increases in intestinal β-glucuronidase levels due to changes in intestinal bacteria [326]. However, many of these studies were unable to assess the effect of CPT-11 throughout the gastrointestinal tract. Our study differed from these studies by investigating histological changes and cytokine expression as well as apoptosis in the ileum, caecum, and colon. The beneficial effects of thalidomide and SJW observed in rats with CPT-11 chemotherapy appeared to be

systemic, as indicated by the protective effects on multiple organs and tissues. Their actions on multiple sites of the host, in particular the intestinal tissues and immune system, may work together to antagonize the toxic effects of CPT-11.

Treatment of CPT-11 caused marked apoptosis in intestinal crypts. An increased number of apoptotic crypt cells and loss of complete epithelial architecture due to inflammation may increase secretion of Cl^- and Na^+ and lead to severe diarrhea. In addition, apoptosis of blood cells may induce hematological toxicity as indicated by marked decrease in leucocytes. It was hypothesized that chemotherapy nonspecifically targeted the rapidly proliferating cells of the basal epithelium, causing the loss of the ability of the tissue to renew itself, which led to atrophy, thinning and ulceration of the mucosal epithelium that is associated with mucositis. Chemotherapy-induced mucositis has mainly been attributed to basal-cell damage that results when drugs permeate to these cells from the submucosal blood supply [326]. Studies have further shown that chemotherapy–induced intestinal mucositis appears to be associated with intestinal exposure to these drugs which induce epithelial apoptosis characterized by the generation of DNA fragments through the action of endogenous endonucleases, decreased crypt cell renewal, and destruction of the mucosal architecture [327]. Treatment with CPT-11 at 100 mg/kg daily for 4 days caused characteristic mucosal changes in murine intestinal tissues including ileum and caecum and severe diarrhea by inducing apoptosis and cell differentiation. Increasing evidence has shown that apoptosis represents an important event during gut inflammatory responses. The findings in our study that thalidomide and SJW exhibited marked *in vivo* anti-apoptotic effects in intestinal epithelial cells associated with alleviated histological toxicity

also provide further support for this apoptosis-associated mechanism for CPT-11 induced toxicity and the protective effects of thalidomide and SJW.

Apart from the modulatory effects on intestinal epithelial cellular apoptosis, regulation of cytokine expression is also involved in the protective effects of thalidomide and SJW against CPT-11 induced gastrointestinal and hematological toxicity. Cytokines are relatively small molecular weight polypeptides released by all nucleated cells in the body that have specific effects on the interactions and communications between cells. Cytokines mainly include the ILs, lymphocytes and cell signal molecules, such as TNF-α and the IFNs. The majority of cytokines is pleiotropic in their functional activities and they are extracellular signalling molecules essential to host development, maturation, immune, and inflammatory responses, and tissue repair processes [328]. Cytokines are highly inducible and fast turn-over molecules during immunological reactions and inflammatory conditions. Many known cytokines have been shown to mediate predominant proinflammatory effects. TNF-α, IL-1β, IL-6, IL-12, and IFN-γ are cytokines that exert predominant proinflammatory effects *in vitro* and *in vivo*, among which IL-6 can also exert anti-inflammatory effect, depending on the specific physiologic or pathophysiologic state [329].

Over-expressions of TNF-α and other pro-inflammatory cytokines such as IL-1 and IL-6 in intestinal mucosa have been reported to be associated with intestinal toxicities induced by cancer chemotherapy agents [330]. TNF-α, a potent pro-inflammatory cytokine, is mainly produced by activated macrophages and is a key cytokine in the initiation of mucosal immuno-inflammatory responses and damages. TNF-α is a critical cytokine that could orchestrate inflammatory

responses by activating a wide range of cells including neutrophils, macrophages, and NK cells. Activation of these cells in turn induces the production of inflammatory cytokines such as IL-1β, IL-6, and IL-8 and up-regulation of adhesion molecules on cell surface. TNF-α also plays a critical role in initiation of chemotherapy-induced primary mucosal damage responses including early damage to connective tissue and endothelium, reduction of epithelial oxygenation, and ultimately, epithelial basal-cell death and injury [331]. The histological damage including increased intestinal permeability and leukocyte infiltration accompanied with anti-cancer agent such as CPT-11 leads to an inflammatory response through the overproduction of pro-inflammatory cytokines like TNF-α by epithelial cells and infiltrating leukocytes within the intestinal mucosa. Moreover, the overall pathology initiated by CPT-11 cytotoxicity is exacerbated with increased TNF-α expression by TNF-α-mediated apoptosis, tissue matrix degradation and vascular leakage [332]. A study conducted on BALB/c mice treated with combination of RDP58 with CPT-11 also showed over-expression of TNF-α after CPT-11 administration and its role involved in CPT-11 induced histological pathology. Consistent with our data in the rat model, administration of CPT-11 for four consecutive days in rats showed significant increase in TNF-α production in rat intestinal tissues both at protein and mRNA levels, associated with severe diarrhea and histological damages. This finding may support the hypothesis that the intestinal damage induced by CPT-11 results from increased production of pro-inflammatory cytokines like TNF-α. Our studies also showed that co-administration of thalidomide or SJW effectively reduced the diarrhea and intestinal damages induced by CPT-11. Moreover, thalidomide or SJW reduced the TNF-α production at both protein and mRNA levels compared to the control

group treated with CPT-11 alone. This finding indicated that the protective effect of thalidomide or SJW on CPT-11 induced toxicity might be ascribed to its down-regulatory effect on TNF-α over-expression.

The inhibitory effects of thalidomide and SJW on TNF-α protein expression might be ascribed to their effects on mRNA level of TNF-α. As shown in our data, the co-administration of thalidomide or SJW reduced the transcription product levels of TNF-α mRNA compared to the group treated with CPT-11 alone, which might be attributed to the increased degradation of TNF-α mRNA by thalidomide [329]. Besides, inhibitory effects on the translational and post-translational expression of TNF-α by thalidomide or SJW could not be excluded. The expression patterns of the protein and mRNA of TNF-α in both control and combination groups are consistent. However, there is some inconsistency between the protein expression and mRNA transcription levels of TNF-α in the same group of rats. Most of protein expression of TNF-α reached peak levels on day 5 and then slowly decreased; while of the expression of mRNA transcripts reached a maximum level on day 7 or day 9. This might be attributed to the differences in the translational and post-translational modification in the intestines.

A close interaction between intestinal epithelial cellular apoptosis and intestinal pro-inflammatory cytokines expression was observed. TNF-α has been shown to play an essential role in regulating intestinal epithelial cell apoptosis and/or survival during chronic inflammation [333]. Members of the TNF-superfamily, such as Fas/CD95/APO-1 and TRAIL, are involved in the extrinsic pathway for production of apoptosis and play a role in apoptosis induced by chemotherapy and cellular immunity. TNF-α has been shown to share common intracellular

pathways of apoptosis with Fas and has the ability to modulate Fas expression itself [334]. The inhibition of intestinal apoptosis by thalidomide or SJW might be partially ascribed to the inhibition of TNF-α expression. Studies also showed venous congestion induced mucosal apoptosis via TNF-α-mediated cell death in the rat small intestine with a variety of intermediates and protein-protein interactions involved [335]. This finding is consistent with our result that congestion is observed in intestinal tissues accompanied with increased TNF-α level and apoptosis after CPT-11 treatment. The reduced TNF-α level after thalidomide or SJW combination also inhibited the intestinal damages caused by apoptosis, arising from venous congestion. SJW and quercetin have also been reported to inhibit apoptosis induced by various mechanisms in several cell lines and exerted protective effects against H_2O_2-induced apoptosis in human neuroblastoma cells, cardiomyoblast cells and macrophages. Hypericin prevented the apoptosis induced in murine L-cells with recombinant TNF-α [309], while quercetin protected glomerular mesangial cells from oxidant-triggered apoptosis [331]. In addition, SJW extract modulated apoptosis in mice splenic lymphocytes *in vivo*. The splenic lymphocytes from mice treated with SJW extract at 100 mg/kg per day for 14 days were significantly more resistant to apoptosis than those from mice treated only with the vehicle [336]. This action could be mediated in part by a decrease in Fas-Ag expression and in part by an increase in Bcl-2 expression. This was consistent with our study that combination of SJW with CPT-11 offered marked protective effect on CPT-11 induced leukocyte decrease, which might be ascribed to the modulation effect of SJW on apoptosis in leukocytes.

TNF-α, the main lethal mediator of sepsis and inhibitor for the toxic effects of bacterial endotoxins, has been identified as a key inflammatory mediator. The development of anti-TNF-α molecules (soluble receptors and antibodies) for important diseases including rheumatoid arthritis and Crohn's disease is now under research [334]. Infliximab, the human-mouse anti-TNF antibody cA2, has shown efficacy in patients with Crohn's disease or rheumatoid arthritis [332]. Etanercept (human p75 TNF receptor-IgG fusion protein) and adalimumab (human anti-TNF monoclonal antibody) are being evaluated in patients for the treatment of Crohn's disease [334]. These monoclonal antibodies against TNF-α may act by neutralizing TNF-α and reducing the expression of adhesion molecules and other cytokines [332]. However, the use of TNF-α antibodies has been associated with increased risk of tuberculosis [337]. Besides TNF-α antibodies, a variety of small molecular weight molecules also showed TNF-α inhibitory effects with therapeutic benefits in experimental colitis [337]. For example, selective inhibitors of the phosphodiesterase (PDE) are potent inhibitors of TNF-α synthesis. Recently, some thalidomide analogs such as lenalidomide and Revlimid have been found to have potent inhibitory effects on TNF-α [338]. Thalidomide has been widely used in the treatment of various inflammatory and autoimmune disorders including Crohn's disease, Bechcet's disease, and rheumatoid arthritis [334]. The TNF-α antagonist property of thalidomide may partly explain its beneficial effects in these TNF-α-associated complications [335]. The pivotal role of TNF-α in mucosal inflammation and injury might infer that, inhibition of TNF-α production may become a potential approach for managing chemotherapy-induced intestinal mucositis. In the present study, we investigated the efficacy and potential mechanism of action of anti-TNF-α

treatment in chemotherapy-induced intestinal damages. We report herein that administration of thalidomide, as a TNF-α inhibitor, efficiently reduced CPT-11 induced diarrhea and mucosal inflammation in rats. Furthermore, our results showed that anti-TNF-α treatment suppressed the overproduction of pro-inflammatory cytokines in intestinal tissues and reduced intestinal epithelium cellular apoptosis. Taken together, these data indicated that the increased intestinal TNF-α expression and epithelial apoptosis by chemotherapy could be suppressed by anti-TNF-α agent such as thalidomide. In addition, the protective effect of SJW against CPT-11 induced toxicity could also be attributed to the suppression of TNF-α expression. So, the protective effects of thalidomide and SJW on CPT-11 induced complications could provide alternatives for chemotherapy-associated histological damages by anti-TNF-α agent by inhibiting inflammatory cytokines expression and intestinal epithelial cellular apoptosis.

TNF-α can potentiate the immune response of many other pro-inflammatory cytokines including IL-1β, IL-2, IL-6, and IFN-γ. Modulation of these cytokines may also play a role in the anti-inflammatory effects of thalidomide and SJW. IL-1β plays a central role in mediating immune and inflammatory responses. Although normal production of IL-1β is obviously critical for initiation of normal host responses to injury and infection, inappropriate or prolonged production of IL-1β has been implicated in the production of a variety of pathological conditions including intestinal inflammatory damages. The naturally occurring IL-1 receptor antagonist (IL-1ra, anakinra or Kineret) has been approved for the treatment of rheumatoid arthritis with large amounts (100 mg) daily [339]. Thus, as shown in our results, the inhibition of IL-1β may contribute to the protective effect on CPT-11 associated intestinal inflammation by combination with thalidomide. In

159

addition, the modulatory effect of thalidomide on IL-1β may be attributed to its inhibitory effect on TNF-α. However, no inhibitory effect for IL-1β was observed for the SJW combination.

Thalidomide also suppressed the production of IL-6 and SJW inhibited the production of IFN-γ. IL-6 is a multifunctional protein that plays important roles in host defense, acute phase reactions, immune responses, and hematopoiesis [340]. IL-6 is expressed by a variety of normal and transformed cells including T cells, B cells, and macrophages [330]. Its expression is increased in Crohn's disease and leads to suppression in growth. Application of IL-6 antibody restore linear growth but did not suppress intestinal inflammation. A mouse monoclonal antibody that blocks IL-6 action has shown hints of efficacy in B-lymphoproliferative disorders and Castleman's disease in small trials [330]. In addition, increased IL-6 expression was seen in the peripheral blood and/or mucosa of patients and animals with chemotherapy-induced mucositis. IFN-γ is produced by CD8^{+}, NK, and Th1 (T helper) cells, that documented antiviral, anti-protozoal and immunomodulatory effects on cell proliferation and apoptosis, as well as the stimulation and repression of a variety of genes. As a pro-inflammatory cytokine, IFN-γ was shown to mediate pleiotropic effects in the innate and adaptive response to infection and sensitize intestinal epithelial cells to physiological and therapeutic inducers of apoptosis via up-regulation of caspases-1 [341]. In the present study, down-regulated intestinal IL-6 by thalidomide and IFN-γ by SJW is probably due to the inhibition of TNF-α production and direct inhibitory effect on local immunocompetent cells. Studies have shown that TNF-α activates invading T cells and NK cells to produce IFN-γ, which directly leads to increased mucosal damage [342]. Reduced TNF-α expression may consecutively lead to a reduced

synthesis of IFN-γ and a reduced infiltration of activated lymphocytes. In addition, studies have shown that blockade of TNF abrogated the production of IL-6 [342].

IL-2 is a pleiotropic cytokine produced primarily by mitogen- or antigen-activated T lymphocytes. It plays a key role in promoting the clonal expansion of antigen-specific T cells by binding sequentially to the α, β, and common γ chain receptor subunits [343]. IL-2 mediates multiple immune responses on a variety of cell types including stimulation of the proliferation and differentiation of activated B cells and induction of cytokine production such as TNF-α and IFN-γ and cytolytic activity by NK cells [343]. IL-2 administration results in expansion of lymphoid cells, but also associated with a variety of autoimmune disorders, including immune thyroiditis, rheumatoid arthritis, and other arthropathies. The combination of CPT-11 with thalidomide decreased the expression of IL-2 compared to treatment with only CPT-11, as IL-2 may have attenuated the effect of thalidomide on CPT-11 induced histological damage.

Besides, a recent mouse study indicated that thalidomide treatment at 200 mg/kg orally significantly lowered the severity of colon injury induced by dinitrobenzene sulfonic acid [344]. This was accompanied with a substantial reduction of the increase in intestinal myeloperoxidase activity, TNF-α, IL-1β, vascular endothelial growth factor, and intercellular adhesion molecule-1. In experimental models, it has been found that increased expression of TNF-α is believed to be the major reason that leads to sepsis, while increased IL-12, IFN-γ, GM-CSF, and IL-8 expression may each play a part. In addition, modulation of other cytokines, such as IL-10, COX-2, and NF-κB transcription factor, is involved. Other

161

mechanisms related to epithelial or endothelial function or growth could also be involved. Thalidomide may inhibit TNF-α-driven calcium and potassium secretion directly or through inhibition of cyclooxygenase [345]. Thalidomide also increases T-helper-2 cell (humoral) immune function and decreases T-helper-1 cell (cellular) immune function by upregulating IL-4 and IL-5, and downregulating the IL-12. In addition, a number of studies have shown that COX-2 is overexpressed in many forms of human cancers [346]. A direct link between COX-2 overexpression and tumorigenesis has been observed. Inhibition of apoptosis, increased angiogenesis, increased invasiveness, modulation of inflammation/immunosuppression, and conversion of procarcinogens to carcinogens by COX-2 are involved in this contribution [347]. CPT-11-induced diarrhea is reported to be, at least in part, mediated by a COX-2-dependent mechanism. Thalidomide could have inhibited the lipopolysaccharide-mediated induction of COX-2 in murine macrophages, which could explain how thalidomide reduce the severity of CPT-11-induced diarrhea in human patients [213, 348]. In addition, to elucidate the mechanism underlying the reduction of the side effect, the thalidomide/St. John's Wort-regulated NF-κB activity should also be investigated in the future studies.

Moreover, the hematological toxicity as the dose-limiting toxicity of CPT-11 administration could also be involved in the induction of late-onset diarrhea. Serious leukopenia induced by CPT-11 administration could assist the bacteria in adversely infecting the intestinal epithelium. Clinically, granulocyte colony-stimulating factor can be co-administered to inhibit the exacerbation of the hematologic toxicity induced by dose-escalating CPT-11 [349], and may alleviate the diarrheal symptoms by inhibiting opportunistic bacterial infection of the

intestinal tissue. Results in our study are consistent with reduction in numbers of leucocytes and reduced gastrointestinal toxicity.

Taken together, the protective effects of thalidomide and SJW on CPT-11 induced complications may be ascribed to the modulation of intestinal epithelial cellular apoptosis and cytokine expression. The greater understanding on the involvement of TNF-α in CPT-11 induced toxicity and the similar modulation effects of both SJW and thalidomide on TNF-α expression may provide a new treatment for chemotherapy-associated histological damages by an anti-TNF-α agent through the inhibition of inflammatory cytokines expression and intestinal epithelial cellular apoptosis.

6.3 PHARMACOKINETIC MECHANISMS OF THE PROTECTIVE EFFECTS OF THALIDOMIDE AND ST. JOHN'S WORT

Although the modulation of cytokine levels and intestinal epithelial cellular apoptosis could partially explain the protective effects of thalidomide and SJW on CPT-11 induced toxicity, pharmacokinetic interactions between CPT-11 with thalidomide/SJW might be also involved. We have examined the effects of thalidomide and SJW on the plasma pharmacokinetics of CPT-11 and its major metabolites, SN-38 and SN-38 glucuronide, and explored the kinetic interactions using the *in vivo* rat and *in vitro* models.

Different effects were observed for the pharmacokinetic interactions between CPT-11/thalidomide and CPT-11/SJW combinations. Both single and multiple dosage regimens of thalidomide exhibited similar modulations on pharmacokinetic parameters of CPT-11, whereas, only long term treatment with

SJW affected pharmacokinetics of CPT-11. Thalidomide showed more modulatory effects on the plasma pharmacokinetic profiles of CPT-11 compared with SJW, which might be ascribed to the complexity, purity and efficacy of SJW, as a herbal medicine. However, thalidomide, as a pure compound, may exert its effects faster than SJW. In addition, the pharmacokinetic properties of both combinations in the rat model were comparable to those observed in clinical studies though some discrepancies existed. In a clinical pilot study in cancer patients [255], combination of thalidomide only increased AUC and decreased $t_{1/2}$ of CPT-11 with significant effects but had no effect on SN-38 pharmacokinetic profiles while another clinical study revealed that combination of thalidomide decreased CL and C_{max} of CPT-11, decreased AUC of SN-38 but increased AUC of SN-38G. Combination of SJW not only reduced C_{max} of SN-38 but also decreased AUC of SN-38 in a clinical study. This might be ascribed to the species differences in drug metabolism and transport between humans and rats. It has been reported that the duration of exposure to CPT-11 and SN-38 may affect the severity of intestinal cytotoxicity, because DNA topo I inhibitors appear to be cell-cycle specific and SN-38 is much more cytotoxic than CPT-11. Therefore, SN-38 exposure is assumed to be the principal cause of late-onset diarrhea. A clear correlation between the toxicity of CPT-11 and C_{max} of SN-38 was also observed in cancer patients. In our study, both the incidence of late-onset diarrhea and the degree of impairment of the intestinal epithelium depended on the duration (AUC) and plasma concentration of SN-38. Thus, the reduction in the AUC or C_{max} of SN-38 after thalidomide or SJW pre-treatment might partially explain the finding that co-administered thalidomide and SJW reduced the gastrointestinal toxicity of CPT-11.

The significant decreased V_d of CPT-11 in rats receiving CPT-11 with combined thalidomide compared with those rats receiving CPT-11 and control vehicle (1% DMSO, v/v) in the 5-day multiple-dosing study may reflect an effect of thalidomide and its metabolites on the plasma protein binding of CPT-11. However, this was not supported by our *in vitro* plasma protein binding results in which thalidomide at a high dose of 250 µM did not cause significant effect in the f_u of CPT-11. However, modulation of the tissue binding of CPT-11 and its binding to target protein (Topo I) by thalidomide and its metabolites is possible. The reason for the reduced plasma SN-38 levels by SJW may be due to the induced CYP3A expression. SJW is a potential inducer of CYP3A4 in human [350]. In a study, the administration of SJW to rats for 14 days resulted in a 2.5-fold increase in hepatic CYP3A2 expression. This may subsequently lead to the increased metabolism from CPT-11 to APC and NPC, though the latter one can be partially converted into SN-38 by carboxylesterases. In addition, the induction of Pgp (MDR1) and MRP1-2 by SJW may contribute to the altered SN-38's pharmacokinetics, given that CPT-11, SN-38 and SN-38G are known substrates for Pgp, MRP1, and MRP2.

Rat liver microsomes were used as an *in vitro* model to study the metabolism of CPT-11 and SN-38. The hydrolysis of CPT-11 to form SN-38 and SN-38 glucuronidation followed Michaelis-Menten kinetics, with a two and one binding-site model being the best fit for CPT-11 hydrolysis and SN-38 glucuronidation, respectively. The estimated K_{m1} and K_{m2} for CPT-11 hydrolysis were 0.50 and 78 µM, respectively; and V_{max1} and V_{max2} were 0.58 and 2.34 pmol/min/mg protein, respectively. This indicates that there are at least two CEs with differential affinity and catalysing capacity involved in the hydrolysis of CPT-11 in rat liver

165

microsomes. The estimated K_m for SN-38 glucuronidation was 18.2 μM and a V_{max} of 185.6 pmol/min/mg protein. This suggests a predominant UGT1A enzyme or multiple UGT1A enzymes with similar affinity catalyze SN-38 glucuronidation in rat liver microsomes. These observed constants for CPT-11 and SN-38 metabolism are comparable with those reported previously in rat or human liver microsomes. Some dissimilarity existed for the hydrolysis of CPT-11 between rat liver microsomes and H4-II-E cells. This may be due to the presence of competition between metabolism, efflux and binding to target protein for SN-38 in H4-II-E cells, but not in rat liver microsomes. When SN-38 was incubated with H4-II-E cells, the formation of SN-38G was comparable with that in rat liver microsomes. Replacement of DMEM with HBSS just slightly affected the metabolism of CPT-11 and SN-38 with comparable K_m and V_{max} values, indicating that fetal bovine serum had little effect on the metabolism of CPT-11 and SN-38 in H4-II-E cells. In addition, there are similarities and differences with regard to concentrations of enzymes metabolizing CPT-11 and SN-38 in the two *in vitro* systems that were used in this study.

In rat liver microsomes, a 16% decrease ($P < 0.05$) in the hydrolysis of CPT-11 at 0.5 μM by the hydrolytic products of thalidomide (10 μM), instead of thalidomide, was observed. Such inhibitory effect was dependent on the total concentration of the hydrolytic products of thalidomide. This inhibitory effect could also be seen for the hydrolysis of CPT-11 at a higher concentration (78 μM) without significant effect. This may explain the increased AUC and C_0 of CPT-11 by combination of thalidomide. In the rat hepatic microsomes, combination of SJW ethanolic extracts significantly reduced SN-38 glucuronidation. Additionally, the induction effects of SJW on CE and UGT1A activities were not

166

clearly demonstrated in our study, as there was no significant difference between the K_m and V_{max} values for CPT-11 hydrolysis and SN-38 glucuronidation in SJW-induced microsomes and control microsomes. Also in the long-term incubation study, the SN-38G levels were not significantly influenced by SJW, suggesting the lack of inducing effect of SJW on UGT1As or induction of multiple drug metabolizing enzymes and transporters with negating effect.

H4-II-E cells were also used to investigate the accumulation of CPT-11 and SN-38 and the effects of thalidomide, its hydrolytic products, SJW and its major components on their accumulation. The mechanism for the accumulation of CPT-11 and SN-38 by H4-II-E cells is unknown, but both active and passive transport are likely to be involved. CPT-11 and SN-38 can be readily taken up by human intestinal Caco-2 cells through passive diffusion [103, 351]. However, the best fit of one binding-site model for the accumulation of both CPT-11 and SN-38 in H4-II-E cells indicates the involvement of one predominant transporter or multiple transporters with similar affinity to the substrates, whereas passive diffusion played a minor or negligible role. The accumulation of both CPT-11 and SN-38 in H4-II-E cells appeared to saturate within several minutes after incubation of the cells with the drug. Pgp, MRP1-2 and MRP4 are all possibly involved in the transport (mainly efflux) of SN-38 in H4-II-E cells, as verapamil (a Pgp inhibitor) and MK-571 [an inhibitor for MRP1-4 [294]] could significantly increased the intracellular accumulation of SN-38. The uptake of CPT-11 in H4-II-E cells appears to be mediated by MRP1-4 as MK-571, but verapamil or nifedipine did not significantly increased its uptake. Both CPT-11 and SN-38 appeared to enter tumor cells at a rapid rate, and are then distributed within cells and bound by subcellular organelles, drug metabolizing enzymes located on endoplasmic

reticulum and the target protein in nucleus (Topo I). The organelles may represent a store of active drug. Both drugs are finally cleared from the cells by metabolism and transporter-mediated efflux. Notably, the accumulation profile of CPT-11 in H4-II-E cells is different from that of SN-38 with differential Michaelis-Menten constants. This may be due mainly to the different physico-chemical properties of the two compounds. For example, SN-38 has higher lipophilicity than CPT-11, probably resulting in different affinity to the transporters, uptake, subcellular compartmentation, and efflux of the two drugs. Different uptake rate and extent of CPT-11 and SN-38 have also been observed in intestinal and lung cancer cells [97, 352]. Metabolism is considered an important determinant for the intracellular accumulation of CPT-11 and SN-38. CPT-11 is hydrolysed by cellular carboxylesterase, whereas SN-38 is readily conjugated by UGT1A1/1A9 which is associated with increased efflux of the drug from HT29 and HCT116 cells.

Interestingly, the metabolism study in H4-II-E cells for the combination of thalidomide with CPT-11 showed similar effects with those observed in microsomes, as indicated that incubation of total hydrolytic products of thalidomide at 10 μM, PGA at 10 μM, and thalidomide at 25 μM all decreased CPT-11 hydrolysis, which might have contributed to the decreased AUC of SN-38 but increased AUC of CPT-11. It seemed that thalidomide could affect the main metabolic pathway of CPT-11 that yields SN-38 though, up to date, little is known concerning drugs that could interact with carboxylesterases, except for ciprofloxacin and loperamide. The metabolism study in H4-II-E cells for the combination of CPT-11 and SJW showed that SJW increased the glucuronidation of SN-38 which was different from those observed in microsomes. This could be attributed to similarities and differences with regard to the concentrations of

enzymes. In addition, competition between metabolism, efflux, and binding to target protein could occur for SN-38 in H4-II-E cells, but not in rat liver microsomes. The increased glucuronidation of SN-38 could explain the decreased C_{max} of SN-38 when combined with SJW.

In the accumulation study, our results showed that thalidomide at 250 μM, PGA at 10 μM, or thalidomide hydrolytic products at 10 μM increased the cellular accumulation of SN-38 in H4-II-E cells. Same trends could be observed for the preincubation of SJW extract and its major components. The increased accumulation of SN-38 into rat hepatoma cells might increase its metabolism via glucuronidation due to increased substrate availability for UGT1As, thus resulting in decreased SN-38 plasma levels. The mechanism for the increased accumulation of SN-38 by thalidomide, its hydrolytic metabolites, SJW, and its major components is unknown, but their inhibitory effects on SN-38 transporters such as Pgp and MRP2 are implicated. The increased accumulation cannot be attributable to damage of the cellular plasma membrane, which in turn could increase drug influx. The tumor cells remained viable during drug accumulation studies over 180 min as measured using trypan blue exclusion. Co-administered thalidomide has been found to inhibit the MRP2-mediated biliary excretion of the glucuronides of the anti-vascular agent DMXAA and decreased the clearance of cyclophosphamide [267], a potential substrate for MRP4, in mice. However, thalidomide did not induce Pgp expression in LS180 cells and affect the uptake of rhodamine 123 in leukaemia cell line over-expressing Pgp. Interestingly, long-term thalidomide therapy resulted in lack of *MDR1* gene expression in a patient with primary resistant multiple myeloma. These results indicate that thalidomide does not interact with Pgp, neither as a substrate nor as an inhibitor, but it may be

169

a suppressor of *MDR1* gene. Thalidomide and/or its metabolites, however, may be substrates or modulators for other drug transporters and they may modulate the transport and excretion of the substrates of these transporters. The increased accumulation of the active metabolite of CPT-11, SN-38, by thalidomide and SJW has important clinical implication. Tumor cells generally exhibit high levels of expression of Pgp or MRPs, thus co-administration of thalidomide and SJW, might enhance the anti-cancer effects of CPT-11 by inhibiting these transporters. In addition, the possible reduced biliary excretion of SN-38 caused by decreased transport of SN-38 may lead to the decrease in $t_{1/2}$ of SN-38 observed in the plasma pharmacokinetic study for the combination of thalidomide. Additionally, our study also showed that PGA increased accumulation of CPT-11 while hypericin and hyperforin reduced it in H4-II-E cells, leading to decreased substrate for hCE, followed by decreased SN-38 plasma levels.

CYP2C-mediated metabolism only plays a minor role in thalidomide elimination [290]. Since thalidomide is a poor substrate for CYPs and it does not inhibit the metabolism of CYP-specific substrates, thalidomide is not involved in clinically important drug-drug interactions caused by inhibition of CYP-mediated drug metabolism. However, given that thalidomide can be hydrolysed to more than a dozen of metabolites *in vivo* [353], it can be expected that these hydrolytic metabolites may have a modulating effect on the metabolism and transport of CPT-11 and SN-38, thus causing altered pharmacokinetics *in vivo*. This study demonstrated that the total hydrolytic products of thalidomide modulated the *in vitro* metabolism of CPT-11, but intact thalidomide at high concentration, hydrolytic products of thalidomide, and PGA affected SN-38 transport. Modulation of the metabolism and transport of CPT-11 and its metabolites was

also observed for the extract of SJW and its major components. These findings indicate that intact thalidomide and its hydrolytic products as well as SJW and its major components have differential effects on drug metabolism and transport, probably due to their different affinities to drug metabolizing enzymes (e.g. CEs) and drug transporters. However, the specific thalidomide hydrolytic products and SJW components responsible for these effects have not been identified in our study. Further studies are needed to identify these compounds and this may lead to the development of new CE and drug transporter modulators. Additionally, to fully understand the mechanism for the reduced metabolism, the expression of phase I and phase II enzymes and transporters should be studied.

The present study demonstrated that concomitant CPT-11 did not significantly alter the plasma pharmacokinetics of thalidomide in rats. This is not surprising, as spontaneous hydrolysis is the major elimination pathway of thalidomide, while CYP2C-mediated metabolism plays only a minor role in its elimination. The V_d of thalidomide was insignificantly altered in rats receiving combination therapy compared to those receiving thalidomide and control vehicle, indicating that CPT-11 and SN-38 did not influence the binding of thalidomide to serum and tissue proteins.

In summary, the results from the pharmacokinetic studies in the rat provided partial explanation for the observation that co-administered thalidomide or SJW reduced the gastrointestinal and blood toxicities of CPT-11. The rat is a suitable model for the pharmacokinetic and toxicological study of CPT-11 in combination with thalidomide. Mechanistic studies on *in vitro* models including rat liver microsomes, rat hepatoma cell line H4-II-E cells indicated that the hydrolytic

products of thalidomide exhibited inhibitory effects on the hydrolysis of CPT-11, and increased the intracellular accumulation of SN-38, probably resulting from inhibition of Pgp and MRPs that transport SN-38; whereas the combination of CPT-11 and SJW increased the glucuronidation and cellular accumulation of SN-38, which may explain the pharmacokinetic interactions for the combination of thalidomide or SJW with CPT-11.

6.4   CONCLUSION

In summary, our study showed that the combination of thalidomide or SJW with CPT-11 both ameliorated the gastrointestinal and hematological toxicities of CPT-11 in rats, as indicated by alleviation of histological damages and up-regulation of decreased leukocyte counts. These protective effects might be attributed to the modulation of cytokine expression and inhibition of intestinal epithelial cellular apoptosis as well as modulation of CPT-11 pharmacokinetic profiles. The achievement in abolition or alleviation of chemotherapy-induced complication may reduce mortality caused by severe diarrhea and inflammation and avoid overall reduction in effectiveness of therapy caused by interruptions or dose reductions during treatment.

The major concern for the combination of CPT-11 with thalidomide is the reduction of plasma levels of SN-38, thereby compromising the anti-tumor activity of CPT-11. In addition, our study showed that thalidomide brought down the increased intestinal TNF-α expression and diminished intestinal epithelial cellular apoptosis, thus TNF-α expression and apoptosis in tumor tissues might be alleviated too, and again diminishing the anti-tumor activity of CPT-11. However, thalidomide has been demonstrated to possess anti-neoplastic activity in several

tumor models when used alone and in combination with cytotoxic drugs, with variable degrees of success. So the combination with thalidomide may increase anti-tumor activity of CPT-11. Furthermore, it has been demonstrated that thalidomide targets both the cancer cell and its microenvironment [210, 354]. So combination of chemotherapeutic agent CPT-11 with thalidomide, an anti-angiogenic agent, may further strengthen the anti-tumor activity of CPT-11 by targeting endothelial cells, which could become a new approach to resolve both toxicity and resistance phenomena for conventional cancer treatment. Moreover, clinical trials have shown that a good response rate was demonstrated in patients with metastatic cancer treated with the CPT-11/thalidomide combination [255]. therefore the combination could be promising for alleviation of CPT-11 induced toxicity and possibly enhancement of its anti-tumor activity. Further studies are warranted to establish whether the anti-tumor activity is improved in this strategy. If a positive response obtained, then the clinical relevance of the results obtained in the rat model system needs to be validated and confirmed using large-scale, comparative clinical trials.

The same concern was observed for the combination of CPT-11 with SJW, as indicated by decreased plasma levels of SN-38, accompanied with decrease in TNF-α levels, which may also compromise the anti-tumor activity of CPT-11. However, it is reported that hypericin and hyperforin induced apoptosis in a variety of tumor cell lines and inhibited cancer invasion and metastasis [244, 355] and some studies showed that quercetin induced apoptosis and inhibited the growth of tumor cells *in vitro* and *in vivo*. Furthermore, several studies established that hypericin and hyperforin expressed powerful *in vivo* and *in vitro* anti-neoplastic and apoptosis-inducing activities upon photoactivation with either

173

visible or UV light. These findings indicate that both hyperforin and hypericin are potent inducers of tumor cell apoptosis by targeting multiple signalling molecules. This may provide a rationale for the combination use of SJW with other chemotherapeutic agents for increasing efficacy. However, as a herbal medicine, SJW contains over two dozens of constituents and the contents of hyperforin and hypericin in SJW are very low (the contents of hypericin and hyperforin in the SJW tablets have been standardized to 0.3% and 5%, respectively, by the manufacturer) so that they may not potentiate the anti-tumor activity of the chemotherapy when combined with CPT-11. The decrease in the plasma level of the active metabolite SN-38 could suggest that patients receiving CPT-11 treatment should refrain from SJW, although the TNF-α level and cellular apoptosis may be not suppressed in tumor tissues. The SJW combination may compromise overall anti-tumor activity of CPT-11 although CPT-11 toxicity is altered. Specific dosing guidelines should be be given when patients are given such combinations.

Furthermore, the underlying pharmacokinetic study for the combination of SJW with CPT-11 indicated that the altered pharmacokinetic profiles of CPT-11 by SJW may be ascribed to the modulation of SJW and its component on CPT-11/SN-38 metabolism and transport, thus resulting in decreased SN-38 plasma levels. Therefore, caution should be taken when chemotherapeutic agents, that are substrates for cytochrome P450 and MDR1 P-glycoprotein, are taken with herbal medicines that are modulators of such enzymes and transporters, as the pharmacokinetic profiles of the anti-cancer agent could be changed, leading to a deleterious impact on treatment outcome.

Our preliminary toxicity studies further support the hypothesis that the intestinal damages induced by CPT-11 results from increased production of pro-inflammatory cytokines like TNF-α and epithelial apoptosis. The underlying mechanisms for the protective effects of thalidomide and SJW against CPT-11 induced complications may provide a new treatment approach for chemotherapy-associated histological damages using anti-TNF-α agents through the inhibition of pro-inflammatory cytokine expression and intestinal epithelial cellular apoptosis. However, the anti-tumor activity of this combination therapy should also be evaluated.

For the future direction of this project, anti-tumor activity study should be firstly performed for the identification of the feasibility of these two combinations. In the mean time, in order to further understand the mechanism for the reduced metabolism of CPT-11 by thalidomide and SJW, the expression of phase I and phase II enzymes and transporters should be involved. Similarly, to understand the mechanism of reduced side effect, the thalidomide/SJW-regulated NF-κB activity should be examined. In addition, the protective effects of thalidomide/SJW on CPT-11 induced toxicity should be evaluated using animal model with colon cancer, such results will be more persuasive compared with normal animal model. In order to mimic the clinical conditions, the colon cancer animal model should be pre-treated firstly with 5-FU/CPT-11 before the administration of thalidomide or SJW.

In conclusion, based on our experimental observations, the combination with thalidomide would be a promising strategy for reducing CPT-11's toxicity with possible enhanced anti-cancer activity, whereas CPT-11 should not be

coadministered with SJW to patients receiving CPT-11 therapy to avoid a deleterious treatment outcome. Furthermore, caution should be taken when chemotherapeutic agents are coadministered with herbal medicines that are modulators of drug enzymes and transporters. In addition, anti-TNF-α agents could be promising candidates for alleviating chemotherapy-associated histological damages.

Bibliography

1. *World Health Organization Fact Sheets.* World Health Organization Website, 2006. **http://www.who.int/mediacentre/factsheets/fs297/en/**.
2. Yokota, J., *Tumor progression and metastasis.* Carcinogenesis, 2000. **21**(3): p. 497-503.
3. Gibbs, J.B., *Mechanism-based target identification and drug discovery in cancer research.* Science, 2000. **287**(5460): p. 1969-73.
4. Fidler, I.J. and L.M. Ellis, *Chemotherapeutic drugs - More really is not better.* Nat Med, 2000. **6**(5): p. 500-2.
5. Ratain, M.J., *Pharmacology of cancer chemotherapy*, in *Principles and Practice of Oncology*, V.T. DeVita, S. Hellman, and S.A. Rosenberg, Editors. 1997, Lippincott-Raven Publishers: Philadelphia. p. 375-509.
6. Schwartzman, R.A. and J.A. Cidlowski, *Apoptosis: the biochemistry and molecular biology of programmed cell death.* Endocr Rev, 1993. **14**(2): p. 133-51.
7. Bosman, F.T., B.C. Visser, and J. van Oeveren, *Apoptosis: pathophysiology of programmed cell death.* Pathol Res Pract, 1996. **192**(7): p. 676-83.
8. Basu, A. and A. Miura, *Differential regulation of extrinsic and intrinsic cell death pathways by protein kinase C.* Int J Mol Med, 2002. **10**(5): p. 541-5.
9. Bossy-Wetzel, E., D.D. Newmeyer, and D.R. Green, *Mitochondrial cytochrome c release in apoptosis occurs upstream of DEVD-specific caspase activation and independently of mitochondrial transmembrane depolarization.* Embo J, 1998. **17**(1): p. 37-49.
10. Clerici, M., A. Sarin, P.A. Henkart, and G.M. Shearer, *Apoptotic cell death and cytokine dysregulation in human immunodeficiency virus infection: pivotal factors in disease progression.* Cell Death Differ, 1997. **4**(8): p. 699-706.
11. Smale, G., N.R. Nichols, D.R. Brady, C.E. Finch, and W.E. Horton, Jr., *Evidence for apoptotic cell death in Alzheimer's disease.* Exp Neurol, 1995. **133**(2): p. 225-30.
12. Podlesniy, P., A. Kichev, C. Pedraza, J. Saurat, M. Encinas, B. Perez, I. Ferrer, and C. Espinet, *Pro-NGF from Alzheimer's disease and normal human brain displays distinctive abilities to induce processing and nuclear translocation of intracellular domain of p75NTR and apoptosis.* Am J Pathol, 2006. **169**(1): p. 119-31.
13. Takeshita, H., K. Kusuzaki, T. Ashihara, M.C. Gebhardt, H.J. Mankin, and Y. Hirasawa, *Intrinsic resistance to chemotherapeutic agents in murine osteosarcoma cells.* J Bone Joint Surg Am, 2000. **82-A**(7): p. 963-9.
14. Levchenko, A., B.M. Mehta, X. Niu, G. Kang, L. Villafania, D. Way, D. Polycarpe, M. Sadelain, and S.M. Larson, *Intercellular transfer of P-glycoprotein mediates acquired multidrug resistance in tumor cells.* Proc Natl Acad Sci U S A, 2005. **102**(6): p. 1933-8.
15. Hill, B.T., S.A. Shellard, L.K. Hosking, A.M. Fichtinger-Schepman, and P. Bedford, *Enhanced DNA repair and tolerance of DNA damage associated with resistance to cis-diammine-dichloroplatinum (II) after in vitro*

exposure of a human teratoma cell line to fractionated X-irradiation. Int J Radiat Oncol Biol Phys, 1990. **19**(1): p. 75-83.

16. Fuchs, E.J., K.A. McKenna, and A. Bedi, *p53-dependent DNA damage-induced apoptosis requires Fas/APO-1-independent activation of CPP32beta.* Cancer Res, 1997. **57**(13): p. 2550-4.

17. Sugiyama, Y., Y. Kato, and X. Chu, *Multiplicity of biliary excretion mechanisms for the camptothecin derivative irinotecan (CPT-11), its metabolite SN-38, and its glucuronide: role of canalicular multispecific organic anion transporter and P-glycoprotein.* Cancer Chemother Pharmacol, 1998. **42 Suppl**: p. S44-9.

18. Hughes, B., D. Yip, D. Goldstein, P. Waring, V. Beshay, and G. Chong, *Cerebral relapse of metastatic gastrointestinal stromal tumor during treatment with imatinib mesylate: case report.* BMC Cancer, 2004. **4**: p. 74.

19. Teicher, B.A., T.S. Herman, S.A. Holden, Y.Y. Wang, M.R. Pfeffer, J.W. Crawford, and E. Frei, 3rd, *Tumor resistance to alkylating agents conferred by mechanisms operative only in vivo.* Science, 1990. **247**(4949 Pt 1): p. 1457-61.

20. Gupta, E., T.M. Lestingi, R. Mick, J. Ramirez, E.E. Vokes, and M.J. Ratain, *Metabolic fate of irinotecan in humans: correlation of glucuronidation with diarrhea.* Cancer Res, 1994. **54**(14): p. 3723-5.

21. Motzer, R.J., B.I. Rini, R.M. Bukowski, B.D. Curti, D.J. George, G.R. Hudes, B.G. Redman, K.A. Margolin, J.R. Merchan, G. Wilding, M.S. Ginsberg, J. Bacik, S.T. Kim, C.M. Baum, and M.D. Michaelson, *Sunitinib in patients with metastatic renal cell carcinoma.* Jama, 2006. **295**(21): p. 2516-24.

22. Melkoumian, Z.K., X. Peng, B. Gan, X. Wu, and J.L. Guan, *Mechanism of cell cycle regulation by FIP200 in human breast cancer cells.* Cancer Res, 2005. **65**(15): p. 6676-84.

23. Willett, C.G., Y. Boucher, E. di Tomaso, D.G. Duda, L.L. Munn, R.T. Tong, D.C. Chung, D.V. Sahani, S.P. Kalva, S.V. Kozin, M. Mino, K.S. Cohen, D.T. Scadden, A.C. Hartford, A.J. Fischman, J.W. Clark, D.P. Ryan, A.X. Zhu, L.S. Blaszkowsky, H.X. Chen, P.C. Shellito, G.Y. Lauwers, and R.K. Jain, *Direct evidence that the VEGF-specific antibody bevacizumab has antivascular effects in human rectal cancer.* Nat Med, 2004. **10**(2): p. 145-7.

24. Kabbinavar, F.F., J. Schulz, M. McCleod, T. Patel, J.T. Hamm, J.R. Hecht, R. Mass, B. Perrou, B. Nelson, and W.F. Novotny, *Addition of bevacizumab to bolus fluorouracil and leucovorin in first-line metastatic colorectal cancer: results of a randomized phase II trial.* J Clin Oncol, 2005. **23**(16): p. 3697-705.

25. Hewett, P.W., E.L. Daft, C.A. Laughton, S. Ahmad, A. Ahmed, and J.C. Murray, *Selective Inhibition of the Human tie-1 Promoter with Triplex-Forming Oligonucleotides Targeted to Ets Binding Sites.* Mol Med, 2006.

26. Kovacs, M.J., D.E. Reece, D. Marcellus, R.M. Meyer, S. Mathews, R.P. Dong, and E. Eisenhauer, *A phase II study of ZD6474 (Zactimatrade mark), a selective inhibitor of VEGFR and EGFR tyrosine kinase in patients with relapsed multiple myeloma-NCIC CTG IND.145.* Invest New Drugs, 2006.

27. Nair, R.E., M.O. Kilinc, S.A. Jones, and N.K. Egilmez, *Chronic immune therapy induces a progressive increase in intratumoral T suppressor activity and a concurrent loss of tumor-specific CD8+ T effectors in her-2/neu transgenic mice bearing advanced spontaneous tumors.* J Immunol, 2006. **176**(12): p. 7325-34.

28. Ramirez-Montagut, T., A. Chow, D. Hirschhorn-Cymerman, T.H. Terwey, A.A. Kochman, S. Lu, R.C. Miles, S. Sakaguchi, A.N. Houghton, and M.R. van den Brink, *Glucocorticoid-induced TNF receptor family related gene activation overcomes tolerance/ignorance to melanoma differentiation antigens and enhances antitumor immunity.* J Immunol, 2006. **176**(11): p. 6434-42.

29. Mathijssen, R.H., S. Marsh, M.O. Karlsson, R. Xie, S.D. Baker, J. Verweij, A. Sparreboom, and H.L. McLeod, *Irinotecan pathway genotype analysis to predict pharmacokinetics.* Clin Cancer Res, 2003. **9**(9): p. 3246-53.

30. Ayyoub, M., N.E. Souleimanian, E. Godefroy, L. Scotto, C.S. Hesdorffer, L.J. Old, and D. Valmori, *A phenotype based approach for the immune monitoring of NY-ESO-1-specific CD4+ T cell responses in cancer patients.* Clin Immunol, 2006. **118**(2-3): p. 188-94.

31. Ando, Y., D.K. Price, W.L. Dahut, M.C. Cox, E. Reed, and W.D. Figg, *Pharmacogenetic associations of CYP2C19 genotype with in vivo metabolisms and pharmacological effects of thalidomide.* Cancer Biol Ther, 2002. **1**(6): p. 669-73.

32. Chabot, G.G., D. Abigerges, G. Catimel, S. Culine, M. de Forni, J.M. Extra, M. Mahjoubi, P. Herait, J.P. Armand, and R. Bugat, *Population pharmacokinetics and pharmacodynamics of irinotecan (CPT-11) and active metabolite SN-38 during phase I trials.* Ann Oncol, 1995. **6**(2): p. 141-51.

33. Klein, C.E., E. Gupta, J.M. Reid, P.J. Atherton, J.A. Sloan, H.C. Pitot, M.J. Ratain, and H. Kastrissios, *Population pharmacokinetic model for irinotecan and two of its metabolites, SN-38 and SN-38 glucuronide.* Clin Pharmacol Ther, 2002. **72**(6): p. 638-47.

34. Urien, S., K. Rezai, and F. Lokiec, *Pharmacokinetic modelling of 5-FU production from capecitabine--a population study in 40 adult patients with metastatic cancer.* J Pharmacokinet Pharmacodyn, 2005. **32**(5-6): p. 817-33.

35. Pizzolato, J.F. and L.B. Saltz, *The camptothecins.* Lancet, 2003. **361**(9376): p. 2235-42.

36. Redinbo, M.R., L. Stewart, P. Kuhn, J.J. Champoux, and W.G. Hol, *Crystal structures of human topoisomerase I in covalent and noncovalent complexes with DNA.* Science, 1998. **279**(5356): p. 1504-13.

37. Stewart, L., M.R. Redinbo, X. Qiu, W.G. Hol, and J.J. Champoux, *A model for the mechanism of human topoisomerase I.* Science, 1998. **279**(5356): p. 1534-41.

38. Jung, L.L. and W.C. Zamboni, *Cellular, pharmacokinetic, and pharmacodynamic aspects of response to camptothecins: can we improve it?* Drug Resist Updat, 2001. **4**(4): p. 273-88.

39. Brown, P.O. and N.R. Cozzarelli, *Catenation and knotting of duplex DNA by type 1 topoisomerases: a mechanistic parallel with type 2 topoisomerases.* Proc Natl Acad Sci U S A, 1981. **78**(2): p. 843-7.

40. Kirkegaard, K. and J.C. Wang, *Escherichia coli DNA topoisomerase I catalyzed linking of single-stranded rings of complementary base sequences.* Nucleic Acids Res, 1978. **5**(10): p. 3811-20.

41. Yeh, Y.C., H.F. Liu, C.A. Ellis, and A.L. Lu, *Mammalian topoisomerase I has base mismatch nicking activity.* J Biol Chem, 1994. **269**(22): p. 15498-504.

42. Hsiang, Y.H., R. Hertzberg, S. Hecht, and L.F. Liu, *Camptothecin induces protein-linked DNA breaks via mammalian DNA topoisomerase I.* J Biol Chem, 1985. **260**(27): p. 14873-8.

43. Yamashita, Y., N. Fujii, C. Murakata, T. Ashizawa, M. Okabe, and H. Nakano, *Induction of mammalian DNA topoisomerase I mediated DNA cleavage by antitumor indolocarbazole derivatives.* Biochemistry, 1992. **31**(48): p. 12069-75.

44. Permana, P.A., R.M. Snapka, L.L. Shen, D.T. Chu, J.J. Clement, and J.J. Plattner, *Quinobenoxazines: a class of novel antitumor quinolones and potent mammalian DNA topoisomerase II catalytic inhibitors.* Biochemistry, 1994. **33**(37): p. 11333-9.

45. Goldwasser, F., T. Shimizu, J. Jackman, Y. Hoki, P.M. O'Connor, K.W. Kohn, and Y. Pommier, *Correlations between S and G2 arrest and the cytotoxicity of camptothecin in human colon carcinoma cells.* Cancer Res., 1996. **56**(19): p. 4430-7.

46. Wall, M., Wani MC, Cook CE, Palmer KH, Mcphail AT, Sim GA, *Plant antitumor agents: 1, the isolation and structure of camptothecin, anovel alkaloidal leukemia and tumor inhibitor from Camptotheca acuminata.* J Am Chem Soc., 1966. **88**: p. 3888-90.

47. Cortesi, R., Esposito, E., Maietti, A., Menegatti, E., Nastruzzi, C.,, *Formulation study for the antitumor drug camptothecin: liposomes, micellar solutions and a microemulsion.* Int. J. Pharm. , 1997. **159**: p. 95-103.

48. Kang, J., V. Kumar, D. Yang, P.R. Chowdhury, and R.J. Hohl, *Cyclodextrin complexation: influence on the solubility, stability, and cytotoxicity of camptothecin, an antineoplastic agent.* Eur J Pharm Sci, 2002. **15**(2): p. 163-70.

49. Tsuruo, T., T. Matsuzaki, M. Matsushita, H. Saito, and T. Yokokura, *Antitumor effect of CPT-11, a new derivative of camptothecin, against pleiotropic drug-resistant tumors in vitro and in vivo.* Cancer Chemother Pharmacol, 1988. **21**(1): p. 71-4.

50. Kudoh, S., Y. Fujiwara, Y. Takada, H. Yamamoto, A. Kinoshita, Y. Ariyoshi, K. Furuse, and M. Fukuoka, *Phase II study of irinotecan combined with cisplatin in patients with previously untreated small-cell lung cancer. West Japan Lung Cancer Group.* J Clin Oncol, 1998. **16**(3): p. 1068-74.

51. Irvin, W.P., F.V. Price, H. Bailey, M. Gelder, R. Rosenbluth, H.J. Durivage, and R.K. Potkul, *A phase II study of irinotecan (CPT-11) in patients with advanced squamous cell carcinoma of the cervix.* Cancer, 1998. **82**(2): p. 328-33.

52. Verschraegen, C.F., T. Levy, A.P. Kudelka, E. Llerena, K. Ende, R.S. Freedman, C.L. Edwards, M. Hord, M. Steger, A.L. Kaplan, D. Kieback, A. Fishman, and J.J. Kavanagh, *Phase II study of irinotecan in prior*

chemotherapy-treated squamous cell carcinoma of the cervix. J Clin Oncol, 1997. **15**(2): p. 625-31.

53.   Shimizu, Y., S. Umezawa, and K. Hasumi, *[Successful treatment of clear cell adenocarcinoma of the ovary (OCCA) with a combination of CPT-11 and mitomycin C].* Gan To Kagaku Ryoho, 1996. **23**(5): p. 587-93.

54.   Ota, K., R. Ohno, S. Shirakawa, T. Masaoka, K. Okada, Y. Ohashi, and T. Taguchi, *[Late phase II clinical study of irinotecan hydrochloride (CPT-11) in the treatment of malignant lymphoma and acute leukemia. The CPT-11 Research Group for Hematological Malignancies].* Gan To Kagaku Ryoho, 1994. **21**(7): p. 1047-55.

55.   Mathijssen, R.H., W.J. Loos, J. Verweij, and A. Sparreboom, *Pharmacology of topoisomerase I inhibitors irinotecan (CPT-11) and topotecan.* Curr Cancer Drug Targets, 2002. **2**(2): p. 103-23.

56.   Jeung, H.C., S.Y. Rha, S.H. Noh, J.K. Roh, and H.C. Chung, *A phase II trial of weekly fractionated irinotecan and cisplatin for advanced gastric cancer.* Cancer Chemother Pharmacol, 2006.

57.   Sanli, U.A., B. Karabulut, R. Uslu, M. Korkut, and E. Goker, *Single-agent irinotecan for recurrent/metastatic colorectal cancer: a retrospective analysis.* Med Princ Pract, 2006. **15**(4): p. 288-92.

58.   Klautke, G., S. Fahndrich, S. Semrau, C. Buscher, C. Virchow, and R. Fietkau, *Simultaneous chemoradiotherapy with irinotecan and cisplatin in limited disease small cell lung cancer a phase I study.* Lung Cancer, 2006.

59.   Shimoyama, T., F. Koizumi, H. Fukumoto, K. Kiura, M. Tanimoto, N. Saijo, and K. Nishio, *Effects of different combinations of gefitinib and irinotecan in lung cancer cell lines expressing wild or deletional EGFR.* Lung Cancer, 2006. **53**(1): p. 13-21.

60.   Ducreux, M.P., V. Boige, S. Leboulleux, D. Malka, P. Kergoat, C. Dromain, D. Elias, T. de Baere, J.C. Sabourin, P. Duvillard, P. Lasser, M. Schlumberger, and E. Baudin, *A phase II study of irinotecan with 5-fluorouracil and leucovorin in patients with pretreated gastroenteropancreatic well-differentiated endocrine carcinomas.* Oncology, 2006. **70**(2): p. 134-40.

61.   Van Cutsem, E., D. Cunningham, W.W. Ten Bokkel Huinink, C.J. Punt, C.G. Alexopoulos, L. Dirix, M. Symann, G.H. Blijham, P. Cholet, G. Fillet, C. Van Groeningen, J.M. Vannetzel, F. Levi, G. Panagos, C. Unger, J. Wils, C. Cote, C. Blanc, P. Herait, and H. Bleiberg, *Clinical activity and benefit of irinotecan (CPT-11) in patients with colorectal cancer truly resistant to 5-fluorouracil (5-FU).* Eur J Cancer, 1999. **35**(1): p. 54-9.

62.   Ulukan, H. and P.W. Swaan, *Camptothecins: a review of their chemotherapeutic potential.* Drugs, 2002. **62**(14): p. 2039-57.

63.   Bailly, C., *Topoisomerase I poisons and suppressors as anticancer drugs.* Curr Med Chem, 2000. **7**(1): p. 39-58.

64.   Burris, H.A., 3rd and S.M. Fields, *Topoisomerase I inhibitors. An overview of the camptothecin analogs.* Hematol Oncol Clin North Am, 1994. **8**(2): p. 333-55.

65.   Xie, R., R.H. Mathijssen, A. Sparreboom, J. Verweij, and M.O. Karlsson, *Clinical pharmacokinetics of irinotecan and its metabolites in relation with diarrhea.* Clin Pharmacol Ther, 2002. **72**(3): p. 265-75.

66.   Chabot, G.G., *Clinical pharmacokinetics of irinotecan.* Clin Pharmacokinet, 1997. **33**(4): p. 245-59.

67. Rivory, L.P., M.C. Haaz, P. Canal, F. Lokiec, J.P. Armand, and J. Robert, *Pharmacokinetic interrelationships of irinotecan (CPT-11) and its three major plasma metabolites in patients enrolled in phase I/II trials.* Clin Cancer Res, 1997. **3**(8): p. 1261-66.

68. Gupta, E., R. Mick, J. Ramirez, X. Wang, T.M. Lestingi, E.E. Vokes, and M.J. Ratain, *Pharmacokinetic and pharmacodynamic evaluation of the topoisomerase inhibitor irinotecan in cancer patients.* J Clin Oncol, 1997. **15**(4): p. 1502-10.

69. Abigerges, D., G.G. Chabot, J.P. Armand, P. Herait, A. Gouyette, and D. Gandia, *Phase I and pharmacologic studies of the camptothecin analog irinotecan administered every 3 weeks in cancer patients.* J Clin Oncol, 1995. **13**(1): p. 210-21.

70. Pitot, H.C., R.M. Goldberg, J.M. Reid, J.A. Sloan, P.A. Skaff, C. Erlichman, J. Rubin, P.A. Burch, A.A. Adjei, S.A. Alberts, L.J. Schaaf, G. Elfring, and L.L. Miller, *Phase I dose-finding and pharmacokinetic trial of irinotecan hydrochloride (CPT-11) using a once-every-three-week dosing schedule for patients with advanced solid tumor malignancy.* Clin Cancer Res, 2000. **6**(6): p. 2236-44.

71. Schoemaker, N.E., I.E. Kuppens, W.W. Huinink, P. Lefebvre, J.H. Beijnen, S. Assadourian, G.J. Sanderink, and J.H. Schellens, *Phase I study of an oral formulation of irinotecan administered daily for 14 days every 3 weeks in patients with advanced solid tumours.* Cancer Chemother Pharmacol, 2005. **55**(3): p. 263-70.

72. Drengler, R.L., J.G. Kuhn, L.J. Schaaf, G.I. Rodriguez, M.A. Villalona-Calero, L.A. Hammond, J.A. Stephenson, Jr., S. Hodges, M.A. Kraynak, B.A. Staton, G.L. Elfring, P.K. Locker, L.L. Miller, D.D. Von Hoff, and M.L. Rothenberg, *Phase I and pharmacokinetic trial of oral irinotecan administered daily for 5 days every 3 weeks in patients with solid tumors.* J Clin Oncol, 1999. **17**(2): p. 685-96.

73. Tsuji, T., N. Kaneda, K. Kado, T. Yokokura, T. Yoshimoto, and D. Tsuru, *CPT-11 converting enzyme from rat serum: purification and some properties.* J Pharmacobiodyn, 1991. **14**(6): p. 341-9.

74. Satoh, T., M. Hosokawa, R. Atsumi, W. Suzuki, H. Hakusui, and E. Nagai, *Metabolic activation of CPT-11, 7-ethyl-10-[4-(1-piperidino)-1-piperidino]carbonyloxycamptothecin, a novel antitumor agent, by carboxylesterase.* Biol Pharm Bull, 1994. **17**(5): p. 662-4.

75. Rivory, L.P., M.R. Bowles, J. Robert, and S.M. Pond, *Conversion of irinotecan (CPT-11) to its active metabolite, 7-ethyl-10-hydroxycamptothecin (SN-38), by human liver carboxylesterase.* Biochem Pharmacol, 1996. **52**(7): p. 1103-11.

76. Humerickhouse, R., K. Lohrbach, L. Li, W.F. Bosron, and M.E. Dolan, *Characterization of CPT-11 hydrolysis by human liver carboxylesterase isoforms hCE-1 and hCE-2.* Cancer Res, 2000. **60**(5): p. 1189-92.

77. Ma, M.K. and H.L. McLeod, *Lessons learned from the irinotecan metabolic pathway.* Curr Med Chem, 2003. **10**(1): p. 41-9.

78. Mathijssen, R.H., R.J. van Alphen, J. Verweij, W.J. Loos, K. Nooter, G. Stoter, and A. Sparreboom, *Clinical pharmacokinetics and metabolism of irinotecan (CPT-11).* Clin Cancer Res, 2001. **7**(8): p. 2182-94.

79. Kawato, Y., M. Aonuma, Y. Hirota, H. Kuga, and K. Sato, *Intracellular roles of SN-38, a metabolite of the camptothecin derivative CPT-11, in the antitumor effect of CPT-11.* Cancer Res, 1991. **51**(16): p. 4187-91.

80. Hanioka, N., S. Ozawa, H. Jinno, M. Ando, Y. Saito, and J. Sawada, *Human liver UDP-glucuronosyltransferase isoforms involved in the glucuronidation of 7-ethyl-10-hydroxycamptothecin.* Xenobiotica, 2001. **31**(10): p. 687-99.

81. Kuhn, J.G., *Pharmacology of irinotecan.* Oncology (Huntingt), 1998. **12**(8 Suppl 6): p. 39-42.

82. Chu, X.Y., Y. Kato, and Y. Sugiyama, *Multiplicity of biliary excretion mechanisms for irinotecan, CPT-11, and its metabolites in rats.* Cancer Res, 1997. **57**(10): p. 1934-8.

83. Takasuna, K., T. Hagiwara, M. Hirohashi, M. Kato, M. Nomura, E. Nagai, T. Yokoi, and T. Kamataki, *Involvement of beta-glucuronidase in intestinal microflora in the intestinal toxicity of the antitumor camptothecin derivative irinotecan hydrochloride (CPT-11) in rats.* Cancer Res, 1996. **56**(16): p. 3752-7.

84. Rivory, L.P., J.F. Riou, M.C. Haaz, S. Sable, M. Vuilhorgne, A. Commercon, S.M. Pond, and J. Robert, *Identification and properties of a major plasma metabolite of irinotecan (CPT-11) isolated from the plasma of patients.* Cancer Res, 1996. **56**(16): p. 3689-94.

85. Haaz, M.C., L. Rivory, C. Riche, L. Vernillet, and J. Robert, *Metabolism of irinotecan (CPT-11) by human hepatic microsomes: participation of cytochrome P-450 3A and drug interactions.* Cancer Res, 1998. **58**(3): p. 468-72.

86. Santos, A., S. Zanetta, T. Cresteil, A. Deroussent, F. Pein, E. Raymond, L. Vernillet, M.L. Risse, V. Boige, A. Gouyette, and G. Vassal, *Metabolism of irinotecan (CPT-11) by CYP3A4 and CYP3A5 in humans.* Clin Cancer Res, 2000. **6**(5): p. 2012-20.

87. Dodds, H.M., M.C. Haaz, J.F. Riou, J. Robert, and L.P. Rivory, *Identification of a new metabolite of CPT-11 (irinotecan): pharmacological properties and activation to SN-38.* J Pharmacol Exp Ther, 1998. **286**(1): p. 578-83.

88. Kehrer, D.F., W. Yamamoto, J. Verweij, M.J. de Jonge, P. de Bruijn, and A. Sparreboom, *Factors involved in prolongation of the terminal disposition phase of SN-38: clinical and experimental studies.* Clin Cancer Res, 2000. **6**(9): p. 3451-8.

89. Rivory, L.P., *Metabolism of CPT-11. Impact on activity.* Ann N Y Acad Sci, 2000. **922**: p. 205-15.

90. de Jonge, M.J., J. Verweij, P. de Bruijn, E. Brouwer, R.H. Mathijssen, R.J. van Alphen, M.M. de Boer-Dennert, L. Vernillet, C. Jacques, and A. Sparreboom, *Pharmacokinetic, metabolic, and pharmacodynamic profiles in a dose-escalating study of irinotecan and cisplatin.* J Clin Oncol, 2000. **18**(1): p. 195-203.

91. Shepard, D.R., J. Ramirez, L. lyer, and M.J. Ratain, *Metabolism of SN-38 by CYP3A4 and microsomes from human liver.* Proc. Am.Soc.Oncol., 1999. **18**: p. 176a.

92. Potmesil, M., *Camptothecins: from bench research to hospital wards.* Cancer Res, 1994. **54**(6): p. 1431-9.

93.   Fassberg, J. and V.J. Stella, *A kinetic and mechanistic study of the hydrolysis of camptothecin and some analogues.* J Pharm Sci, 1992. **81**(7): p. 676-84.

94.   Burke, T.G. and Z. Mi, *Ethyl substitution at the 7 position extends the half-life of 10-hydroxycamptothecin in the presence of human serum albumin.* J Med Chem, 1993. **36**(17): p. 2580-2.

95.   Mi, Z., H. Malak, and T.G. Burke, *Reduced albumin binding promotes the stability and activity of topotecan in human blood.* Biochemistry, 1995. **34**(42): p. 13722-8.

96.   Slichenmyer, W.J., E.K. Rowinsky, R.C. Donehower, and S.H. Kaufmann, *The current status of camptothecin analogues as antitumor agents.* J Natl Cancer Inst, 1993. **85**(4): p. 271-91.

97.   Kobayashi, K., B. Bouscarel, Y. Matsuzaki, S. Ceryak, S. Kudoh, and H. Fromm, *pH-dependent uptake of irinotecan and its active metabolite, SN-38, by intestinal cells.* Int J Cancer, 1999. **83**(4): p. 491-6.

98.   Kobayashi, K., B. Bouscarel, Y. Matsuzaki, S. Ceryak, and H. Fromm, *Uptake mechanism of irinotecan (CPT-11) and its metabolite (SN-38) by hamster intestinal cells.* Gastroenterology, 1998. **114**: p. G2578.

99.   Combes, O., J. Barre, J.C. Duche, L. Vernillet, Y. Archimbaud, M.P. Marietta, J.P. Tillement, and S. Urien, *In vitro binding and partitioning of irinotecan (CPT-11) and its metabolite, SN-38, in human blood.* Invest New Drugs, 2000. **18**(1): p. 1-5.

100.   Burke, T.G. and Z. Mi, *The structural basis of camptothecin interactions with human serum albumin: impact on drug stability.* J Med Chem, 1994. **37**(1): p. 40-6.

101.   Mi, Z., H. Malak, and T.G. Burke, *Reduced albumin binding promotes the stability and activity of topotecan in human blood.* Biochemistry, 1995. **34**(42): p. 13722-8.

102.   Yang, C.J., J.K. Horton, K.H. Cowan, and E. Schneider, *Cross-resistance to camptothecin analogues in a mitoxantrone-resistant human breast carcinoma cell line is not due to DNA topoisomerase I alterations.* Cancer Res, 1995. **55**(18): p. 4004-9.

103.   Chu, X.Y., H. Suzuki, K. Ueda, Y. Kato, S. Akiyama, and Y. Sugiyama, *Active efflux of CPT-11 and its metabolites in human KB-derived cell lines.* J Pharmacol Exp Ther, 1999. **288**(2): p. 735-41.

104.   Maliepaard, M., M.A. van Gastelen, A. Tohgo, F.H. Hausheer, R.C. van Waardenburg, L.A. de Jong, D. Pluim, J.H. Beijnen, and J.H. Schellens, *Circumvention of breast cancer resistance protein (BCRP)-mediated resistance to camptothecins in vitro using non-substrate drugs or the BCRP inhibitor GF120918.* Clin Cancer Res, 2001. **7**(4): p. 935-41.

105.   Schellens, J.H., M. Maliepaard, R.J. Scheper, G.L. Scheffer, J.W. Jonker, J.W. Smit, J.H. Beijnen, and A.H. Schinkel, *Transport of topoisomerase I inhibitors by the breast cancer resistance protein. Potential clinical implications.* Ann N Y Acad Sci, 2000. **922**: p. 188-94.

106.   Luo, F.R., P.V. Paranjpe, A. Guo, E. Rubin, and P. Sinko, *Intestinal transport of irinotecan in Caco-2 cells and MDCK II cells overexpressing efflux transporters Pgp, cMOAT, and MRP1.* Drug Metab Dispos, 2002. **30**(7): p. 763-70.

107.   Yamamoto, W., J. Verweij, P. de Bruijn, M.J. de Jonge, H. Takano, M. Nishiyama, M. Kurihara, and A. Sparreboom, *Active transepithelial*

transport of irinotecan (CPT-11) and its metabolites by human intestinal Caco-2 cells. Anticancer Drugs, 2001. **12**(5): p. 419-32.

108.   Chu, X.Y., Y. Kato, K. Ueda, H. Susuki, K. Niinuma, C.A. Tyson, V. Weizer, J.E. Dabbs, R. Froehlich, C.E. Green, and Y. Sugiyama, *Biliary excretion mechanism of CPT-11 and its metabolites in humans: involvement of primary active transporters.* Cancer Res, 1998. **58**(22): p. 5137-43.

109.   Gupta, E., A.R. Safa, X. Wang, and M.J. Ratain, *Pharmacokinetic modulation of irinotecan and metabolites by cyclosporin A.* Cancer Res, 1996. **56**(6): p. 1309-14.

110.   Chu, X.Y., Y. Kato, and Y. Sugiyama, *Possible involvement of P-glycoprotein in biliary excretion of CPT-11 in rats.* Drug Metab Dispos, 1999. **27**(4): p. 440-1.

111.   Sparreboom, A., M.J. de Jonge, P. de Bruijn, E. Brouwer, K. Nooter, W.J. Loos, R.J. van Alphen, R.H. Mathijssen, G. Stoter, and J. Verweij, *Irinotecan (CPT-11) metabolism and disposition in cancer patients.* Clin Cancer Res, 1998. **4**(11): p. 2747-54.

112.   Slatter, J.G., L.J. Schaaf, J.P. Sams, K.L. Feenstra, M.G. Johnson, P.A. Bombardt, K.S. Cathcart, M.T. Verburg, L.K. Pearson, L.D. Compton, L.L. Miller, D.S. Baker, C.V. Pesheck, and R.S. Lord, 3rd, *Pharmacokinetics, metabolism, and excretion of irinotecan (CPT-11) following I.V. infusion of [(14)C]CPT-11 in cancer patients.* Drug Metab Dispos, 2000. **28**(4): p. 423-33.

113.   Itoh, T., I. Takemoto, S. Itagaki, K. Sasaki, T. Hirano, and K. Iseki, *Biliary excretion of irinotecan and its metabolites.* J Pharm Pharm Sci, 2004. **7**(1): p. 13-8.

114.   Atsumi, R., W. Suzuki, and H. Hakusui, *Identification of the metabolites of irinotecan, a new derivative of camptothecin, in rat bile and its biliary excretion.* Xenobiotica, 1991. **21**(9): p. 1159-69.

115.   Kaneda, N. and T. Yokokura, *Nonlinear pharmacokinetics of CPT-11 in rats.* Cancer Res, 1990. **50**(6): p. 1721-5.

116.   Takasuna, K., Y. Kasai, Y. Kitano, K. Mori, R. Kobayashi, T. Hagiwara, K. Kakihata, M. Hirohashi, M. Nomura, E. Nagai, and et al., *Protective effects of kampo medicines and baicalin against intestinal toxicity of a new anticancer camptothecin derivative, irinotecan hydrochloride (CPT-11), in rats.* Jpn J Cancer Res, 1995. **86**(10): p. 978-84.

117.   Gandia, D., D. Abigerges, J.P. Armand, G. Chabot, L. Da Costa, M. De Forni, A. Mathieu-Boue, and P. Herait, *CPT-11-induced cholinergic effects in cancer patients.* J Clin Oncol, 1993. **11**(1): p. 196-7.

118.   Hecht, J.R., *Gastrointestinal toxicity or irinotecan.* Oncology (Huntingt), 1998. **12**(8 Suppl 6): p. 72-8.

119.   Sargent, D.J., D. Niedzwiecki, M.J. O'Connell, and R.L. Schilsky, *Recommendation for caution with irinotecan, fluorouracil, and leucovorin for colorectal cancer.* N Engl J Med, 2001. **345**(2): p. 144-5; author reply 146.

120.   Rougier, P., R. Bugat, J.Y. Douillard, S. Culine, E. Suc, P. Brunet, Y. Becouarn, M. Ychou, M. Marty, J.M. Extra, J. Bonneterre, A. Adenis, J.F. Seitz, G. Ganem, M. Namer, T. Conroy, S. Negrier, Y. Merrouche, F. Burki, M. Mousseau, P. Herait, and M. Mahjoubi, *Phase II study of irinotecan in the treatment of advanced colorectal cancer in*

chemotherapy-naive patients and patients pretreated with fluorouracil-based chemotherapy. J Clin Oncol, 1997. **15**(1): p. 251-60.

121. Sasaki, Y., H. Hakusui, and S. Mizuno, *A pharmacokinetic and pharmacodynamic analysis of CPT-11 and its active metabolite SN-38.* Jpn J Cancer Res, 1995. **86**(1): p. 101-10.

122. Chabot, G.G., D. Abigerges, G. Catimel, S. Culine, M. de Forni, J.M. Extra, M. Mahjoubi, P. Herait, J.P. Armand, R. Bugat, and et al., *Population pharmacokinetics and pharmacodynamics of irinotecan (CPT-11) and active metabolite SN-38 during phase I trials.* Ann Oncol, 1995. **6**(2): p. 141-51.

123. de Forni, M., R. Bugat, G.G. Chabot, S. Culine, J.M. Extra, A. Gouyette, I. Madelaine, M.E. Marty, and A. Mathieu-Boue, *Phase I and pharmacokinetic study of the camptothecin derivative irinotecan, administered on a weekly schedule in cancer patients.* Cancer Res, 1994. **54**(16): p. 4347-54.

124. Kurita, A., S. Kado, N. Kaneda, M. Onoue, S. Hashimoto, and T. Yokokura, *Alleviation of side effects induced by irinotecan hydrochloride (CPT-11) in rats by intravenous infusion.* Cancer Chemother Pharmacol, 2003. **52**(5): p. 349-60.

125. Kurita, A., S. Kado, N. Kaneda, M. Onoue, S. Hashimoto, and T. Yokokura, *Modified irinotecan hydrochloride (CPT-11) administration schedule improves induction of delayed-onset diarrhea in rats.* Cancer Chemother Pharmacol, 2000. **46**(3): p. 211-20.

126. Catimel, G., G.G. Chabot, J.P. Guastalla, A. Dumortier, C. Cote, C. Engel, A. Gouyette, A. Mathieu-Boue, M. Mahjoubi, and M. Clavel, *Phase I and pharmacokinetic study of irinotecan (CPT-11) administered daily for three consecutive days every three weeks in patients with advanced solid tumors.* Ann Oncol, 1995. **6**(2): p. 133-40.

127. Kudoh, S., M. Fukuoka, N. Masuda, A. Yoshikawa, Y. Kusunoki, K. Matsui, S. Negoro, N. Takifuji, K. Nakagawa, and T. Hirashima, *Relationship between the pharmacokinetics of irinotecan and diarrhea during combination chemotherapy with cisplatin.* Jpn J Cancer Res, 1995. **86**(4): p. 406-13.

128. Siu, L.L. and E.K. Rowinsky, *A risk-benefit assessment of irinotecan in solid tumours.* Drug Saf, 1998. **18**(6): p. 395-417.

129. Tukey, R.H., C.P. Strassburg, and P.I. Mackenzie, *Pharmacogenomics of human UDP-glucuronosyltransferases and irinotecan toxicity.* Mol Pharmacol, 2002. **62**(3): p. 446-50.

130. Herben, V.M., J.H. Schellens, M. Swart, G. Gruia, L. Vernillet, J.H. Beijnen, and W.W. ten Bokkel Huinink, *Phase I and pharmacokinetic study of irinotecan administered as a low-dose, continuous intravenous infusion over 14 days in patients with malignant solid tumors.* J Clin Oncol, 1999. **17**(6): p. 1897-905.

131. Canal, P., C. Gay, A. Dezeuze, J.Y. Douillard, R. Bugat, R. Brunet, A. Adenis, P. Herait, F. Lokiec, and A. Mathieu-Boue, *Pharmacokinetics and pharmacodynamics of irinotecan during a phase II clinical trial in colorectal cancer. Pharmacology and Molecular Mechanisms Group of the European Organization for Research and Treatment of Cancer.* J Clin Oncol, 1996. **14**(10): p. 2688-95.

132.   Rowinsky, E.K., L.B. Grochow, D.S. Ettinger, S.E. Sartorius, B.G. Lubejko, T.L. Chen, M.K. Rock, and R.C. Donehower, *Phase I and pharmacological study of the novel topoisomerase I inhibitor 7-ethyl-10-[4-(1-piperidino)-1-piperidino]carbonyloxycamptothecin (CPT-11) administered as a ninety-minute infusion every 3 weeks.* Cancer Res, 1994. **54**(2): p. 427-36.

133.   Kawato, Y., M. Sekiguchi, K. Akahane, Y. Tsutomi, Y. Hirota, H. Kuga, W. Suzuki, H. Hakusui, and K. Sato, *Inhibitory activity of camptothecin derivatives against acetylcholinesterase in dogs and their binding activity to acetylcholine receptors in rats.* J Pharm Pharmacol, 1993. **45**(5): p. 444-8.

134.   Chen, G., R. Portman, and A. Wickel, *Pharmacology of 1,1-dimethyl-4-phenyl-piperazinium iodide, a ganglion-stimulating agent.* J Pharmacol Exp Ther, 1951. **103**: p. 330-6.

135.   Takasuna, K., Y. Kasai, Y. Kitano, K. Mori, K. Kakihata, M. Hirohashi, and M. Nomura, *[Study on the mechanisms of diarrhea induced by a new anticancer camptothecin derivative, irinotecan hydrochloride (CPT-11), in rats].* Nippon Yakurigaku Zasshi, 1995. **105**(6): p. 447-60.

136.   Saliba, F., R. Hagipantelli, J.L. Misset, G. Bastian, G. Vassal, M. Bonnay, P. Herait, C. Cote, M. Mahjoubi, D. Mignard, and E. Cvitkovic, *Pathophysiology and therapy of irinotecan-induced delayed-onset diarrhea in patients with advanced colorectal cancer: a prospective assessment.* J Clin Oncol, 1998. **16**(8): p. 2745-51.

137.   Alimonti, A., F. Satta, I. Pavese, E. Burattini, V. Zoffoli, and A. Vecchione, *Prevention of irinotecan plus 5-fluorouracil/leucovorin-induced diarrhoea by oral administration of neomycin plus bacitracin in first-line treatment of advanced colorectal cancer.* Ann Oncol, 2003. **14**(5): p. 805-6.

138.   Takasuna, K., T. Hagiwara, M. Hirohashi, M. Kato, M. Nomura, E. Nagai, T. Yokoi, and T. Kamataki, *Inhibition of intestinal microflora beta-glucuronidase modifies the distribution of the active metabolite of the antitumor agent, irinotecan hydrochloride (CPT-11) in rats.* Cancer Chemother Pharmacol, 1998. **42**(4): p. 280-6.

139.   Wadkins, R.M., J.L. Hyatt, K.J. Yoon, C.L. Morton, R.E. Lee, K. Damodaran, P. Beroza, M.K. Danks, and P.M. Potter, *Discovery of novel selective inhibitors of human intestinal carboxylesterase for the amelioration of irinotecan-induced diarrhea: synthesis, quantitative structure-activity relationship analysis, and biological activity.* Mol Pharmacol, 2004. **65**(6): p. 1336-43.

140.   Kase, Y., T. Hayakawa, M. Aburada, Y. Komatsu, and T. Kamataki, *Preventive effects of Hange-shashin-to on irinotecan hydrochloride-caused diarrhea and its relevance to the colonic prostaglandin E2 and water absorption in the rat.* Jpn J Pharmacol, 1997. **75**(4): p. 407-13.

141.   Eisenkraft, A., S. Luria, E. Robenshtok, and A. Hourvitz, *Using thalidomide against pathological neovascularization.* Harefuah, 2003. **142**(3): p. 212-6, 237.

142.   Kase, Y., T. Hayakawa, Y. Togashi, and T. Kamataki, *Relevance of irinotecan hydrochloride-induced diarrhea to the level of prostaglandin E2 and water absorption of large intestine in rats.* Jpn J Pharmacol, 1997. **75**(4): p. 399-405.

143. Suzuki, T., H. Sakai, and A. Ikari, *Inhibition of thromboxane A2-induced Cl- secretion by antidiarrhea drug loperamide in isolated rat colon.* J Pharm and Experiment therapeutics, 2000. **295**(1): p. 233-38.

144. Sakai, H., T. Sato, N. Hamada, M. Yasue, A. Ikari, B. Kakinoki, and N. Takeguchi, *Thromboxane A2, released by the anti-tumour drug irinotecan, is a novel stimulator of Cl- secretion in isolated rat colon.* J Physiol, 1997. **505 (Pt 1)**: p. 133-44.

145. Trifan, O.C., W.F. Durham, V.S. Salazar, J. Horton, B.D. Levine, B.S. Zweifel, T.W. Davis, and J.L. Masferrer, *Cyclooxygenase-2 inhibition with celecoxib enhances antitumor efficacy and reduces diarrhea side effect of CPT-11.* Cancer Res, 2002. **62**(20): p. 5778-84.

146. Ghezzi, P. and A. Cerami, *Tumor necrosis factor as a pharmacological target.* Methods Mol Med, 2004. **98**: p. 1-8.

147. TsujI, E., N. Hiki, S. Nomura, R. Fukushima, J. Kojima, T. Ogawa, K. Mafune, Y. Mimura, and M. Kaminishi, *Simultaneous onset of acute inflammatory response, sepsis-like symptoms and intestinal mucosal injury after cancer chemotherapy.* Int J Cancer., 2003. **107**(2): p. 303-8.

148. Tonini, G., D. Santini, B. Vincenzi, D. Borzomati, G. Dicuonzo, A. La Cesa, N. Onori, and R. Coppola, *Oxaliplatin may induce cytokine-release syndrome in colorectal cancer patients.* J Biol Regul Homeost Agents., 2002. **16**(2): p. 105-9.

149. Ikegami, T., L. Ha, K. Arimori, P. Latham, K. Kobayashi, S. Ceryak, Y. Matsuzaki, and B. Bouscarel, *Intestinal alkalization as a possible preventive mechanism in irinotecan (CPT-11)-induced diarrhea.* Cancer Res, 2002. **62**(1): p. 179-87.

150. Kehrer, D.F., A. Sparreboom, J. Verweij, P. de Bruijn, C.A. Nierop, J. van de Schraaf, E.J. Ruijgrok, and M.J. de Jonge, *Modulation of irinotecan-induced diarrhea by cotreatment with neomycin in cancer patients.* Clin Cancer Res, 2001. **7**(5): p. 1136-41.

151. Horikawa, M., Y. Kato, and Y. Sugiyama, *Reduced gastrointestinal toxicity following inhibition of the biliary excretion of irinotecan and its metabolites by probenecid in rats.* Pharm Res, 2002. **19**(9): p. 1345-53.

152. Zampa, G., E. Magnolfi, and A. Borgomastro, *Premedication for irinotecan.* J Clin Oncol, 2000. **18**(1): p. 237.

153. Yumuk, P.F., S.Z. Aydin, F. Dane, M. Gumus, M. Ekenel, M. Aliustaoglu, A. Karamanoglu, M. Sengoz, and S.N. Turhal, *The absence of early diarrhea with atropine premedication during irinotecan therapy in metastatic colorectal patients.* Int J Colorectal Dis, 2004. **19**(6): p. 609-10.

154. Petit, R., M. Rothenberg, and E. Mitchell, *Cholinergic symptoms following CPT-11 infusion in a phase II multicenter trial of 250mg/m2 irinotecan (CPT-11) given every 2 weeks (abstract).* Proc Am Soc Clin Oncol, 1997. **16**: p. 268a.

155. Suzuki, T., H. Sakai, A. Ikari, and N. Takeguchi, *Inhibition of thromboxane A(2)-induced Cl(-) secretion by antidiarrhea drug loperamide in isolated rat colon.* J Pharmacol Exp Ther, 2000. **295**(1): p. 233-8.

156. Tobin, P.J., Y. Hong, J.P. Seale, L.P. Rivory, and A.J. McLachlan, *Loperamide inhibits the biliary excretion of irinotecan (CPT-11) in the rat isolated perfused liver.* J Pharm Pharmacol, 2005. **57**(1): p. 39-45.

157. Ratain, M., *Insights into the pharmacokinetics and pharmacodynamics of irinotecan.* Clin Cancer Res., 2000. **6**(9): p. 3393-4.

158. Gupta, E., A. Safa, X. Wang, and M. Ratain, *Pharmacokinetic modulation of irinotecan and metabolites by cyclosporin A.* Cancer Res., 1996. **56**(6): p. 1309-14.

159. Arimori, K., N. Kuroki, M. Hidaka, T. Iwakiri, K. Yamsaki, M. Okumura, H. Ono, N. Takamura, M. Kikuchi, and M. Nakano, *Effect of P-glycoprotein modulator, cyclosporin A, on the gastrointestinal excretion of irinotecan and its metabolite SN-38 in rats.* Pharm Res, 2003. **20**(6): p. 910-7.

160. Iyer, L., D. Hall, S. Das, M.A. Mortell, J. Ramirez, S. Kim, A. Di Rienzo, and M.J. Ratain, *Phenotype-genotype correlation of in vitro SN-38 (active metabolite of irinotecan) and bilirubin glucuronidation in human liver tissue with UGT1A1 promoter polymorphism.* Clin Pharmacol Ther, 1999. **65**(5): p. 576-82.

161. Chester, J.D., S.P. Joel, S.L. Cheeseman, G.D. Hall, M.S. Braun, J. Perry, T. Davis, C.J. Button, and M.T. Seymour, *Phase I and pharmacokinetic study of intravenous irinotecan plus oral ciclosporin in patients with fuorouracil-refractory metastatic colon cancer.* J Clin Oncol, 2003. **21**(6): p. 1125-32.

162. Innocenti, F., S.D. Undevia, J. Ramirez, S. Mani, R.L. Schilsky, N.J. Vogelzang, M. Prado, and M.J. Ratain, *A phase I trial of pharmacologic modulation of irinotecan with cyclosporine and phenobarbital.* Clin Pharmacol Ther, 2004. **76**(5): p. 490-502.

163. Govindarajan, R., *Irinotecan/thalidomide in metastatic colorectal cancer.* Oncology (Huntingt), 2002. **16**(4 Suppl 3): p. 23-6.

164. Govindarajan, R., *Irinotecan and thalidomide in metastatic colorectal cancer.* Oncology (Huntingt), 2000. **14**(12 Suppl 13): p. 29-32.

165. Govindarajan, R., K.M. Heaton, R. Broadwater, A. Zeitlin, N.P. Lang, and M. Hauer-Jensen, *Effect of thalidomide on gastrointestinal toxic effects of irinotecan.* Lancet, 2000. **356**(9229): p. 566-7.

166. Onn, A., J.E. Tseng, and R.S. Herbst, *Thalidomide, cyclooxygenase-2, and angiogenesis: potential for therapy.* Clin Cancer Res, 2001. **7**(11): p. 3311-3.

167. Zhao, J., L. Huang, N. Belmar, R. Buelow, and T. Fong, *Oral RDP58 allows CPT-11 dose intensification for enhanced tumor response by decreasing gastrointestinal toxicity.* Clin Cancer Res., 2004. **10**(8): p. 2851-9.

168. Shinohara, H., J.J. Killion, C.D. Bucana, S. Yano, and I.J. Fidler, *Oral administration of the immunomodulator JBT-3002 induces endogenous interleukin 15 in intestinal macrophages for protection against irinotecan-mediated destruction of intestinal epithelium.* Clin Cancer Res, 1999. **5**(8): p. 2148-56.

169. Cao, S., J.D. Black, A.B. Troutt, and Y.M. Rustum, *Interleukin 15 offers selective protection from irinotecan-induced intestinal toxicity in a preclinical animal model.* Cancer Res, 1998. **58**(15): p. 3270-4.

170. Reardon, D.A., J.A. Quinn, J. Vredenburgh, J.N. Rich, S. Gururangan, M. Badruddoja, J.E. Herndon, 2nd, J.M. Dowell, A.H. Friedman, and H.S. Friedman, *Phase II trial of irinotecan plus celecoxib in adults with recurrent malignant glioma.* Cancer, 2005. **103**(2): p. 329-38.

171. Barbounis, V., G. Koumakis, M. Vassilomanolakis, M. Demiri, and A.P. Efremidis, *Control of irinotecan-induced diarrhea by octreotide after loperamide failure.* Support Care Cancer, 2001. **9**(4): p. 258-60.

172. Pro, B., R. Lozano, and J.A. Ajani, *Therapeutic response to octreotide in patients with refractory CPT-11 induced diarrhea.* Invest New Drugs, 2001. **19**(4): p. 341-3.

173. Maeda, Y., T. Ohune, M. Nakamura, M. Yamasaki, Y. Kiribayashi, and T. Murakami, *Prevention of irinotecan-induced diarrhoea by oral carbonaceous adsorbent (Kremezin) in cancer patients.* Oncol Rep, 2004. **12**(3): p. 581-5.

174. Michael, M., M. Brittain, J. Nagai, R. Feld, D. Hedley, A. Oza, L. Siu, and M.J. Moore, *Phase II study of activated charcoal to prevent irinotecan-induced diarrhea.* J Clin Oncol, 2004. **22**(21): p. 4410-7.

175. Hardman, W.E., M.P. Moyer, and I.L. Cameron, *Fish oil supplementation enhanced CPT-11 (irinotecan) efficacy against MCF7 breast carcinoma xenografts and ameliorated intestinal side-effects.* Br J Cancer, 1999. **81**(3): p. 440-8.

176. Chowbay, B., A. Sharma, Q.Y. Zhou, Y.B. Cheung, and E.J. Lee, *The modulation of irinotecan-induced diarrhoea and pharmacokinetics by three different classes of pharmacologic agents.* Oncol Rep, 2003. **10**(3): p. 745-51.

177. Mathijssen, R.H., J. Verweij, P. de Bruijn, W.J. Loos, and A. Sparreboom, *Effects of St. John's wort on irinotecan metabolism.* J Natl Cancer Inst, 2002. **94**(16): p. 1247-9.

178. Parman, T., M.J. Wiley, and P.G. Wells, *Free radical-mediated oxidative DNA damage in the mechanism of thalidomide teratogenicity.* Nat Med, 1999. **5**(5): p. 582-5.

179. Eriksson, T., S. Bjorkman, A. Fyge, and H. Ekberg, *Determination of thalidomide in plasma and blood by high-performance liquid chromatography: avoiding hydrolytic degradation.* J Chromatogr, 1992. **582**(1-2): p. 211-6.

180. Reiriz, A.B., M.F. Richter, S. Fernandes, A.I. Cancela, T.D. Costa, L.P. Di Leone, and G. Schwartsmann, *Phase II study of thalidomide in patients with metastatic malignant melanoma.* Melanoma Res, 2004. **14**(6): p. 527-31.

181. Raza, A., P. Meyer, D. Dutt, F. Zorat, L. Lisak, F. Nascimben, M. du Randt, C. Kaspar, C. Goldberg, J. Loew, S. Dar, S. Gezer, P. Venugopal, and J. Zeldis, *Thalidomide produces transfusion independence in long-standing refractory anemias of patients with myelodysplastic syndromes.* Blood, 2001. **98**(4): p. 958-65.

182. Kaufmann, H., M. Raderer, S. Wohrer, A. Puspok, A. Bankier, C. Zielinski, A. Chott, and J. Drach, *Antitumor activity of rituximab plus thalidomide in patients with relapsed/refractory mantle cell lymphoma.* Blood, 2004. **104**(8): p. 2269-71.

183. Fine, H.A., P.Y. Wen, E.A. Maher, E. Viscosi, T. Batchelor, N. Lakhani, W.D. Figg, B.W. Purow, and C.B. Borkowf, *Phase II trial of thalidomide and carmustine for patients with recurrent high-grade gliomas.* J Clin Oncol, 2003. **21**(12): p. 2299-304.

184. Amato, R.J., *Thalidomide therapy for renal cell carcinoma.* Crit Rev Oncol Hematol, 2003. **46 Suppl**: p. S59-65.

185.   Hwu, W.J., S.E. Krown, J.H. Menell, K.S. Panageas, J. Merrell, L.A. Lamb, L.J. Williams, C.J. Quinn, T. Foster, P.B. Chapman, P.O. Livingston, J.D. Wolchok, and A.N. Houghton, *Phase II study of temozolomide plus thalidomide for the treatment of metastatic melanoma.* J Clin Oncol, 2003. **21**(17): p. 3351-6.

186.   Dahut, W.L., J.L. Gulley, P.M. Arlen, Y. Liu, K.M. Fedenko, S.M. Steinberg, J.J. Wright, H. Parnes, C.C. Chen, E. Jones, C.E. Parker, W.M. Linehan, and W.D. Figg, *Randomized phase II trial of docetaxel plus thalidomide in androgen-independent prostate cancer.* J Clin Oncol, 2004. **22**(13): p. 2532-9.

187.   Singhal, S., J. Mehta, R. Desikan, D. Ayers, P. Roberson, P. Eddlemon, N. Munshi, E. Anaissie, C. Wilson, M. Dhodapkar, J. Zeddis, and B. Barlogie, *Antitumor activity of thalidomide in refractory multiple myeloma.* N Engl J Med, 1999. **341**(21): p. 1565-71.

188.   Glasmacher, A. and M. von Lilienfeld-Toal, *The current status of thalidomide in the management of multiple myeloma.* Acta Haematol, 2005. **114 Suppl 1**: p. 3-7.

189.   Boccadoro, M., J. Blade, M. Attal, and A. Palumbo, *The future role of thalidomide in multiple myeloma.* Acta Haematol, 2005. **114 Suppl 1**: p. 18-22.

190.   Barlogie, B., R. Desikan, P. Eddlemon, T. Spencer, J. Zeldis, N. Munshi, A. Badros, M. Zangari, E. Anaissie, J. Epstein, J. Shaughnessy, D. Ayers, D. Spoon, and G. Tricot, *Extended survival in advanced and refractory multiple myeloma after single-agent thalidomide: identification of prognostic factors in a phase 2 study of 169 patients.* Blood, 2001. **98**(2): p. 492-4.

191.   Cavo, M., E. Zamagni, P. Tosi, C. Cellini, D. Cangini, P. Tacchetti, N. Testoni, M. Tonelli, A. de Vivo, G. Palareti, S. Tura, and M. Baccarani, *First-line therapy with thalidomide and dexamethasone in preparation for autologous stem cell transplantation for multiple myeloma.* Haematologica, 2004. **89**(7): p. 826-31.

192.   Schwartzman, R.J., E. Chevlen, and K. Bengtson, *Thalidomide has activity in treating complex regional pain syndrome.* Arch Intern Med, 2003. **163**(12): p. 1487-8; author reply 1488.

193.   Vogelsang, G.B., E.R. Farmer, A.D. Hess, V. Altamonte, W.E. Beschorner, D.A. Jabs, R.L. Corio, L.S. Levin, O.M. Colvin, and J.R. Wingard, *Thalidomide for the treatment of chronic graft-versus-host disease.* N Engl J Med, 1992. **326**(16): p. 1055-8.

194.   Strupp, C., U. Germing, M. Aivado, E. Misgeld, R. Haas, and N. Gattermann, *Thalidomide for the treatment of patients with myelodysplastic syndromes.* Leukemia, 2002. **16**(1): p. 1-6.

195.   Sharpstone, D., A. Rowbottom, N. Francis, G. Tovey, D. Ellis, M. Barrett, and B. Gazzard, *Thalidomide: a novel therapy for microsporidiosis.* Gastroenterology, 1997. **112**(6): p. 1823-9.

196.   Facchini, S., M. Candusso, S. Martelossi, M. Liubich, E. Panfili, and A. Ventura, *Efficacy of long-term treatment with thalidomide in children and young adults with Crohn disease: preliminary results.* J Pediatr Gastroenterol Nutr, 2001. **32**(2): p. 178-81.

197.   Wines, N.Y., A.J. Cooper, and M.P. Wines, *Thalidomide in dermatology.* Australas J Dermatol, 2002. **43**(4): p. 229-38; quiz 239-40.

198. Elaraj, D.M., D.E. White, S.M. Steinberg, L. Haworth, S.A. Rosenberg, and J.C. Yang, *A pilot study of antiangiogenic therapy with bevacizumab and thalidomide in patients with metastatic renal cell carcinoma.* J Immunother, 2004. **27**(4): p. 259-64.

199. Hada, M. and K. Mizutari, *[A case of advanced pancreatic cancer with remarkable response to thalidomide, celecoxib and gemcitabine].* Gan To Kagaku Ryoho, 2004. **31**(6): p. 959-61.

200. Singhal, S. and J. Mehta, *Thalidomide in cancer.* Biomed Pharmacother, 2002. **56**(1): p. 4-12.

201. Sleijfer, S., W.H. Kruit, and G. Stoter, *Thalidomide in solid tumours: the resurrection of an old drug.* Eur J Cancer, 2004. **40**(16): p. 2377-82.

202. Marriott, J.B., I.A. Clarke, K. Dredge, G. Muller, D. Stirling, and A.G. Dalgleish, *Thalidomide and its analogues have distinct and opposing effects on TNF-alpha and TNFR2 during co-stimulation of both CD4(+) and CD8(+) T cells.* Clin Exp Immunol, 2002. **130**(1): p. 75-84.

203. Keifer, J.A., D.C. Guttridge, B.P. Ashburner, and A.S. Baldwin, Jr., *Inhibition of NF-kappa B activity by thalidomide through suppression of IkappaB kinase activity.* J Biol Chem, 2001. **276**(25): p. 22382-7.

204. Marriott, J.B., I.A. Clarke, A. Czajka, K. Dredge, K. Childs, H.W. Man, P. Schafer, S. Govinda, G.W. Muller, D.I. Stirling, and A.G. Dalgleish, *A novel subclass of thalidomide analogue with anti-solid tumor activity in which caspase-dependent apoptosis is associated with altered expression of bcl-2 family proteins.* Cancer Res, 2003. **63**(3): p. 593-9.

205. Moreira, A.L., E.P. Sampaio, A. Zmuidzinas, P. Frindt, K.A. Smith, and G. Kaplan, *Thalidomide exerts its inhibitory action on tumor necrosis factor alpha by enhancing mRNA degradation.* J Exp Med, 1993. **177**(6): p. 1675-80.

206. McHugh, S.M., I.R. Rifkin, J. Deighton, A.B. Wilson, P.J. Lachmann, C.M. Lockwood, and P.W. Ewan, *The immunosuppressive drug thalidomide induces T helper cell type 2 (Th2) and concomitantly inhibits Th1 cytokine production in mitogen- and antigen-stimulated human peripheral blood mononuclear cell cultures.* Clin Exp Immunol, 1995. **99**(2): p. 160-7.

207. Moreira, A.L., L. Tsenova-Berkova, J. Wang, P. Laochumroonvorapong, S. Freeman, V.H. Freedman, and G. Kaplan, *Effect of cytokine modulation by thalidomide on the granulomatous response in murine tuberculosis.* Tuber Lung Dis, 1997. **78**(1): p. 47-55.

208. Moller, D.R., M. Wysocka, B.M. Greenlee, X. Ma, L. Wahl, D.A. Flockhart, G. Trinchieri, and C.L. Karp, *Inhibition of IL-12 production by thalidomide.* J Immunol, 1997. **159**(10): p. 5157-61.

209. Walchner, M., M. Meurer, G. Plewig, and G. Messer, *Clinical and immunologic parameters during thalidomide treatment of lupus erythematosus.* Int J Dermatol, 2000. **39**(5): p. 383-8.

210. D'Amato, R.J., M.S. Loughnan, E. Flynn, and J. Folkman, *Thalidomide is an inhibitor of angiogenesis.* Proc Natl Acad Sci U S A, 1994. **91**(9): p. 4082-5.

211. Sampaio, E.P., E.N. Sarno, R. Galilly, Z.A. Cohn, and G. Kaplan, *Thalidomide selectively inhibits tumor necrosis factor alpha production by stimulated human monocytes.* J Exp Med, 1991. **173**(3): p. 699-703.

212. Kedar, I., W. Mermershtain, and H. Ivgi, *Thalidomide reduces serum C-reactive protein and interleukin-6 and induces response to IL-2 in a fraction of metastatic renal cell cancer patients who failed IL-2-based therapy.* Int J Cancer, 2004. **110**(2): p. 260-5.

213. Fujita, J., J.R. Mestre, J.B. Zeldis, K. Subbaramaiah, and A.J. Dannenberg, *Thalidomide and its analogues inhibit lipopolysaccharide-mediated Iinduction of cyclooxygenase-2.* Clin Cancer Res, 2001. **7**(11): p. 3349-55.

214. Folkman, J. and M. Klagsbrun, *Angiogenic factors.* Science, 1987. **235**(4787): p. 442-7.

215. Cross, M.J. and L. Claesson-Welsh, *FGF and VEGF function in angiogenesis: signalling pathways, biological responses and therapeutic inhibition.* Trends Pharmacol Sci, 2001. **22**(4): p. 201-7.

216. Klement, G., S. Baruchel, J. Rak, S. Man, K. Clark, D.J. Hicklin, P. Bohlen, and R.S. Kerbel, *Continuous low-dose therapy with vinblastine and VEGF receptor-2 antibody induces sustained tumor regression without overt toxicity.* J Clin Invest, 2000. **105**(8): p. R15-24.

217. Schiller, J.H. and G. Bittner, *Potentiation of platinum antitumor effects in human lung tumor xenografts by the angiogenesis inhibitor squalamine: effects on tumor neovascularization.* Clin Cancer Res, 1999. **5**(12): p. 4287-94.

218. Merchant, J.J., K. Kim, M.P. Mehta, G.H. Ripple, M.L. Larson, D.J. Brophy, L.C. Hammes, and J.H. Schiller, *Pilot and safety trial of carboplatin, paclitaxel, and thalidomide in advanced non small-cell lung cancer.* Clin Lung Cancer, 2000. **2**(1): p. 48-52; discussion 53-4.

219. Teicher, B.A., E.A. Sotomayor, and Z.D. Huang, *Antiangiogenic agents potentiate cytotoxic cancer therapies against primary and metastatic disease.* Cancer Res, 1992. **52**(23): p. 6702-4.

220. Boehm, T., J. Folkman, T. Browder, and M.S. O'Reilly, *Antiangiogenic therapy of experimental cancer does not induce acquired drug resistance.* Nature, 1997. **390**(6658): p. 404-7.

221. Chen, T.L., G.B. Vogelsang, B.G. Petty, R.B. Brundrett, D.A. Noe, G.W. Santos, and O.M. Colvin, *Plasma pharmacokinetics and urinary excretion of thalidomide after oral dosing in healthy male volunteers.* Drug Metab Dispos, 1989. **17**(4): p. 402-5.

222. Piscitelli, S.C., W.D. Figg, B. Hahn, G. Kelly, S. Thomas, and R.E. Walker, *Single-dose pharmacokinetics of thalidomide in human immunodeficiency virus-infected patients.* Antimicrob Agents Chemother, 1997. **41**(12): p. 2797-9.

223. Teo, S.K., W.A. Colburn, and S.D. Thomas, *Single-dose oral pharmacokinetics of three formulations of thalidomide in healthy male volunteers.* J Clin Pharmacol, 1999. **39**(11): p. 1162-8.

224. Eriksson, T., S. Bjorkman, and P. Hoglund, *Clinical pharmacology of thalidomide.* Eur J Clin Pharmacol, 2001. **57**(5): p. 365-76.

225. Figg, W.D., S. Raje, K.S. Bauer, A. Tompkins, D. Venzon, R. Bergan, A. Chen, M. Hamilton, J. Pluda, and E. Reed, *Pharmacokinetics of thalidomide in an elderly prostate cancer population.* J Pharm Sci, 1999. **88**(1): p. 121-5.

226. Braun, A.G., F.A. Harding, and S.L. Weinreb, *Teratogen metabolism: thalidomide activation is mediated by cytochrome P-450.* Toxicol Appl Pharmacol, 1986. **82**(1): p. 175-9.

227.	Eriksson, T., S. Bjorkman, B. Roth, and P. Hoglund, *Intravenous formulations of the enantiomers of thalidomide: pharmacokinetic and initial pharmacodynamic characterization in man.* J Pharm Pharmacol, 2000. **52**(7): p. 807-17.

228.	Eriksson, T., P. Hoglund, I. Turesson, A. Waage, B.R. Don, J. Vu, M. Scheffler, and G.A. Kaysen, *Pharmacokinetics of thalidomide in patients with impaired renal function and while on and off dialysis.* J Pharm Pharmacol, 2003. **55**(12): p. 1701-6.

229.	Hoglund, P., T. Eriksson, and S. Bjorkman, *A double-blind study of the sedative effects of the thalidomide enantiomers in humans.* J Pharmacokinet Biopharm, 1998. **26**(4): p. 363-83.

230.	Gunzler, V., *Thalidomide in human immunodeficiency virus (HIV) patients. A review of safety considerations.* Drug Saf, 1992. **7**(2): p. 116-34.

231.	Wulff, C.H., H. Hoyer, G. Asboe-Hansen, and H. Brodthagen, *Development of polyneuropathy during thalidomide therapy.* Br J Dermatol, 1985. **112**(4): p. 475-80.

232.	Neubert, D., *Never-ending tales of the mode of the teratogenic action of thalidomide.* Teratog Carcinog Mutagen, 1997. **17**(1): p. i-ii.

233.	Linde, K., C.D. Mulrow, M. Berner, and M. Egger, *St John's wort for depression.* Cochrane Database Syst Rev, 2005(2): p. CD000448.

234.	Butterweck, V., *Mechanism of action of St John's wort in depression : what is known?* CNS Drugs, 2003. **17**(8): p. 539-62.

235.	Tedeschi, E., M. Menegazzi, D. Margotto, H. Suzuki, U. Forstermann, and H. Kleinert, *Anti-inflammatory actions of St. John's wort: inhibition of human inducible nitric-oxide synthase expression by down-regulating signal transducer and activator of transcription-1alpha (STAT-1alpha) activation.* J Pharmacol Exp Ther, 2003. **307**(1): p. 254-61.

236.	Barnes, J., L.A. Anderson, and J.D. Phillipson, *St John's wort (Hypericum perforatum L.): a review of its chemistry, pharmacology and clinical properties.* J Pharm Pharmacol, 2001. **53**(5): p. 583-600.

237.	Bork, P.M., S. Bacher, M.L. Schmitz, U. Kaspers, and M. Heinrich, *Hypericin as a non-antioxidant inhibitor of NF-kappa B.* Planta Med, 1999. **65**(4): p. 297-300.

238.	Raso, G.M., M. Pacilio, G. Di Carlo, E. Esposito, L. Pinto, and R. Meli, *In-vivo and in-vitro anti-inflammatory effect of Echinacea purpurea and Hypericum perforatum.* J Pharm Pharmacol, 2002. **54**(10): p. 1379-83.

239.	Agostinis, P., A. Donella-Deana, J. Cuveele, A. Vandenbogaerde, S. Sarno, W. Merlevede, and P. de Witte, *A comparative analysis of the photosensitized inhibition of growth-factor regulated protein kinases by hypericin-derivatives.* Biochem Biophys Res Commun, 1996. **220**(3): p. 613-7.

240.	Chibowska, M., D. Krasowska, and J. Weglarz, *Pentoxyfilline treatment does not influence the plasma levels of IL-2 and sIL-2R in limited scleroderma patients.* Med Sci Monit, 2001. **7**(2): p. 282-8.

241.	Fiebich, B.L., A. Hollig, and K. Lieb, *Inhibition of substance P-induced cytokine synthesis by St. John's wort extracts.* Pharmacopsychiatry, 2001. **34 Suppl 1**: p. S26-8.

242.	Dona, M., I. Dell'Aica, E. Pezzato, L. Sartor, F. Calabrese, M. Della Barbera, A. Donella-Deana, G. Appendino, A. Borsarini, R. Caniato, and

S. Garbisa, *Hyperforin inhibits cancer invasion and metastasis.* Cancer Res, 2004. **64**(17): p. 6225-32.

243. Takahashi, I., S. Nakanishi, E. Kobayashi, H. Nakano, K. Suzuki, and T. Tamaoki, *Hypericin and pseudohypericin specifically inhibit protein kinase C: possible relation to their antiretroviral activity.* Biochem Biophys Res Commun, 1989. **165**(3): p. 1207-12.

244. Thomas, C. and R.S. Pardini, *Oxygen dependence of hypericin-induced phototoxicity to EMT6 mouse mammary carcinoma cells.* Photochem Photobiol, 1992. **55**(6): p. 831-7.

245. Martarelli, D., B. Martarelli, D. Pediconi, M.I. Nabissi, M. Perfumi, and P. Pompei, *Hypericum perforatum methanolic extract inhibits growth of human prostatic carcinoma cell line orthotopically implanted in nude mice.* Cancer Lett, 2004. **210**(1): p. 27-33.

246. Miccoli, L., A. Beurdeley-Thomas, G. De Pinieux, F. Sureau, S. Oudard, B. Dutrillaux, and M.F. Poupon, *Light-induced photoactivation of hypericin affects the energy metabolism of human glioma cells by inhibiting hexokinase bound to mitochondria.* Cancer Res, 1998. **58**(24): p. 5777-86.

247. Durr, D., B. Stieger, G.A. Kullak-Ublick, K.M. Rentsch, H.C. Steinert, P.J. Meier, and K. Fattinger, *St John's Wort induces intestinal P-glycoprotein/MDR1 and intestinal and hepatic CYP3A4.* Clin Pharmacol Ther, 2000. **68**(6): p. 598-604.

248. Hennessy, M., D. Kelleher, J.P. Spiers, M. Barry, P. Kavanagh, D. Back, F. Mulcahy, and J. Feely, *St Johns wort increases expression of P-glycoprotein: implications for drug interactions.* Br J Clin Pharmacol, 2002. **53**(1): p. 75-82.

249. Wang, Z., M.A. Hamman, S.M. Huang, L.J. Lesko, and S.D. Hall, *Effect of St John's wort on the pharmacokinetics of fexofenadine.* Clin Pharmacol Ther, 2002. **71**(6): p. 414-20.

250. Izzo, A.A., *Drug interactions with St. John's Wort (Hypericum perforatum): a review of the clinical evidence.* Int J Clin Pharmacol Ther, 2004. **42**(3): p. 139-48.

251. Schulz, V., *Incidence and clinical relevance of the interactions and side effects of Hypericum preparations.* Phytomedicine, 2001. **8**(2): p. 152-60.

252. Schulz, V., *[Incidence and clinical relevance of interactions and side-effects of hypericum preparations].* Schweiz Rundsch Med Prax, 2000. **89**(50): p. 2131-40.

253. Hwang, J.J., S.G. Eisenberg, and J.L. Marshall, *Improving the toxicity of irinotecan/5-FU/leucovorin: a 21-day schedule.* Oncology (Huntingt), 2003. **17**(9 Suppl 8): p. 37-43.

254. Dranitsaris, G., J. Maroun, and A. Shah, *Severe chemotherapy-induced diarrhea in patients with colorectal cancer: a cost of illness analysis.* Support Care Cancer, 2004.

255. Allegrini, G., A. Di Paolo, E. Cerri, S. Cupini, F. Amatori, G. Masi, R. Danesi, L. Marcucci, G. Bocci, M. Del Tacca, and A. Falcone, *Irinotecan in combination with thalidomide in patients with advanced solid tumors: a clinical study with pharmacodynamic and pharmacokinetic evaluation.* Cancer Chemother Pharmacol, 2006: p. 585-93.

256. Tchekmedyian, N.S., *Thalidomide and irinotecan-associated diarrhea.* Am J Clin Oncol, 2002. **25**(3): p. 324.

257. Itoh, T., S. Itagaki, K. Sasaki, T. Hirano, I. Takemoto, and K. Iseki, *Pharmacokinetic modulation of irinotecan metabolites by sulphobromophthalein in rats*. J Pharm Pharmacol, 2004. **56**(6): p. 809-12.

258. Aviles, A., M.J. Nambo, N. Neri, E. Murillo, C. Castaneda, S. Cleto, A. Talavera, and M. Gonzalez, *Biological modifiers as cytoreductive therapy before stem cell transplant in previously untreated patientswith multiple myeloma*. Ann Oncol, 2005. **16**(2): p. 219-21.

259. Candoni, A., A. Raza, F. Silvestri, L. Lisak, N. Galili, M. Mumtaz, F. Kikic, and R. Fanin, *Response rate and survival after thalidomide-based therapy in 248 patients with myelodysplastic syndromes*. Ann Hematol, 2005. **84**(7): p. 479-81.

260. Patt, Y.Z., M.M. Hassan, R.D. Lozano, A.K. Nooka, Schnirer, II, J.B. Zeldis, J.L. Abbruzzese, and T.D. Brown, *Thalidomide in the treatment of patients with hepatocellular carcinoma*. Cancer, 2005. **103**(4): p. 749-55.

261. Wu, K.L., H.H. Helgason, B. van der Holt, P.W. Wijermans, H.M. Lokhorst, W.M. Smit, and P. Sonneveld, *Analysis of efficacy and toxicity of thalidomide in 122 patients with multiple myeloma: response of soft-tissue plasmacytomas*. Leukemia, 2005. **19**(1): p. 143-5.

262. Franks, M.E., G.R. Macpherson, and W.D. Figg, *Thalidomide*. Lancet, 2004. **363**(9423): p. 1802-11.

263. Royce, M.E., D. Medgyesy, T.H. Zukowski, S. Dwivedy, P.M. Hoff, and R. Pazdur, *Colorectal cancer: chemotherapy treatment overview*. Oncology (Huntingt), 2000. **14**(12 Suppl 14): p. 40-6.

264. Heere-Ress, E., J. Boehm, C. Thallinger, C. Hoeller, V. Wacheck, P. Birner, K. Wolff, H. Pehamberger, and B. Jansen, *Thalidomide enhances the anti-tumor activity of standard chemotherapy in a human melanoma xenotransplatation model*. J Invest Dermatol, 2005. **125**(2): p. 201-6.

265. Fujii, T., M. Tachibana, D.K. Dhar, S. Ueda, S. Kinugasa, H. Yoshimura, H. Kohno, and N. Nagasue, *Combination therapy with paclitaxel and thalidomide inhibits angiogenesis and growth of human colon cancer xenograft in mice*. Anticancer Res, 2003. **23**(3B): p. 2405-11.

266. Verheul, H.M., D. Panigrahy, J. Yuan, and R.J. D'Amato, *Combination oral antiangiogenic therapy with thalidomide and sulindac inhibits tumour growth in rabbits*. Br J Cancer, 1999. **79**(1): p. 114-8.

267. Ding, Q., P. Kestell, B.C. Baguley, B.D. Palmer, J.W. Paxton, G. Muller, and L.M. Ching, *Potentiation of the antitumour effect of cyclophosphamide in mice by thalidomide*. Cancer Chemother Pharmacol, 2002. **50**(3): p. 186-92.

268. Hovenga, S., S.M. Daenen, J.T. de Wolf, G.W. van Imhoff, H.C. Kluin-Nelemans, W.J. Sluiter, and E. Vellenga, *Combined thalidomide and cyclophosphamide treatment for refractory or relapsed multiple myeloma patients: a prospective phase II study*. Ann Hematol, 2004.

269. Hwu, W.J., E. Lis, J.H. Menell, K.S. Panageas, L.A. Lamb, J. Merrell, L.J. Williams, S.E. Krown, P.B. Chapman, P.O. Livingston, J.D. Wolchok, and A.N. Houghton, *Temozolomide plus thalidomide in patients with brain metastases from melanoma: a phase II study*. Cancer, 2005. **103**(12): p. 2590-7.

270. Zhu, A.X., C.S. Fuchs, J.W. Clark, A. Muzikansky, K. Taylor, S. Sheehan, K. Tam, E. Yung, M.H. Kulke, and D.P. Ryan, *A phase II study of*

epirubicin and thalidomide in unresectable or metastatic hepatocellular carcinoma. Oncologist, 2005. **10**(6): p. 392-8.

271. Hwu, W.J., S.E. Krown, K.S. Panageas, J.H. Menell, P.B. Chapman, P.O. Livingston, L.J. Williams, C.J. Quinn, and A.N. Houghton, *Temozolomide plus thalidomide in patients with advanced melanoma: results of a dose-finding trial.* J Clin Oncol, 2002. **20**(11): p. 2610-5.

272. Terpos, E., D. Mihou, R. Szydlo, K. Tsimirika, C. Karkantaris, M. Politou, E. Voskaridou, A. Rahemtulla, M.A. Dimopoulos, and K. Zervas, *The combination of intermediate doses of thalidomide with dexamethasone is an effective treatment for patients with refractory/relapsed multiple myeloma and normalizes abnormal bone remodeling, through the reduction of sRANKL/osteoprotegerin ratio.* Leukemia, 2005. **19**(11): p. 1969-76.

273. Kerst, J.M., A. Bex, H. Mallo, L. Dewit, J.B. Haanen, W. Boogerd, H.J. Teertstra, and G.C. de Gast, *Prolonged low dose IL-2 and thalidomide in progressive metastatic renal cell carcinoma with concurrent radiotherapy to bone and/or soft tissue metastasis: a phase II study.* Cancer Immunol Immunother, 2005. **54**(9): p. 926-31.

274. Hernberg, M., P. Virkkunen, P. Bono, H. Ahtinen, H. Maenpaa, and H. joensuu, *Interferon alfa-2b three times daily and thalidomide in the treatment of metastatic renal cell carcinoma.* J Clin Oncol, 2003. **21**(20): p. 3770-6.

275. Villalona-Calero, M., L. Schaaf, G. Phillips, G. Otterson, K. Panico, W. Duan, B. Kleiber, M. Shah, D. Young, W.H. Wu, and J. Kuhn, *Thalidomide and celecoxib as potential modulators of irinotecan's activity in cancer patients.* Cancer Chemother Pharmacol, 2007. **59**(1): p. 23-33.

276. Goto, S., T. Okutomi, Y. Suma, J. Kera, G. Soma, and S. Takeuchi, *Induction of tumor necrosis factor by a camptothecin derivative, irinotecan, in mice and human mononuclear cells.* Anticancer Res, 1996. **16**(5A): p. 2507-11.

277. Sonis, S.T., *The pathobiology of mucositis.* Nat Rev Cancer, 2004. **4**(4): p. 277-84.

278. Marini, M., G. Bamias, J. Rivera-Nieves, C.A. Moskaluk, S.B. Hoang, W.G. Ross, T.T. Pizarro, and F. Cominelli, *TNF-alpha neutralization ameliorates the severity of murine Crohn's-like ileitis by abrogation of intestinal epithelial cell apoptosis.* Proc Natl Acad Sci U S A, 2003. **100**(14): p. 8366-71.

279. Fernandez-Martinez, E., M.S. Morales-Rios, V. Perez-Alvarez, and P. Muriel, *Immunomodulatory effects of thalidomide analogs on LPS-induced plasma and hepatic cytokines in the rat.* Biochem Pharmacol, 2004. **68**(7): p. 1321-9.

280. Schneider, J., W. Bruckmann, and K. Zwingenberger, *Extravasation of leukocytes assessed by intravital microscopy: effect of thalidomide.* Inflamm Res, 1997. **46**(10): p. 392-7.

281. Farese, J.P., L.E. Fox, C.J. Detrisac, J.M. Van Gilder, S.L. Roberts, and J.M. Baldwin, *Effect of thalidomide on growth and metastasis of canine osteosarcoma cells after xenotransplantation in athymic mice.* Am J Vet Res, 2004. **65**(5): p. 659-64.

282. Kruschewski, M., T. Foitzik, A. Perez-Canto, A. Hubotter, and H.J. Buhr, *Changes of colonic mucosal microcirculation and histology in two colitis*

models: an experimental study using intravital microscopy and a new histological scoring system. Dig Dis Sci, 2001. **46**(11): p. 2336-43.

283. Bradford, M.M., *A rapid and sensitive method for the quantitation of microgram quantities of protein utilizing the principle of protein-dye binding.* Anal Biochem, 1976. **72**: p. 248-54.

284. Miampamba, M., E.J. Parr, D.M. McCafferty, J.L. Wallace, and K.A. Sharkey, *Effect of intracolonic benzalkonium chloride on trinitrobenzene sulphonic acid-induced colitis in the rat.* Aliment Pharmacol Ther, 1998. **12**(3): p. 219-28.

285. Thompson, C., *Thalidomide effective for AIDS-related oral ulcers.* Lancet, 1995. **346**(8985): p. 1289.

286. Zhao, J., L. Huang, N. Belmar, R. Buelow, and T. Fong, *Optimal antidiarrhea treatment for antitumor agent irinotecan hydrochloride (CPT-11)-induced delayed diarrhea.* Clin Cancer Res, 2004. **10**(8): p. 2851-9.

287. Dinarello, C.A., *Interleukin-1 and interleukin-1 antagonism.* Blood, 1991. **77**(8): p. 1627-52.

288. Brennan, F.M., D. Chantry, A. Jackson, R. Maini, and M. Feldmann, *Inhibitory effect of TNF alpha antibodies on synovial cell interleukin-1 production in rheumatoid arthritis.* Lancet, 1989. **2**(8657): p. 244-7.

289. Charles, P., M.J. Elliott, D. Davis, A. Potter, J.R. Kalden, C. Antoni, F.C. Breedveld, J.S. Smolen, G. Eberl, K. deWoody, M. Feldmann, and R.N. Maini, *Regulation of cytokines, cytokine inhibitors, and acute-phase proteins following anti-TNF-alpha therapy in rheumatoid arthritis.* J Immunol, 1999. **163**(3): p. 1521-8.

290. Ando, Y., E. Fuse, and W.D. Figg, *Thalidomide metabolism by the CYP2C subfamily.* Clin Cancer Res, 2002. **8**(6): p. 1964-73.

291. Lu, J., B.D. Palmer, P. Kestell, P. Browett, B.C. Baguley, G. Muller, and L.M. Ching, *Thalidomide metabolites in mice and patients with multiple myeloma.* Clin Cancer Res, 2003. **9**(5): p. 1680-8.

292. Kestell, P., L. Zhao, B.C. Baguley, B.D. Palmer, G. Muller, J.W. Paxton, and L.M. Ching, *Modulation of the pharmacokinetics of the antitumour agent 5,6-dimethylxanthenone-4-acetic acid (DMXAA) in mice by thalidomide.* Cancer Chemother Pharmacol, 2000. **46**(2): p. 135-41.

293. Pollard, M. and J. McGivan, *The rat hepatoma cell line H4-II-E-C3 expresses high activities of the high-affinity glutamate transporter GLT-1A.* FEBS Lett, 2000. **484**(2): p. 74-6.

294. Jones, T.R., R. Zamboni, M. Belley, E. Champion, L. Charette, A.W. Ford-Hutchinson, R. Frenette, J.Y. Gauthier, S. Leger, and P. Masson, *Pharmacology of L-660,711 (MK-571): a novel potent and selective leukotriene D4 receptor antagonist.* Can J Physiol Pharmacol, 1989. **67**(1): p. 17-28.

295. Sasaki, Y., H. Hakusui, S. Mizuno, M. Morita, T. Miya, K. Eguchi, T. Shinkai, T. Tamura, Y. Ohe, and N. Saijo, *A pharmacokinetic and pharmacodynamic analysis of CPT-11 and its active metabolite SN-38.* Jpn J Cancer Res, 1995. **86**(1): p. 101-10.

296. Charasson, V., M.C. Haaz, and J. Robert, *Determination of drug interactions occurring with the metabolic pathways of irinotecan.* Drug Metab Dispos, 2002. **30**(6): p. 731-3.

297. Teo, S.K., P.J. Sabourin, K. O'Brien, K.A. Kook, and S.D. Thomas, *Metabolism of thalidomide in human microsomes, cloned human cytochrome P-450 isozymes, and Hansen's disease patients.* J Biochem Mol Toxicol, 2000. **14**(3): p. 140-7.

298. Birdsall, T.C., *St. John's wort and irinotecan-induced diarrhea.* Toxicol Appl Pharmacol, 2007. **220**(1): p. 108; author reply 109-10.

299. Blank, M., M. Mandel, Y. Keisari, D. Meruelo, and G. Lavie, *Enhanced ubiquitinylation of heat shock protein 90 as a potential mechanism for mitotic cell death in cancer cells induced with hypericin.* Cancer Res, 2003. **63**(23): p. 8241-7.

300. Chen, B., T. Roskams, Y. Xu, P. Agostinis, and P.A. de Witte, *Photodynamic therapy with hypericin induces vascular damage and apoptosis in the RIF-1 mouse tumor model.* Int J Cancer, 2002. **98**(2): p. 284-90.

301. Chen, B., Y. Xu, T. Roskams, E. Delaey, P. Agostinis, J.R. Vandenheede, and P. de Witte, *Efficacy of antitumoral photodynamic therapy with hypericin: relationship between biodistribution and photodynamic effects in the RIF-1 mouse tumor model.* Int J Cancer, 2001. **93**(2): p. 275-82.

302. Meltzer-Brody, S.E., *St. John's Wort: Clinical Status in Psychiatry.* CNS Spectr, 2001. **6**(10): p. 835-40.

303. Kobak, K.A., L.V. Taylor, G. Warner, and R. Futterer, *St. John's wort versus placebo in social phobia: results from a placebo-controlled pilot study.* J Clin Psychopharmacol, 2005. **25**(1): p. 51-8.

304. Rezvani, A.H., D.H. Overstreet, Y. Yang, and E. Clark, Jr., *Attenuation of alcohol intake by extract of Hypericum perforatum (St. John's Wort) in two different strains of alcohol-preferring rats.* Alcohol Alcohol, 1999. **34**(5): p. 699-705.

305. Shibayama, Y., R. Ikeda, T. Motoya, and K. Yamada, *St. John's Wort (Hypericum perforatum) induces overexpression of multidrug resistance protein 2 (MRP2) in rats: a 30-day ingestion study.* Food Chem Toxicol, 2004. **42**(6): p. 995-1002.

306. Winkler, C., B. Wirleitner, K. Schroecksnadel, H. Schennach, and D. Fuchs, *St. John's wort (Hypericum perforatum) counteracts cytokine-induced tryptophan catabolism in vitro.* Biol Chem, 2004. **385**(12): p. 1197-202.

307. Ishikawa, Y. and M. Kitamura, *Bioflavonoid quercetin inhibits mitosis and apoptosis of glomerular cells in vitro and in vivo.* Biochem Biophys Res Commun, 2000. **279**(2): p. 629-34.

308. Lavie, G., D. Meruelo, K. Aroyo, and M. Mandel, *Inhibition of the CD8+ T cell-mediated cytotoxicity reaction by hypericin: potential for treatment of T cell-mediated diseases.* Int Immunol, 2000. **12**(4): p. 479-86.

309. Di Carlo, G., I. Nuzzo, R. Capasso, M.R. Sanges, E. Galdiero, F. Capasso, and C.R. Carratelli, *Modulation of apoptosis in mice treated with Echinacea and St. John's wort.* Pharmacol Res, 2003. **48**(3): p. 273-7.

310. Wu, B., T. Fujise, R. Iwakiri, A. Ootani, S. Amemori, S. Tsunada, S. Toda, and K. Fujimoto, *Venous congestion induces mucosal apoptosis via tumor necrosis factor-alpha-mediated cell death in the rat small intestine.* J Gastroenterol, 2004. **39**(11): p. 1056-62.

311. O'Connell, J., M.W. Bennett, K. Nally, G.C. O'Sullivan, J.K. Collins, and F. Shanahan, *Interferon-gamma sensitizes colonic epithelial cell lines to*

physiological and therapeutic inducers of colonocyte apoptosis. J Cell Physiol, 2000. **185**(3): p. 331-8.

312. Xie, R., R.H. Mathijssen, A. Sparreboom, J. Verweij, and M.O. Karlsson, *Clinical pharmacokinetics of irinotecan and its metabolites in relation with diarrhea.* Clin Pharmacol Ther, 2002. **72**(3): p. 265-75.

313. Xie, R., R.H. Mathijssen, A. Sparreboom, J. Verweij, and M.O. Karlsson, *Clinical pharmacokinetics of irinotecan and its metabolites: a population analysis.* J Clin Oncol, 2002. **20**(15): p. 3293-301.

314. Wang, Z.Q., C. Gorski, M.A. Hamman, S.M. Huang, L.J. Lesko, and S.D. Hall, *The effects of St John's wort (Hypericum perforatum) on human cytochrome P450 activity.* Clin Pharmacol Ther, 2001. **70**(4): p. 317-26.

315. Markowitz, J.S., C.L. DeVane, D.W. Boulton, S.W. Carson, Z. Nahas, and S.C. Risch, *Effect of St. John's wort (Hypericum perforatum) on cytochrome P-450 2D6 and 3A4 activity in healthy volunteers.* Life Sci, 2000. **66**(9): p. PL133-9.

316. Markowitz, J.S., J.L. Donovan, C.L. DeVane, R.M. Taylor, Y. Ruan, J.S. Wang, and K.D. Chavin, *Effect of St John's wort on drug metabolism by induction of cytochrome P450 3A4 enzyme.* JAMA, 2003. **290**(11): p. 1500-4.

317. Wang, Z., J.C. Gorski, M.A. Hamman, S.M. Huang, L.J. Lesko, and S.D. Hall, *The effects of St John's wort (Hypericum perforatum) on human cytochrome P450 activity.* Clin Pharmacol Ther, 2001. **70**(4): p. 317-26.

318. Chu, X.Y., Y. Kato, K. Niinuma, K.I. Sudo, H. Hakusui, and Y. Sugiyama, *Multispecific organic anion transporter is responsible for the biliary excretion of the camptothecin derivative irinotecan and its metabolites in rats.* J Pharmacol Exp Ther, 1997. **281**(1): p. 304-14.

319. Yoshikawa, M., Y. Ikegami, K. Sano, H. Yoshida, H. Mitomo, S. Sawada, and T. Ishikawa, *Transport of SN-38 by the wild type of human ABC transporter ABCG2 and its inhibition by quercetin, a natural flavonoid.* J Exp Ther Oncol, 2004. **4**(1): p. 25-35.

320. Martinez-Poveda, B., *Hyperforin, a bio-active compound of St. John's Wort, is a new inhibitor of angiogenesis targeting several key steps of the process.* Int. J. Cancer, 2005. **117**: p. 775–80.

321. Lavie, G., M. Mandel, S. Hazan, T. Barliya, M. Blank, A. Grunbaum, D. Meruelo, and A. Solomon, *Anti-angiogenic activities of hypericin in vivo: potential for ophthalmologic applications.* Angiogenesis, 2005. **8**(1): p. 35-42.

322. Sharma, R., P. Tobin, and S.J. Clarke, *Management of chemotherapy-induced nausea, vomiting, oral mucositis, and diarrhoea.* Lancet Oncol, 2005. **6**(2): p. 93-102.

323. Wadler, S., A.B. Benson, 3rd, C. Engelking, R. Catalano, M. Field, S.M. Kornblau, E. Mitchell, J. Rubin, P. Trotta, and E. Vokes, *Recommended guidelines for the treatment of chemotherapy-induced diarrhea.* J Clin Oncol, 1998. **16**(9): p. 3169-78.

324. Rothenberg, M.L., J.R. Eckardt, J.G. Kuhn, H.A. Burris, 3rd, J. Nelson, S.G. Hilsenbeck, G.I. Rodriguez, A.M. Thurman, L.S. Smith, S.G. Eckhardt, G.R. Weiss, G.L. Elfring, D.A. Rinaldi, L.J. Schaaf, and D.D. Von Hoff, *Phase II trial of irinotecan in patients with progressive or rapidly recurrent colorectal cancer.* J Clin Oncol, 1996. **14**(4): p. 1128-35.

325. Abigerges, D., J.P. Armand, G.G. Chabot, L. Da Costa, E. Fadel, C. Cote, P. Herait, and D. Gandia, *Irinotecan (CPT-11) high-dose escalation using intensive high-dose loperamide to control diarrhea.* J Natl Cancer Inst, 1994. **86**(6): p. 446-9.

326. Ikuno, N., H. Soda, M. Watanabe, and M. Oka, *Irinotecan (CPT-11) and characteristic mucosal changes in the mouse ileum and cecum.* J Natl Cancer Inst, 1995. **87**(24): p. 1876-83.

327. Lenardo, M., K.M. Chan, F. Hornung, H. McFarland, R. Siegel, J. Wang, and L. Zheng, *Mature T lymphocyte apoptosis--immune regulation in a dynamic and unpredictable antigenic environment.* Annu Rev Immunol, 1999. **17**: p. 221-53.

328. Standiford, T.J., *Anti-inflammatory cytokines and cytokine antagonists.* Curr Pharm Des, 2000. **6**(6): p. 633-49.

329. Bang, S., E.J. Jeong, I.K. Kim, Y.K. Jung, and K.S. Kim, *Fas- and tumor necrosis factor-mediated apoptosis uses the same binding surface of FADD to trigger signal transduction. A typical model for convergent signal transduction.* J Biol Chem, 2000. **275**(46): p. 36217-22.

330. Haddad, E., S. Paczesny, V. Leblond, J.M. Seigneurin, M. Stern, A. Achkar, M. Bauwens, V. Delwail, D. Debray, C. Duvoux, P. Hubert, B. Hurault de Ligny, J. Wijdenes, A. Durandy, and A. Fischer, *Treatment of B-lymphoproliferative disorder with a monoclonal anti-interleukin-6 antibody in 12 patients: a multicenter phase 1-2 clinical trial.* Blood, 2001. **97**(6): p. 1590-7.

331. Sarzi-Puttini, P., F. Atzeni, A. Doria, L. Iaccarino, and M. Turiel, *Tumor necrosis factor-alpha, biologic agents and cardiovascular risk.* Lupus, 2005. **14**(9): p. 780-4.

332. Blam, M.E., R.B. Stein, and G.R. Lichtenstein, *Integrating anti-tumor necrosis factor therapy in inflammatory bowel disease: current and future perspectives.* Am J Gastroenterol, 2001. **96**(7): p. 1977-97.

333. Ormerod, L.P., *Tuberculosis and anti-TNF-alpha treatment.* Thorax, 2004. **59**(11): p. 921.

334. Feldmann, M. and R.N. Maini, *Lasker Clinical Medical Research Award. TNF defined as a therapeutic target for rheumatoid arthritis and other autoimmune diseases.* Nat Med, 2003. **9**(10): p. 1245-50.

335. Sansonetti, P.J., *War and peace at mucosal surfaces.* Nat Rev Immunol, 2004. **4**(12): p. 953-64.

336. Cottone, M., A. Orlando, A. Casa, and L. Oliva, *Maintenance infliximab for Crohn's disease.* Lancet, 2002. **360**(9345): p. 1602; author reply 1602-3.

337. Loher, F., K. Schmall, P. Freytag, N. Landauer, R. Hallwachs, C. Bauer, B. Siegmund, F. Rieder, H.A. Lehr, M. Dauer, J.F. Kapp, S. Endres, and A. Eigler, *The specific type-4 phosphodiesterase inhibitor mesopram alleviates experimental colitis in mice.* J Pharmacol Exp Ther, 2003. **305**(2): p. 549-56.

338. Bartlett, J.B., K. Dredge, and A.G. Dalgleish, *The evolution of thalidomide and its IMiD derivatives as anticancer agents.* Nat Rev Cancer, 2004. **4**(4): p. 314-22.

339. Cohen, S., E. Hurd, J. Cush, M. Schiff, M.E. Weinblatt, L.W. Moreland, J. Kremer, M.B. Bear, W.J. Rich, and D. McCabe, *Treatment of rheumatoid arthritis with anakinra, a recombinant human interleukin-1 receptor*

antagonist, in combination with methotrexate: results of a twenty-four-week, multicenter, randomized, double-blind, placebo-controlled trial. Arthritis Rheum, 2002. **46**(3): p. 614-24.

340. Sawczenko, A., O. Azooz, J. Paraszczuk, M. Idestrom, N.M. Croft, M.O. Savage, A.B. Ballinger, and I.R. Sanderson, *Intestinal inflammation-induced growth retardation acts through IL-6 in rats and depends on the -174 IL-6 G/C polymorphism in children.* Proc Natl Acad Sci U S A, 2005. **102**(37): p. 13260-5.

341. Novelli, F. and J.L. Casanova, *The role of IL-12, IL-23 and IFN-gamma in immunity to viruses.* Cytokine Growth Factor Rev, 2004. **15**(5): p. 367-77.

342. O'Shea, J.J., A. Ma, and P. Lipsky, *Cytokines and autoimmunity.* Nat Rev Immunol, 2002. **2**(1): p. 37-45.

343. Anderson, P.O., A. Sundstedt, Z. Yazici, S. Minaee, E.J. O'Neill, R. Woolf, K. Nicolson, N. Whitley, L. Li, S. Li, D.C. Wraith, and P. Wang, *IL-2 overcomes the unresponsiveness but fails to reverse the regulatory function of antigen-induced T regulatory cells.* J Immunol, 2005. **174**(1): p. 310-9.

344. Mazzon, E., C. Muia, R. Di Paola, T. Genovese, A. De Sarro, and S. Cuzzocrea, *Thalidomide treatment reduces colon injury induced by experimental colitis.* Shock, 2005. **23**(6): p. 556-64.

345. Williams, C.S., M. Tsujii, J. Reese, S.K. Dey, and R.N. DuBois, *Host cyclooxygenase-2 modulates carcinoma growth.* J Clin Invest, 2000. **105**(11): p. 1589-94.

346. Prescott, S.M. and F.A. Fitzpatrick, *Cyclooxygenase-2 and carcinogenesis.* Biochim Biophys Acta, 2000. **1470**(2): p. M69-78.

347. Yeoh, A.S., J.M. Bowen, R.J. Gibson, and D.M. Keefe, *Nuclear factor kappaB (NFkappaB) and cyclooxygenase-2 (Cox-2) expression in the irradiated colorectum is associated with subsequent histopathological changes.* Int J Radiat Oncol Biol Phys, 2005. **63**(5): p. 1295-303.

348. Dempke, W., C. Rie, A. Grothey, and H.J. Schmoll, *Cyclooxygenase-2: a novel target for cancer chemotherapy?* J Cancer Res Clin Oncol, 2001. **127**(7): p. 411-7.

349. Sugita, K., S. Hayakawa, M. Karasaki-Suzuki, H. Hagiwara, F. Chishima, S. Aleemuzaman, J.A. Li, S. Nishinarita, and T. Yamamoto, *Granulocyte colony stimulation factor (G-CSF) suppresses interleukin (IL)-12 and/or IL-2 induced interferon (IFN)-gamma production and cytotoxicity of decidual mononuclear cells.* Am J Reprod Immunol, 2003. **50**(1): p. 83-9.

350. Xie, R., L.H. Tan, E.C. Polasek, C. Hong, M. Teillol-Foo, T. Gordi, A. Sharma, D.J. Nickens, T. Arakawa, D.W. Knuth, and E.J. Antal, *CYP3A and P-Glycoprotein Activity Induction With St. John's Wort in Healthy Volunteers From 6 Ethnic Populations.* J Clin Pharmacol, 2005. **45**(3): p. 352-6.

351. van Ark-Otte, J., M.A. Kedde, W.J. van der Vijgh, A.M. Dingemans, W.J. Jansen, H.M. Pinedo, E. Boven, and G. Giaccone, *Determinants of CPT-11 and SN-38 activities in human lung cancer cells.* Br J Cancer, 1998. **77**(12): p. 2171-6.

352. Itoh, T., S. Itagaki, Y. Sumi, T. Hirano, I. Takemoto, and K. Iseki, *Uptake of irinotecan metabolite SN-38 by the human intestinal cell line Caco-2.* Cancer Chemother Pharmacol, 2005. **55** (5): p. 420-4.

353. Fabro, S.E., H. Schumacher, R.L. Smith, and R.T. Williams, *[Metabolism of Thalidomide. I. The Spontaneous Hydrolysis of Thalidomide.]*. Boll Soc Ital Biol Sper, 1963. **39**: p. 1921-5.

354. Kruse, F.E., A.M. Joussen, K. Rohrschneider, M.D. Becker, and H.E. Volcker, *Thalidomide inhibits corneal angiogenesis induced by vascular endothelial growth factor.* Graefes Arch Clin Exp Ophthalmol, 1998. **236**(6): p. 461-6.

355. Agostinis, P., A. Vantieghem, W. Merlevede, and P.A.M. de Witte, *Hypericin in cancer treatment: more light on the way.* Int J Biochem Cell Biol, 2002. **34**(3): p. 221-41.